UNIVERSITAT POLITÈCNICA DE VALÈNCIA

dma
Departament de Matemàtica Aplicada

Advances on Differential Equations with Uncertainties and their Applications to Probabilistic Mechanics Engineering

PhD Thesis

PhD Candidate
Elena López Navarro

Supervisors
PhD Juan Carlos Cortés López
PhD M. Dolores Roselló Ferragud

València, Autumn 2024

UNIVERSITAT
POLITÈCNICA
DE VALÈNCIA

Advances on Differential Equations with Uncertainties and their Applications to Probabilistic Mechanics Engineering

Author: Elena López Navarro

Supervisors: PhD Juan Carlos Cortés López
PhD María Dolores Roselló Ferragud

Declaration of Authorship

PhD Juan Carlos Cortés López and PhD María Dolores Roselló Ferragud, full professors at the Universitat Politècnica de València,

CERTIFY that the present PhD thesis entitled: *Advances on Differential Equations with Uncertainties and their Applications to Probabilistic Mechanics Engineering* has been performed under our supervision at the *Instituto Universitario de Matemática Multidisciplinar* in the Universitat Politècnica de València by Elena López Navarro. It constitutes her thesis dissertation to obtain the PhD degree in Mathematics with international mention.

In compliance with the current legislation, we authorize the presentation of this dissertation signing the present certificate.

València - Autumn 2024

JUAN CARLOS\| CORTES\| LOPEZ

Firmado digitalmente por JUAN CARLOS\| CORTES\|LOPEZ
Fecha: 2024.10.17 21:02:02 +02'00'

PhD Juan Carlos Cortés López

MARIA DOLORES\| ROSELLO\| FERRAGUD

Firmado digitalmente por MARIA DOLORES\| ROSELLO\| FERRAGUD
Fecha: 2024.10.17 21:52:59 +02'00'

PhD María Dolores Roselló Ferragud

Everything changes and nothing stands still.
Heraclitus

A todas aquellas personas que me han apoyado y aguantado durante esta aventura. Gracias.

Resumen

Las ecuaciones diferenciales son herramientas fundamentales para modelizar y analizar sistemas dinámicos en Ingeniería. Las ecuaciones diferenciales permiten a los ingenieros describir cómo cambian en el tiempo y/o en el espacio las magnitudes físicas como, por ejemplo, la posición de un sistema vibratorio (como puede ser un muelle), la deflexión de un estructura mecánica (como puede ser una viga), etc. Por otra parte, muchos sistemas del mundo real están afectados por incertidumbres. Por ejemplo, los errores de medición, la comprensión incompleta de fenómenos físicos complejos, el ruido termal en los circuitos electrónicos o las variaciones en las propiedades de los materiales debido a su heterogeneidad son factores que involucran cierto nivel de aleatoriedad que debe tenerse en cuenta en la modelización. Esta modelización suele realizarse en muchos casos mediante ecuaciones diferenciales que, por tanto, contienen en su formulación magnitudes con incertidumbre, dando lugar a ecuaciones diferenciales aleatorias/estocásticas. Proporcionar métodos rigurosos para estudiar dichas ecuaciones es fundamental para desarrollar soluciones robustas y fiables de problemas de Ingeniería.

Esta tesis presenta un análisis probabilístico de tres clases de problemas de Ingeniería Mecánica, como son los sistemas vibratorios (osciladores), las estructuras mecánicas (deflexión de vigas) y un problema mecánico modelado por una ecuación diferencial fraccionaria aleatoria. A lo largo del trabajo se han aplicado diferentes técnicas probabilísticas para lograr una comprensión más profunda del comportamiento de estos sistemas bajo excitaciones aleatorias. Además, en esta tesis nos hemos centrado en construir aproximaciones, no sólo de los momentos estadísticos principales (media, varianza, etc.), sino también la función de densidad de probabilidad de la respuesta (solución) de los distintos modelos estudiados. Proporcionar una descripción probabilística completa de este tipo de modelos mecánicos es un tema que ha atraído un notable interés tanto de matemáticos como de ingenieros durante las últimas décadas.

En primer lugar, se estudian dos osciladores aleatorios no lineales en los que el término de restauración depende de la posición, en el primer caso, y de la posición y la velocidad, en el segundo. El término no lineal está afectado por un pequeño

parámetro de perturbación. Como en ambos casos no podemos obtener la solución explícitamente, utilizaremos el método de perturbación estocástica para construir aproximaciones de la solución estocástica y sus primeros momentos estadísticos. Esto, en combinación con el principio de máxima entropía, nos permitirá obtener aproximaciones de la función de densidad de probabilidad estacionaria de la solución. En segundo lugar, se aborda el estudio de dos modelos estáticos aleatorios que describen la deflexión de una viga en voladizo. Se distinguen dos escenarios con respecto al tipo de procesos estocásticos que modelan la distribución de la carga que soporta la viga, y suponiendo que algunos parámetros del modelo, como el módulo de Young o el parámetro de rigidez flexural, pueden ser aleatorios. Adaptamos convenientemente distintas técnicas estocásticas para calcular de forma exacta o aproximada la función de densidad de probabilidad de la deflexión de la viga en voladizo en cada uno de los dos modelos antes mencionados.

Por último, se revisita un modelo sencillo propuesto recientemente para estudiar una clase de osciladores aleatorios formulados mediante la derivada fraccionaria de Caputo. Concretamente se construyen aproximaciones de la función de densidad de probabilidad de la respuesta estocástica aprovechando el método de transformación de variables aleatorias adaptado a procesos estocásticos. En este estudio se dan condiciones suficientes sobre los parámetros (que son variables aleatorias) del modelo para garantizar la convergencia de estas aproximaciones. Los resultados de este estudio pueden ser de utilidad para acometer en el futuro el estudio de osciladores aleatorios más complejos formulados mediante ecuaciones diferenciales fraccionarias.

Resum

Les equacions diferencials són ferramentes fonamentals per a modelitzar i analitzar sistemes dinàmics en Enginyeria. Les equacions diferencials permeten als enginyers descriure com canvien en el temps i/o l'espai les magnituds físiques com, per exemple, la posició d'un sistema vibratori (com pot ser un moll), la deflexió d'una estructura mecànica (com pot ser una viga), etc. Per altra banda, molts sistemes del món real estan afectats per incerteses. Per exemple, els errors de mesurament, la comprensió incompleta de fenòmens físics complexos, el soroll termal en els circuits electrònics i les variacions en les propietats dels materials a causa de la seua heterogeneïtat són factors que involucren cert nivell d'aleatorietat que ha de tindre's en compte en la modelització. Esta modelització sol realitzar-se en molts casos mitjançant equacions diferencials que, per tant, contindrà en la seua formulació incertesa, donant lloc a equacions diferencials aleatòries/estocàstiques. Proporcionar mètodes rigorosos per a estudiar estes equacions és fonamental per a desenvolupar solucions robustes i fiables de problemes d'Enginyeria.

Esta tesi presenta una anàlisi probabilística de tres classes de problemes d'Enginyeria Mecànica, com són els sistemes vibratoris (oscil·ladors), les estructures mecàniques (deflexió de bigues) i un problema mecànic modelat per una equació diferencial fraccionària aleatòria. Al llarg del nostre treball, hem aplicat diferents tècniques matemàtiques per a aconseguir una comprensió més profunda del comportament d'estos sistemes sota excitacions aleatòries. A més a més, en esta tesi ens hem centrat en construir aproximacions, no sols dels moments estadístics principals (mitjana, variància, etc.), sinó també la funció de densitat de probabilitat de la resposta (solució) dels diferents models estudiats. Proporcionar una descripció probabilística completa d'esta mena de models mecànics és un tema que ha atret l'interés tant de matemàtics com d'enginyers durant les últimes dècades.

En primer lloc, estudiem dos oscil·ladors aleatoris no lineals en els quals el terme de restauració depén de la posició, en el primer cas, i de la posició i la velocitat, en el segon. El terme no lineal està afectat per un xicotet paràmetre de pertorbació. Com en tots dos casos no podem obtindre la solució explícitament, utilitzarem el mètode de pertorbació estocàstica per a construir aproximacions de la solució

estocàstica i els seus primers moments estadístics. Això, en combinació amb el principi de màxima entropia, ens permetrà obtindre aproximacions fiables de la funció de densitat de probabilitat estacionària de la solució. En segon lloc, s'aborda l'estudi de dos models estàtics aleatoris que descriuen la deflexió d'una biga en volada. Distingim dos escenaris diferents respecte al tipus de processos estocàstics que modelen la distribució de la càrrega que suporta la biga i suposant aleatorietat per a alguns paràmetres del model, com el mòdul de Young o el paràmetre de rigidesa flexural. Adaptem convenientment diferents tècniques estocàstiques per a calcular de manera exacta o aproximada la funció de densitat de probabilitat de la deflexió de la biga en volada en cadascun dels dos models abans esmentats.

Finalment, es revisita un model senzill proposat recentment per a estudiar una classe d'oscil·ladors aleatoris formulats mitjançant la derivada fraccionària de Caputo. Concretament, es construïxen aproximacions de la funció de densitat de probabilitat de la resposta estocàstica aprofitant el mètode de transformació de variables aleatòries adaptat a processos estocàstics. En este estudi es donen condicions suficients sobre els paràmetres (que són variables aleatòries) del model per a garantir la convergència d'estes aproximacions. Els resultats d'este estudi poden ser d'utilitat per emprendre en el futur l'estudi d'oscil·ladors aleatoris més complexos formulats mitjançant equacions diferencials fraccionàries.

Abstract

Differential equations in Engineering are fundamental tools for modelling and analysing dynamical systems. Differential equations allow engineers to describe how physical quantities change over time and/or space, such as vibratory systems, mechanical structures, etc. However, many real-world systems are influenced by uncertainties. For instance, measurement errors, incomplete understanding of complex physical phenomena, random fluctuations like electronic circuit noise, and unpredictable material properties variations are aleatoric factors. Understanding both deterministic and random/stochastic differential equations is, therefore, vital for developing robust and reliable engineering solutions in a random world.

This thesis presents a comprehensive probabilistic analysis of three mechanical engineering problems: vibratory systems (oscillators), mechanical structures (deflection of beams), and a foundational mechanical problem modelled by a random fractional differential equation. Throughout our work, we have applied different mathematical techniques to better understand these system's behavior under random excitations. A significant focus has been on accurately approximating not only the main statistical moments but also the probability density function of the model's response (solution) of the models studied throughout this dissertation. Providing a complete probabilistic description of such types of mechanical models is a topic that has attracted the interest of mathematicians and engineers during the last decades.

In the first place, we will study two nonlinear random oscillators where the restoring term depends on the position, in the first case, and on the position and velocity, in the second one. The nonlinear term is affected by a small perturbative parameter. As in both cases, we cannot obtain the solution explicitly, we will use the stochastic perturbation method to construct approximations of the stochastic solution and its first statistical moments. This, in combination with the principle of maximum entropy, will result in obtaining reliable approximations of the stationary probability density function of the response. Second, we will study two models describing the deflection of a random static cantilever beam. We distinguish two different scenarios with respect to the type of stochastic processes modelling the

distribution of the load spanned the beam and assuming randomness for some model parameters such as the Young's modulus or the flexural rigidity parameter. We then conveniently adapt different stochastic techniques to calculate exactly or approximately the probability density function of the deflection of the cantilever.

Finally, we will revisit a simple model recently proposed to study a class of random oscillators formulated via the Caputo fractional derivative. We will construct approximations of the probability density function of the stochastic response, taking advantage of the random variable transformation method. We rigorously prove the convergence of these approximations under mild conditions of the model's parameters. This approach can inspire the study of more complex oscillators formulated via fractional differential equations.

Contents

List of Figures

List of Tables

Glossary

1-PDF	First probability density function
i.i.d.	Independent and identically distributed
m.s	Mean square
PCE	Polynomial chaos expansion
PDF	Probability density function
PI	Probabilistic intervals
PME	Principle of Maximum Entropy
RDE	Random differential equation
RFDE	Random fractional differential equations
RFIVP	Random fractional initial value problem
RIVP	Random initial value problem
SFDE	Stochastic fractional differential equations
w.p. 1	With probability 1
w.r.t.	With respect to

Chapter 1

General Introduction

In modern engineering, the modelling of complex systems often involves uncertainties that cannot be ignored. Many problems arising in Physics and Engineering lead to differential equations whose data (initial/boundary conditions, forcing term and/or coefficients) must be set from experimental information that involves what is usually termed, *epistemic* (or reducible) randomness [74]. Despite this type of uncertainty can possibly be reduced by using accurate measurements or improvements in the modelling process, there is another uncertainty source often met in mathematical modelling of real-world problems called *aleatory* (or irreducible) randomness, which comes from the intrinsic variability of the phenomenon to be modelled. This approach leads to the formulation of random/stochastic differential equations [89, 54]. Apart from answering fundamental questions about the existence, uniqueness, and continuous dependence of the solution with respect to the model parameter or stability, solving a random differential equation means not only calculating, exact or approximately, its solution, which is a stochastic process but also to determine its main statistical information like the expectation or the variance. However, a more ambitious goal is to calculate the finite distribution functions (usually termed the *fidis*) of the solution, being the first probability density function (1-PDF), the main *fidis* since by integration, one can calculate

any one-dimensional moment (so including the mean and the variance), and also the probability that the solution lies within an interval of specific interest [89]. In real-world applications of Physics or Engineering, this fact is a key point since it allows us to calculate relevant information such as, for example, the probability that the position and velocity of an oscillator subject to stochastic inputs lie on a specific interval or the probability of collapsing a cantilever beam whose loads are randomly distributed, etc.

This thesis applies differential equations with uncertainties to study three classes of mechanical engineering problems: vibratory systems (oscillators), mechanical structures (deflection of beams), and a foundational mechanical problem modelled by a random fractional differential equation. To face these probabilistic models, we first construct, exactly or approximately, the solution of the corresponding model using different analytical methods, such as the Laplace transform and the stochastic perturbation technique. Afterward, we apply some probabilistic techniques, such as the Random Variable Transformation (RVT) method and the Principle of Maximum Entropy (PME), to obtain the probability density function (PDF) to the solutions of those models. This approach is crucial for better describing the dynamics of the engineering systems under study.

Before studying the aforementioned probabilistic models from Chapter 3 to Chapter 7, we first include, in Chapter 2 the main definitions and results that will be required throughout the thesis.

In Chapter 3 and Chapter 4, we analyze two families of nonlinear oscillators subject to random external forces utilizing the stochastic perturbation method as a unifying technique. These types of oscillators can be formulated through differential equations of the form

$$\ddot{X}(t) + f(\dot{X}(t), X(t))) = Y(t), \quad t > 0, \tag{1.1}$$

where $f(\cdot)$ is a nonlinear function and $Y(t)$ is a stochastic external source, which acts upon the system producing random vibrations.

The study of this type of vibratory system is encountered, for example, in Physics (in the analysis of different types of oscillators) and in Engineering (in the analysis

of road vehicles and the response of structures to earthquakes' excitations or to sea waves). For example, the model (1.1) where $f(\dot{X}(t), X(t))) := 2\beta\dot{X}(t)+\omega_0^2 X(t)$, has been used, from the original contribution [11], to describe the effect on earthbound structures of earthquake-type disturbances being $X(t)$ the relative horizontal displacement of, for example, the roof of a building with respect to the ground [98]. The nature of vibrations in this type of system is usually random because they are spawned by complex factors that are not known deterministically but are statistically characterized via measurements that often contain errors and uncertainties. While oscillators in Physics and Engineering systems have been extensively studied in deterministic settings [2, 28], particularly in nonlinear cases [106, 52, 53], stochastic analysis is more appropriate as it provides a deeper understanding of their dynamics under real-world conditions. As previously said, this will be the focus of our study in Chapter 3 and Chapter 4. Specifically, in Chapter 3, the restoring term depends only on the position, while, in Chapter 4, it depends on both position and velocity. This apparently small change in the restoring term entails the study of the above-mentioned oscillators, which must be performed separately. In both chapters, assuming that $Y(t)$ satisfies certain hypotheses that will be specified later, we compute reliable approximations, not only of the mean, the variance, and the covariance (as is usually done) but of higher moments of the steady-state nonlinear oscillator. We then combine the foregoing information related to higher moments and the PME method to construct reliable approximations of the PDF of the steady-state solution. To show the versatility of the theoretical results obtained in these two chapters, different types of external stochastic inputs, such as the white noise, Ornstein-Uhlenbeck, or trigonometric process, are considered in the numerical examples.

The aim of Chapter 5 and Chapter 6 is to contribute to the development and application of stochastic methods to study foundational problems in the realm of civil engineering structures. In particular, we will address the stochastic analysis of the deflection experienced by a load-carrying beam and, more specifically, a cantilever beam.

Beams are considered one of the most important structural elements in civil engineering. They are key elements to support the floor of a building, as structural components of bridges, or to build balconies, just to cite a few. If we apply loads

to these above-mentioned beams, for example, the weight of building materials or furniture, the flow of cars on a bridge, or people on the balcony, we have to ensure that the structure can support these loads so as not to collapse. To properly design a beam, it is necessary to know some key engineering characteristics, such as the static deflection, the bending moment, or the shear force. To mathematically describe these characteristics, as a first simplified approach, we can use Euler-Bernoulli's beam theory, also called shear rigid-beam or classical beam theory, [75]. In the context of this theory, the equation governing the deflection, $Y(x)$, of a beam under a distributed load $Q(x)$ is given by the following fourth-order differential equation

$$\frac{\mathrm{d}^2}{\mathrm{d}x^2}\left(EI\frac{\mathrm{d}^2Y(x)}{\mathrm{d}x^2}\right) = Q(x), \tag{1.2}$$

where E represents Young's modulus of the material, and I is the moment of inertia of the beam's cross-section. This model is a simplification of the theory of elasticity that allows us to model the deflection of a static straight-axis beam as a function of the applied load, provided it undergoes small deflections. The deflection of a beam using Euler-Bernoulli's beam model has been widely studied from a deterministic point of view [84, 9, 18]. However, it is more realistic to approach the corresponding study from a stochastic standpoint since uncertainties are often present due to, for example, the heterogeneity of the beam materials or the lack of knowledge of the physical phenomenon because of its own inherent complexity. More accurately, the heterogeneity of the beam materials makes it more realistic to assume that both the values of the beam's moment of inertia and Young's modulus are random variables rather than deterministic constants. In addition, the loads applied on a beam may vary randomly at each of its spatial points due to environmental factors (such as the wind pressure or the snow load on the ground) or to the use for which it has been built (such as the flow of people on balconies, or vehicles on bridges), for instance. This latter motivates modeling the load on a beam by a spatial stochastic process rather than via a deterministic function. These reasons have motivated numerous probability-based methods over the last few decades to better design and analyze civil engineering structures. For instance, in [65], it is obtained the mean and covariance of the deflection of a simply supported beam with stochastic bending flexibility, assuming that the load is deterministic. In [43], authors assume that elastic modulus is a random

variable, and then the stochastic finite element method is applied to calculate the mean, standard deviation, and coefficient of displacements. In [76], the authors combine polynomial chaos with Neumann expansion method to obtain closed-form expressions for the first two response moments and, then they apply the results to a cantilever beam, where the bending rigidity of the beam is assumed to be a stationary Gaussian random field.

Assuming that the beam is fixed at the origin, i.e., $Y(0) = Y'(0) = 0$, and adding adequate endpoint values, model (1.2) allows us to study the deflection of beams with different supports: simply supported ($Y(l) = Y''(l) = 0$), built-in or fixed end ($Y(l) = Y'(l) = 0$) and free end ($Y''(l) = Y'''(l) = 0$), for example. As previously indicated, in this thesis, we focus on the stochastic analysis of the cantilever case, where the beam is firmly fastened at the origin, $x = 0$, but with no support at the end, $x = l$. The boundary conditions for this configuration are:

$$\begin{aligned} &Y(0) = 0, \quad \text{(null deflection at the embedment)},\\ &Y'(0) = 0, \quad \text{(null slope at the embedment)},\\ &Y''(l) = 0, \quad \text{(null moment at the free end)},\\ &Y'''(l) = 0, \quad \text{(null shear at the free end)}. \end{aligned} \tag{1.3}$$

While this thesis deals primarily with the stochastic analysis of the cantilever case, the same probabilistic techniques presented throughout Chapters 5 and 6 can also be applied to beams with simply supported or fixed ends.

Specifically, in Chapter 5, we study model (1.2) in the case that Young's modulus, E, is a random variable with an arbitrary PDF while the loads are randomly distributed according to different stochastic processes describing punctual and continuous loads. In Chapter 6, we face the most challenging scenario where the flexural rigidity, EI, is random, and the loads are applied on the beam according to a Poisson delta-correlated process. This latter scenario describes the complex case of cars crossing a bridge or the loads on a balcony occupied by people in movement. In both chapters, we focus on the computation of the 1-PDF of the deflection and the PDF of other mechanical quantities of interest, such as the shear force or the bending moment. The main stochastic tools to conduct the

study are the RVT method in Chapter 5 and the PME method in Chapter 6. In both chapters, all the theoretical findings are illustrated by different numerical experiments.

Over the last few decades, many contributions have proposed reformulations of classical models in Mechanics using generalized derivatives. More specifically, fractional derivatives have been utilized to model memory effects, aging in devices and/or structures, viscoelasticity in materials, etc., [80, 5, 57]. On the other hand, we have already pointed out the importance of including uncertainties when modelling physical processes. On account of these two inspiring approaches, several stochastic/random mechanical models using fractional derivatives have been proposed in recent publications, [80, 86, 29]. The aim of Chapter 7 is to extend the random analysis of a foundational mechanical model recently studied in [12], taking advantage of the RVT method. Specifically, in this chapter, we compute approximations of the PDF of the solution stochastic process of a random fractional differential equation having a power-law generalized coefficient that includes, as a particular case, the harmonic oscillator, so extending the classical deterministic theory. The theoretical results are illustrated with different examples. These instances are validated against the non-fractional model by imposing the order of the fractional derivative approaches to 2, which corresponds to the random harmonic oscillator.

The main conclusions of the thesis are presented in Chapter 8.

Finally, we want to point out that this thesis, heavily related to Probabilistic Mechanical Engineering, has been developed within some of the goals of the two following competitive research projects, whose principal investigators have been, respectively, the advisors:

- *Ecuaciones Diferenciales Aleatorias. Cuantificación de la Incertidumbre y Aplicaciones*. PID2020-115270GB-I00. IPs: Juan Carlos Cortés López and Rafael Villanueva Micó. Agencia Estatal de Investigación.

- *Métodos Computacionales para Ecuaciones Diferenciales Aleatorias. Aplicación a Sistemas Vibratorios*. AICO/2021/302. IPs: María Dolores Roselló Ferragud and Julia Irene Real Herráiz. Generalitat Valenciana.

Chapter 2

Stochastic Preliminaries

For the sake of completeness, in this chapter, we will briefly summarise some important definitions, properties, and results for random variables and stochastic processes that will be required throughout the thesis.

2.1 Probability, random variables and stochastic processes

To properly approach the study of random and stochastic differential equations, it is essential to first establish a solid background in the fundamental concepts of probability theory. Hereinafter, we will follow the definitions and notations given in [63], [17], and [89]. We briefly start by defining what a probability space, a random variable, and a stochastic process are.

A probability space, $(\Omega, \mathcal{F}, \mathbb{P})$, is a triplet made up of a sample space Ω, which includes all possible outcomes of a random experiment, a σ-algebra, $\mathcal{F}$, that is a family of subsets of Ω, usually call events, that includes all the sets resulting from operations such as union, intersection, etc., of a numerable collection of themselves, and a probability measure, $\mathbb{P}$, which assigns a probability to each event in $\mathcal{F}$.

A random variable is a measurable function from a probability space to the real numbers. Formally, given a probability space $(\Omega, \mathcal{F}, P)$, a random variable X maps outcomes in Ω to real numbers such that for every Borel set B in $\mathbb{R}$, the preimage $X^{-1}(B)$ belongs to $\mathcal{F}$. Recall that intervals are typical examples of Borel sets in the real line. Random variables enable the quantification and analysis of random phenomena by translating abstract outcomes into numerical values.

A stochastic process is a collection of random variables indexed by time (or space), $\{X(t), t \in T\}$, where T is the index set. For each $t \in T$, $X(t)$ is a random variable defined on a common probability space $(\Omega, \mathcal{F}, P)$. Stochastic processes model dynamic systems where states evolve randomly over time (or space), allowing the analysis and prediction of complex systems under uncertainty.

Next, we will define second-order variables and processes and explore their properties, including mean square convergence, continuity, differentiability, and integrability.

A real random variable, X, that satisfies $\mathbb{E}\left[X^2\right] < \infty$ is termed a second-order random variable. Here $\mathbb{E}[\cdot]$ denotes the expectation operator. The space $(L_2(\Omega), \langle \cdot, \cdot \rangle)$ is the set of all second-order random variables endowed of the following inner product $\langle X, Y \rangle = \sqrt{\mathbb{E}\left[XY\right]}$. From this inner product, one derives the following norm, usually called 2-norm, $\|X\|_2 = \sqrt{\mathbb{E}\left[X^2\right]} < +\infty$. It can be proved that $(L_2(\Omega), \langle \cdot, \cdot \rangle)$ is a Hilbert space.

In this space, a key inequality, usually referred to as Schwarz's inequality, is the following:

$$\mathbb{E}\left[XY\right] \leq \|X\|_2 \|Y\|_2, \quad X, Y \in L_2(\Omega). \tag{2.1}$$

A stochastic process $\{X(t), t \in T\}$, where T is a closed interval in $\mathbb{R}$, is called a second-order stochastic process if, for each $t \in T$, $X(t)$ is a second-order random variable.

A sequence $\{X_n : n \geq 0\}$ defined in $L_2(\Omega)$ is said to converge in mean square (m.s.) to a random variable $X \in L_2(\Omega)$ if the following condition holds:

$$\lim_{n \to \infty} \|X_n - X\|_2 = 0.$$

When this condition is met, we denote this convergence as $X_n \xrightarrow[n\to\infty]{\text{m.s.}} X$.

A second-order stochastic process $\{X(t), t \in T\}$ is m.s. continuous at $t \in T$ if

$$X(t+\Delta t) \xrightarrow[\Delta t\to 0]{\text{m.s.}} X(t).$$

The m.s. derivative of the second-order stochastic process $\{X(t), t \in T\}$, denoted as $\{\frac{\mathrm{d}X(t)}{\mathrm{d}t}, t \in T\}$, if the following m.s. convergence

$$\frac{X(t+\Delta t)-X(t)}{\Delta t} \xrightarrow[\Delta t\to 0]{\text{m.s.}} \frac{\mathrm{d}X(t)}{\mathrm{d}t},$$

holds.

Consider a partition $P = \{a = t_{n,0} < t_{n,1} < \cdots < t_{n,n} = b\}$ of the interval $[a,b] \subset \mathbb{R}$, such that $\Delta_n = \max\{t_{n,k} - t_{n,k-1} : k = 1,\ldots,n\} \to 0$ as $n \to +\infty$. Let $t'_{n,k}$ be an arbitrary point in $[t_{n,k-1}, t_{n,k})$. Suppose $f(t,u)$ is a deterministic function defined on the interval $[a,b]$ and Riemann integrable for every $u \in U$, where U is a subset of $\mathbb{R}$. We say that the second-order stochastic process $\{f(t,u)X(t) : t \in T\}$ is m.s. Riemann integrable over $[a,b]$ if for each $u \in U$, the following m.s. limit exists for some sequence of partitions of $[a,b]$

$$\sum_{k=1}^{n} f(t'_{n,k},u)X(t'_{n,k})(t_{n,k}-t_{n,k-1}) \xrightarrow[n\to+\infty]{\text{m.s.}} Y(u),$$

where $Y(u) = \int_a^b f(t,u)X(t)\mathrm{d}t$.

One function whose calculation will be a main objective throughout this thesis is the PDF of the solution of a random differential equation.

Let $X = X(t)$, $t \in T \subset \mathbb{R}$ be a stochastic process, being T an interval of the real line. The probability distribution of X is characterized by its finite-dimensional distributions. These describe the distributions of the random vectors

$$(X_{t_1},\ldots,X_{t_n}), \quad t_1,\ldots,t_n \in \mathrm{T},\ n \geq 1.$$

For every finite set $\{t_1, t_2, \ldots, t_n\}$ of T, there exist corresponding random variables $X_1 = X(t_1), X_2 = X(t_2), \ldots, X_n = X(t_n)$ with a well-defined joint distribution function

$$F_{X_1,X_2,\ldots,X_n}(x_1, t_1; x_2, t_2; \ldots; x_n, t_n)$$

$$= \mathbb{P}\left[\{\omega \in \Omega : X_1(t_1)(\omega) \leq x_1, X_2(t_2)(\omega) \leq x_2, \ldots, X_n(t_n)(\omega) \leq x_n\}\right], \, n \geq 1.$$

This joint distribution function is often denoted as $F_n(x_1, t_1; x_2, t_2; \ldots; x_n, t_n)$, and referred to it as n–th distribution function. Its associated n–th PDF is defined by

$$f_n(x_1, t_1; x_2, t_2; \ldots; x_n, t_n) = \frac{\partial^n F_n(x_1, t_1; x_2, t_2, \ldots; x_n, t_n)}{\partial x_1 \partial x_2 \ldots \partial x_n},$$

provided the previous partial derivatives exist.

For fixed $n \geq 1$, the collections $\{F_1, \ldots, F_n\}$ or $\{f_1, \ldots, f_n\}$ are known as the *fidis*. When $n = 1$, we call it the 1-PDF, which we will work with throughout the thesis. We will denote it as $f_{X(t)}(x)$, where $X(t)$ is a stochastic process with $t \in T$.

The calculation of the 1-PDF is of great usefulness from a practical standpoint since it permits determining the mean, $\mu_X(t)$, and the variance, $\sigma_X^2(t)$, at each point $t \in T$,

$$\mu_X(t) = \mathbb{E}[X(t)] = \int_{-\infty}^{\infty} x f_{X(t)}(x) \, \mathrm{d}x, \tag{2.2}$$

and

$$\sigma_X^2(t) = \mathbb{E}[(X(t) - \mu_X(t))^2] = \mathbb{E}[(X(t))^2] - (\mu_X(t))^2, \tag{2.3}$$

respectively. Additionally, further one-dimensional higher moments with respect to (w.r.t.) the origin and centered at the mean can also be calculated by means of the 1-PDF,

$$\mathbb{E}[(X(t))^m] = \int_{-\infty}^{\infty} x^m f_{X(t)}(x) \, \mathrm{d}x, \qquad m = 1, 2, \ldots,$$

and

$$\mathbb{E}[(X(t) - \mu_X(t))^m] = \int_{-\infty}^{\infty} (x - \mu_X(t))^m f_{X(t)}(x) \, \mathrm{d}x, \qquad m = 1, 2, \ldots,$$

respectively, provided the above integrals exist and are finite. Fixed an arbitrary point $t \in T$, the 1-PDF is also particularly relevant to calculate the probability that $X(t)$ lies on a certain interval of specific interest, say $[x_1, x_2]$,

$$\mathbb{P}[x_1 \leq X(t) \leq x_2] = \int_{x_1}^{x_2} f_{X(t)}(x)\mathrm{d}x.$$

Let $\{X(t) : t \in \mathrm{T}\}$ be a stochastic process. Its n–th characteristic function is defined by

$$\begin{aligned}\varphi_{n,X}(u_1, t_1; \ldots; u_n, t_n) &= \mathbb{E}\left[\mathrm{e}^{\mathrm{i}\sum_{j=1}^{n} u_j X(t_j)}\right] \\ &= \int_{-\infty}^{\infty} \cdots \int_{-\infty}^{\infty} \mathrm{e}^{\mathrm{i}\sum_{j=1}^{n} u_j x_j} f_n(x_1, t_1; \ldots; x_n, t_n)\mathrm{d}x_1 \cdots \mathrm{d}x_n,\end{aligned}$$

where $\mathrm{i} = \sqrt{-1}$ is the imaginary unit. An important property of this function is that always exists.

In addition to the one-dimensional functions $\mu_X(t)$ (mean) and $\sigma_X^2(t)$ (variance), which have been previously defined via the 1-PDF, one can also introduce the following two-dimensional associated with a second-order stochastic process,

$$\Gamma_X(t_1, t_2) = \mathbb{E}[X(t_1)X(t_2)], \quad t_1, t_2 \in \mathrm{T},$$

$$\begin{aligned}\mathbb{C}\mathrm{ov}_X(t_1, t_2) = \mathbb{C}\mathrm{ov}\left[X_{t_1}, X_{t_2}\right] &= \mathbb{E}[(X(t_1) - \mu_X(t_1))(X(t_2) - \mu_X(t_2))] \\ &= \Gamma_X(t_1, t_2) - \mu_X(t_1)\mu_X(t_2), \quad t_1, t_2 \in \mathrm{T},\end{aligned}$$

called correlation function and covariance function, respectively.

The correlation function has the following properties that will be utilized in some chapters of this thesis,

- Symmetry: $\Gamma_X(t_1, t_2) = \Gamma_X(t_2, t_1)$. This means that the correlation between $X(t_1)$ and $X(t_2)$ does not depend on the order of t_1 and t_2.
- Boundedness: $\Gamma_X(t_1, t_2) \leq \Gamma_X(t_1, t_1)\Gamma_X(t_2, t_2)$.

- Positive-definite: $\sum_{i=1}^{n}\sum_{j=1}^{n}\Gamma_X(t_i,t_j)f(t_i)f(t_j) \geq 0$, $\forall t_1,\ldots,t_n \in \mathrm{T}$ and an arbitrary function $f(t)$.

When considering two different stochastic processes, say $X(t)$ and $Y(t)$, the so called cross-correlation function is defined as

$$\Gamma_{XY}(t_1,t_2) = \mathbb{E}[X(t_1)Y(t_2)], \quad t_1,t_2 \in \mathrm{T}.$$

Notice that when $X(t) = Y(t)$, the cross-correlation function becomes the correlation function. It motivates the following notation $\Gamma_{XX}(t_1,t_2) = \Gamma_X(t_1,t_2)$ is used in interchangeably throughout this thesis. The cross-correlation function has similar properties as the correlation function, namely

- Symmetry: $\Gamma_{XY}(t_1,t_2) = \Gamma_{YX}(t_2,t_1)$.
- Boundedness: $\Gamma^2_{XY}(t_1,t_2) \leq \Gamma_{XX}(t_1,t_1)\Gamma_{YY}(t_2,t_2)$.

This thesis uses tools from analyzing stationary stochastic processes and processes with independent increments to model and analyse different problems. Next, we introduce the main definitions and results related to these stochastic processes.

In certain situations, the original data may not exhibit useful mathematical properties, but its increments (differences) do. In such a case, modelling may be performed using a stochastic process, say $X(t)$, whose increments satisfy some properties. Two important cases are:

1. Independent increment stochastic process are random functions such that the following time-increments, $X(t_1,t_2) := X(t_2) - X(t_1)$, ..., $X(t_{n-1},t_n) := X(t_n) - X(t_{n-1})$, which are random variables, are mutually independent, for $t_1 \leq t_2 \leq \cdots \leq t_{n-1} \leq t_n$;
2. When, in addition, the probability distributions of these independent increments depend only on the differences between the time parameters, such as $t_2 - t_1, \ldots, t_n - t_{n-1}$, respectively, the stochastic process is called stationary.

The statistical distributions of stationary stochastic processes do not significantly change w.r.t. their parameters. This type of process is particularly useful in contexts where the statistical behaviour of the system is assumed not to change over time, allowing for a more consistent and predictable analysis of the data. However, checking that a stochastic process is stationary is very difficult in practice. This motivates using a weaker definition called wide-sense or weak stationary stochastic process.

We say that a second-order stochastic process, $\{X(t) : t \in \mathrm{T}\}$, is wide-sense stationary if:

$$\mu_X(t) = \mu_X \text{ is constant}, \quad \mathbb{C}\mathrm{ov}_X(t,s) = \mathbb{C}\mathrm{ov}_X(\tau) \text{ only depends on } \tau = |t-s|.$$

For wide-sense stationary stochastic processes, the correlation function only depends on a single variable, $\Gamma_X(\tau) = \mathbb{E}[X(t)X(t+\tau)]$ and has the following properties that we will be used in Chapters 3 and 4:

- $\Gamma_X(\tau)$ is an even function, i.e., $\Gamma_X(\tau) = \Gamma_X(-\tau), \quad \tau > 0$.
- If $\Gamma_X(0)$ exists, then $\Gamma_X(\tau)$ always exists and is finite. In fact, $|\Gamma_X(\tau)| \leq \Gamma_X(0)$.
- $\Gamma_X(\tau)$ is nonnegative definite in τ.

2.2 Some relevant stochastic processes

In this section, we will briefly define some of the stochastic processes that we will utilize throughout the numerical examples of the thesis. Their properties will be listed as they are necessary to carry out the corresponding computations.

Gaussian stochastic process. We say that $\{X(t) : t \in \mathrm{T}\}$ is a Gaussian stochastic process if its *fidis* are multidimensional Gaussian. It is important to note that a Gaussian distribution is characterized by its mean vector, $\boldsymbol{\mu}$, and covariance matrix, $\boldsymbol{\Sigma}$. Consequently, a Gaussian stochastic process is determined by the values of $\boldsymbol{\mu}$ and $\boldsymbol{\Sigma}$ for every *fidis*.

This definition can also be expressed in terms of the joint characteristic function. Specifically, $\{X(t) : t \in \mathrm{T}\}$ is a Gaussian stochastic process if, for every finite set $t_1, \ldots, t_n$, the joint characteristic function of the random variables $X(t_1), \ldots, X(t_n)$ is given by:

$$\varphi_n(u_1, t_1; \ldots; u_n, t_n) = \mathrm{e}^{\mathrm{i}(\boldsymbol{\mu}(t_i))^{\mathrm{T}}\mathbf{u} - \frac{1}{2}\mathbf{u}^{\mathrm{T}}\boldsymbol{\Sigma}(t_i,t_j)\mathbf{u}},$$

where $\mathbf{u}^{\mathrm{T}} = (u_1, \ldots, u_n)$, $(\boldsymbol{\mu}(t_i))^{\mathrm{T}} = (\mathbb{E}[X(t_1)], \ldots, \mathbb{E}[X(t_n)])$ is the mean vector and $\boldsymbol{\Sigma}(t_i, t_j) = (\boldsymbol{\mu}_{i,j})_{n\times n}$ is the covariance matrix associated to $X(t_1), \ldots, X(t_n)$:

$$\boldsymbol{\mu}_{i,j} = \mathbb{E}[(X(t_i) - \boldsymbol{\mu}(t_i))(X(t_j) - \boldsymbol{\mu}(t_j))], \quad 1 \leq i, j \leq n.$$

In some texts, this definition is also provided in terms of the joint probability density function. However, such a definition is more restrictive and less general, as the joint probability density function may not always exist and requires the covariance matrix to be invertible, which is not always the case.

Gaussian trigonometric stochastic process. This stochastic process is defined by a linear combination of independent Gaussian variables where the coefficients are trigonometric functions, typically sine and cosine. An example of this kind of process will be used in Chapter 4 in the following form

$$Y(t) = \xi_1 \cos(t) + \xi_2 \sin(t),$$

where $\xi_1, \xi_2 \sim \mathrm{N}(0, 1)$ independent and identically distributed (i.i.d.) random variables. This process is used to model phenomena where the underlying dynamics have cyclical patterns or oscillations, exhibiting periodic behaviour.

Let us see that this stochastic process fulfills some of the properties we will need later,

- Zero-mean, i.e., $\mu_Y(t) = \mathbb{E}[Y(t)] = 0$:

$$\mathbb{E}[Y(t)] = \mathbb{E}[\xi_1 \cos(t) + \xi_2 \sin(t)] = \cos(t)\mathbb{E}[\xi_1] + \sin(t)\mathbb{E}[\xi_2] = 0.$$

- Wide-sense stationary. In the previous item, we have already seen that the mean is constant. So, let us see now if the covariance function only depends

on $\tau = |t - s|$:

$$\begin{aligned}\mathbb{C}\mathrm{ov}_Y(t,s) &= \mathbb{E}\left[(Y(t) - \mu_Y(t))(Y(s) - \mu_Y(s))\right] \\ &= \mathbb{E}\left[(\xi_1 \cos(t) + \xi_2 \sin(t))\,(\xi_1 \cos(s) + \xi_2 \sin(s))\right] \\ &= \mathbb{E}\left[\xi_1^2\right]\cos(t)\cos(s) + \mathbb{E}\left[\xi_2^2\right]\sin(t)\sin(s) \\ &= \cos(t-s) = \cos(\tau).\end{aligned}$$

In this case, the covariance function coincides with the correlation function, $\Gamma_{YY}(t,s) = \cos(t-s)$.

Standard Wiener process. This stochastic process, $\{W(t) : t \geq 0\} \equiv \{B(t) : t \geq 0\}$, also called Brownian motion, is a continuous-time stochastic process that models random motion. It satisfies the following conditions:

- It starts at zero with probability 1 (w.p. 1): $\mathbb{P}\left[\{\omega \in \Omega : W(0)(\omega) = 0\}\right] = \mathbb{P}\left[W(0) = 0\right] = 1$.
- It has independent increments: $W(t_2) - W(t_1), \ldots, W(t_n) - W(t_{n-1})$ are independent, $\forall \{t_i : 1 \leq i \leq n\} : 0 \leq t_1 < t_2 < \cdots < t_{n-1} < t_n < \infty,\ n \geq 1$.
- It has stationary increments and Gaussian with zero-mean and variance $|t-s|$: $W(t) - W(s) \sim \mathrm{N}(0; |t-s|)$, for all $t, s \geq 0$.

From this definition, some important properties can be deduced (see [17, p. 216]):

- $W(t)$ is Gaussian.
- It has zero-mean, $\mu_W(t) = 0$.
- The covariance function is $\mathbb{C}\mathrm{ov}_W(t,s) = \min(t,s)$. In particular, its variance function is $\sigma_W^2(t) = t$.

As throughout this thesis, we will work mainly with static mechanical problems, the independent variable of this process will be denoted by x (denoting space) instead of t (time). This motivates the Brownian motion will be denoted by $B(x)$ (or $W(x)$). The Brownian motion will be used in Chapter 3 and Chapter 5.

For the latter, to perform the stochastic analysis, we will take advantage of the Karhunen–Loève expansion of the Brownian motion [64, Ch. 5]

$$B(x) = \mu_B(x) + \sum_{j=1}^{\infty} \sqrt{\nu_j}\phi_j(x)\xi_j(\omega), \quad \omega \in \Omega,\ 0 < x \leq l, \tag{2.4}$$

where the mean is null: $\mu_B(x) = 0$; $\xi_j(\omega) \sim \mathrm{N}(0,1)$, $j = 1, 2, \ldots$ are i.i.d. standard Gaussian random variables, and $\{\nu_j, \phi_j(x)\}$ are the eigenpairs (eigenvalues and eigenfunctions) obtained when solving the following homogeneous Fredholm integral equation of second kind

$$\int_0^l c_B(x_1, x_2)\, \phi_j(x_2)\, \mathrm{d}x_2 = \nu_j\, \phi_j(x_1).$$

Here, $c_B(x_1, x_2) = \mathbb{C}\mathrm{ov}_B(x_1, x_2) = \min(x_1, x_2)$, $(x_1, x_2) \in [0, l] \times [0, l]$ is the covariance function of the Brownian motion, $B(x)$. It can be seen that [64, p. 216]

$$\nu_j = \frac{4l^2}{\pi^2(2j-1)^2}, \quad \phi_j(x) = \sqrt{\frac{2}{l}} \sin\left(\frac{(2j-1)\pi}{2l}x\right), \quad j = 1, 2, \ldots$$

White Gaussian noise stochastic process. Although the Brownian motion is neither m.s. differentiable nor pathwise differentiable, it can be differentiated in a generalized sense (using the theory of distributions), and the resulting process is called white noise

$$\frac{\mathrm{d}B(t)}{\mathrm{d}t} = \xi(t), \quad t \geq 0.$$

It can be shown that the white noise is a stationary zero-mean Gaussian stochastic process, whose correlation function is given by $\Gamma_{\xi\xi}(\tau) = \frac{1}{2}W\delta(\tau)$, where $\delta(\cdot)$ is the Dirac delta function and W is the noise power [88].

Ornstein–Uhlenbeck stochastic process. This stochastic process is a continuous-time process that describes the velocity of a particle undergoing Brownian motion with friction. Mathematically, the Ornstein-Uhlenbeck stochastic process, $X(t)$ is defined as the stationary solution of the Langevin equation

$$\frac{\mathrm{d}X(t)}{\mathrm{d}t} + \alpha X(t) = \sigma\frac{\mathrm{d}W(t)}{\mathrm{d}t}, \quad \alpha > 0,$$

where $W(t)$ is the standard Wiener process.

This stochastic process will be used in Chapter 3. It can be shown that is a stationary zero-mean Gaussian stochastic process, and whose correlation function is given by $\Gamma_{XX}(\tau) = \sigma^2 \, \mathrm{e}^{-\alpha|\tau|}$, [103].

Random pulses. The following stochastic process will be extensively utilized in Chapter 6. Let

$$Z(x) = \sum_{i=1}^{N(l)} U_i v(x, x_i) \tag{2.5}$$

be a stochastic process constructed by the superposition of pulses at the spatial points x_i whose shape is defined by a deterministic function $v = v(x, x_i)$ and having pulse intensities given by a family of i.i.d. random variables U_i, and $N(l)$ is a counting process, [58]. This stochastic process, $Z(x)$, will be defined in the time domain (position) $(0, l]$. In Chapter 6, specifically, we will handle this stochastic process by taking the deterministic function, $v(x, x_i)$, as the Dirac delta function, $\delta(x - x_i)$ (to represent pulses). Then, briefly, it will be a superposition of random delta pulses correlated at random instants according to a Poisson-type counting process.

2.3 Some important properties of Gaussian random variables and stochastic processes

In this section, we will introduce some technical stochastic results of Gaussian random variables and stochastic processes.

The following properties will be applied to calculate some higher-order moments of the solution stochastic process, $X(t)$, in Chapter 3 and in Chapter 4, since as it shall be seen later, $X(t)$ depends on a product of the stochastic excitation, $Y(t)$, evaluated at a finite number of instants, say $t_1, t_2, \ldots, t_n$, $Y(t_i) = Y_i$, $1 \leq i \leq n$.

Proposition 2.1 *[89, p. 28]. Let the random variables $Y_1, Y_2, \ldots, Y_n$ be jointly Gaussian with zero-mean, $\mathbb{E}[Y_i] = 0$, $1 \leq i \leq n$. Then, all odd-order moments of*

these random variables vanish, and for n even,

$$\mathbb{E}\left[Y_1 Y_2 \cdots Y_n\right] = \sum_{m_1, m_2, \ldots, m_n} \mathbb{E}\left[Y_{m_1} Y_{m_2}\right] \mathbb{E}\left[Y_{m_3} Y_{m_4}\right] \cdots \mathbb{E}\left[Y_{m_{n-1}} Y_{m_n}\right].$$

The sum above is taken over all possible combinations of $n/2$ pairs of n random variables. The number of terms in the summation is $1 \cdot 3 \cdot 5 \cdots (n-3) \cdot (n-1)$.

Sometimes, we will use this property reformulated in the following way, and in this form, it is often called the Isserlis or Wick theorem [70, 48].

Proposition 2.2 *Consider a zero-mean multivariate normal vector, say $(Y_1, \ldots, Y_n)$. Then the expected value of their product can be expressed as a sum over all possible pairings of the variables in terms of its correlation matrix*

$$\mathbb{E}\left[Y_1 \cdots Y_n\right] = \sum_{p \in P_n^2} \prod_{\{i,j\} \in p} \mathbb{E}\left[Y_i Y_j\right] = \sum_{p \in P_n^2} \prod_{\{i,j\} \in p} \Gamma(Y_i, Y_j),$$

where $\Gamma(Y_i, Y_j)$ stands for the correlation of vector (Y_i, Y_j). The sum is over all distinct ways of partitioning the set of indexes $\{1, 2, \ldots, n\}$ into pairs $\{i, j\}$ (the set of these pairs is denoted by P_n^2), and the product is over these pairs.

The following results permit interchanging the expectation operator with the mean square derivative and the mean square integral. In [89, Eq. (4.130) in Sec. 4.4.2], the first result is established for $n = 2$, and then it follows straightforwardly by induction.

Proposition 2.3 *Let $\{Y(t) : t \geq 0\}$ be a mean square differentiable stochastic process. Then,*

$$\mathbb{E}\{Y(t_1) \cdots Y(t_{n-1}) \dot{Y}(t_n)\} = \frac{\partial}{\partial t_n} (\mathbb{E}\{Y(t_1) \cdots Y(t_n)\}), \quad t_1, \ldots, t_n \geq 0,$$

provided the above expectations exist.

Proposition 2.4 *[89, p. 104]. Let $\{Y(t) : -\infty \leq a \leq t \leq b \leq +\infty\}$ be a second-order stochastic process integrable in the mean square sense and $h(t)$ a Riemann*

integrable deterministic function on $t \in (a, b)$. *Then,*

$$\mathbb{E}\left\{\int_a^b h(t)Y(t)\,\mathrm{d}t\right\} = \int_a^b h(t)\mathbb{E}\{Y(t)\}\,\mathrm{d}t.$$

The following is a distinctive property of Gaussian processes since they preserve Gaussianity under mean square integration:

Proposition 2.5 *[89, p. 112]. Let* $\{Y(t) : a \leq t \leq \infty\}$ *be a Gaussian process and let* $h(t)$ *be a Riemann integrable deterministic function on* (a, t) *such that the following mean square integral,*

$$X(t) = \int_a^t h(t, \tau)Y(\tau)\mathrm{d}\tau,$$

exists, then $\{X(t) : t \geq a\}$, *is a Gaussian process.*

We close this section by stating the mean square Leibniz rule for differentiating a mean square integral stochastic process:

Proposition 2.6 *[89, p. 104]. Let* $Y(t) \equiv \{Y(t) : a \leq t \leq b\}$ *be a mean square integrable stochastic process. Let* $f(t, s)$ *be a continuous deterministic function on* $t, s \in (a, b)$, $-\infty \leq a < b \leq \infty$ *with finite first partial derivative* $\frac{\partial f(t,s)}{\partial t}$. *Then, the mean square derivative of*

$$Z(t) = \int_a^t f(t, s)Y(s)\mathrm{d}s, \quad a \leq t \leq b, \tag{2.6}$$

exists for all $t \in (a, b)$ *and is given by*

$$\dot{Z}(t) = f(t, t)Y(t) + \int_a^t \frac{\partial f(t, s)}{\partial t}Y(s)\mathrm{d}s, \quad a \leq t \leq b. \tag{2.7}$$

2.4 Perturbation technique

The perturbation technique is a powerful mathematical method used to find approximate solutions to complex problems by introducing a small parameter into the system. This technique is well established in the analysis of deterministic nonlinear problems but can also be used for nonlinear random differential equations with random inputs under specific conditions, as discussed, among others, in [89], [72] and [45]. We will use this technique in Chapter 3 and 4.

Let's look at a simple example of how this method works. Consider a second-order system governed by the differential equation

$$a\ddot{X}(t) + b\dot{X}(t) + \epsilon g(X(t)) = Y(t) \tag{2.8}$$

where $Y(t)$ is a random input and the nonlinear function, $g(X(t))$, is considered differentiable w.r.t. X until an appropriate order.

The perturbation method relies on the premise that the solution process $X(t)$ can be expressed as a series expansion in powers of the parameter ϵ, that is

$$X(t) = X_0(t) + \epsilon X_1(t) + \epsilon^2 X_2(t) + \cdots \tag{2.9}$$

Now, if we replace Eq. (2.9) in Eq.(2.8) and group the terms of the same order of ϵ, we obtain the following system of random differential equations which can be solved in cascade

$$\begin{array}{lcccc} \epsilon^0 & : & a\ddot{X}_0(t) + b\dot{X}_0(t) & = & Y(t), \\ \epsilon^1 & : & a\ddot{X}_1(t) + b\dot{X}_1(t) & = & -g(X_0(t)), \\ \epsilon^2 & : & a\ddot{X}_2(t) + b\dot{X}_2(t) & = & -X_1(t)g'(X_0(t)), \\ \vdots & \vdots & \vdots & \vdots & \vdots \end{array} \tag{2.10}$$

This technique is usually applied by truncating the expansion (2.9) to the first-order approximation

$$\widehat{X}(t) = X_0(t) + \epsilon X_1(t), \tag{2.11}$$

since as ϵ is small, the terms associated to higher powers ($X_n(t)\epsilon^n$, $n = 2, 3, \ldots$) in the series expansion can usually be neglected. This fact determines the legitimacy of the approximation only for a small range for the values of parameter ϵ, which is consistent with the initial assumption that ϵ is a small parameter [50]. It is important to point out that, as already reported in [89, Ch. 7], no proof is available to show that the stochastic process $X(t)$ given in (2.9) converges in the mean square sense (or other probabilistic convergences), while some restrictive convergence conditions have been established in the deterministic framework [92]. Therefore, the convergence of $X(t)$ can be formulated in terms of strong hypotheses about its sample behaviour, which, in practice, results in very restrictive assumptions.

2.5 Random Variable Transformation method

When we have a random initial value problem (RIVP), for which it is possible to obtain an explicit expression of the solution (which will depend on the random variables that define the initial condition, source term and/or coefficients), it is sometimes possible to define a transformation that allows us to obtain the PDF of the RIVP solution. For this purpose, the following result, which allows us to determine the PDF of a random vector V resulting from the transformation of another random vector U whose PDF is known, will be very useful, as will be shown in Chapters 5 and 7.

Theorem 2.1 (RVT method) *[89, page 25]. Let us consider* $\mathbf{U} = (U_1, \ldots, U_n)$ *and* $\mathbf{V} = (V_1, \ldots, V_n)$ *two n-dimensional continuous random vectors defined on a complete probability space* $(\Omega, \mathcal{F}, \mathbb{P})$. *Let* $\mathbf{r} : \mathbb{R}^n \to \mathbb{R}^n$ *be a one-to-one deterministic transformation of* $\mathbf{U}$ *into* $\mathbf{V}$, *i.e.,* $\mathbf{V} = \mathbf{r}(\mathbf{U})$. *Assume that* $\mathbf{r}$ *is continuous in* $\mathbf{U}$ *and has continuous partial derivatives w.r.t. each* U_i, $1 \leq i \leq n$. *Then, if* $f_{\mathbf{U}}(\mathbf{u})$ *denotes the joint PDF of random vector* $\mathbf{U}$, *and* $\mathbf{s} = \mathbf{r}^{-1} = (s_1(v_1, \ldots, v_n), \ldots, s_n(v_1, \ldots, v_n))$ *represents the inverse mapping of* $\mathbf{r} = (r_1(u_1, \ldots, u_n), \ldots, r_n(u_1, \ldots, u_n))$, *the joint PDF of random vector* $\mathbf{V}$ *is given by*

$$f_{\mathbf{V}}(\mathbf{v}) = f_{\mathbf{U}}\left(\mathbf{s}(\mathbf{v})\right) |\mathcal{J}| \,,$$

where $|\mathcal{J}|$, which is assumed to be different from zero, is the absolute value of the Jacobian, that is defined by the determinant

$$\mathcal{J} = \det\left(\frac{\partial \mathbf{s}}{\partial \mathbf{v}}\right) = \det\begin{pmatrix} \frac{\partial s_1(v_1,\ldots,v_n)}{\partial v_1} & \cdots & \frac{\partial s_n(v_1,\ldots,v_n)}{\partial v_1} \\ \vdots & \ddots & \vdots \\ \frac{\partial s_1(v_1,\ldots,v_n)}{\partial v_n} & \cdots & \frac{\partial s_n(v_1,\ldots,v_n)}{\partial v_n} \end{pmatrix}.$$

2.6 Principle of Maximum Entropy

Sometimes, it is not possible to use the RVT method, either because it is not possible to obtain an explicit solution or because, even having such an expression, it is impossible to define a transformation fulfilling the conditions of the theorem. In this case, an alternative to constructing the PDF of the RIVP is based on the application of the PME method described below. This technique will be used in Chapters 3, 4, and 6 to obtain an approximation of the PDF of the stochastic solution.

As detailed in [69], the PME is an efficient method to determine the PDF, $f_X(x)$, of a random variable, say X, constrained by the statistical information available (domain, expectation, variance, symmetry, kurtosis, etc.) on X. The method consists of determining $f_X(x)$ such that it maximizes the so-called Shannon's entropy (also referred to as differential entropy), which is given by $\mathcal{S}\{f_X\} = -\int_{x_1}^{x_2} f_X(x)\log(f_X(x))\,\mathrm{d}x$, subject to several constraints, which are usually defined by the N first moments, say a_n, $n = 1, 2, \ldots, N$, of the random variable X together with the normalization condition, $\int_{x_1}^{x_2} f_X(x)\,\mathrm{d}x = 1$. In this context, the admissible set of solutions is then defined by $\mathcal{A} = \{f_X : [x_1, x_2] \longrightarrow \mathbb{R} : \int_{x_1}^{x_2} x^n f_X(x)\,\mathrm{d}x = a_n,\ n = 0, 1, \ldots, N\}$. Notice that $n = 0$ corresponds to the normalization condition (i.e., the integral of the PDF is one), and that the rest of the restrictions are defined by the statistical moments, $\mathbb{E}[X^n] = a_n$, $n = 1, 2, \ldots, N$. It can be seen, by applying the functional version of Lagrange multipliers associated with $\mathcal{A}$, that

$$f_X(x) = \mathbb{1}_{[x_1,x_2]}(x)\,\mathrm{e}^{-\sum_{i=0}^{N}\lambda_i x^i}, \qquad \mathbb{1}_{[x_1,x_2]}(x) = \begin{cases} 1, & x \in [x_1, x_2], \\ 0, & x \notin [x_1, x_2]. \end{cases} \tag{2.12}$$

In practice, the Lagrange multipliers, λ_i, $i = 0, 1, \ldots, N$, are determined by numerically solving the following system of $N + 1$ nonlinear equations defined by the constraints

$$\int_{x_1}^{x_2} x^n \mathbb{1}_{[x_1,x_2]}(x)\, \mathrm{e}^{-\sum_{i=0}^{N} \lambda_i x^i}\, \mathrm{d}x = a_n, \qquad n = 0, 1, \ldots, N. \tag{2.13}$$

In other words, the PME method selects the one that maximizes the Shannon or differential entropy as a measure of randomness among all the PDFs that satisfy the constraints given by the available statistical information. This can be naively interpreted as looking for the PDF, which maximizes the uncertainty from the minimal quantity of information [69].

2.7 Monte Carlo simulations

The Monte Carlo method is a popular, intuitive, and flexible approach to uncertainty quantification in virtually any class of mathematical problems whose data is affected by randomness. It is based on performing simulations of the random data according to their corresponding associated probabilistic laws. So, the method heavily relies on good random number generators. In its crude form, the error convergence rate is inversely proportional to the square root of the number of realizations of the random inputs. The Monte Carlo has been demonstrated to be a powerful tool to deal with stochastic/random engineering problems [66, 105]. The Monte Carlo simulations will be used to compare and validate the numerical results obtained by the different stochastic methods developed in this thesis.

Chapter 3

Probabilistic analysis of random nonlinear oscillators subject to small perturbations in the restoring term depending on the position

In this chapter, we study a class of single-degree-of-freedom oscillators whose restoring function, which depends only on the position, is affected by small nonlinearities and excited by stationary Gaussian stochastic processes. We obtain, via the stochastic perturbation technique, approximations of the main statistics of the steady-state, which is a random variable, including the first moments, and the correlation and power spectral functions. Additionally, we combine this key information with the Principle of Maximum Entropy to construct approximations of the probability density function of the steady-state. We include two numerical examples where the advantages and limitations of the stochastic perturbation method are discussed with regard to certain general properties that must be preserved.

3.1 Introduction

Many vibratory systems are governed by differential equations with small nonlinear terms of the following form

$$\ddot{X}(t) + 2\beta\dot{X}(t) + \omega_0^2(X(t) + \epsilon g(X(t))) = Y(t), \quad t > 0. \tag{3.1}$$

Here, $X(t)$ denotes the position (usually of the angle w.r.t. an origin) of the oscillatory system at the time instant t, the parameter $2\beta > 0$ is the damping coefficient, $\omega_0 > 0$ the undamped angular frequency and, finally, ϵ is a small perturbation ($|\epsilon| << 1$) affecting the restoring term via a nonlinear function of the position, $g(X(t))$. The expression $X(t) + \epsilon g(X(t))$ is referred to as the nonlinear restoring term. The right-hand side term, $Y(t)$, represents an external source/forcing term (vibration) acting upon the system. In the setting of random vibration systems, $Y(t)$ is assumed to be a stochastic process, termed stochastic excitation, having certain characteristics that will be specified later in the present study. This equation corresponds to the one seen in the Introduction Chapter, Eq. (1.1), by taking $f(\dot{X}(t), X(t))) = 2\beta\dot{X}(t) + \omega_0^2(X(t) + \epsilon g(X(t)))$.

Notice that the nonlinear restoring term in Eq. (3.1) involves the parameter ϵ, which determines the magnitude of the nonlinear perturbation, whose shape is given by $g(X(t))$. When $\epsilon = 0$, Eq. (3.1) describes a random linear oscillator. In [15], authors analyse this class of oscillators considering two cases for the stochastic source term $Y(t)$, first, when it is Gaussian and, secondly, when it can be represented via a Karhunen-Loève expansion. In the case that $\epsilon \neq 0$, the inclusion of the nonlinear term makes it more difficult (even simply impossible) to exactly solve Eq. (3.1). An effective method to construct reliable approximations of Eq. (3.1) in the case that ϵ represents a small parameter is the perturbation technique [45, 72, 8, 85, 40]. In the stochastic setting, this method has been successfully applied to study different types of oscillators subject to random vibrations. After pioneer contributions by Crandall [27, 26], the analysis of random vibration systems has attracted many researchers (see, for instance, [46, 73, 40] for a full overview of this topic). In [32], approximations of quadratic and cubic nonlinear oscillators subject to white noise excitations are constructed by combining the Wiener-Hermite expansion and the homotopy perturbation technique. The aforementioned approximations correspond

to the first statistical moments (mean and variance) since, as the authors indicate in the introduction section, the computation of the PDF is usually very difficult to obtain. In [30] authors extend the previous analysis to compute higher-order statistical moments of the oscillator response in the case the nonlinearity is only quadratic. The previous methodology is extended and algorithmically-automated in [31]. In [39], the author considers the interesting scenario of a harmonic oscillator with a random mass and analyses important dynamic characteristics such as stochastic stability and resonance phenomena. A new type of Brownian motion was introduced to conduct that study. The perturbation technique has also been used to approximate the first moments, mainly the mean and the variance, of some oscillators subject to small nonlinearities. The computational procedures of this method often require amendments to the existing solution codes, so it is classified as an intrusive method. A spectral technique that allows overcoming this drawback is non-intrusive PCE (polynomial chaos expansion), in which simulations are used as black boxes, and the calculation of chaos expansion coefficients for response metrics of interest is based on a set of simulation response evaluations. In the recent paper [37], authors design an interesting hybrid non-intrusive procedure that combines PCE with the Chebyshev Surrogate Method to analyse a number of uncertain physical parameters and the corresponding transient responses of a rotating system.

Besides computing the first statistical moments of the response or performing a stability analysis of systems under stochastic vibrations, we must emphasize that the computation of the *fidis* associated with the stationary solution, and particularly of the stationary PDF, is also a major goal in the realm of vibratory systems with uncertainties. Some interesting contributions in this regard include [109, 20]. In [109], authors first present a complete overview of methods and techniques available to determine the stationary PDF of nonlinear oscillators excited by random functions. Secondly, nonlinear stochastic oscillators excited by a combination of Gaussian and Poisson white noises are fully analysed. The study is based on solving the forward generalized Kolmogorov partial differential equation (PDE) using the exponential-polynomial closure method. The theoretical analysis is accompanied by several illustrative examples. In the recent contribution [20], authors propose a new method to compute a closed-form solution of stationary PDF of single-

degree-of-freedom vibro-impact systems under Gaussian white noise excitation. The density is obtained by solving the Fokker-Planck-Kolmogorov PDE using the iterative method of weighted residue combined with the concepts of circulatory and potential probability flows. Apart from obtaining the density of the solutions, it is worth pointing out that some recent contributions deal with the calculation of the densities of quantities of interest, that belong to Reliability Theory, like the first-passage time for vibro-impact systems with randomly fluctuating restoring and damping terms (see [77] and references therein).

The goal of this chapter is to tackle the stochastic study of oscillators of the form (3.1) in the case that the nonlinear term g is a transcendental function using a polynomial approximation, based on Taylor's expansions, and then to apply the stochastic perturbation method to approximate the main statistical functions of the steady-state. Afterward, we take advantage of the PME to determine approximations of the PDF of the stationary solution. To conduct our study we have chosen a general form of the pendulum equation

$$\ddot{X}(t) + 2\beta\dot{X} + \omega_0^2(X(t) + \epsilon\sin(X(t))) = Y(t), \quad t > 0, \tag{3.2}$$

where we will assume that β and ω_0 are positive parameters, and the external source, $Y(t)$, is defined via zero-mean Gaussian stationary stochastic process, which corresponds to an important case in the analysis of vibratory systems [59, 100]. Assuming that $Y(t)$ is a stationary and Gaussian stochastic process is a rather intuitive concept, which has been extensively used in both theoretical and practical studies [60, 61]. Stationarity means that the statistical properties of the process do not vary significantly over time/space. This feature is usually met in a number of modeling problems as the surface of the sea in both spatial and time coordinates, noise in time in electric circuits under steady-state operations, homogeneous impurities in engineering materials and media, for example, [89, Ch. 3].

This chapter is organized as follows: In Section 3.2 we will obtain the main theoretical results for the stochastic model (3.2). Afterward, in Section 3.3, we perform a numerical analysis through two examples, with criticism about the

validity of the results obtained via the stochastic perturbation method. Conclusions are drawn in Section 3.4.

Finally, we want to point out that the nonlinear term, $\sin(X(t))$, that we have chosen in our subsequent analysis, could be represented by other transcendental functions, admitting polynomial approximations. With this observation, we want to highlight the generality of the study presented in this chapter.

3.2 Probabilistic model study

This section is devoted to studying, from a probabilistic standpoint, the steady-state of model (3.2). It is important to point out that the non-perturbated associated model

$$\ddot{X}(t) + 2\beta\dot{X}(t) + \omega_0^2 X(t) = Y(t), \quad t > 0, \tag{3.3}$$

has a steady-state solution provided $\beta > 0$ and regardless the value of ω_0^2. For the sake of completeness, we discuss this issue in the general setting that $Y(t)$ is a causal stationary Gaussian process and also in connection with the examples presented later.

Using the classical change of variable $\mathbf{X} = (X_1(t), X_2(t))^\top = (X(t), \dot{X}(t))^\top$, Eq. (3.3) can be written (using for convenience the differential notation) as

$$\frac{\mathrm{d}\mathbf{X}(t)}{\mathrm{d}t} = \begin{pmatrix} 0 & 1 \\ -\omega_0^2 & -2\beta \end{pmatrix} \mathbf{X}(t) + \begin{pmatrix} 0 \\ 1 \end{pmatrix} Y(t), \tag{3.4}$$

i.e.,

$$\mathrm{d}\mathbf{X}(t) = \begin{pmatrix} 0 & 1 \\ -\omega_0^2 & -2\beta \end{pmatrix} \mathbf{X}(t)\mathrm{d}t + \begin{pmatrix} 0 \\ 1 \end{pmatrix} Y(t)\mathrm{d}t. \tag{3.5}$$

In the case that $Y(t) = \xi(t)$ is the white noise (a zero-mean, Gaussian and stationary process), i.e., $\xi(t) = \dot{W}(t)$ ($W(t)$ is the standard Wiener process), Eq. (3.5) writes

$$\mathrm{d}\mathbf{X}(t) = \begin{pmatrix} 0 & 1 \\ -\omega_0^2 & -2\beta \end{pmatrix} \mathbf{X}(t)\mathrm{d}t + \begin{pmatrix} 0 \\ 1 \end{pmatrix} \dot{W}(t)\mathrm{d}t,$$

or

$$\mathrm{d}\mathbf{X}(t) = \begin{pmatrix} 0 & 1 \\ -\omega_0^2 & -2\beta \end{pmatrix} \mathbf{X}(t)\mathrm{d}t + \begin{pmatrix} 0 \\ 1 \end{pmatrix} \mathrm{d}W(t).$$

It is well known that this last equation has a stationary or steady-state solution if the real parts of the eigenvalues of the matrix

$$\mathbf{F} = \begin{pmatrix} 0 & 1 \\ -\omega_0^2 & -2\beta \end{pmatrix}$$

are negative (in other words, $\mathbf{F}$ is a Hurwitz matrix). Assuming $\beta > 0$, it is easy to check that this condition fulfills since the spectrum of $\mathbf{F}$ is given by

$$\sigma(\mathbf{F}) = \left\{ \lambda_1 = -\beta + \sqrt{\beta^2 - \omega_0^2},\ \ \lambda_2 = -\beta - \sqrt{\beta^2 - \omega_0^2} \right\},$$

and $\mathrm{Re}(\lambda_1) = \mathrm{Re}(\lambda_2) = -\beta < 0$ ($\mathrm{Re}(\cdot)$ denotes the real part). Observe that in the underdamped case ($\beta^2/\omega_0^2 < 1$), λ_1 and λ_2 are complex conjugate. This fact is used in Example 3.1 where $\beta = \frac{1}{20} > 0$ to guarantee the existence of the steady-state solution. In the more general case that $Y(t)$ in (3.4) is such that satisfies a state-space SDE of the form

$$\mathrm{d}Y(t) = r_1 Y(t)\mathrm{d}t + r_2 \mathrm{d}W(t), \tag{3.6}$$

model (3.4) together with (3.6) can be written as

$$\begin{cases} \mathrm{d}X_1(t) &= X_2(t)\mathrm{d}t, \\ \mathrm{d}X_2(t) &= -\omega_0^2 X_1(t)\mathrm{d}t - 2\beta X_2(t)\mathrm{d}t + Y(t)\mathrm{d}t, \\ \mathrm{d}Y(t) &= r_1 Y(t)\mathrm{d}t + r_2 \mathrm{d}W(t). \end{cases} \tag{3.7}$$

This system is of the form

$$\mathrm{d}\tilde{\mathbf{X}}(t) = \tilde{\mathbf{F}}\tilde{\mathbf{X}}(t)\mathrm{d}t + \tilde{\mathbf{G}}\mathrm{d}W(t), \tag{3.8}$$

where

$$\tilde{\mathbf{X}}(t) = \begin{pmatrix} X_1(t) \\ X_2(t) \\ Y(t) \end{pmatrix}, \quad \tilde{\mathbf{F}} = \begin{pmatrix} 0 & 1 & 0 \\ -\omega_0^2 & -2\beta & 1 \\ 0 & 0 & r_1 \end{pmatrix}, \quad \tilde{\mathbf{G}} = \begin{pmatrix} 0 \\ 0 \\ r_2 \end{pmatrix}. \tag{3.9}$$

The well-known results about the existence of a steady-state solution of Itô SDEs then apply to study the larger dimensional system (3.7) (or equivalently (3.8) and (3.9)). Consequently, it is enough to check that the real parts of all the eigenvalues of matrix $\tilde{\mathbf{F}}$ are negative. In this case,

$$\sigma(\tilde{\mathbf{F}}) = \left\{ \lambda_1 = r_1, \lambda_2 = -\beta + \sqrt{\beta^2 - \omega_0^2}, \lambda_3 = -\beta - \sqrt{\beta^2 - \omega_0^2} \right\}.$$

Hence, since $\beta > 0$, it is sufficient that $r_1 < 0$. Notice that in Example 3.2, which we will present later, $Y(t)$ is the Ornstein-Uhlenbeck process and $r_1 = -\alpha < 0$ (since $\alpha > 0$), so the existence of the steady-state will also be guaranteed. Finally, it is interesting to point out that in the general case $Y(t)$ is a (zero-mean) stationary Gaussian process (like the white noise and Ornstein-Uhlenbeck processes in the Examples 3.1 and 3.2, respectively), it is possible to use state-space representations of the form (3.8) to reduce a (stationary) Gaussian process driven ordinary differential equation of the form

$$\frac{\mathrm{d}\mathbf{X}(t)}{\mathrm{d}t} = \mathbf{F}\mathbf{X}(t) + \mathbf{G}Y(t),$$

as (3.4) into a larger dimensional ordinary differential equation driven by white noise, i.e., a linear Itô SDE. This can be done when the spectral density of the covariance function of $Y(t)$ is a rational function.

In the following subsections, we will apply the stochastic perturbation method to approximate its stationary solution, which is a random variable. After that, we will perform a stochastic analysis addressed to obtain the main statistical functions of the stationary solution. In particular, we will obtain the first one-dimensional moments and the correlation function.

3.2.1 Stochastic perturbation expansion

In the case of model (3.2), the method of perturbation consists, as we have seen in Chapter 2, in expanding the unknown, $X(t)$, in terms of a formal power series of the perturbative parameter ϵ, which is assumed to have a small value ($|\epsilon| \ll 1$),

$$X(t) = X_0(t) + \epsilon X_1(t) + \epsilon^2 X_2(t) + \cdots , \tag{3.10}$$

where the coefficients $X_n(t)$, $n \geq 0$ need to be determined.

As we have mentioned before, this technique is usually applied by truncating the expansion (3.10) to the first-order approximation

$$\widehat{X}(t) = X_0(t) + \epsilon X_1(t), \tag{3.11}$$

since $|\epsilon| \ll 1$, higher-order terms may not provide significant additional insights.

On the other hand, to derive a solvable family of differential equations after applying the perturbation method to model (3.2), we will also use a double approximation for the nonlinear term $\sin(X(t))$. Specifically, we first apply a truncation of its Taylor's series

$$\sin(X(t)) \approx \sum_{m=0}^{M} \frac{(-1)^m}{(2m+1)!}(X(t))^{2m+1}, \tag{3.12}$$

and secondly, we approximate $X(t)$ using (3.11), i.e.

$$\sin(X(t)) \approx \sin(\widehat{X}(t)) \approx \sum_{m=0}^{M} \frac{(-1)^m}{(2m+1)!}(X_0(t) + \epsilon X_1(t))^{2m+1}. \tag{3.13}$$

Substituting the expansions (3.13) and (3.11) into (3.2), and equating terms with the same power of ϵ, leads to the two following linear differential equations

$$\begin{aligned} \epsilon^0 \quad &: \quad \ddot{X}_0(t) + 2\beta\dot{X}_0(t) + \omega_0^2 X_0(t) \quad = \quad Y(t), \\ \epsilon^1 \quad &: \quad \ddot{X}_1(t) + 2\beta\dot{X}_1(t) + \omega_0^2 X_1(t) \quad = \quad \omega_0^2 \left(\sum_{m=0}^{M} \frac{(-1)^{m+1}}{(2m+1)!}(X_0(t))^{2m+1} \right), \end{aligned} \tag{3.14}$$

that can be solved in cascade. Although the method can be applied for any order of truncation associated with Taylor's expansion (3.12), in practice, the value of

M is set when the approximations obtained with M and $M+1$ are very closed with reference to a prefixed error or tolerance. In our subsequent analysis, we will consider $M = 2$ (that corresponds to Taylor's approximation of order 5, $\sin(X(t)) \approx X(t) - 1/3!(X(t))^3 + 1/5!(X(t))^5$), since, as we shall show later, the approximations of the main statistics of the solution stochastic process do not significantly change w.r.t. $M = 1$ (that corresponds to Taylor's approximation of order 3, $\sin(X(t)) \approx X(t) - 1/3!(X(t))^3$). To summarize, we have performed a double truncation. The first one, based on Taylor expansion for the nonlinear term ($\sin(X(t))$), and the second one, when applying the stochastic perturbation expansion given in expression (3.11) (this latter approximation is fixed in our analysis at order 1 in ϵ, as it is usually done in the literature). Notice that the order M of the Taylor truncation is independent of the order of truncation applied for the perturbation method.

As previously indicated, we are interested in the stochastic analysis of the stationary solution or steady-state. Based upon the linear theory of Laplace transformation [68], the solutions $X_0(t)$ and $X_1(t)$ are given by

$$X_0(t) = \int_0^\infty h(s) Y(t-s)\, \mathrm{d}s, \tag{3.15}$$

and

$$X_1(t) = \omega_0^2 \sum_{m=0}^{M} \int_0^\infty h(s) \frac{(-1)^{m+1}}{(2m+1)!} (X_0(t-s))^{2m+1}\, \mathrm{d}s, \tag{3.16}$$

where, for the underdamped case ($\frac{\beta^2}{\omega_0^2} < 1$),

$$h(t) = \begin{cases} \left(\omega_0^2 - \beta^2\right)^{-\frac{1}{2}} \mathrm{e}^{-\beta t} \sin\left(\left(\omega_0^2 - \beta^2\right)^{\frac{1}{2}} t\right), & \text{if} \quad t > 0, \\ 0, & \text{if} \quad t \leq 0. \end{cases} \tag{3.17}$$

Physically this situation corresponds to the case that the oscillator approaches zero oscillating about this value [91]. Finally, we point out that the integrals defining $X_0(t)$ and $X_1(t)$ in (3.15) and (3.16) must be probabilistically interpreted in the mean square sense [89, Ch. 4].

3.2.2 Constructing approximations of the main statistical moments of the stationary solution

It is important to point out that the solution of model (3.2) is not Gaussian, so in order to probabilistically describe the stationary solution, the approximations of the mean and the variance (or more generally, the correlation) functions are not enough. This fact motivates that this subsection is addressed to construct reliable approximations of higher moments of the stationary solution (represented by the first-order approximation (3.11)). This key information will be used in the next section to obtain approximations of the stationary PDF, which in turn permits the obtaining of any one-dimensional moment of the stationary solution.

Specifically, in the subsequent development we will compute any statistical moments of odd order, $\mathbb{E}\left[(\widehat{X}(t))^{2i+1}\right]$, $i = 0, 1, 2, \ldots$, the second order moment, $\mathbb{E}\left[(\widehat{X}(t))^2\right]$, the correlation function, $\Gamma_{\widehat{X}\widehat{X}}(\tau)$, the variance, $\mathbb{V}\left[\widehat{X}(t)\right]$, and the spectral density function, $S_{\widehat{X}(t)}(f)$.

As indicated in Section 3.1, we shall assume that the stochastic external source, $Y(t)$, is a stationary Gaussian stochastic process centered at the origin, i.e. $\mathbb{E}\left[Y(t)\right] = 0$, being $\Gamma_{YY}(\tau)$, its correlation function. Notice that the hypothesis $\mathbb{E}\left[Y(t)\right] = 0$ is not restrictive since otherwise we can work, without loss of generality, with the process $\tilde{Y}(t) = Y(t) - \mathbb{E}\left[Y(t)\right]$, whose mean is null.

The mean of the first-order approximation is calculated taking the expectation operator in (3.11) and using its linearity,

$$\mathbb{E}\left[\widehat{X}(t)\right] = \mathbb{E}\left[X_0(t)\right] + \epsilon\mathbb{E}\left[X_1(t)\right]. \tag{3.18}$$

To compute $\mathbb{E}\left[X_0(t)\right]$, we take the expectation operator in (3.15), then we first apply the commutation of the expectation and the mean square integral by applying Proposition 2.4, and, secondly, we use that $\mathbb{E}\left[Y(t)\right] = 0$,

$$\mathbb{E}\left[X_0(t)\right] = \mathbb{E}\left[\int_0^\infty h(s)Y(t-s)\,\mathrm{d}s\right] = \int_0^\infty h(s)\mathbb{E}\left[Y(t-s)\right]\mathrm{d}s = 0. \tag{3.19}$$

To compute $\mathbb{E}\left[X_1(t)\right]$, we take the expectation operator in (3.16) (recall that we take $M = 2$) and we again apply the commutation between the expectation and

the mean square integral as well as the integral representation of $X_0(t)$ given in (3.15),

$$\begin{aligned}
&\mathbb{E}\left[X_1(t)\right] \\
&\quad = \mathbb{E}\left[-\omega_0^2 \int_0^\infty h(s) X_0(t-s)\,\mathrm{d}s + \frac{\omega_0^2}{3!}\int_0^\infty h(s)(X_0(t-s))^3\,\mathrm{d}s\right. \\
&\qquad \left. -\frac{\omega_0^2}{5!}\int_0^\infty h(s)(X_0(t-s))^5\,\mathrm{d}s\right] \\
&\quad = -\omega_0^2 \int_0^\infty h(s)\int_0^\infty h(s_1)\mathbb{E}\left[Y(t-s-s_1)\right]\mathrm{d}s_1\,\mathrm{d}s \\
&\qquad + \frac{\omega_0^2}{3!}\int_0^\infty h(s)\int_0^\infty h(s_1)\int_0^\infty h(s_2)\int_0^\infty h(s_3)\mathbb{E}\left[Y(t-s-s_1)\right. \\
&\qquad \left. \cdot\, Y(t-s-s_2)Y(t-s-s_3)\right]\mathrm{d}s_3\,\mathrm{d}s_2\,\mathrm{d}s_1\,\mathrm{d}s \\
&\qquad - \frac{\omega_0^2}{5!}\int_0^\infty h(s)\int_0^\infty h(s_1)\int_0^\infty h(s_2)\int_0^\infty h(s_3)\int_0^\infty h(s_4)\int_0^\infty h(s_5)\mathbb{E}\left[Y(t-s-s_1)\right. \\
&\qquad \left. \cdot\, Y(t-s-s_2)Y(t-s-s_3)Y(t-s-s_4)Y(t-s-s_5)\right]\mathrm{d}s_5\,\mathrm{d}s_4\,\mathrm{d}s_3\,\mathrm{d}s_2\,\mathrm{d}s_1\,\mathrm{d}s\,.
\end{aligned} \tag{3.20}$$

Now, observe that

$$\mathbb{E}\left[Y(t-s-s_1)Y(t-s-s_2)Y(t-s-s_3)Y(t-s-s_4)(t-s-s_5)\right] = 0,$$

since $Y(t)$ is a zero-mean Gaussian process, see Proposition 2.1. Then, from (3.20) one gets

$$\mathbb{E}\left[Y_1(t)\right] = 0. \tag{3.21}$$

Substituting (3.21) and (3.19) into (3.18), one obtains

$$\mathbb{E}\left[\widehat{X}(t)\right] = \mathbb{E}\left[X_0(t)\right] + \epsilon\mathbb{E}\left[X_1(t)\right] = 0. \tag{3.22}$$

To obtain the second-order moment, $\mathbb{E}\left[(\widehat{X}(t))^2\right]$, we square the expression (3.11), but retaining up to the first-order approximation in the parameter ϵ,

$$\mathbb{E}\left[(\widehat{X}(t))^2\right] = \mathbb{E}\left[(X_0(t))^2\right] + 2\epsilon\mathbb{E}\left[X_0(t)X_1(t)\right]. \tag{3.23}$$

To calculate $\mathbb{E}\left[(X_0(t))^2\right]$, we substitute expression (3.15) and apply Fubini's theorem,

$$\begin{aligned}\mathbb{E}\left[(X_0(t))^2\right] &= \mathbb{E}\left[\left(\int_0^\infty h(s)Y(t-s)\,\mathrm{d}s\right)\left(\int_0^\infty h(s_1)Y(t-s_1)\,\mathrm{d}s_1\right)\right] \\ &= \int_0^\infty h(s)\int_0^\infty h(s_1)\mathbb{E}\left[Y(t-s)Y(t-s_1)\right]\mathrm{d}s_1\,\mathrm{d}s\,.\end{aligned} \tag{3.24}$$

Now, $\mathbb{E}\left[Y(t-s)Y(t-s_1)\right]$ can be expressed in terms of the correlation function, $\Gamma_{YY}(\cdot)$, $\mathbb{E}\left[Y(t-s)Y(t-s_1)\right] = \Gamma_{YY}(t-s_1-(t-s)) = \Gamma_{YY}(s-s_1)$. Then, (3.24) writes

$$\mathbb{E}\left[(X_0(t))^2\right] = \int_0^\infty h(s)\int_0^\infty h(s_1)\Gamma_{YY}(s-s_1)\,\mathrm{d}s_1\,\mathrm{d}s\,. \tag{3.25}$$

Observe that the correlation function is a deterministic function of a single variable since $Y(t)$ is a stationary process. To calculate the term $\mathbb{E}\left[X_0(t)X_1(t)\right]$ in (3.23), we substitute the expressions of $X_0(t)$ and $X_1(t)$ given in (3.15) and (3.16) (recall that we take $M=2$), and apply Fubini's theorem,

$$\begin{aligned}&\mathbb{E}\left[\,X_0(t)\,X_1(t)\right] \\ &= \mathbb{E}\left[X_0(t)\left(-\omega_0^2\int_0^\infty h(s)X_0(t-s)\,\mathrm{d}s + \frac{\omega_0^2}{3!}\int_0^\infty h(s)(X_0(t-s))^3\,\mathrm{d}s\right.\right. \\ &\quad \left.\left. -\frac{\omega_0^2}{5!}\int_0^\infty h(s)(X_0(t-s))^5\,\mathrm{d}s\right)\right] \\ &= \int_0^\infty h(s)\mathbb{E}\left[X_0(t)\left(-\omega_0^2X_0(t-s) + \frac{\omega_0^2}{3!}(X_0(t-s))^3 - \frac{\omega_0^2}{5!}(X_0(t-s))^5\right)\right]\mathrm{d}s \\ &= -\omega_0^2\int_0^\infty h(s)\int_0^\infty h(s_1)\int_0^\infty h(s_2)\mathbb{E}\left[Y(t-s_1)Y(t-s-s_2)\right]\mathrm{d}s_2\,\mathrm{d}s_1\,\mathrm{d}s \\ &\quad + \frac{\omega_0^2}{3!}\int_0^\infty h(s)\int_0^\infty h(s_1)\int_0^\infty h(s_2)\int_0^\infty h(s_3)\int_0^\infty h(s_4) \\ &\quad \cdot\mathbb{E}\left[Y(t-s_1)Y(t-s-s_2)Y(t-s-s_3)Y(t-s-s_4)\right]\mathrm{d}s_4\,\mathrm{d}s_3\,\mathrm{d}s_2\,\mathrm{d}s_1\,\mathrm{d}s \\ &\quad - \frac{\omega_0^2}{5!}\int_0^\infty h(s)\int_0^\infty h(s_1)\int_0^\infty h(s_2)\int_0^\infty h(s_3)\int_0^\infty h(s_4)\int_0^\infty h(s_5)\int_0^\infty h(s_6) \\ &\quad \cdot\mathbb{E}\left[Y(t-s_1)Y(t-s-s_2)Y(t-s-s_3)Y(t-s-s_4)Y(t-s-s_5)\right. \\ &\quad \left.\cdot Y(t-s-s_6)\right]\mathrm{d}s_6\,\mathrm{d}s_5\,\mathrm{d}s_4\,\mathrm{d}s_3\,\mathrm{d}s_2\,\mathrm{d}s_1\,\mathrm{d}s\,.\end{aligned} \tag{3.26}$$

Now, we express the expectations that appear in the above integrals in terms of the correlation function, $\Gamma_{YY}(\cdot)$, taking into account that $Y(t)$ is stationary. For the first expectation, one gets

$$\mathbb{E}\left[Y(t-s_1)Y(t-s-s_2)\right] = \Gamma_{YY}(s_1-s-s_2). \tag{3.27}$$

To calculate the other two expectations, we will apply the symmetry in the subindexes and the Proposition 2.2, taking into account that $Y(t)$ is a zero-mean stationary Gaussian process. To determine the second expectation in (3.26), we will denote $u_1 = t-s_1$, $u_2 = t-s-s_2$, $u_3 = t-s-s_3$ and $u_4 = t-s-s_4$ to facilitate the presentation of our computations

$$\begin{aligned}
&\mathbb{E}\Big[Y(t-s_1)Y(t-s-s_2)Y(t-s-s_3)Y(t-s-s_4)\Big] \\
&\quad = \mathbb{E}\left[Y(u_1)Y(u_2)\right]\mathbb{E}\left[Y(u_3)Y(u_4)\right] + \mathbb{E}\left[Y(u_1)Y(u_3)\right]\mathbb{E}\left[Y(u_2)Y(u_4)\right] \\
&\qquad + \mathbb{E}\left[Y(u_1)Y(u_4)\right]\mathbb{E}\left[Y(u_2)Y(u_3)\right] \\
&\quad = \Gamma_{YY}(u_2-u_1)\Gamma_{YY}(u_4-u_3) + \Gamma_{YY}(u_3-u_1)\Gamma_{YY}(u_4-u_2) \\
&\qquad + \Gamma_{YY}(u_4-u_1)\Gamma_{YY}(u_3-u_2) \\
&\quad = \Gamma_{YY}(s_1-s-s_2)\Gamma_{YY}(s_3-s_4) + \Gamma_{YY}(s_1-s-s_3)\Gamma_{YY}(s_2-s_4) \\
&\qquad + \Gamma_{YY}(s_1-s-s_4)\Gamma_{YY}(s_2-s_3).
\end{aligned}$$

Then, the second integral in (3.26) can be computed as

$$\begin{aligned}
&\int_0^\infty h(s)\int_0^\infty h(s_1)\int_0^\infty h(s_2)\int_0^\infty h(s_3)\int_0^\infty h(s_4) \\
&\quad \cdot \mathbb{E}\left[Y(t-s_1)Y(t-s-s_2)Y(t-s-s_3)Y(t-s-s_4)\right]\mathrm{d}s_4\,\mathrm{d}s_3\,\mathrm{d}s_2\,\mathrm{d}s_1\,\mathrm{d}s \\
&= \int_0^\infty h(s)\int_0^\infty h(s_1)\int_0^\infty h(s_2)\int_0^\infty h(s_3)\int_0^\infty h(s_4)\,(\Gamma_{YY}(s_1-s-s_2)\Gamma_{YY}(s_3-s_4) \\
&\quad + \Gamma_{YY}(s_1-s-s_3)\Gamma_{YY}(s_2-s_4) \\
&\quad + \Gamma_{YY}(s_1-s-s_4)\Gamma_{YY}(s_2-s_3))\,\mathrm{d}s_4\,\mathrm{d}s_3\,\mathrm{d}s_2\,\mathrm{d}s_1\,\mathrm{d}s \\
&= 3\int_0^\infty h(s)\int_0^\infty h(s_1)\int_0^\infty h(s_2)\int_0^\infty h(s_3)\int_0^\infty h(s_4) \\
&\quad \cdot \Gamma_{YY}(s_1-s-s_2)\Gamma_{YY}(s_3-s_4)\,\mathrm{d}s_4\,\mathrm{d}s_3\,\mathrm{d}s_2\,\mathrm{d}s_1\,\mathrm{d}s\,.
\end{aligned} \tag{3.28}$$

Notice that we have taken advantage of the symmetry of the correlation function, $\Gamma_{YY}(\cdot)$, to express the last multidimensional integral. The third expectation in (3.26) can be analogously calculated

$$\begin{aligned}
\mathbb{E}\Big[Y(t-s_1)Y(t-s-s_2)Y(t-s-s_3)Y(t-s-s_4)Y(t-s-s_5)Y(t-s-s_6)\Big] \\
=&\Gamma_{YY}(s_1-s-s_2)\Gamma_{YY}(s_3-s_4)\Gamma_{YY}(s_5-s_6) \\
&+\Gamma_{YY}(s_1-s-s_2)\Gamma_{YY}(s_3-s_5)\Gamma_{YY}(s_4-s_6) \\
&+\Gamma_{YY}(s_1-s-s_2)\Gamma_{YY}(s_3-s_6)\Gamma_{YY}(s_4-s_5) \\
&+\Gamma_{YY}(s_1-s-s_3)\Gamma_{YY}(s_2-s_4)\Gamma_{YY}(s_5-s_6) \\
&+\Gamma_{YY}(s_1-s-s_3)\Gamma_{YY}(s_2-s_5)\Gamma_{YY}(s_4-s_6) \\
&+\Gamma_{YY}(s_1-s-s_3)\Gamma_{YY}(s_2-s_6)\Gamma_{YY}(s_4-s_5) \\
&+\Gamma_{YY}(s_1-s-s_4)\Gamma_{YY}(s_2-s_3)\Gamma_{YY}(s_5-s_6) \\
&+\Gamma_{YY}(s_1-s-s_4)\Gamma_{YY}(s_2-s_5)\Gamma_{YY}(s_3-s_6) \\
&+\Gamma_{YY}(s_1-s-s_4)\Gamma_{YY}(s_2-s_6)\Gamma_{YY}(s_3-s_5) \\
&+\Gamma_{YY}(s_1-s-s_5)\Gamma_{YY}(s_2-s_3)\Gamma_{YY}(s_4-s_6) \\
&+\Gamma_{YY}(s_1-s-s_5)\Gamma_{YY}(s_2-s_4)\Gamma_{YY}(s_3-s_6) \\
&+\Gamma_{YY}(s_1-s-s_5)\Gamma_{YY}(s_2-s_6)\Gamma_{YY}(s_3-s_4) \\
&+\Gamma_{YY}(s_1-s-s_6)\Gamma_{YY}(s_2-s_3)\Gamma_{YY}(s_4-s_5) \\
&+\Gamma_{YY}(s_1-s-s_6)\Gamma_{YY}(s_2-s_4)\Gamma_{YY}(s_3-s_5) \\
&+\Gamma_{YY}(s_1-s-s_6)\Gamma_{YY}(s_2-s_5)\Gamma_{YY}(s_3-s_4).
\end{aligned} \tag{3.29}$$

Then, substituting (3.28) and (3.29) into (3.26), and taking again advantage of the symmetry of the correlation function, $\Gamma_{YY}(\cdot)$, to simplify the representation

of the last multidimensional integral, one obtains

$$\begin{aligned}\mathbb{E}\left[X_0(t)\ X_1(t)\right] = &-\omega_0^2 \int_0^\infty h(s) \int_0^\infty h(s_1) \int_0^\infty h(s_2) \Gamma_{YY}(s_1 - s - s_2)\,\mathrm{d}s_2\,\mathrm{d}s_1\,\mathrm{d}s \\ &+ \frac{\omega_0^2}{2} \int_0^\infty h(s) \int_0^\infty h(s_1) \int_0^\infty h(s_2) \int_0^\infty h(s_3) \int_0^\infty h(s_4) \Gamma_{YY}(s_1 - s - s_2) \\ &\quad \cdot \Gamma_{YY}(s_3 - s_4)\,\mathrm{d}s_4\,\mathrm{d}s_3\,\mathrm{d}s_2\,\mathrm{d}s_1\,\mathrm{d}s \\ &- \frac{\omega_0^2}{8} \int_0^\infty h(s) \int_0^\infty h(s_1) \int_0^\infty h(s_2) \int_0^\infty h(s_3) \int_0^\infty h(s_4) \int_0^\infty h(s_5) \int_0^\infty h(s_6) \\ &\cdot \Gamma_{YY}(s_1 - s - s_2)\Gamma_{YY}(s_3 - s_4)\Gamma_{YY}(s_5 - s_6)\,\mathrm{d}s_6\,\mathrm{d}s_5\,\mathrm{d}s_4\,\mathrm{d}s_3\,\mathrm{d}s_2\,\mathrm{d}s_1\,\mathrm{d}s\,.\end{aligned} \tag{3.30}$$

So, substituting expressions (3.25) and (3.30) into (3.23), we obtain an explicit approximation of the second-order moment for the approximation $\widehat{X}(t)$,

$$\begin{aligned}\mathbb{E}\left[\ (\widehat{X}(t))^2\right] = &\int_0^\infty h(s) \int_0^\infty h(s_1) \Gamma_{YY}(s - s_1)\,\mathrm{d}s_1\,\mathrm{d}s \\ &+ 2\epsilon \Bigg(- \omega_0^2 \int_0^\infty h(s) \int_0^\infty h(s_1) \int_0^\infty h(s_2) \Gamma_{YY}(s_1 - s - s_2)\,\mathrm{d}s_2\,\mathrm{d}s_1\,\mathrm{d}s \\ &+ \frac{\omega_0^2}{2} \int_0^\infty h(s) \int_0^\infty h(s_1) \int_0^\infty h(s_2) \int_0^\infty h(s_3) \int_0^\infty h(s_4) \\ &\quad \cdot \Gamma_{YY}(s_1 - s - s_2)\Gamma_{YY}(s_3 - s_4)\,\mathrm{d}s_4\,\mathrm{d}s_3\,\mathrm{d}s_2\,\mathrm{d}s_1\,\mathrm{d}s \\ &- \frac{\omega_0^2}{8} \int_0^\infty h(s) \int_0^\infty h(s_1) \int_0^\infty h(s_2) \int_0^\infty h(s_3) \int_0^\infty h(s_4) \int_0^\infty h(s_5) \int_0^\infty h(s_6) \\ &\quad \cdot \Gamma_{YY}(s_1 - s - s_2)\Gamma_{YY}(s_3 - s_4)\Gamma_{YY}(s_5 - s_6)\,\mathrm{d}s_6\,\mathrm{d}s_5\,\mathrm{d}s_4\,\mathrm{d}s_3\,\mathrm{d}s_2\,\mathrm{d}s_1\,\mathrm{d}s \Bigg).\end{aligned} \tag{3.31}$$

Now, we compute the third-order moment of $\widehat{X}(t)$, using the first-order approximation w.r.t. the perturbative parameter ϵ,

$$\mathbb{E}\left[(\widehat{X}(t))^3\right] = \mathbb{E}\left[(X_0(t))^3\right] + 3\epsilon\mathbb{E}\left[(X_0(t))^2 X_1(t)\right]. \tag{3.32}$$

By reasoning analogously as in the calculation of the foregoing statistical moments, we obtain

$$\begin{aligned}&\mathbb{E}\left[\,(X_0(t))^3\right]\\&\quad=\int_0^\infty h(s)\int_0^\infty h(s_1)\int_0^\infty h(s_2)\mathbb{E}\left[Y(t-s)Y(t-s_1)Y(t-s_2)\right]\mathrm{d}s_2\,\mathrm{d}s_1\,\mathrm{d}s\\&\quad=0,\end{aligned}\tag{3.33}$$

and

$$\begin{aligned}&\mathbb{E}\left[\,(X_0(t))^2X_1(t)\right]\\&\quad=\int_0^\infty h(s)\mathbb{E}\left[X_0^2(t)\left(-\omega_0^2X_0(t-s)+\frac{\omega_0^2}{3!}(X_0(t-s))^3-\frac{\omega_0^2}{5!}(X_0(t-s))^5\right)\right]\mathrm{d}s\\&\quad=0.\end{aligned}\tag{3.34}$$

We here omit the details of these calculations since they are somewhat cumbersome and they can easily inferred from our previous developments. Then, substituting (3.33) and (3.34) into (3.32), we obtain

$$\mathbb{E}\left[(\widehat{X}(t))^3\right]=\mathbb{E}\left[(X_0(t))^3\right]+3\epsilon\mathbb{E}\left[(X_0(t))^2X_1(t)\right]=0.$$

In general, it can be straightforwardly shown that the statistical moments of odd order are null,

$$\mathbb{E}\left[(\widehat{X}(t))^{2n+1}\right]=0,\quad n=0,1,2,\ldots\tag{3.35}$$

The correlation function of $\widehat{X}(t)$, using the approximation of first-order w.r.t. the perturbative parameter ϵ, is given by

$$\begin{aligned}\Gamma_{\widehat{X}\widehat{X}}(\tau)&=\mathbb{E}\left[\widehat{X}(t)\widehat{X}(t+\tau)\right]\\&=\mathbb{E}\left[X_0(t)X_0(t+\tau)\right]+\epsilon\left(\mathbb{E}\left[X_0(t)X_1(t+\tau)\right]+\mathbb{E}\left[X_1(t)X_0(t+\tau)\right]\right).\end{aligned}\tag{3.36}$$

The first term of (3.36) corresponds to the correlation function of $X_0(t)$. It is determined, in terms of the correlation function $\Gamma_{YY}(\cdot)$, by applying the Fubini's

theorem and the stationarity of $Y(t)$,

$$\begin{aligned}\mathbb{E}\left[X_0(t)X_0(t+\tau)\right] &= \int_0^\infty h(s)\int_0^\infty h(s_1)\mathbb{E}\left[Y(t-s)Y(t+\tau-s_1)\right]\mathrm{d}s_1\,\mathrm{d}s \\ &= \int_0^\infty h(s)\int_0^\infty h(s_1)\Gamma_{YY}(\tau-s_1+s)\,\mathrm{d}s_1\,\mathrm{d}s\,.\end{aligned} \tag{3.37}$$

The two last expectations on the right-hand side of (3.36), correspond to the cross-correlation function of $X_0(t)$ and $X_1(t)$. They can be expressed explicitly in terms of the correlation function $\Gamma_{YY}(\cdot)$,

$$\begin{aligned}&\mathbb{E}\left[\ X_0(t)X_1(t+\tau)\right] \\ &= \int_0^\infty h(s)\mathbb{E}\left[X_0(t)\left(-\omega_0^2X_0(t+\tau-s)+\frac{\omega_0^2}{3!}\left(X_0(t+\tau-s)\right)^3-\frac{\omega_0^2}{5!}\left(X_0(t+\tau-s)\right)^5\right)\right]\mathrm{d}s \\ &= -\omega_0^2\int_0^\infty h(s)\int_0^\infty h(s_1)\int_0^\infty h(s_2)\Gamma_{YY}(s_1+\tau-s-s_2)\,\mathrm{d}s_2\,\mathrm{d}s_1\,\mathrm{d}s \\ &\quad+\frac{\omega_0^2}{2}\int_0^\infty h(s)\int_0^\infty h(s_1)\int_0^\infty h(s_2)\int_0^\infty h(s_3)\int_0^\infty h(s_4) \\ &\quad\cdot\Gamma_{YY}(s_1+\tau-s-s_2)\Gamma_{YY}(s_3-s_4)\,\mathrm{d}s_4\,\mathrm{d}s_3\,\mathrm{d}s_2\,\mathrm{d}s_1\,\mathrm{d}s \\ &\quad-\frac{\omega_0^2}{8}\int_0^\infty h(s)\int_0^\infty h(s_1)\int_0^\infty h(s_2)\int_0^\infty h(s_3)\int_0^\infty h(s_4)\int_0^\infty h(s_5)\int_0^\infty h(s_6) \\ &\quad\cdot\Gamma_{YY}(s_1+\tau-s-s_2)\Gamma_{YY}(s_3-s_4)\Gamma_{YY}(s_5-s_6)\,\mathrm{d}s_6\,\mathrm{d}s_5\,\mathrm{d}s_4\,\mathrm{d}s_3\,\mathrm{d}s_2\,\mathrm{d}s_1\,\mathrm{d}s\end{aligned} \tag{3.38}$$

and

$$\begin{aligned}&\mathbb{E}\left[\ X_1(t)X_0(t+\tau)\right] \\ &= \int_0^\infty h(s)\mathbb{E}\left[X_0(t+\tau)\left(-\omega_0^2X_0(t-s)+\frac{\omega_0^2}{3!}\left(X_0(t-s)\right)^3-\frac{\omega_0^2}{5!}\left(X_0(t-s)\right)^5\right)\right]\mathrm{d}s \\ &= -\omega_0^2\int_0^\infty h(s)\int_0^\infty h(s_1)\int_0^\infty h(s_2)\Gamma_{YY}(s_1-\tau-s-s_2)\,\mathrm{d}s_2\,\mathrm{d}s_1\,\mathrm{d}s \\ &\quad+\frac{\omega_0^2}{2}\int_0^\infty h(s)\int_0^\infty h(s_1)\int_0^\infty h(s_2)\int_0^\infty h(s_3)\int_0^\infty h(s_4) \\ &\quad\cdot\Gamma_{YY}(s_1-\tau-s-s_2)\Gamma_{YY}(s_3-s_4)\,\mathrm{d}s_4\,\mathrm{d}s_3\,\mathrm{d}s_2\,\mathrm{d}s_1\,\mathrm{d}s \\ &\quad-\frac{\omega_0^2}{8}\int_0^\infty h(s)\int_0^\infty h(s_1)\int_0^\infty h(s_2)\int_0^\infty h(s_3)\int_0^\infty h(s_4)\int_0^\infty h(s_5)\int_0^\infty h(s_6) \\ &\quad\cdot\Gamma_{YY}(s_1-\tau-s-s_2)\Gamma_{YY}(s_3-s_4)\Gamma_{YY}(s_5-s_6)\,\mathrm{d}s_6\,\mathrm{d}s_5\,\mathrm{d}s_4\,\mathrm{d}s_3\,\mathrm{d}s_2\,\mathrm{d}s_1\,\mathrm{d}s\,.\end{aligned} \tag{3.39}$$

From expressions (3.37)–(3.39), we observe that the correlation function, $\Gamma_{\widehat{X}\widehat{X}}(\tau)$, given by (3.36), only depends on the difference τ between two different instants, t and $t+\tau$ (as it has been anticipated in the notation in (3.36)). This fact together with $\mathbb{E}\left[\widehat{X}(t)\right] = 0$ (see (3.22)), allows us to say that the first-order approximation, $\widehat{X}(t)$, given in (3.11) and obtained via the perturbation technique, is a stationary stochastic process. Additionally, it is clear that the covariance function of the steady-state coincides with the correlation function, i.e. $\mathbb{C}\mathrm{ov}\left[\widehat{X}(t_1), \widehat{X}(t_2)\right] = \Gamma_{\widehat{X}\widehat{X}}(\tau)$, where $\tau = |t_1 - t_2|$ and, also the variance matches the second-order moment, which in turn can be calculated evaluating the correlation function at the origin,

$$\mathbb{V}\left[\widehat{X}(t)\right] = \mathbb{E}\left[\widehat{X}(t)^2\right] = \Gamma_{\widehat{X}\widehat{X}}(0). \tag{3.40}$$

From the correlation function, $\Gamma_{\widehat{X}\widehat{X}}(\tau)$, it is straightforward to also determine the power spectral density function (or simply, the power spectrum) of $\widehat{X}(t)$

$$S_{\widehat{X}(t)}(f) = \int_{-\infty}^{\infty} \mathrm{e}^{-\mathrm{i}f\tau}\, \Gamma_{\widehat{X}\widehat{X}}(\tau)\mathrm{d}\tau, \tag{3.41}$$

here, $\mathrm{i} = \sqrt{-1}$ is the imaginary unit and f is the angular frequency. Observe that, $S_{\widehat{X}(t)}(f)$ is the Fourier transform of the correlation function of $\widehat{X}(t)$. This function plays a key role in describing the distribution of power into frequency components composing a signal represented via stationary stochastic process [93].

3.3 Numerical examples

In the previous section, we have obtained approximations of the main statistical moments of the steady-state of problem (3.2). In this section, we combine this key information, together with the PME technique, to construct approximations of the PDF of the stationary solution. We will show two examples where important stochastic processes play the role of the external source, $Y(t)$, in problem (3.2). In the first example, we will take the white Gaussian noise as $Y(t)$, while in the second one, the Ornstein-Uhlenbeck stochastic process will be considered. Since the validity of the perturbation method is restricted to small values of the perturbative parameter ϵ, the numerical experiments are carried out with criticism to this key point taking into account that the numerical approximations must retain certain

universal properties such as the positivity of even order statistical moments (for any stochastic process); the symmetry of the correlation and power spectral functions; the correlation function reaches its maximum value at the origin and the positivity of the spectral function, in the case of stationary stochastic processes.

For the sake of completeness, down below we revise the main definition and results about the power spectral function, $S_{\widehat{X}(t)}(f)$ defined in (3.41), that will be used throughout the two numerical examples.

Using the Euler identity $\mathrm{e}^{\mathrm{i}x} = \cos(x) + \mathrm{i}\sin(x)$, it is easy to check that, for any stationary process, the power spectral density is an even function,

$$S_{\widehat{X}(t)}(f) = \int_{-\infty}^{\infty} \cos(f\tau)\Gamma_{\widehat{X}\widehat{X}}(\tau)\mathrm{d}\tau = 2\int_{0}^{\infty} \cos(f\tau)\Gamma_{\widehat{X}\widehat{X}}(\tau)\mathrm{d}\tau = S_{\widehat{X}(t)}(-f). \tag{3.42}$$

This property is also fulfilled by the correlation function, $\Gamma_{\widehat{X}\widehat{X}}(\tau) = \Gamma_{\widehat{X}\widehat{X}}(-\tau)$ [89, Ch. 3]. Moreover, the correlation function reaches its maximum at the origin, i.e. $|\Gamma_{\widehat{X}\widehat{X}}(\tau)| \leq \Gamma_{\widehat{X}\widehat{X}}(0)$ [89, Ch. 3], while it can be proved that the power spectral function is non-negative, $S_{\widehat{X}(t)}(f) \geq 0$ [93]. To reject the possible spurious approximations obtained via the stochastic perturbation method, we will check in our numerical experiments whether all these properties are preserved. We will also take advantage of the approximations of the power spectral density and of the correlation function to obtain the two following important parameters associated with a stationary stochastic process, the noise intensity ($\mathcal{D}$) and the correlation time ($\hat{\tau}$), respectively defined by

$$\mathcal{D} = \int_{0}^{\infty} \Gamma_{\widehat{X}\widehat{X}}(\tau)\mathrm{d}\tau = \frac{1}{2}S_{\widehat{X}(t)}(0), \qquad \hat{\tau} = \frac{\int_{0}^{\infty}\Gamma_{\widehat{X}\widehat{X}}(\tau)\mathrm{d}\tau}{\Gamma_{\widehat{X}\widehat{X}}(0)} = \frac{\mathcal{D}}{\Gamma_{\widehat{X}\widehat{X}}(0)}. \tag{3.43}$$

Notice that the value of $\mathcal{D}$ comes from evaluating $S_{\widehat{X}(t)}(f)$ at $f = 0$ in (3.42). So, the noise intensity is defined as the area beneath the correlation function $\Gamma_{\widehat{X}\widehat{X}}(\tau)$, while the correlation time is a standardized noise intensity [7]. The parameters $\mathcal{D}$ and $\hat{\tau}$ indicate how strongly the stochastic process is correlated over time.

In both examples, the numerical results that we shall show correspond to 3rd-order Taylor's approximations of the nonlinear term $\sin(X(t))$ in (3.13), since we

have checked that no significant differences are obtained using 5th order Taylor's approximations.

Example 3.1 *Let us consider as external source the stochastic process* $Y(t) = \xi(t)$*, where* $\xi(t)$ *is a white Gaussian noise, i.e. is a stationary Gaussian stochastic process with zero-mean,* $\mathbb{E}[Y(t)] = 0$*, and flat power spectral density,* $S_{Y(t)}(f) = \frac{N_0}{2}$*, for all* f*. Then, its correlation function is given by* $\Gamma_{YY}(\tau) = \frac{N_0}{2}\delta(\tau)$*, where* $\delta(\tau)$ *is the Dirac delta function. We will take the following data for the parameters involved in model* (3.2)*,* $\omega_0 = 1$*,* $\beta = \frac{5}{100}$ *and* $N_0 = \frac{1}{100}$ *(that satisfy the conditions explained in Section 3.2, so ensuring the existence of the steady-state solution), so the nonlinear random oscillator is formulated by*

$$\frac{\mathrm{d}^2X(t)}{\mathrm{d}t^2} + \frac{1}{10}\frac{\mathrm{d}X(t)}{\mathrm{d}t} + X(t) + \epsilon\sin(X(t)) = \xi(t), \quad t > 0. \tag{3.44}$$

We will now take advantage of the results derived in Subsection 3.2.2, to calculate the following statistical information of the first-order approximation, $\widehat{X}(t)$*, obtained via the perturbation method and given in* (3.11)*: (1) the moments up to order 3, i.e.* $\mathbb{E}\left[(\widehat{X}(t))^i\right]$*,* $i = 1, 2, 3$*; (2) the variance,* $\mathbb{V}\left[\widehat{X}(t)\right]$*, and (3) the correlation function,* $\Gamma_{\widehat{X}\widehat{X}}(\tau)$*. We will use this information to compute approximations, first of the stationary PDF of* $\widehat{X}(t)$*, using the PME, and, secondly, of the spectral density function of* $\widehat{X}(t)$*.*

From expression (3.35)*, in particular, we know that* $\mathbb{E}\left[\widehat{X}(t)\right]$ *and* $\mathbb{E}\left[(\widehat{X}(t))^3\right]$ *are null. For the second-order moment,* $\mathbb{E}\left[(\widehat{X}(t))^2\right]$*, using the expression* (3.31) *we obtain*

$$\mathbb{E}\left[(\widehat{X}(t))^2\right] = \frac{1}{40} - \frac{12641}{512000}\epsilon.$$

This value is also the variance since $\mathbb{E}\left[\widehat{X}(t)\right] = 0$*. On the other hand, as* $\mathbb{E}\left[(\widehat{X}(t))^2\right]$ *is always positive, we can obtain the following bound for the perturbative parameter,* $\epsilon < 1.01258$*. Although this value provides a bound for the validity of the perturbation method, we show that it is a conservative bound down below.*

To this end, we will compare the mean and standard deviation of $\widehat{X}(t)$ *obtained via the perturbation method and the ones computed by Kloeden-Platen-Schurz algorithm [54]. The results are shown in Table 3.1. We can observe that both approximations are accurate for* $\epsilon = 0$ *(which corresponds to the linearization of model* (3.2)*),* $\epsilon = 0.01$ *and* $\epsilon = 0.1$*. But significant differences in the standard deviation are revealed for* $\epsilon = 0.5$ *and* $\epsilon = 1$*.*

		Perturbation method	Kloeden-Platen-Schurz (1000 simulations)	Kloeden-Platen-Schurz (10000 simulations)
$\epsilon = 0$	Mean	0	0.00135	0.00027
	sd	0.15811	0.16031	0.15873
$\epsilon = 0.01$	Mean	0	0.00009	-0.00028
	sd	0.15733	0.15419	0.15732
$\epsilon = 0.1$	Mean	0	0.00022	$-1.806 \cdot 10^{-6}$
	sd	0.15010	0.14933	0.14992
$\epsilon = 0.5$	Mean	0	$-3.124 \cdot 10^{-7}$	0.00006
	sd	0.11249	0.12931	0.12954
$\epsilon = 1$	Mean	0	0.00028	0.00010
	sd	0.01762	0.11646	0.11267

Table 3.1: Comparison between stochastic perturbation method and Kloeden-Platen-Schurz algorithm for different values of ϵ with regard to the approximations of the mean and the standard deviation (sd) of the steady-state. Example 3.1.

According to expressions (3.36)–(3.39)*, the approximation of the correlation function is given by*

$$\Gamma_{\widehat{X}\widehat{X}}(\tau) = \begin{cases} f_1(\tau), & \text{if } \tau > 0, \\ f_2(\tau), & \text{if } \tau < 0, \\ \dfrac{1}{40} - \dfrac{12641}{512000}\epsilon, & \text{if } \tau = 0. \end{cases} \tag{3.45}$$

where,

$$f_1(\tau) = \frac{\mathrm{e}^{-\tau/20}}{81510912000}\left(399\,(5107200 + 12641\epsilon(-399 + 10\tau))\cos\left(\frac{\sqrt{399}\tau}{20}\right)\right.$$
$$\left. +\sqrt{399}(5107200 - 12641\epsilon(599 + 3990\tau))\sin\left(\frac{\sqrt{399}\tau}{20}\right)\right),$$

and,

$$f_2(\tau) = -\frac{\mathrm{e}^{\tau/20}}{81510912000}\left(399(-5107200+12641\epsilon(399+10\tau))\cos\left(\frac{\sqrt{399}\tau}{20}\right)\right.$$
$$\left.+\sqrt{399}(5107200+12641\epsilon(-599+3990\tau))\sin\left(\frac{\sqrt{399}\tau}{20}\right)\right).$$

Notice that, in full agreement with expression (3.40)*, it is satisfied that*

$$\mathbb{E}\left[(\widehat{X}(t))^2\right] = \mathbb{V}\left[\widehat{X}(t)\right] = \Gamma_{\widehat{X}\widehat{X}}(0) = \frac{1}{40} - \frac{12641}{512000}\epsilon.$$

In Figure 3.1, we show the graphical representation of the correlation function, $\Gamma_{\widehat{X}\widehat{X}}(\tau)$*, plotted from the expression* (3.45) *and using different values of the perturbative parameter* ϵ*. To emphasize this dependence on the parameter* ϵ*, hereinafter we will denote this function by* $\Gamma_{\widehat{X}\widehat{X}}(\tau,\epsilon)$*. In Figure 3.1a, we observe that the approximations of the* $\Gamma_{\widehat{X}\widehat{X}}(\tau,\epsilon)$ *deteriorate as* ϵ *increases in full agreement with the results obtained in Table 3.1. The deterioration of the approximations as* ϵ *increases can also be confirmed by checking that the general property* $|\Gamma_{\widehat{X}\widehat{X}}(\tau)| \leq \Gamma_{\widehat{X}\widehat{X}}(0)$ *for the correlation function [38], does not fulfill for* $\epsilon = 0.5$ *and* $\epsilon = 1$ *(see Figure 3.1a). In contrast, for smaller values of* $\epsilon \in \{0, 0.01, 0.1\}$ *this property holds. Notice that the correlation functions for* $\epsilon = 0$ *and* $\epsilon = 0.01$ *are quite similar, as expected. For the sake of clarity, we have plotted these results in Figure 3.1b. Finally, in Figure 3.1c we show* $\Gamma_{\widehat{X}\widehat{X}}(\tau,\epsilon)$ *as a surface varying* $(\tau,\epsilon) \in [-20,20]\times[0,0.1]$*.*

Now, we compute the approximation of the PDF, $f_{\widehat{X}(t)}(x)$*, of the steady-state, using the PME, taking* $N = 3$ *(see Section 2.6). Therefore, according to the PME, the PDF is sought in the form*

$$f_{\widehat{X}(t)}(x) = \mathrm{e}^{-1-\lambda_0-\lambda_1 x-\lambda_2 x^2-\lambda_3 x^3},$$

where, in our case, λ_0*,* λ_1*,* λ_2 *and* λ_3 *are determined numerically solving the system* (2.13) *with* $a_0 = 1$*,* $a_1 = 0$*,* $a_2 = \frac{1}{40} - \frac{12641}{512000}\epsilon$ *and* $a_3 = 0$*. In Table 3.2, we show the values of* λ_0*,* λ_1*,* λ_2 *and* λ_3 *and the corresponding domain* $[x_1, x_2]$ *for the following values of the perturbative parameter* $\epsilon \in \{0, 0.01, 0.1\}$*. The domain has been determined using the Bienaymé–Chebyshev inequality* $[\mu - k\sigma, \mu + k\sigma]$ *(in*

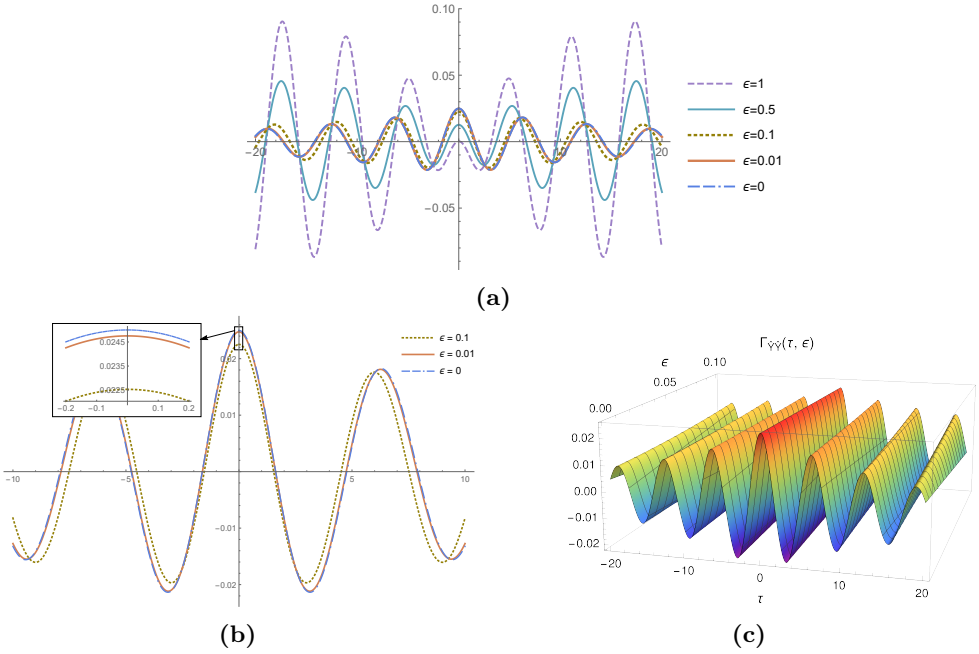

Figure 3.1: Correlation function $\Gamma_{\widehat{X}\widehat{X}}(\tau,\epsilon)$ of $\widehat{X}(t)$. (3.1a) and (3.1b): 2D-representation of $\Gamma_{\widehat{X}\widehat{X}}(\tau,\epsilon)$ for fixed values of ϵ. (3.1c): 3D-representation of $\Gamma_{\widehat{X}\widehat{X}}(\tau,\epsilon)$ for $\epsilon \in [0, 0.1]$. Example 3.1.

our case $\mu = 0$) with $k = 10$, see [19]. This guarantees the 99% of the probability is contained in the above interval $[\mu - k\sigma, \mu + k\sigma]$ regardless of the distribution of the corresponding random variable [19]. In Figure 3.2, we compare the graphical representations of the PDF, $f_{\widehat{X}(t)}(y)$. From them, we can observe that the plots are quite similar.

To complete our numerical analysis, in Figure 3.3 we show a graphical representation of the power spectral density for $\epsilon \in \{0, 0.01, 0.1\}$. We observe that the approximation obtained via the stochastic perturbation method is able to retain the properties of symmetry and positivity of the power spectral density for $\epsilon \in \{0, 0.01\}$, however, positivity begins to slightly fail for $\epsilon = 0.1$, therefore restricting the validity of the results provided by the stochastic perturbation method. In Table 3.3, the noise intensity ($\mathcal{D}$) and the correlation time ($\hat{\tau}$) have been calculated for $\epsilon \in \{0, 0.01\}$.

	$\epsilon = 0$	$\epsilon = 0.01$	$\epsilon = 0.1$
λ_0	-1.92550119	-1.93046362	-1.977491823
λ_1	$1.16917582 \cdot 10^{-8}$	$2.28178507 \cdot 10^{-8}$	$1.72829555 \cdot 10^{-10}$
λ_2	19.9999999	20.19948570	22.19159320
λ_3	$-8.23925883 \cdot 10^{-8}$	$-3.07272453 \cdot 10^{-7}$	$-5.17949495 \cdot 10^{-9}$
$[x_1, x_2]$	$[-1.581138, 1.581138]$	$[-1.573311, 1.573311]$	$[-1.501034, 1.501034]$

Table 3.2: Values for λ_i, $i \in \{0, 1, 2, 3\}$ and the domain $[x_1, x_2]$ obtained via the PME method, for $\epsilon \in \{0, 0.01, 0.1\}$. Example 3.1.

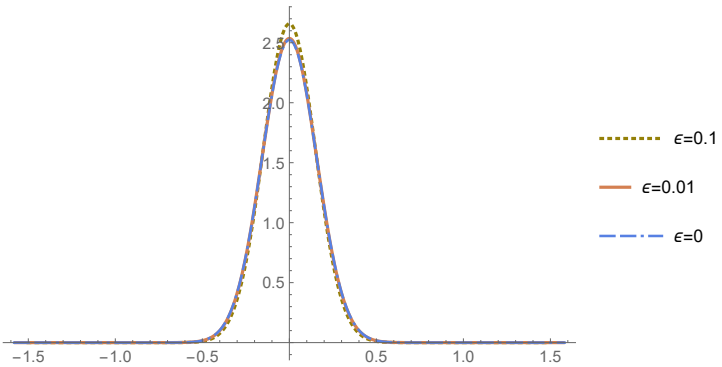

Figure 3.2: Approximate PDF, $f_{\widehat{X}(t)}(y)$, of steady-state, $\widehat{X}(t)$, for $\epsilon \in \{0, 0.01, 0.1\}$. Example 3.1.

Example 3.2 *In this second example, let us consider the Ornstein-Uhlenbeck stochastic process to play the role of the external source, $Y(t)$. As we have seen in Section 2.2, it is defined as the stationary solution of the Langevin equation*

$$\frac{\mathrm{d}Y(t)}{\mathrm{d}t} + \alpha Y(t) = \sigma \frac{\mathrm{d}W(t)}{\mathrm{d}t}, \quad \alpha > 0,$$

where $W(t)$ is the standard Wiener process [54]. Notice that $\alpha > 0$ is a necessary and sufficient condition for a stationary solution. $Y(t)$ satisfies the hypotheses so that the stochastic perturbation method can be applied, i.e., is a zero-mean stationary Gaussian stochastic process, being $\Gamma_{YY}(\tau) = \sigma^2 \, \mathrm{e}^{-\alpha|\tau|}$ its correlation function. We take the following values for the parameters in equation (3.2), $\omega_0 = 1$, $\beta = 1/100$, $\sigma = 1/100$ and $\alpha = 1/2$ (thus, it ensures the existence of the steady-state

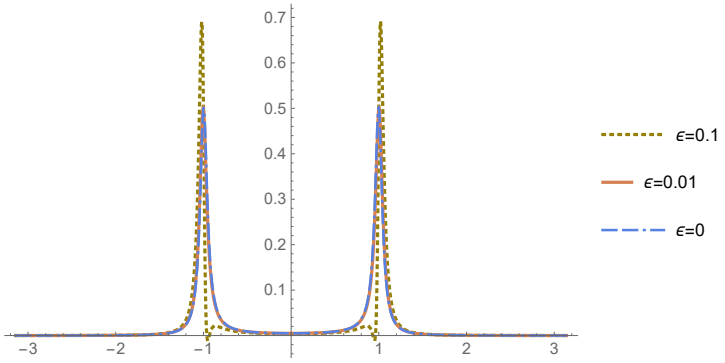

Figure 3.3: Power spectral density of the approximation solution $\widehat{X}(t)$, $S_{\widehat{X}(t)}(f)$, for $\epsilon \in \{0, 0.01, 0.1\}$. Example 3.1.

	$\epsilon = 0$	$\epsilon = 0.01$
$\mathcal{D}$	0.0025	0.00245062
$\hat{\tau}$	0.1	0.0990026

Table 3.3: Values for $\mathcal{D}$ and $\hat{\tau}$, defined in (3.43), for $\epsilon \in \{0, 0.01\}$. Example 3.1.

solution). So, in this case, the nonlinear random oscillator is given by

$$\ddot{X}(t) + \frac{1}{50}\dot{X}(t) + X(t) + \epsilon \sin(X(t)) = Y(t), \quad t > 0. \tag{3.46}$$

We will now apply the same steps as in Example 3.1 to obtain approximations of the main statistical functions of the approximate stochastic solution $\widehat{X}(t)$. First, we will determine the three first statistical moments. From expression (3.35), $\mathbb{E}\left[\widehat{X}(t)\right]$ *and* $\mathbb{E}\left[\widehat{X}^3(t)\right]$ *are null. For the second-order moment,* $\mathbb{E}\left[\widehat{X}^2(t)\right]$*, using the expression* (3.23) *we obtain*

$$\mathbb{E}\left[\widehat{X}^2(t)\right] = \frac{13}{6300} - \frac{465955883861}{126023688000000}\epsilon. \tag{3.47}$$

From this expression, we can obtain a rough bound for ϵ, since $\mathbb{E}\left[\widehat{X}^2(t)\right] > 0$*. In this case, $\epsilon < 0.558098$. To check that our second-order moment approximation is consistent, we will compare it with the random linear oscillator obtained when*

$\epsilon \to 0$ *[89, Example 7.2],*

$$\ddot{X}(t) + \frac{1}{50}\dot{X}(t) + X(t) = Y(t), \quad t > 0.$$

Notice that, according to (3.40)*, expression* (3.47) *is also the variance of* $\widehat{X}(t)$*,* $\mathbb{V}\left[\widehat{X}(t)\right]$*.*

In Figure 3.4, we can observe that for t *large enough (corresponding in the limit as* $t \to \infty$ *to the steady-state), the second-order moment of the random linear equation approaches to our approximation for* $\epsilon = 0$*. Observe in the plot that the* $\mathbb{E}\left[X^2(t)\right] \to 0.00206349 \approx \frac{13}{6300}$ *as* $t \to \infty$*, in accordance with* (3.47)*.*

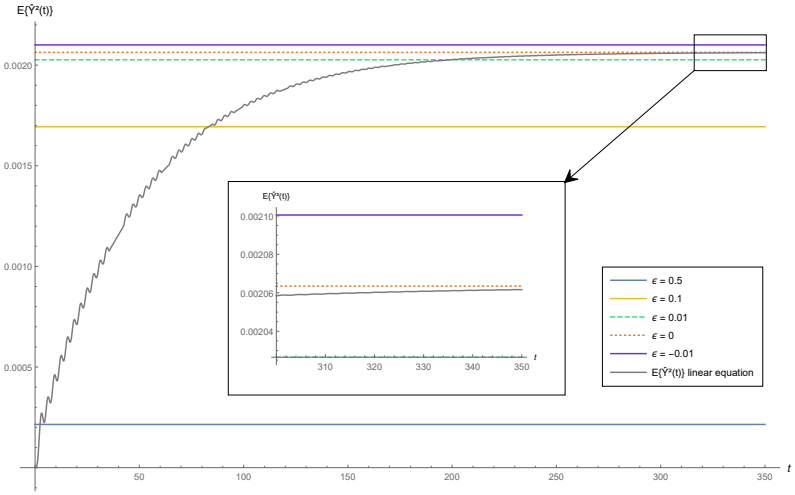

Figure 3.4: Comparison of second-order moments between linear and nonlinear random oscillator for small values of ϵ and t large (corresponding to the steady-state). Example 3.2.

Once we have obtained the mean, $\mathbb{E}\left[\widehat{X}(t)\right]$ *and the standard deviation,* $\sqrt{\mathbb{V}\left[\widehat{X}(t)\right]}$*, of* $\widehat{X}(t)$ *via the perturbation method, we compare them with the ones computed by Kloeden-Platen-Schurz algorithm. The results are shown in Table 3.4. We can observe that both approximations are accurate for* $\epsilon \in \{0, 0.01, 0.1\}$*, however, significant differences in the standard deviation are shown for* $\epsilon = 0.5$*, thus showing the perturbation method does not provide acceptable approximations.*

		Perturbation method	Kloeden-Platen-Schurz (1000 simulations)	Kloeden-Platen-Schurz (10000 simulations)
$\epsilon = 0$	Mean	0	-0.01267	-0.01283
	sd	0.04542	0.04422	0.04447
$\epsilon = 0.01$	Mean	0	0.00737	0.00725
	sd	0.04501	0.04437	0.04394
$\epsilon = 0.1$	Mean	0	-0.00265	-0.00222
	sd	0.04115	0.04081	0.04083
$\epsilon = 0.5$	Mean	0	-0.00626	-0.00643
	sd	0.01465	0.03234	0.03246

Table 3.4: Comparison of the mean and the standard deviation (sd) between the stochastic perturbation method and the Kloeden-Platen-Schurz algorithm for different values of ϵ. Example 3.2.

The approximation of the correlation function, $\Gamma_{\widehat{X}\widehat{X}}(\tau)$*, using* (3.36) *together with expressions* (3.37)–(3.39) *is given by*

$$\Gamma_{\widehat{X}\widehat{X}}(\tau) = \begin{cases} f_1(\tau), & \text{if } \tau < 0, \\ f_2(\tau), & \text{if } \tau > 0, \\ \dfrac{13}{6300} - \dfrac{465955883861}{126023688000000}\epsilon, & \text{if } \tau = 0, \end{cases} \tag{3.48}$$

where,

$$\begin{aligned} f_1(\tau) = &- \frac{\mathrm{e}^{\tau/100}}{298974181793219856000000} \Big(19286265625\,\mathrm{e}^{\frac{49\tau}{100}}(1585962845\epsilon \\ &-992186496) + \sqrt{1111}\sin\left(\frac{3\sqrt{1111}\tau}{100}\right)(317192569(28243342050\tau \\ &-3197833091)\epsilon + 466418810254320000) \\ &+1111\cos\left(\frac{3\sqrt{1111}\tau}{100}\right)(317192569(22036350\tau + 3050020523)\epsilon \\ &-538069558062960000))\,, \end{aligned}$$

and

$$
\begin{aligned}
f_2(\tau) =& \frac{\mathrm{e}^{-\frac{\tau}{2}}}{29897418179321985600000}\left(1111\cos\left(\frac{3\sqrt{1111}\tau}{100}\right)(317192569\right.\\
&\cdot(22036350\tau-3050020523)\epsilon+538069558062960000)\\
&+\mathrm{e}^{\frac{49\tau}{100}}\left(\sqrt{1111}\sin\left(\frac{3\sqrt{1111}\tau}{100}\right)(466418810254320000\right.\\
&-317192569(28243342050\tau+3197833091)\epsilon))\\
&\left.-19286265625(1585962845\epsilon-992186496)\right).
\end{aligned}
$$

Then, we can check that property (3.40) *holds.*

In Figure 3.5, we show the graphical representations of the correlation function, given by the expression (3.48)*, for different values of the perturbative parameter* ϵ*. First, in Figure 3.5a, we can observe that for* $\epsilon = 0.1$ *and* 0.2 *the property* $|\Gamma_{\widehat{X}\widehat{X}}(\tau)| \leq \Gamma_{\widehat{X}\widehat{X}}(0)$ *is not fulfilled, so showing the perturbations method does not provide reliable approximations for such values of* ϵ*. For the other values of* ϵ*, we have represented the correlation function (see Figure 3.5b). One observes that* $\Gamma_{\widehat{X}\widehat{X}}(\tau,\epsilon)$ *for* $\epsilon \in \{0, 0.01\}$ *are quite similar. Finally, in Figure 3.5c we show* $\Gamma_{\widehat{X}\widehat{X}}(\tau,\epsilon)$ *as a surface varying* $(\tau,\epsilon) \in [-20,20]\times[-0.01,0.01]$*.*

Now, we will obtain the approximation of the stationary PDF in the form $f_{\widehat{X}(t)}(x) = \mathrm{e}^{-1-\lambda_0-\lambda_1 x-\lambda_2 x^2-\lambda_3 x^3}$ *using the PME, taking* $N = 3$ *(see Section 2.6). The values of* λ_0*,* λ_1*,* λ_2 *and* λ_3 *are shown in Table 3.5 together with the domain* $[x_1, x_2]$ *for the following values of the perturbative parameter* $\epsilon \in \{0, 0.01, 0.1\}$*. As in Example 3.1, the intervals* $[x_1, x_2]$ *have been computed using the Bienaymé–Chebyshev inequality.*

In Figure 3.6, we compare the graphical representations of the PDF, $f_{\widehat{X}(t)}(x)$*. From them, we can observe that the approximations are very similar.*

To complete our numerical example, we have calculated graphical representations of the power spectral density, $S_{\widehat{X}(t)}(f)$*, of the* $\widehat{X}(t)$*. In Figure 3.7, we show two plots. Panel left corresponds to* $\epsilon \in \{0, 0.01\}$*, and panel right to* $\epsilon \in \{0, 0.001\}$*. We observe that the property of symmetry breaks down when* ϵ *increases while positivity is retained. In Table 3.6,* $\mathcal{D}$ *and* $\hat{\tau}$ *have been calculated for* $\epsilon \in \{0, 0.001\}$*.*

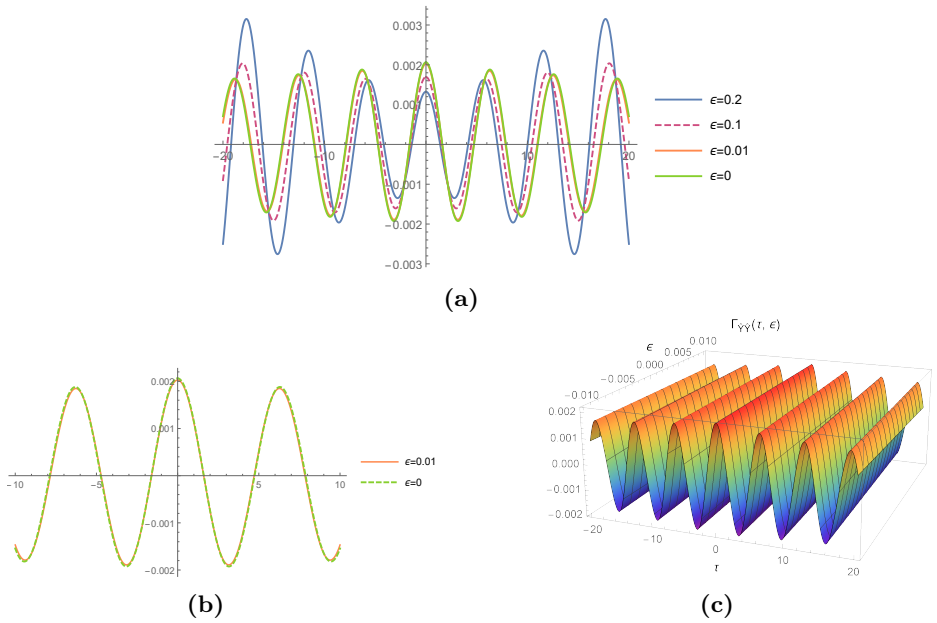

Figure 3.5: Correlation function $\Gamma_{\widehat{X}\widehat{X}}(\tau,\epsilon)$ of $\widehat{X}(t)$. (3.5a) and (3.5b): 2D-representation of $\Gamma_{\widehat{X}\widehat{X}}(\tau,\epsilon)$ for fixed values of ϵ. (3.5c): 3D-representation of $\Gamma_{\widehat{X}\widehat{X}}(\tau,\epsilon)$ for $\epsilon \in [-0.01, 0.01]$. Example 3.2.

3.4 Conclusions

In this chapter, we have studied a class of stochastic nonlinear oscillators whose restoring term is a transcendental function that depends only on the position. We have assumed that the oscillator is excited by a zero-mean stationary Gaussian process. Since the nonlinear term is affected by a small parameter, to conduct our probabilistic analysis, we have approximated the nonlinear term using Taylor's polynomial, and then we applied the stochastic perturbation method to obtain the main statistical moments of the stationary solution. After this theoretical analysis, we have carried out numerical examples where the stochastic excitation is driven by two important stochastic processes, the Gaussian white noise and the Ornstein-Uhlenbeck processes. Since a key point when applying the perturbation method is the accuracy of the approximations in terms of the size of the perturbative parameter, from the numerical results obtained in the two examples, we have

	$\epsilon = 0$	$\epsilon = 0.01$
λ_0	-3.17273924	-3.181779485
λ_1	$-1.282642481 \cdot 10^{-11}$	$2.017945566 \cdot 10^{-10}$
λ_2	$2.423076923 \cdot 10^{2}$	246.7285778
λ_3	$1.474799603 \cdot 10^{-9}$	$-2.2037993478 \cdot 10^{-8}$
$[x_1, x_2]$	$[-0.454256, 0.454256]$	$[-0.450168, 0.450168]$

Table 3.5: Values of λ_i, $i = \{0, 1, 2, 3\}$ and the domain $[x_1, x_2]$ obtained via PME, for $\epsilon = 0$ and 0.01. Example 3.2.

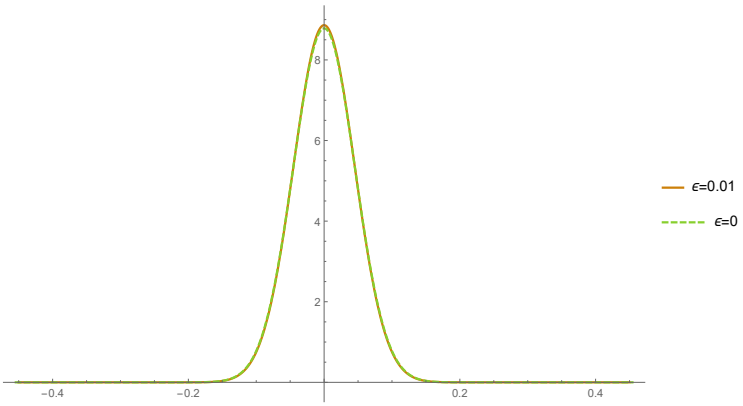

Figure 3.6: PDF of $\widehat{X}(t)$, $f_{\widehat{X}(t)}(x)$, for $\epsilon = 0$ and 0.01. Example 3.2.

performed a critical analysis checking whether some important general properties of the statistics associated to the stationary solution are correctly preserved. To better check the accuracy of the approximations of the mean and the standard deviation via the perturbation method, we have compared them with the ones calculated by means of an accurate numerical scheme, showing good agreement for certain sizes of the perturbative parameter. This comparative analysis includes the linear case obtained when the perturbative parameter is null. In this limit case, the results are also fully consistent. In summary, our study shows that, by means of a class of stochastic nonlinear oscillators, the double approximation Taylor-perturbation method is able to approximate the statistics of the stationary solution. Additionally, we have taken advantage of the above-computed statistics,

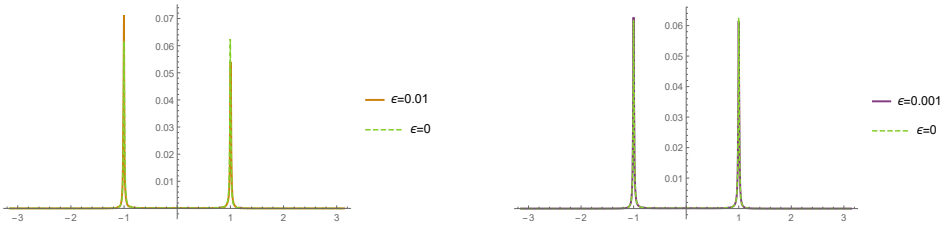

Figure 3.7: Power spectral density, $S_{\widehat{X}(t)}(f)$, of $\widehat{X}(t)$. Panel left: $\epsilon \in \{0, 0.01\}$. Panel right: $\epsilon \in \{0, 0.001\}$. Example 3.2.

	$\epsilon = 0$	$\epsilon = 0.001$
$\mathcal{D}$	0.0002	0.0001996
$\hat{\tau}$	0.0969231	0.0969031

Table 3.6: Values for $\mathcal{D}$ and $\hat{\tau}$, defined in (3.43), for $\epsilon \in \{0, 0.001\}$. Example 3.2.

in combination with the Principle of Maximum Entropy, to construct reliable approximations of the density of the steady-state. Our analysis has been performed with criticism with regard to the size of the perturbative parameter, as required when applying the stochastic perturbation method. Our approach can be useful to study other stochastic nonlinear oscillators whose small perturbations affect transcendental functions with the additional advantage of computing the density of the stationary solution.

Publications associated with this chapter

The results of this chapter have been presented at the International Symposium & International Student Workshop on Interdisciplinary Mathematics in the CiTi areas (ISIM & ISWIM) in Budapest (Romania) from June 27-30, 2023. The talk, titled *Probabilistic analysis of a random nonlinear oscillator via the random perturbation technique*, was published in the conference proceedings with ISSN-L 2821–8779. Additionally, a complete version of the chapter's findings has been published in the paper [25].

Chapter 4

Probabilistic analysis of random nonlinear oscillators subject to small perturbations in the restoring term depending on the position and velocity

In this chapter, we combine the stochastic perturbation method with the Principle of Maximum Entropy to construct approximations of the first probability density function of the steady-state solution of a class of nonlinear oscillators, whose restoring function, which depends on the position and velocity, is affected by small perturbations and driven by a stochastic excitation. The excitation is given by a stationary Gaussian stochastic process with certain additional properties. Furthermore, we approximate higher-order moments, the variance, and the correlation functions of the solution. The theoretical findings are illustrated via some numerical experiments that confirm that our approximations are reliable.

4.1 Introduction

When dealing with oscillators, the term $g(X(t))$ that appears in Eq. (3.1) may not only depend on position but may also depend on velocity. In this chapter, we address the study of random cross-nonlinear oscillators subject to small perturbations affecting the nonlinear term, g, which depend on both the position, $X(t)$, and the velocity, $\dot{X}(t)$,

$$\ddot{X}(t) + 2\zeta\omega_0\dot{X}(t) + \epsilon g(X(t), \dot{X}(t)) + \omega_0^2 X(t) = Y(t), \tag{4.1}$$

where $X(t)$ denotes the position of the oscillatory system at the time instant t, ζ is the damping constant, $\omega_0 > 0$ is the undamped angular frequency, and finally, ϵ is the small perturbation parameter.

Here, the stochastic derivatives are understood in the mean square sense [89, Ch. 4]. In our subsequent analysis, we will consider the case that $g(X(t), \dot{X}(t)) = X^2(t)\dot{X}(t)$, which corresponds to the most complicated scenario, sometimes called *cross-nonlinearity* [26, 23], and the excitation $Y(t)$ is a causal mean square differentiable and stationary zero-mean Gaussian stochastic process whose correlation function, $\Gamma_{YY}(\tau)$, is known. The intuitive and physical interpretations of these hypotheses have been explained in Section 3.1.

To the best of our knowledge, this is the first time that stochastic nonlinear oscillators with the above-described type of cross-nonlinearities is studied using our approach, i.e., combining mean square calculus and the stochastic perturbation method. In this sense, we think that our approach may be useful to extend our study to stochastic nonlinear oscillators having more general cross-nonlinearities, in particular of the form $g(X(t), \dot{X}(t)) = \sum_{n=1}^{N}\sum_{m=1}^{M} X^n(t)\dot{X}^m(t)$. This in turn, can be utilized for the case that the expression of $g(X(t), \dot{X}(t))$ is given by an analytic function of $X(t)$ and $\dot{X}(t)$, such that $g(0,0) = 0$, by representing it by means of the truncation of its Taylor expansion of order (N, M). For instance, this happens when $g(X(t), \dot{X}(t)) = \sin(X(t)\dot{X}(t))$.

The chapter is organized as follows. Section 4.2 is divided into two parts. In Subsection 4.2.1, we apply the perturbation technique to construct a first-order

approximation of the stationary solution stochastic process of model (4.1) with $g(X(t), \dot{X}(t)) = X^2(t)\dot{X}(t)$. In Subsection 4.2.2, we determine expressions for the first higher-order moments, the variance, the covariance and the correlation of the aforementioned first-order approximation. These expressions will be given in terms of certain integrals of the correlation function of the Gaussian noise, $Y(t)$, and of the classical impulse response function to the linearized oscillator associated with Eq. (4.1). In Section 4.3 we illustrate all theoretical findings by means of several illustrative examples. Our numerical results are compared with Monte Carlo simulations and with the application of the Euler-Maruyama numerical scheme, showing full agreement. Conclusions are drawn in Section 4.4.

4.2 Probabilistic model study

As it has been indicated in Section 4.1, in this chapter, we will study, from a probabilistic standpoint, the random cross-nonlinear oscillator

$$\ddot{X}(t) + 2\zeta\omega_0\dot{X}(t) + \epsilon X^2(t)\dot{X}(t) + \omega_0^2 X(t) = Y(t). \tag{4.2}$$

The analysis will be divided into two steps. First, in Subsection 4.2.1, we will apply the perturbation technique to obtain an approximation, $\widehat{X}(t)$, of the stationary solution stochastic process, $X(t)$. Then, in Subsection 4.2.2 we will take advantage of $\widehat{X}(t)$ to determine reliable approximations of the main statistical functions of $X(t)$, namely, the first higher-order moments, $\mathbb{E}\left[X^n(t)\right], n = 1, \ldots, 5$, the variance, $\mathbb{V}\left[X(t)\right]$, the covariance, $\mathbb{C}\mathrm{ov}\left[X(t_1), X(t_2)\right]$, and the correlation, $\Gamma_{XX}(\tau)$.

4.2.1 Stochastic perturbation expansion

Let us consider the Eq. (4.2). The main idea of the stochastic perturbation technique, as we have seen in Chapter 2, is to consider that the solution $X(t)$ can be expanded in the powers of the small parameter ϵ ($|\epsilon| \ll 1$),

$$X(t) = X_0(t) + \epsilon X_1(t) + \epsilon^2 X_2(t) + \cdots \tag{4.3}$$

Replacing expression (4.3) into Eq. (4.2), yields the following sequence of linear differential equations with random inputs

$$\begin{array}{lcll} \epsilon^0 & : & \ddot{X}_0(t) + 2\zeta\omega_0\dot{X}_0(t) + \omega_0^2 X_0(t) & = & Y(t), \\ \epsilon^1 & : & \ddot{X}_1(t) + 2\zeta\omega_0\dot{X}_1(t) + \omega_0^2 X_1(t) & = & -X_0^2(t)\dot{X}_0(t), \\ \epsilon^2 & : & \ddot{X}_2(t) + 2\zeta\omega_0\dot{X}_2(t) + \omega_0^2 X_2(t) & = & -2X_0(t)X_1(t)\dot{X}_0(t) - X_0^2(t)\dot{X}_1, \\ \vdots & \vdots & \vdots & \vdots & \vdots \end{array} \tag{4.4}$$

Notice that each equation can be solved in cascade. As usual, when applying the perturbation technique, we take the first-order approximation

$$\widehat{X}(t) = X_0(t) + \epsilon X_1(t). \tag{4.5}$$

This entails that in our subsequent development we will only need the two first equations listed in (4.4).

As indicated in Section 4.1, now we will focus on the analysis of the steady-state solution. Using the linear theory, the two first equations in (4.4) can be solved using the convolution integral [68]:

$$X_0(t) = \int_0^\infty h(s)Y(t-s)\,\mathrm{d}s, \tag{4.6}$$

and

$$X_1(t) = \int_0^\infty h(s)\left(-X_0^2(t-s)\dot{X}_0(t-s)\right)\mathrm{d}s, \tag{4.7}$$

where

$$h(t) = \begin{cases} \left(\omega_0^2 - \zeta^2\omega_0^2\right)^{-\frac{1}{2}} \mathrm{e}^{-\zeta\omega_0 t}\sin\left(\left(\omega_0^2 - \zeta^2\omega_0^2\right)^{\frac{1}{2}} t\right), & \text{if } t > 0, \\ 0, & \text{if } t \leq 0, \end{cases} \tag{4.8}$$

is the impulse response function for the underdamped case $\zeta^2 < 1$. This situation corresponds to the condition in which damping of an oscillator causes it to return to equilibrium with the amplitude gradually decreasing to zero (in our random setting, it means that the expectation of the amplitude is null); the system returns to equilibrium faster but overshoots and crosses the equilibrium position one or

more times. Although they are not treated hereinafter, two more situations are also possible, namely, critical damping and overdamping. The former corresponds to $\zeta^2 = 1$ and in that case the damping of an oscillator causes it to return as quickly as possible to its equilibrium position without oscillating back and forth about this position, while the latter corresponds to $\zeta^2 > 1$, and in this situation damping of an oscillator causes it to return to equilibrium without oscillating; oscillator moves more slowly toward equilibrium than in the critically damped system [91].

4.2.2 Constructing approximations of the main statistical moments of the stationary solution

This subsection is devoted to calculating the main probabilistic information of the stationary solution stochastic process, $X(t)$, of model (4.2). As it has been previously pointed out, to this end, we assume that the input term $Y(t)$ is a stationary zero-mean ($\mathbb{E}[Y(t)] = 0$) Gaussian stochastic process whose correlation function, $\Gamma_{YY}(\tau)$, is given. We will further assume that $Y(t)$ is mean square differentiable. This additional hypothesis will be apparent later. At this point, it is convenient to recall that for any stationary stochastic process, its correlation function is even, so $\Gamma_{YY}(\tau) = \Gamma_{YY}(-\tau)$, [89, p. 47]. This property will be extensively applied throughout our subsequent developments.

To compute the mean of the approximation, we first take the expectation operator in (4.5),

$$\mathbb{E}\left[\widehat{X}(t)\right] = \mathbb{E}[X_0(t)] + \epsilon\mathbb{E}[X_1(t)]\,. \tag{4.9}$$

So, we now need to determine both $\mathbb{E}[X_0(t)]$ and $\mathbb{E}[X_1(t)]$. To compute the $\mathbb{E}[X_0(t)]$, we again use the expectation operator in (4.6),

$$\mathbb{E}[X_0(t)] = \mathbb{E}\left[\int_0^\infty h(s)Y(t-s)\,\mathrm{d}s\right] = \int_0^\infty h(s)\mathbb{E}[Y(t-s)]\,\mathrm{d}s = 0, \tag{4.10}$$

where we have applied Prop. 2.4 and that $\mathbb{E}[Y(t)] = 0$.

Now, we deal with the computation of $\mathbb{E}\left[X_1(t)\right]$ in an analogous manner but using the representation of $X_1(t)$ given in (4.7),

$$\begin{aligned}\mathbb{E}\left[X_1(t)\right] &= \mathbb{E}\left[\int_0^\infty h(s)\left(-X_0^2(t-s)\dot{X}_0(t-s)\right)\mathrm{d}s\right] \\ &= \int_0^\infty h(s)\mathbb{E}\left[-X_0^2(t-s)\dot{X}_0(t-s)\right]\mathrm{d}s \\ &= -\int_0^\infty h(s)\int_0^\infty h(s_1)\int_0^\infty h(s_2)\int_0^\infty h(s_3)\mathbb{E}\left[Y(t-s-s_1)\right. \\ &\quad \left.\cdot Y(t-s-s_2)\dot{Y}(t-s-s_3)\right]\mathrm{d}s_3\,\mathrm{d}s_2\,\mathrm{d}s_1\,\mathrm{d}s \\ &= 0.\end{aligned} \tag{4.11}$$

Notice that the assumption of mean square differentiability of the input process $Y(t)$ appears naturally at this stage.

Let us justify the last step in expression (4.11). Let us denote $u_1 = t-s-s_1$, $u_2 = t-s-s_2$ and $u_3 = t-s-s_3$, then applying Prop. 2.3 and Prop. 2.1, both with $n=3$, one gets

$$\begin{aligned}\mathbb{E}\left[Y(t-s-s_1)Y(t-s-s_2)\dot{Y}(t-s-s_3)\right] &= \mathbb{E}\left[Y(u_1)Y(u_2)\dot{Y}(u_3)\right] \\ &= \frac{\partial}{\partial u_3}\mathbb{E}\left[Y(u_1)Y(u_2)Y(u_3)\right] = 0.\end{aligned}$$

So, substituting (4.10) and (4.11) into (4.9), we obtain the expectation of the approximation is null,

$$\mathbb{E}\left[\widehat{X}(t)\right] = \mathbb{E}\left[X_0(t)\right] + \epsilon\mathbb{E}\left[X_1(t)\right] = 0. \tag{4.12}$$

From the approximation (4.5) and neglecting the term ϵ^2, the second-order moment for $\widehat{X}(t)$ is given by

$$\mathbb{E}\left[\widehat{X}^2(t)\right] = \mathbb{E}\left[X_0^2(t)\right] + 2\epsilon\mathbb{E}\left[X_0(t)X_1(t)\right]. \tag{4.13}$$

The first addend can be calculated using expression (4.6) and Fubini's theorem,

$$\begin{aligned}\mathbb{E}\left[X_0^2(t)\right] &= \int_0^\infty h(s)\int_0^\infty h(s_1)\mathbb{E}\left[Y(t-s)Y(t-s_1)\right]\mathrm{d}s_1\,\mathrm{d}s \\ &= \int_0^\infty h(s)\int_0^\infty h(s_1)\Gamma_{YY}(s-s_1)\,\mathrm{d}s_1\,\mathrm{d}s\,.\end{aligned} \tag{4.14}$$

Notice that we have used that $Y(t)$ is a stationary process, so

$$\mathbb{E}\left[Y(t-s)Y(t-s_1)\right] = \Gamma_{YY}(t-s_1-(t-s)) = \Gamma_{YY}(s-s_1).$$

Now, we calculate the second addend in (4.13). To this end, we substitute the expressions of $X_0(t)$ and $X_1(t)$ given in (4.6) and (4.7), respectively,

$$\begin{aligned}
\mathbb{E}[\,X_0(t)X_1(t)] &= \int_0^\infty h(s)\mathbb{E}\left[X_0(t)\left(-X_0^2(t-s)\dot{X}_0(t-s)\right)\right]\mathrm{d}s \\
&= \int_0^\infty h(s)\mathbb{E}\left[-\int_0^\infty h(s_1)Y(t-s_1)\,\mathrm{d}s_1\int_0^\infty h(s_2)Y(t-s-s_2)\,\mathrm{d}s_2\right. \\
&\quad \left.\cdot\int_0^\infty h(s_3)Y(t-s-s_3)\,\mathrm{d}s_3\int_0^\infty h(s_4)\dot{Y}(t-s-s_4)\,\mathrm{d}s_4\right]\mathrm{d}s \\
&= -\int_0^\infty h(s)\int_0^\infty h(s_1)\int_0^\infty h(s_2)\int_0^\infty h(s_3)\int_0^\infty h(s_4)\mathbb{E}\left[Y(t-s_1)Y(t-s-s_2)\right. \\
&\quad \left.\cdot Y(t-s-s_3)\dot{Y}(t-s-s_4)\right]\mathrm{d}s_4\,\mathrm{d}s_3\,\mathrm{d}s_2\,\mathrm{d}s_1\,\mathrm{d}s \\
&\overset{\text{(I)}}{=} -\int_0^\infty h(s)\int_0^\infty h(s_1)\int_0^\infty h(s_2)\int_0^\infty h(s_3)\int_0^\infty h(s_4)\Big(\Gamma_{YY}(s_1-s-s_2)\Gamma'_{YY}(s_3-s_4) \\
&\quad +\Gamma_{YY}(s_1-s-s_3)\Gamma'_{YY}(s_2-s_4)+\Gamma'_{YY}(s_1-s-s_4)\Gamma_{YY}(s_2-s_3)\Big)\,\mathrm{d}s_4\,\mathrm{d}s_3\,\mathrm{d}s_2\,\mathrm{d}s_1\,\mathrm{d}s \\
&\overset{\text{(II)}}{=} -\int_0^\infty h(s)\int_0^\infty h(s_1)\int_0^\infty h(s_2)\int_0^\infty h(s_3)\int_0^\infty h(s_4)\Big(2\Gamma_{YY}(s_1-s-s_2)\Gamma'_{YY}(s_3-s_4) \\
&\quad +\Gamma'_{YY}(s_1-s-s_4)\Gamma_{YY}(s_2-s_3)\Big)\,\mathrm{d}s_4\,\mathrm{d}s_3\,\mathrm{d}s_2\,\mathrm{d}s_1\,\mathrm{d}s\,.
\end{aligned} \tag{4.15}$$

Observe that in step (I) of the above expression, we have first applied Prop. 2.3 and secondly Prop. 2.1–2.2. Indeed, let us denote by $u_1 = t - s_1$, $u_2 = t - s - s_2$,

$u_3 = t - s - s_3$ and $u_4 = t - s - s_4$, then by Prop. 2.3, with $n = 4$, one gets

$$\begin{aligned}\mathbb{E}\left[Y(t-s_1)Y(t-s-s_2)\ Y(t-s-s_3)\dot{Y}(t-s-s_4)\right] \\ = \frac{\partial}{\partial u_4}\mathbb{E}\left[Y(u_1)Y(u_2)Y(u_3)Y(u_4)\right],\end{aligned}$$

and now we apply Prop. 2.1–2.2, with $n = 4$, to the right-hand side. This yields,

$$\begin{aligned}&\mathbb{E}\left[\ Y(t-s_1)Y(t-s-s_2)Y(t-s-s_3)\dot{Y}(t-s-s_4)\right] = \\ &= \frac{\partial}{\partial u_4}\left(\mathbb{E}\left[Y(u_1)Y(u_2)\right]\mathbb{E}\left[Y(u_3)Y(u_4)\right] + \mathbb{E}\left[Y(u_1)Y(u_3)\right]\mathbb{E}\left[Y(u_2)Y(u_4)\right]\right. \\ &\quad \left.+\mathbb{E}\left[Y(u_1)Y(u_4)\right]\mathbb{E}\left[Y(u_2)Y(u_3)\right]\right) \\ &= \frac{\partial}{\partial u_4}\left(\Gamma_{YY}(u_2-u_1)\Gamma_{YY}(u_4-u_3) + \Gamma_{YY}(u_3-u_1)\Gamma_{YY}(u_4-u_2)\right. \\ &\quad \left.+\Gamma_{YY}(u_4-u_1)\Gamma_{YY}(u_3-u_2)\right) \\ &= \Gamma_{YY}(u)|_{u=s_1-s-s_2}\Gamma'_{YY}(u)|_{u=s_3-s_4} + \Gamma_{YY}(u)|_{u=s_1-s-s_3}\Gamma'_{YY}(u)|_{u=s_2-s_4} \\ &\quad + \Gamma'_{YY}(u)|_{u=s_1-s-s_4}\Gamma_{YY}(u)|_{u=s_2-s_3}.\end{aligned}$$

In step (II) of expression (4.15), we have taken advantage of the symmetry of the indexes.

Then, substituing (4.14) and (4.15) in (4.13) one gets,

$$\begin{aligned}\mathbb{E}\left[\widehat{X}^2(t)\right] &= \int_0^\infty h(s)\int_0^\infty h(s_1)\Gamma_{YY}(s-s_1)\,\mathrm{d}s_1\,\mathrm{d}s \\ &\quad - 2\epsilon\left(\int_0^\infty h(s)\int_0^\infty h(s_1)\int_0^\infty h(s_2)\int_0^\infty h(s_3)\int_0^\infty h(s_4)\right. \\ &\quad \cdot\Big(2\Gamma_{YY}(s_1-s-s_2)\Gamma'_{YY}(s_3-s_4) \\ &\quad \left.+\Gamma'_{YY}(s_1-s-s_4)\Gamma_{YY}(s_2-s_3)\Big)\,\mathrm{d}s_4\,\mathrm{d}s_3\,\mathrm{d}s_2\,\mathrm{d}s_1\,\mathrm{d}s\right).\end{aligned} \tag{4.16}$$

Notice that $\mathbb{E}\left[\widehat{X}^2(t)\right]$ does not depend on t. This is consistent with the fact that we are dealing with the stochastic analysis of the stationary solution. The same feature will hold when computing higher-order moments, $\mathbb{E}\left[\widehat{X}^n(t)\right]$, $n > 2$, later.

Since $\mathbb{E}\left[\widehat{X}(t)\right]$ is null (see (4.12)), then the variance of the solution coincides with $\mathbb{E}\left[\widehat{X}^2(t)\right]$.

Now, we calculate the third-order moment of $\widehat{X}(t)$ keeping up to the first-order term of perturbation ϵ. Therefore,

$$\mathbb{E}\left[\widehat{X}^3(t)\right] = \mathbb{E}\left[X_0^3(t)\right] + 3\epsilon\mathbb{E}\left[X_0^2(t)X_1(t)\right]. \tag{4.17}$$

Reasoning analogously as we have shown before, we obtain

$$\begin{aligned}\mathbb{E}\left[X_0^3(t)\right] &= \int_0^\infty h(s)\int_0^\infty h(s_1)\int_0^\infty h(s_2)\mathbb{E}\left[Y(t-s)Y(t-s_1)Y(t-s_2)\right]\mathrm{d}s_2\,\mathrm{d}s_1\,\mathrm{d}s\\ &= 0,\end{aligned} \tag{4.18}$$

where we have applied Prop. 2.1 in the last step.
The second addend in (4.17) is calculated using Prop. 2.3 and Prop. 2.1,

$$\begin{aligned}\mathbb{E}\left[X_0^2(t)X_1(t)\right] &= \int_0^\infty h(s)\mathbb{E}\left[X_0^2(t)\left(-X_0^2(t-s)\dot{X}_0(t-s)\right)\right]\mathrm{d}s\\ &= -\int_0^\infty h(s)\int_0^\infty h(s_1)\int_0^\infty h(s_2)\int_0^\infty h(s_3)\int_0^\infty h(s_4)\int_0^\infty h(s_5)\mathbb{E}\left[Y(t-s)\right.\\ &\quad\left.\cdot Y(t-s_1)Y(t-s-s_3)Y(t-s-s_4)\dot{Y}(t-s-s_5)\right]\mathrm{d}s_5\mathrm{d}s_4\mathrm{d}s_3\mathrm{d}s_2\mathrm{d}s_1\mathrm{d}s\\ &= 0.\end{aligned} \tag{4.19}$$

From (4.18) and (4.19), we obtain

$$\mathbb{E}\left[\widehat{X}^3(t)\right] = \mathbb{E}\left[X_0^3(t)\right] + 3\epsilon\mathbb{E}\left[X_0^2(t)X_1(t)\right] = 0.$$

Using again the first-order approximation of the perturbation ϵ, in general, it can be straightforwardly seen that

$$\mathbb{E}\left[\widehat{X}^n(t)\right] = 0, \qquad n = 1, 3, 5, \ldots. \tag{4.20}$$

Indeed, we know that,

$$\mathbb{E}\left[\widehat{X}^n(t)\right] = \mathbb{E}\left[X_0^n(t)\right] + n\,\epsilon\,\mathbb{E}\left[X_0^{n-1}(t)X_1(t)\right]. \tag{4.21}$$

On the one hand, let us observe that applying first Fubini's theorem and Prop. 2.4, and secondly Prop. 2.1 for n odd, one gets,

$$\begin{aligned}\mathbb{E}\left[X_0^n(t)\right] &= \mathbb{E}\left[\left(\int_0^\infty h(s)Y(t-s)\,\mathrm{d}s\right)^n\right] \\ &= \int_0^\infty h(s_1)\cdots\int_0^\infty h(s_n)\mathbb{E}\left[Y(t-s_1)\cdots Y(t-s_n)\right]\mathrm{d}s_n\cdots\mathrm{d}s_1 = 0.\end{aligned}$$

On the other hand, using the same reasoning as in (4.19),

$$\mathbb{E}\left[X_0^{n-1}(t)X_1(t)\right] = \int_0^\infty h(s)\mathbb{E}\left[X_0^{n-1}(t)\left(-X_0^2(t-s)\dot{X}_0(t-s)\right)\right]\mathrm{d}s = 0,$$

where first we have applied Prop. 2.3, to put the first derivative out of the expectation, and secondly, we have utilized that $X_0^{n-1}(t)$, $X_0^2(t-s)$ and $\dot{X}_0(t-s)$ depend upon $n-1$, 2 and 1 terms of $Y(\cdot)$, respectively, together with Prop. 2.1 (notice that $n+2$ is odd since n is odd).

To complete the information of statistical moments of the approximation, we also determine $\mathbb{E}\left[\widehat{X}^4(t)\right]$.

The fourth-order moment of $\widehat{X}(t)$, based on the first-order approximation via the perturbation method, is given by

$$\mathbb{E}\left[\widehat{X}^4(t)\right] = \mathbb{E}\left[X_0^4(t)\right] + 4\epsilon\mathbb{E}\left[X_0^3(t)X_1(t)\right]. \tag{4.22}$$

Reasoning analogously as we have shown in previous sections, we obtain for the first addend,

$$\mathbb{E}\left[X_0^4(t)\right] = 3\int_0^\infty h(s)\int_0^\infty h(s_1)\int_0^\infty h(s_2)\int_0^\infty h(s_3)\Gamma_{YY}(s-s_1)\Gamma_{YY}(s_2-s_3)\,\mathrm{d}s\,\mathrm{d}s_1\,\mathrm{d}s_2\,\mathrm{d}s_3, \tag{4.23}$$

and for the second addend,

$$\begin{aligned}
&\mathbb{E}\left[X_0^3(t)X_1(t)\right] \\
&\quad = -\int_0^\infty h(s)\int_0^\infty h(s_1)\int_0^\infty h(s_2)\int_0^\infty h(s_3)\int_0^\infty h(s_4)\int_0^\infty h(s_5)\int_0^\infty h(s_6)\mathbb{E}\left[Y(t-s_1)\right. \\
&\qquad \left.\cdot Y(t-s_2)Y(t-s_3)Y(t-s-s_4)Y(t-s-s_5)\dot{Y}(t-s-s_6)\right]\mathrm{d}s\,\mathrm{d}s_1\,\mathrm{d}s_2\,\mathrm{d}s_3\,\mathrm{d}s_4\,\mathrm{d}s_5\,\mathrm{d}s_6 \\
&\quad = -\int_0^\infty h(s)\int_0^\infty h(s_1)\int_0^\infty h(s_2)\int_0^\infty h(s_3)\int_0^\infty h(s_4)\int_0^\infty h(s_5)\int_0^\infty h(s_6)\Big(6\,\Gamma'_{YY}(s_5-s_6) \\
&\qquad \cdot\Gamma_{YY}(s_1-s_2)\Gamma_{YY}(s_3-s-s_4)+3\,\Gamma'_{YY}(s_1-s-s_6)\big(2\,\Gamma_{YY}(s_2-s-s_4)\Gamma_{YY}(s_3-s-s_5) \\
&\qquad +\Gamma_{YY}(s_2-s_3)\Gamma_{YY}(s_4-s_5)\big)\Big)\,\mathrm{d}s\,\mathrm{d}s_1\,\mathrm{d}s_2\,\mathrm{d}s_3\,\mathrm{d}s_4\,\mathrm{d}s_5\,\mathrm{d}s_6\,.
\end{aligned} \tag{4.24}$$

In the last step of the above expression, we first used Prop. 2.3, and secondly, Prop. 2.1–2.2. From this last proposition, we know that exist 15 combinations, but we can reduce the expression by the symmetry of involved indexes.

Now we deal with the approximation of the correlation function of $X(t)$ via (4.5), i.e., taking the first-order approximation of the perturbation expansion,

$$\begin{aligned}
\Gamma_{\widehat{X}\widehat{X}}(\tau) &= \mathbb{E}\left[\widehat{X}(t)\widehat{X}(t+\tau)\right] \\
&= \mathbb{E}\left[X_0(t)X_0(t+\tau)\right]+\epsilon\left(\mathbb{E}\left[X_0(t)X_1(t+\tau)\right]+\mathbb{E}\left[X_1(t)X_0(t+\tau)\right]\right).
\end{aligned} \tag{4.25}$$

The first addend in (4.25) corresponds to the correlation function of $X_0(t)$. It can be expressed as

$$\begin{aligned}
\mathbb{E}\left[X_0(t)X_0(t+\tau)\right] &= \int_0^\infty\int_0^\infty h(s)h(s_1)\mathbb{E}\left[Y(t-s)Y(t+\tau-s_1)\right]\mathrm{d}s\,\mathrm{d}s_1 \\
&= \int_0^\infty\int_0^\infty h(s)h(s_1)\Gamma_{YY}(\tau-s_1+s)\,\mathrm{d}s_1\,\mathrm{d}s\,.
\end{aligned}$$

The two last addends in (4.25) represent the cross-correlation of $X_0(t)$ and $X_1(t)$. They are given, respectively, by

$$\begin{aligned}\mathbb{E}\left[X_0(t)\ X_1(t+\tau)\right] &= \int_0^\infty h(s)\mathbb{E}\left[X_0(t)\left(-X_0^2(t+\tau-s)\dot{X}_0(t+\tau-s)\right)\right]\mathrm{d}s \\ &= -\int_0^\infty h(s)\int_0^\infty h(s_1)\int_0^\infty h(s_2)\int_0^\infty h(s_3)\int_0^\infty h(s_4)\ \big(2\,\Gamma_{YY}(\tau-s-s_2+s_1)\Gamma'_{YY}(s_3-s_4) \\ &\quad +\Gamma'_{YY}(\tau-s-s_4+s_1)\Gamma_{YY}(s_2-s_3)\big)\,\mathrm{d}s_4\,\mathrm{d}s_3\,\mathrm{d}s_2\,\mathrm{d}s_1\,\mathrm{d}s,\end{aligned}$$

and

$$\begin{aligned}\mathbb{E}\left[X_1(t)\ X_0(t+\tau)\right] &= \mathbb{E}\left[\int_0^\infty -h(s)X_0^2(t-s)\dot{X}_0(t-s)X_0(t+\tau)\right]\mathrm{d}s \\ &= -\int_0^\infty h(s)\int_0^\infty h(s_1)\int_0^\infty h(s_2)\int_0^\infty h(s_3)\int_0^\infty h(s_4) \\ &\quad \cdot\left(\Gamma_{YY}(s_1-s_2)\Gamma'_{YY}(\tau-s_4+s+s_3)\right. \\ &\quad \left.+2\,\Gamma'_{YY}(s_1-s_3)\Gamma_{YY}(\tau-s_4+s+s_2)\right)\mathrm{d}s_4\,\mathrm{d}s_3\,\mathrm{d}s_2\,\mathrm{d}s_1\,\mathrm{d}s\,.\end{aligned}$$

Summarizing,

$$\begin{aligned}\Gamma_{\widehat{X}\widehat{X}}(\tau) &= \int_0^\infty\int_0^\infty h(s)h(s_1)\Gamma_{YY}(\tau-s_1+s)\,\mathrm{d}s\,\mathrm{d}s_1 \\ &\quad -\epsilon\int_0^\infty h(s)\int_0^\infty h(s_1)\int_0^\infty h(s_2)\int_0^\infty h(s_3)\int_0^\infty h(s_4)(2\,\Gamma_{YY}(\tau-s-s_2+s_1)\Gamma'_{YY}(s_3-s_4) \\ &\quad +\Gamma'_{YY}(\tau-s-s_4+s_1)\Gamma_{YY}(s_2-s_3)+\Gamma_{YY}(s_1-s_2)\Gamma'_{YY}(\tau-s_4+s+s_3) \\ &\quad +2\,\Gamma'_{YY}(s_1-s_3)\Gamma_{YY}(\tau-s_4+s+s_2))\,\mathrm{d}s_4\,\mathrm{d}s_3\,\mathrm{d}s_2\,\mathrm{d}s_1\,\mathrm{d}s\,.\end{aligned} \tag{4.26}$$

Since $\mathbb{E}\left[\widehat{X}(t)\right]=0$, we observe that the covariance and correlation functions of $\widehat{X}(t)$ coincide,

$$\mathbb{C}\mathrm{ov}\left[\widehat{X}(t_1),\widehat{X}(t_2)\right]=\Gamma_{\widehat{X}\widehat{X}}(\tau),\ \ \tau=|t_1-t_2|.$$

Remark 4.1 *The hypothesis that $Y(t)$ is mean square differentiable can be removed, rewriting the Eq.* (4.6) *in the following way*

$$X(t) = \int_0^\infty h(s)Y(t-s)\mathrm{d}s = \int_{-\infty}^t h(t-s)Y(s)\mathrm{d}s, \tag{4.27}$$

where $h(\cdot)$ is defined in Eq. (4.8)*. Indeed, applying Leibniz's rule (see Prop. 2.6), which is also valid when the partial derivative exists almost everywhere and does not require that it be continuous [99], one gets*

$$\dot{X}(t) = h(0)Y(t) + \int_{-\infty}^t h'(t-s)Y(s)\mathrm{d}s = \int_{-\infty}^t h'(t-s)Y(s)\mathrm{d}s, \tag{4.28}$$

since $h(0) = 0$ (see (4.8)*). In this way, we do not require assuming the mean square differentiability of $Y(t)$. This fact shall be illustrated in the Example 4.2 exhibited in the next section, where $Y(t)$ is chosen as a Gaussian white noise.*

4.3 Numerical examples

This section is devoted to illustrating the theoretical findings obtained in previous sections. We take the following data for the parameters of the random nonlinear oscillator (4.2), $\zeta = 0.05$ ($\zeta^2 < 1$) and $\omega_0 = 1$.

Example 4.1 *Let us consider as input excitation the causal trigonometric stochastic process defined by $Y(t) = \xi_1\cos(t) + \xi_2\sin(t)$, $t \geq 0$, where $\xi_1, \xi_2 \sim \mathrm{N}(0,1)$ are independent. Observe that $Y(t)$ satisfies the hypotheses, i.e., $\mathbb{E}[Y(t)] = 0$, $Y(t)$ is Gaussian, mean square differentiable w.r.t. t and stationary, being its correlation $\Gamma_{YY}(t_1,t_2) = \cos(t_1-t_2)$ or $\Gamma_{YY}(\tau) = \cos(\tau)$. Substituting this data into Eq.* (4.2)*, we obtain,*

$$\ddot{X}(t)+0.1\dot{X}(t)+\epsilon X^2(t)\dot{X}(t)+X(t) = \xi_1\cos(t)+\xi_2\sin(t),\ \xi_1,\xi_2 \sim \mathrm{N}(0,1). \tag{4.29}$$

Now we shall obtain approximations to the first moments, $\mathbb{E}\left[\widehat{X}^i(t)\right], i = 1,\ldots,5$, the correlation function and the variance, $\mathbb{V}\left[\widehat{X}(t)\right]$, of the approximate solution $\widehat{X}(t)$ of random nonlinear oscillator (4.29)*.*

As we have seen in the expression (4.20)*, the moments of odd order are null, so, in this case,* $\mathbb{E}\left[\widehat{X}(t)\right] = \mathbb{E}\left[\widehat{X}^3(t)\right] = \mathbb{E}\left[\widehat{X}^5(t)\right] = 0$*. Now, we sequentially deduce some bounds for the perturbation parameter* ϵ *using the positiveness of even order moments, i.e.,* $\mathbb{E}\left[\widehat{X}^2(t)\right] > 0$ *and* $\mathbb{E}\left[\widehat{X}^4(t)\right] > 0$*. First, it is easy to check that, using expression* (4.16)*, the second-order moment is given by*

$$\mathbb{E}\left[\widehat{X}^2(t)\right] = 100 - 200000\epsilon, \tag{4.30}$$

so we obtain the bound $\epsilon < 0.0005$*. Since* $\mathbb{E}\left[\widehat{X}(t)\right] = 0$*, observe that the variance of the first-order approximation is given by* (4.30)*. Secondly, using expressions* (4.22)–(4.24)*,*

$$\mathbb{E}\left[\widehat{X}^4(t)\right] = 30000 - \frac{1153800000000}{6409}\epsilon. \tag{4.31}$$

This provides a stronger bound, $\epsilon < 0.000166641$*.*
Now, applying (4.26)*, we obtain the following approximation of the correlation function*

$$\Gamma_{\widehat{X}\widehat{X}}(\tau) = 100(1 - 2000\epsilon)\cos(\tau). \tag{4.32}$$

In Figure 4.1 we show the graphical representation of the correlation function, $\Gamma_{\widehat{X}\widehat{X}}(\tau)$*, given in the expression* (4.32) *for different values of* ϵ*. The higher the perturbation* ϵ*, the lower the variability. This graphical behavior fully agrees with the physical interpretation of the oscillator dynamics. Indeed, let us rewrite Eq.* (4.29) *as follows*

$$\ddot{X}(t) + (0.1 + \epsilon X^2(t))\dot{X}(t) + X(t) = \xi_1\cos(t) + \xi_2\sin(t).$$

As $\epsilon > 0$ *increases, the damped coefficient* $0.1 + \epsilon X^2(t)$ *does, so the mechanical system reduces its oscillations. It should be noted that* $\epsilon = 0.0004$ *only satisfies the first bound (*$\epsilon < 0.0005$*); however, we can observe that the corresponding approximation preserves the symmetry of the correlation function. This might be due to the sample regularity of the random excitation,* $Y(t)$*, which is differentiable.*

For the approximation of the stationary PDF, $f_{\widehat{X}(t)}(x)$*, we apply the results exhibited in Section 2.6 based on PME by taking* $N = 5$ *and* $\epsilon = 0.00005$*, which satisfies*

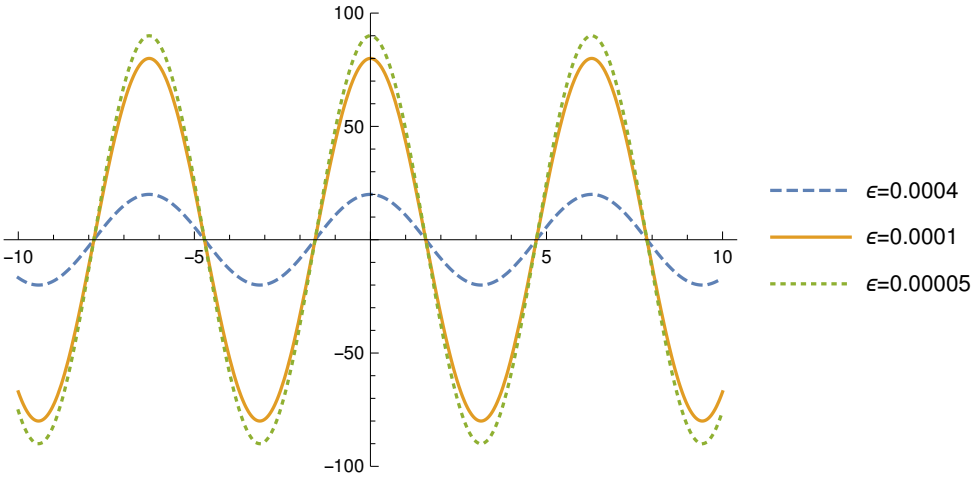

Figure 4.1: Correlation function $\Gamma_{\widehat{X}\widehat{X}}(\tau)$ of $X(t)$ for different values of ϵ. Example 4.1.

the stronger bound previously determined ($\epsilon < 0.000166641$). We first compute the approximation based on the three first moments

$$f_{\widehat{X}(t)}(x) = \mathrm{e}^{-1-2.181+1.045\cdot 10^{-5}x-0.005x^2-4.9217\cdot 10^{-8}x^3},$$

and, secondly, the approximation based on the five first moments

$$f_{\widehat{X}(t)}(x) = \mathrm{e}^{-1-2.243+2.552\cdot 10^{-8}x-0.004x^2-2.177\cdot 10^{-9}x^3-3.789\cdot 10^{-6}x^4+6.754\cdot 10^{-13}x^5}.$$

In Figure 4.2, we compare both graphical representations. From them, we can observe that both plots are quite similar, proving that computations are consistent.

Finally, to check that our approximations are reliable, we compare the mean and standard deviation of the approximate solution obtained via the perturbation method against the ones calculated by Monte Carlo. The results are collected in Table 4.1. We can observe that both approximations agree.

Example 4.2 *To previously perform our theoretical analysis, we have required the stationary Gaussian stochastic excitation $Y(t)$ be differentiable in the mean square sense (or equivalently, its correlation function, $\Gamma_Y(\tau)$, be twice differentiable in the*

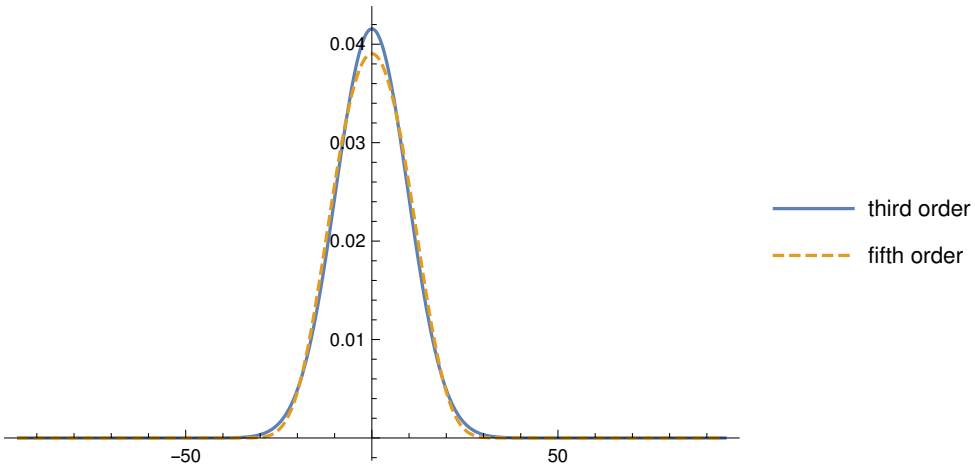

Figure 4.2: Approximation of PDF, $f_{\widehat{X}(t)}(x)$, using until the third and the fifth order moment for $\epsilon = 0.00005$ via the PME. Example 4.1.

	Perturbation method	Monte Carlo (1000 simulations)	Monte Carlo (10000 simulations)
Mean	0	0.188808	-0.114379
Standard deviation	9.48714	9.31356	9.49534

Table 4.1: Comparison between perturbation method and Monte Carlo simulations using $\epsilon = 0.00005$. Example 4.1.

ordinary sense at $\tau = 0$ [89, Ch. 4]), so having differentiable sample trajectories [94]. If we carefully revise our previous development, we can notice this is a hypothesis coming from the fact the nonlinearity cross-term depends upon $\dot{X}(t)$. However, as it has been explained in Remark 4.1, the hypothesis of mean square differentiability of $Y(t)$ can be removed. This example is devised to illustrate this fact by choosing $Y(t) = \xi(t)$, a Gaussian white noise process with zero-mean and correlation function $\Gamma_{YY}(\tau) = \frac{1}{2}W\delta(\tau)$, where $\delta(\tau)$ is the Dirac delta function and W is the noise power. In this example, we take $W = \frac{1}{100}$. This type of random noise has been extensively used in the literature since earliest contributions [26]. Observe that $Y(t) = \xi(t)$ is a stationary zero-mean Gaussian process but is not mean square differentiable (since its correlation function, given by the Dirac delta

function, is not differentiable) and, consequently, its sample trajectories are not differentiable either. In this case, Eq. (4.2) *becomes*

$$\ddot{X}(t) + 0.1\dot{X}(t) + \epsilon X^2(t)\dot{X}(t) + X(t) = \xi(t). \tag{4.33}$$

As in the previous example, we are going to obtain approximations to the five first moments, $\mathbb{E}\left[\widehat{X}^i(t)\right]$, $i = 1, \ldots, 5$, *the correlation function and the variance,* $\mathbb{V}\left[\widehat{X}(t)\right]$, *of the approximate solution* $\widehat{X}(t)$ *of Eq.* (4.33). *To implement the corresponding formulas derived throughout Subsection 4.2.2 saving computational time in Mathematica®, we have taken into account the following properties of the Dirac delta function,*

$$\int_{-\infty}^{\infty} h(t)\delta(t-s)\,\mathrm{d}t = h(s), \quad \int_{-\infty}^{\infty} h(t)\delta'(t-s)\,\mathrm{d}t = -h'(s).$$

As mentioned in Example 4.1, the moments of odd order are null, and using the positiveness of even order moments, we can obtain some bounds for the perturbation parameter ϵ. *First, using expression* (4.16), *the second-order moment is determined by*

$$\mathbb{E}\left[\widehat{X}^2(t)\right] = \frac{1}{40} - \frac{\epsilon}{160}, \tag{4.34}$$

so we obtain the bound $\epsilon < 4$. *Since* $\mathbb{E}\{\widehat{X}(t)\} = 0$, *expression* (4.34) *is also the variance of the first-order approximation. Secondly, using expression* (4.22)–(4.24),

$$\mathbb{E}\left[\widehat{X}^4(t)\right] = \frac{3}{1600} - \frac{759}{644800}\epsilon. \tag{4.35}$$

This provides a stronger bound, $\epsilon < 1.59289$.

Now, applying (4.26), *we obtain the following approximation of the correlation function,*

$$\Gamma_{\widehat{X}\widehat{X}}(\tau) = \begin{cases} f_1(\tau), & \text{if } \tau \geq 0, \\ \\ f_2(\tau), & \text{if } \tau < 0, \end{cases} \tag{4.36}$$

where

$$f_1(\tau) = \frac{\mathrm{e}^{-\tau/20}\left(-399\,(-399+5\epsilon\tau)\cos\left(\frac{\sqrt{399}\tau}{20}\right)+\sqrt{399}(399+100\epsilon)\sin\left(\frac{\sqrt{399}\tau}{20}\right)\right)}{6368040},$$

and

$$f_2(\tau) = \frac{\mathrm{e}^{\tau/20}\left(-399(-399+5\epsilon\tau)\cos\left(\frac{\sqrt{399}\tau}{20}\right)+\sqrt{399}(-399+100\epsilon)\sin\left(\frac{\sqrt{399}\tau}{20}\right)\right)}{6368040}.$$

In Figure 4.3, we show the plot of the correlation function, $\Gamma_{\widehat{X}\widehat{X}}(\tau)$, given in the expression (4.36)*, for different values of ϵ satisfying the weaker and the stronger bounds previously determined. We can observe that for smaller values of ϵ the obtained approximation of the correlation function better preserves the symmetry as expected.*

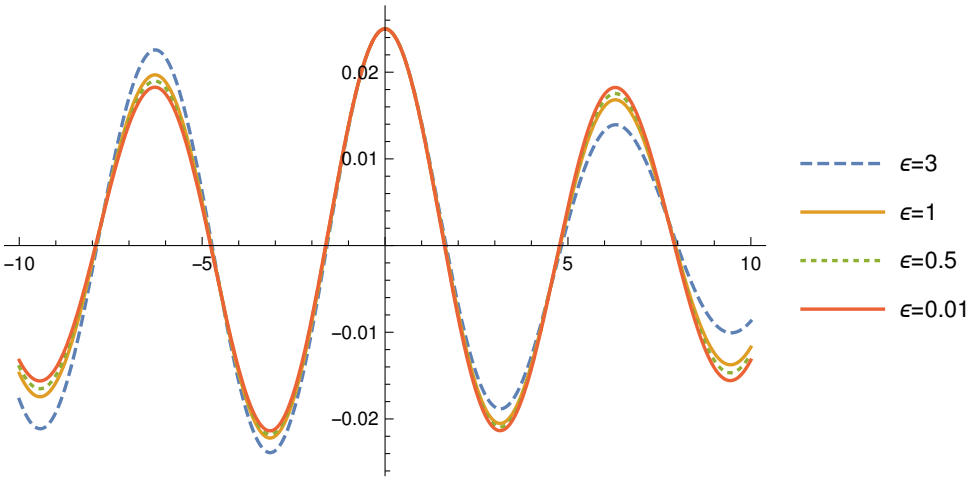

Figure 4.3: Correlation function $\Gamma_{\widehat{X}\widehat{X}}(\tau)$ of $X(t)$ for different values of ϵ. Example 4.2.

Applying the results presented in Section 2.6 taking $N = 5$, we obtain the approximation of the PDF, $f_{\widehat{X}(t)}(x)$, for $\epsilon = 0.5$, which satisfies the stronger bound 1.59289*. We first compute the approximation based on the three first moments*

$$f_{\widehat{X}(t)}(x) = \mathrm{e}^{-1+1.992+1.438\cdot10^{-8}x-22.857x^2-2.197\cdot10^{-7}x^3},$$

and, secondly, the approximation based on the five first moments

$$f_{\widehat{X}(t)}(x) = \mathrm{e}^{-1+1.940-5.226\cdot 10^{-11}x-17.837x^2+1.580\cdot 10^{-9}x^3-42.679x^4-7.904\cdot 10^{-9}x^5}.$$

In Figure 4.4, we compare both graphical representations. We can observe, again, the similarity between them, thus showing full agreement in our numerical computations.

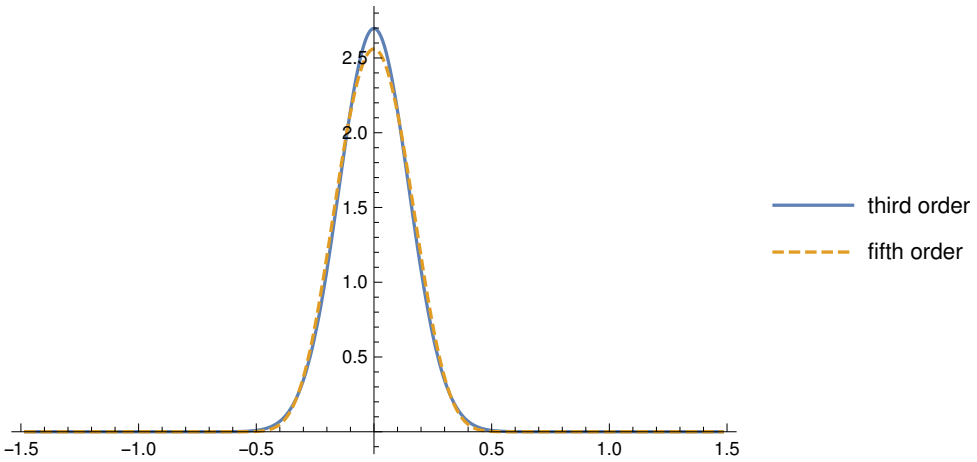

Figure 4.4: Approximation of PDF, $f_{\widehat{X}(t)}(x)$, using until the third and the fifth order moment for $\epsilon = 0.5$ via the PME. Example 4.2.

Finally, to check that our approximations are accurate, we compare the mean and standard deviation of $\widehat{X}(t)$ obtained via the perturbation method against the ones computed by Kloeden-Platen-Schurz numerical scheme [54]. The results are shown in Table 4.2. We can observe that both approximations are similar.

4.4 Conclusions

In this chapter, we have studied, from a probabilistic standpoint, a family of oscillators subject to small perturbations on the nonlinear term that depends both upon the position and the velocity (cross-nonlinearity) and whose forcing source is driven by a mean square differentiable stationary zero-mean Gaussian process. Nevertheless, we have seen that the hypothesis of mean square differentiability

	Perturbation method	Euler-Maruyama (1000 simulations)	Euler-Maruyama (10000 simulations)
Mean	0	0.000281162	-0.0000170694
Standard deviation	0.147902	0.149143	0.149929

Table 4.2: Comparison between perturbation method and Kloeden-Platen-Schurz simulations using $\epsilon = 0.5$. Example 4.2.

of the forcing term can be removed. This latter result has been illustrated by taking the white noise process playing the role of external excitation. On the other hand, we must point out that most contributions dealing with this type of stochastic oscillator focus on the computation of the mean, the variance, and the correlation function. Our main contribution is the computation of reliable approximations of the probability density function of the stationary solution by combining the stochastic perturbation method and the principle of maximum entropy. In this manner, we provide a fuller probabilistic description of the solution since, from the density, one can determine any one-dimensional moment and further probabilistic information of the steady-state. As explained at the end of Section 4.1, the proposed approach can be very useful to open new avenues in the analysis to other kinds of nonlinear oscillators subject to small fluctuations and whose forcing term is a polynomial stochastic process in the position and the velocity or, more generally, an analytical stochastic process that satisfies certain hypotheses.

Publications associated with this chapter

The results of this chapter have been presented at the Mathematical Modelling in Engineering & Human Behaviour 2020 Conference in Valencia (Spain) from July 8-10, 2020. The talk, titled *Analysing nonlinear oscillators subject to Gaussian inputs via the random perturbation technique*, was published in the conference proceedings with ISBN 978-84-09-25132-2. Additionally, a complete version of the chapter's findings has been published in the paper [23].

Chapter 5

Probabilistic analysis of the Euler-Bernoulli model for a static cantilever beam subjected to random loads via probability density functions

This chapter addresses the probabilistic analysis of the deflection of a static cantilever beam by randomizing the classical governing fourth-order differential equation (Euler-Bernoulli model) with null boundary conditions. The probabilistic study is based on the calculation of the first probability density function of the solution, which is a stochastic process, as well as the density function of further quantities of interest associated with this engineering problem such as the maximum slope and deflection at the free end of the cantilever beam, that are treated as random variables. In addition, the probability density function of the bending moment and the shear force will also be computed. The study takes extensive advantage of the so-called random variable transformation method, which allows us to fully unify the probabilistic analysis in three relevant cases commonly studied in the deterministic setting. All the theoretical findings are illustrated via detailed numerical examples corresponding to each one of the three scenarios.

5.1 Introduction

As it has been indicated in Chapter 1, the deflection of a beam subject to different loads can be described by means of the general model given in Eq. 1.2. More specifically, for the case of a static deflection cantilever beam with the flexural rigidity (Ei) constant, the aforementioned model writes [75, Entry 3 of Table 2.4]

$$\frac{\mathrm{d}^4 Y(x)}{\mathrm{d}x^4} = \frac{1}{Ei} Q(x), \quad 0 < x < l, \tag{5.1}$$

with boundary conditions

$$Y(0) = 0, \;\; Y'(0) = 0, \;\; Y''(l) = 0, \;\; Y'''(l) = 0. \tag{5.2}$$

Recall that, here, $Y(x)$ represents the deflection curve of the beam, E is the Young's modulus of elasticity of the material of the beam, i denotes the moment of inertia of the cross-section of the beam around a horizontal line through the centroid of the cross-section, l is the length of the beam and $Q(x)$ represents the density of downward force acting vertically on the beam at the spatial point x, which can be interpreted as load per unit length acting on the beam.

Despite model (5.1)–(5.2) is usually applied to assume a deterministic (nominal) value for the Young's modulus, E, it depends on the physical material properties with which the beam has been built. Due to the heterogeneity of the material, the mathematical nature of the Young's modulus is random rather than deterministic as it has been reported in different investigations [51, 90, 44, 36]. On the other hand, the nature of $Q(x)$ is also stochastic since, as it has been previously indicated, represents the density of downward force acting perpendicularly on the beam. At every spatial point x, the value of $Q(x)$ will depend on the heterogeneity of the material carried on the beam. Additionally, in practice, the value of $Q(x)$ on the whole spatial domain is approximated via measurements, so it contains epistemic errors. All these considerations lead to rigorously treating (5.1) as a random differential equation, where E is a random variable and $Q(x)$ is a stochastic process defined in a common complete probability space $(\Omega, \mathcal{F}, \mathbb{P})$. As it shall be seen later, we will assume that E is an absolutely continuous random variable, so having a PDF, while for $Q(x)$ we will consider both the case that is a parametric

stochastic process, which depends on absolutely continuous random variables, and when it is a non-parametric process.

We point out that throughout the chapter, and following the standard notation in Probability Theory, we will distinguish random variables and their realizations (which are deterministic quantities) by using capital and lowercase letters in the notation, respectively.

Under our approach, the solution of the randomized boundary problem (5.1)–(5.2) is a stochastic process, $Y(x)$, and our goal will be to determine, under very general assumptions on the model parameters, E and $Q(x)$, the so-called 1-PDF of the solution, $f_{Y(x)}(y)$ [89, Ch. 3]. As we have seen in Chapter 2, obtaining the 1-PDF permits determining all the one-dimensional moments, provided they exist, and the probability that the solution lies within a certain interval of specific interest. In the stochastic analysis of civil engineering structures, this information is of paramount importance since it permits the evaluation of the probability of breaking a structure (like a bridge, a balcony, a crane, etc.) that is carrying on distributed or uniform forces. Indeed, this is done by calculating the probability that the deflection of a beam lies within a certain *safety* interval.

Throughout this chapter, we will obtain an explicit expression of the 1-PDF, $f_{Y(x)}(y)$, of the random boundary problem (5.1)–(5.2) by considering different forms of the density downward force, $Q(x)$. The key tool that will be applied to conduct our probabilistic analysis is the RVT method, see Theorem 2.1.

As it shall be seen later, to apply this useful probabilistic result, first, we will take advantage of the Laplace transform to explicitly obtain a solution of model (5.1)–(5.2) for three different forms of $Q(x)$, hereinafter identified with Cases I-III, that are often considered in the analysis of beams in civil engineering.

The analysis of a cantilever beam has been extensively faced, mainly in the deterministic context (see, for example, [79, 108, 56]). In the stochastic setting, the number of contributions is still limited with regard to the specific study of a cantilever beam, although many other types of engineering structures have been studied taking into account uncertainties. Next, we will concentrate on commenting on the three main approaches, namely, polynomial chaos expansions,

Monte Carlo simulation, and stochastic finite elements method, that have been applied to analyse a cantilever beam subject to randomness. The next discussion is presented in connection with the study performed throughout this chapter. In [76], one combines polynomial chaos with the Neumann expansion method to obtain closed-form expressions for the first two response moments in different engineering problems. The authors apply the theoretical results obtained to analyze a cantilever beam, where the bending rigidity of the beam, EI, is assumed to be a stationary Gaussian random field with an exponential-type autocovariance kernel. In [78], it is assumed that all parameters of the classical Euler-Bernoulli cantilever beam are random variables. The study is performed in the case of a single load with constant (deterministic) value W. In that paper, one also studies the case that the Young's modulus is a discrete random field modelled first via simple random walk with stationary independent increments and, secondly, via an adapted autoregressive model with Gaussian distributed random variables. In both cases, authors use Monte Carlo simulations to numerically compute the distribution of the maximum deflection of a cantilever beam. In [55], authors compare stochastic and data-driven finite element methods to study a cantilever by assuming that the Young's modulus is modelled via the fluctuation of a nominal (mean) value using a standard Gaussian random variable. In [10], the multilevel Monte Carlo is combined with a finite element solver to compute the statistical quantities of the static deflection and frequency response function for a cantilever beam with uncertainty in Young's modulus under a static and a dynamic load. The authors show that the multilevel Monte Carlo method provides a significant computational cost reduction compared to the standard (crude) Monte Carlo method. We also mention the use of Bayesian techniques to better account for the deflection of a cantilever in the case that the spatially variable flexibility is described via a random field represented by means of a Karhunen-Loève expansion [101, 64]. It is worth mentioning that, in some contributions, the cantilever beams subject to randomness factors have not been directly analysed, but as specific examples to test new stochastic techniques. In this spirit, we here point out [104], where authors propose a stochastic dynamic load identification algorithm to analyse uncertain dynamic systems with correlated random system parameters. The adopted method is based on the approximation the Green's function by the second-order perturbation method and orthogonal polynomial chaos bases. The authors then apply the theoretical results to perform

numerical simulations and experimental studies with a cantilever beam under a concentrated stochastic force to estimate the statistical characteristics of the stochastic load from the stochastic structural response samples. To the best of our knowledge, there is still an important lack of information regarding the complete stochastic analysis of a cantilever beam that is subject to uncertainties. This extended study should include the computation of the 1-PDF of the deflection in the case that the most important parameters of the Euler-Bernoulli model (5.1) are random variables with arbitrary probability distributions and also when the density of the downward force $Q(x)$ may randomly vary according to different realistic situations. This chapter aims to face these aspects from a very general standpoint, including the computation of the PDF of relevant quantities associated with the analysis of the cantilever beam as the maximum deflection and the maximum slope at the free end of the beam.

The chapter is organized as follows. In Section 5.2, we deal with the Case I, corresponding to the scenario that $Q(x)$ represents two uniform loads characterized by two independent random variables covering the same span on the beam. In Section 5.3, we study the Case II, where multiple independent concentrated loads along the span of the beam are analysed. In this case, $Q(x)$ will be represented by a train of Dirac delta functions whose intensities (loads) are independent random variables. In Section 5.4, we study the third scenario, Case III, where $Q(x)$ models a distributed load with an uncertain value characterized by a constant (nominal) value affected by fluctuating changes due to the heterogeneity of the material at every spatial point. Spatial fluctuations are modelled via a stochastic process. In these three above-mentioned sections, we will extensively apply the RVT technique to obtain an explicit expression of the 1-PDF of the solution stochastic process of model (5.1)–(5.2), and the PDF of other quantities of interest, such as the maximum slope, the maximum deflection, the shear force and the bending moment. The theoretical results obtained in Sections 5.2–5.4, will be fully illustrated with examples in Section 5.5. Conclusions will be drawn in Section 5.6.

Finally, we point out that the results in the three aforementioned Cases I–III will be intentionally presented in an analogous manner for ease of reading but also to show the generality of the RVT method despite each scenario being completely different from a mathematical standpoint.

5.2 Case I: Two loads modelled via random variables

This section is addressed to compute the 1-PDF, $f_{Y(x)}(y)$, of the stochastic solution of the random model (5.1)–(5.2), where

$$Q(x) = \begin{cases} Q_0, & 0 < x \leq l/2, \\ Q_1, & l/2 < x \leq l. \end{cases} \tag{5.3}$$

This model represents the deflection of a cantilever beam with two different loads, represented by Q_0 and Q_1, that occupy the same space on the beam, which is fully loaded. As discussed in the previous section, due to uncertainties associated with data, we will assume that model parameters E, Q_0, and Q_1 are random variables. Hereinafter, $f_{E,Q_0,Q_1}(e, q_0, q_1)$ will denote the joint PDF of the random vector (E, Q_0, Q_1), that can be factorized as the product of the corresponding marginal PDF, i.e. $f_E(e) f_{Q_0}(q_0) f_{Q_1}(q_1)$, in the particular, but the important case that E, Q_0 and Q_1 are mutually independent. In Fig. 5.1 we show a graphical scheme of the model.

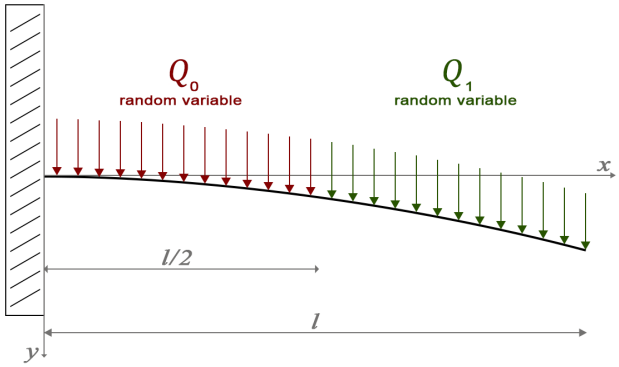

Figure 5.1: Case I: Cantilever beam with two loads modelled via random variables.

At this point, it is interesting to note that in our analysis, arbitrary distributions have been assumed for model parameters, which will provide more generality to our study.

In order to obtain the 1-PDF, $f_{Y(x)}(y)$, taking advantage of the RVT technique (see Th. 2.1), we first need to explicitly calculate the stochastic solution of Eq. (5.1)–(5.2). To this end, several techniques can be utilized. Here, we shall apply the Laplace transform because of the well-known advantages of this integral transform to compactly obtain the solution $Y(x)$ when $Q(x)$ is defined via a piecewise function representing the loads spanned on the beam [47]. Furthermore, the resulting expression of the solution is particularly useful for applying the RVT technique, as it will be apparent throughout our subsequent development. To apply the Laplace transform, we first need to extend the definition of (5.3) as

$$Q(x) = \begin{cases} Q_0, & 0 < x \leq l/2, \\ Q_1, & l/2 < x \leq l, \\ 0, & x > l. \end{cases}$$

The above expression can be written in terms of a unitary Heaviside function, $\mathcal{U}(x)$,

$$Q(x) = Q_0 \left(\mathcal{U}(x) - \mathcal{U}(x - l/2)\right) + Q_1 \left(\mathcal{U}(x - l/2) - \mathcal{U}(x - l)\right). \tag{5.4}$$

Now, applying the Laplace transform, $y(s) = \mathcal{L}\{Y(x)\}(s) = \int_0^\infty \mathrm{e}^{-sx} Y(x)\,\mathrm{d}x$, to (5.1)–(5.2) with $Q(x)$ given by (5.4), using the well-known properties of this integral transform [83, Ch. 2] and isolating $y(s)$, one obtains

$$y(s) = \frac{1}{s^4}\left(sc_1 + c_2 + \frac{1}{Ei}\left(\frac{Q_0}{s} - \frac{Q_0}{s}\mathrm{e}^{-\frac{ls}{2}} + \frac{Q_1}{s}\mathrm{e}^{-\frac{ls}{2}} - \frac{Q_1}{s}\mathrm{e}^{-ls}\right)\right), \tag{5.5}$$

where $c_1 = Y''(0)$ and $c_2 = Y'''(0)$. The next step is to apply the inverse Laplace transform to (5.5)

$$\mathcal{L}^{-1}\{y(s)\} = \mathcal{L}^{-1}\left\{\frac{1}{s^3}c_1 + \frac{1}{s^4}c_2 + \frac{1}{Ei}\left(Q_0\frac{1}{s^5} + (Q_1 - Q_0)\,\frac{1}{s^5}\mathrm{e}^{-\frac{ls}{2}} - Q_1\frac{1}{s^5}\mathrm{e}^{-ls}\right)\right\}.$$

Then, using the inverse Laplace properties [83], and applying the boundary conditions $Y''(l) = 0$ and $Y'''(l) = 0$ in order to obtain the values of c_1 and c_2, we

obtain the solution stochastic process of model (5.1)–(5.2)

$$Y(x) = \begin{cases} Y^{\mathrm{I}}(x; E, Q_0, Q_1), & 0 < x \leq l/2, \\ Y^{\mathrm{I}}(x; E, Q_0, Q_1) + \dfrac{Q_1 - Q_0}{384Ei}(l - 2x)^4, & l/2 < x \leq l, \end{cases} \tag{5.6}$$

where

$$Y^{\mathrm{I}}(x; E, Q_0, Q_1) = \frac{Q_0 + 3Q_1}{16Ei} l^2 x^2 - \frac{Q_0 + Q_1}{12Ei} l x^3 + \frac{Q_0}{24Ei} x^4. \tag{5.7}$$

Observe that the solution $Y(x)$ is differentiable and, therefore continuous at $x = l/2$, which is interesting from an engineering point of view since it informs us that the deflection varies smoothly at the spatial point, $x = l/2$, where the load changes.

Since $Y(x)$ is a piecewise function, the calculation of the 1-PDF of $Y(x)$ will be done separately in the two subdomains $0 < x \leq l/2$ and $l/2 < x \leq l$.

In the first case, we fix $0 < x \leq l/2$ and then we apply the RVT method, i.e. Th. 2.1, to $\mathbf{U} = (E, Q_0, Q_1)$ to obtain the PDF of the random vector $\mathbf{V} = (V_1, V_2, V_3)$, defined by the transformation $\mathbf{r}\colon \mathbb{R}^3 \to \mathbb{R}^3$, whose components are conveniently defined as

$$\begin{aligned} v_1 &= r_1(e, q_0, q_1) = Y^{\mathrm{I}}(x; e, q_0, q_1), \\ v_2 &= r_2(e, q_0, q_1) = q_0, \\ v_3 &= r_3(e, q_0, q_1) = q_1. \end{aligned}$$

The inverse transformation of $\mathbf{r}$, denoted by $\mathbf{s}\colon \mathbb{R}^3 \to \mathbb{R}^3$, is given by

$$\begin{aligned} e &= s_1(v_1, v_2, v_3) = Z^{\mathrm{I}}(x; v_1, v_2, v_3), \\ q_0 &= s_2(v_1, v_2, v_3) = v_2, \\ q_1 &= s_3(v_1, v_2, v_3) = v_3, \end{aligned}$$

where

$$Z^{\mathrm{I}}(x; v_1, v_2, v_3) = \frac{1}{48 v_1 i} \left(3l^2 v_2 x^2 + 9l^2 v_3 x^2 - 4l v_2 x^3 - 4l v_3 x^3 + 2 v_2 x^4\right). \tag{5.8}$$

To compute the PDF of the random vector $\mathbf{V}$, it is necessary to obtain the absolute value of the Jacobian of $\mathbf{s}$,

$$|\mathcal{J}| = \left|\frac{\partial s_1(v_1, v_2, v_3)}{\partial v_1}\right| = \left|\frac{1}{v_1} Z^{\mathrm{I}}(x; v_1, v_2, v_3)\right|,$$

which is well-defined and different from zero w.p. 1 since Q_0, Q_1 and E (hence V_1, V_2 and V_3) are continuous random variables and $i \neq 0$. Applying the RVT method, stated in Th. 2.1, we obtain the PDF of the random vector $\mathbf{V} = (V_1, V_2, V_3)$,

$$f_{V_1,V_2,V_3}(v_1, v_2, v_3) = f_{E,Q_0,Q_1}(Z^{\mathrm{I}}(x; v_1, v_2, v_3), v_2, v_3) \left|\frac{1}{v_1} Z^{\mathrm{I}}(x; v_1, v_2, v_3)\right|.$$

In the particular and important case that E, Q_0 and Q_1 are independent random variables, the above expression writes

$$f_{V_1,V_2,V_3}(v_1, v_2, v_3) = f_E(Z^{\mathrm{I}}(x; v_1, v_2, v_3)) f_{Q_0}(v_2) f_{Q_1}(v_3) \left|\frac{1}{v_1} Z^{\mathrm{I}}(x; v_1, v_2, v_3)\right|.$$

Notice that, according to the previous transformation $\mathbf{r}\colon \mathbb{R}^3 \to \mathbb{R}^3$, the solution of model (5.1)–(5.2) corresponds to its first component v_1, so marginalizing w.r.t. $V_2 = Q_0$ and $V_3 = Q_1$, one obtains the 1-PDF of $Y(x)$,

$$\begin{aligned} f_{Y(x)}(y) \;=\; & \int_{\mathbb{R}^2} f_E\left(\frac{1}{48yi}\left(3l^2q_0x^2 + 9l^2q_1x^2 - 4lq_0x^3 - 4lq_1x^3 + 2q_0x^4\right)\right) f_{Q_0}(q_0) \\ & \cdot f_{Q_1}(q_1) \frac{1}{48y^2i} \left|\left(3l^2q_0x^2 + 9l^2q_1x^2 - 4lq_0x^3 - 4lq_1x^3 + 2q_0x^4\right)\right| \mathrm{d}q_0\, \mathrm{d}q_1. \end{aligned} \tag{5.9}$$

Remark 5.1 *In the latter expression, it can be difficult to calculate the improper multi-integral using quadrature rules. For this reason and from a computational standpoint, it is interesting to express the above integral expression for the 1-PDF in terms of the expectation operator w.r.t. random variables (Q_0, Q_1) as follows*

$$\begin{aligned} f_{Y(x)}(y) \;=\; & \mathbb{E}_{Q_0,Q_1}\left[f_E\left(\frac{1}{48yi}\left(3l^2Q_0x^2 + 9l^2Q_1x^2 - 4lQ_0x^3 - 4lQ_1x^3 + 2Q_0x^4\right)\right)\right. \\ & \left. \cdot \frac{1}{48y^2i}\left|\left(3l^2Q_0x^2 + 9l^2Q_1x^2 - 4lQ_0x^3 - 4lQ_1x^3 + 2Q_0x^4\right)\right|\right], \quad 0 < x \leq l/2, \end{aligned} \tag{5.10}$$

since it permits applying Monte Carlo simulations to approximate the 1-PDF. We will use this remark throughout the chapter.

The computation of the 1-PDF on the second piece of the domain $l/2 < x \leq l$, can be calculated using a similar development as the one we have previously detailed step by step. We omit the technical details that lead to the following explicit expression in terms of the expectation operator

$$\begin{aligned} f_{Y(x)}(y) &= \mathbb{E}_{Q_0,Q_1}\left[f_E\left(\frac{1}{384yi}\left(-l^4Q_0 + l^4Q_1 + 8l^3Q_0x - 8l^3Q_1x + 96l^2Q_1x^2 \right.\right.\right. \\ &\quad \left.\left.\left. -64lQ_1x^3 + 16Q_1x^4\right)\right) \cdot \frac{1}{384y^2i}\left|\left(-l^4Q_0 + l^4Q_1 + 8l^3Q_0x - 8l^3Q_1x \right.\right.\right. \\ &\quad \left.\left.\left. +96l^2Q_1x^2 - 64lQ_1x^3 + 16Q_1x^4\right)\right|\right], \quad l/2 < x \leq l. \end{aligned} \tag{5.11}$$

The maximum slope, S, and the maximum deflection, D, in a cantilever beam represent key information to account for safety and control measures [75, 96, 71]. In the case of a cantilever beam, it is clear they are calculated at the free end of the beam, i.e., $x = l$. It is easy to check that they are given by the following expressions

$$S = Y'(l) = \frac{l^3}{48Ei}\left(Q_0 + 7Q_1\right), \tag{5.12}$$

and,

$$D = Y(l) = \frac{l^4}{384Ei}\left(7Q_0 + 41Q_1\right). \tag{5.13}$$

In our context, S and D are random variables whose respective PDFs, $f_S(s)$ and $f_D(d)$, provide important information about its probabilistic behaviour.

Similar to the above, to obtain the PDF of S, we apply the RVT method stated in Th. 2.1 taking $\mathbf{U} = (E, Q_0, Q_1)$ to obtain the PDF of the random vector $\mathbf{V} = (V_1, V_2, V_3)$, defined by the transformation $\mathbf{r}\colon \mathbb{R}^3 \to \mathbb{R}^3$, whose components are given by

$$\begin{aligned} v_1 &= r_1(e, q_0, q_1) = \frac{l^3}{48ei}\left(q_0 + 7q_1\right), \\ v_2 &= r_2(e, q_0, q_1) = q_0, \\ v_3 &= r_3(e, q_0, q_1) = q_1. \end{aligned}$$

The inverse transformation of $\mathbf{r}$, $\mathbf{s} : \mathbb{R}^3 \to \mathbb{R}^3$, writes

$$\begin{aligned} e &= s_1(v_1, v_2, v_3) = \frac{l^3}{48 v_1 i} (v_2 + 7v_3), \\ q_0 &= s_2(v_1, v_2, v_3) = v_2, \\ q_1 &= s_3(v_1, v_2, v_3) = v_3. \end{aligned}$$

The absolute value of the Jacobian of the inverse transformation is

$$|\mathcal{J}| = \left| \frac{\partial s_1(v_1, v_2, v_3)}{\partial v_1} \right| = \frac{l^3}{48 v_1^2 i} (v_2 + 7v_3) \neq 0, \quad \text{w.p. 1.}$$

So, the PDF of $\mathbf{V}$ is given by

$$f_{V_1,V_2,V_3}(v_1, v_2, v_3) = f_E \left(\frac{l^3}{48 v_1 i} (v_2 + 7v_3) \right) f_{Q_0}(v_2) f_{Q_1}(v_3) \frac{l^3}{48 v_1^2 i} (v_2 + 7v_3).$$

To obtain the PDF of (5.12), which is given by V_1, we marginalize w.r.t. $V_2 = Q_0$ and $V_3 = Q_1$, turning out

$$f_S(s) \quad = \quad \frac{l^3}{48 s^2 i} \int_{\mathbb{R}^2} f_E \left(\frac{l^3}{48 s i} (q_0 + 7q_1) \right) f_{Q_0}(q_0) f_{Q_1}(q_1) (q_0 + 7q_1) \, \mathrm{d}q_0 \, \mathrm{d}q_1.$$

This PDF can be expressed by the expectation of the random vector (Q_0, Q_1) as

$$f_S(s) = \frac{l^3}{48 s^2 i} \mathbb{E}_{Q_0,Q_1} \left[f_E \left(\frac{l^3}{48 s i} (Q_0 + 7Q_1) \right) (Q_0 + 7Q_1) \right]. \tag{5.14}$$

In a similar way, we can obtain the PDF of the maximum deflection (5.13),

$$f_D(d) = \frac{l^4}{384 d^2 i} \mathbb{E}_{Q_0,Q_1} \left[f_E \left(\frac{l^4}{384 d i} (7Q_0 + 41Q_1) \right) (7Q_0 + 41Q_1) \right]. \tag{5.15}$$

From an engineering point of view, it is useful to represent the response of the cantilever beam at each spatial point x in terms of static quantities as the bending moment, $M(x)$, and the shear force, $V(x)$. These relevant quantities can be obtained,

respectively, in terms of the second and third-order derivatives of the deflection [97]

$$M(x) = -EiY''(x), \tag{5.16}$$

and

$$V(x) = -EiY'''(x). \tag{5.17}$$

In our setting problem, the following expressions for the bending moment and the shear force are, respectively, obtained

$$M(x)=\begin{cases} -\frac{1}{8}(Q_0+3Q_1)l^2+\frac{1}{2}(Q_0+Q_1)lx-\frac{1}{2}Q_0x^2, & 0\le x\le l/2, \\ \left(-\frac{1}{2}l^2+lx-\frac{1}{2}x^2\right)Q_1, & l/2<x\le l, \end{cases} \tag{5.18}$$

$$V(x) = \begin{cases} \frac{1}{2}(Q_0+Q_1)l-Q_0x, & 0\le x\le l/2, \\ (l-x)\,Q_1, & l/2<x\le l. \end{cases} \tag{5.19}$$

We can observe that for $x = l$ both the bending moment and the shear force are null ($M(l) = 0$ and $V(l) = 0$). In addition, at $x = 0$ they reach their maximum value (positive or negative).

In order to obtain the PDF of (5.18), and taking into account that it is a piecewise function, we need to calculate the PDF separately in the two subdomains.

To this end, we first fix $x : 0 \le x \le l/2$. Now we apply Theorem 2.1 taking $\mathbf{U} = (Q_1, Q_0)$ to obtain the PDF of the random vector $\mathbf{V} = (V_1, V_2)$, defined by the transformation $\mathbf{r}\colon \mathbb{R}^2 \to \mathbb{R}^2$, whose components are given by

$$\begin{aligned} v_1 &= r_1(q_1, q_0) = -\frac{1}{8}(q_0+3q_1)l^2+\frac{1}{2}(q_0+q_1)lx-\frac{1}{2}q_0x^2, \\ v_2 &= r_2(q_1, q_0) = q_0. \end{aligned}$$

The inverse transformation $\mathbf{s} : \mathbb{R}^2 \to \mathbb{R}^2$ of $\mathbf{r}$ is given by

$$q_1 = s_1(v_1, v_2) = \frac{v_1 - v_2\left(-\frac{1}{8}l^2 + \frac{1}{2}lx - \frac{1}{2}x^2\right)}{\frac{1}{2}lx - \frac{3}{8}l^2},$$
$$q_0 = s_2(v_1, v_2) = v_2.$$

Now, we need to calculate the absolute value of the Jacobian of the previous inverse transformation,

$$|\mathcal{J}| = \left|\frac{\partial s_1(v_1, v_2)}{\partial v_1}\right| = \frac{1}{\left|\frac{1}{2}lx - \frac{3}{8}l^2\right|} \neq 0.$$

Then, applying the RVT method and taking advantage of the expectation operator, we obtain the PDF on the first subdomain $0 \leq x \leq l/2$,

$$f_{M(x)}(m) = \mathbb{E}_{Q_0}\left[f_{Q_1}\left(\frac{m - \left(-\frac{1}{8}l^2 + \frac{1}{2}lx - \frac{1}{2}x^2\right)Q_0}{\frac{1}{2}lx - \frac{3}{8}l^2}\right)\frac{1}{\left|\frac{1}{2}lx - \frac{3}{8}l^2\right|}\right].$$

To complete the analysis on the whole domain, we fix now $x : l/2 < x < l$. In this subdomain, only one random variable appears, so in this case we use the one-dimensional version of the RVT method. Using the same notation as above, we take $U = Q_1$ to obtain the PDF of the random variable $V = V_1$, defined by the transformation $r\colon \mathbb{R} \to \mathbb{R}$ such that

$$v_1 = r(q_1) = \left(-\frac{1}{2}l^2 + lx - \frac{1}{2}x^2\right)q_1.$$

The inverse transformation of r is determined by

$$s(v_1) := r^{-1}(v_1) = \frac{v_1}{-\frac{1}{2}l^2 + lx - \frac{1}{2}x^2}.$$

Finally, we need to calculate the derivative of r^{-1} that is given by

$$\frac{\mathrm{d}s}{\mathrm{d}v_1} = \frac{1}{-\frac{1}{2}l^2 + lx - \frac{1}{2}x^2}.$$

Then applying RVT method, the PDF on $l/2 < x < l$ is

$$f_{M(x)}(m) = f_{Q_1}\left(\frac{m}{-\frac{1}{2}l^2 + lx - \frac{1}{2}x^2}\right)\frac{1}{\left|-\frac{1}{2}l^2 + lx - \frac{1}{2}x^2\right|}.$$

In summary, the PDF of the bending moment is given by

$$f_{M(x)}(m) = \begin{cases} \mathbb{E}_{Q_0}\left[f_{Q_1}\left(\dfrac{m - \left(-\frac{1}{8}l^2 + \frac{1}{2}lx - \frac{1}{2}x^2\right)Q_0}{\frac{1}{2}lx - \frac{3}{8}l^2}\right)\dfrac{1}{\left|\frac{1}{2}lx - \frac{3}{8}l^2\right|}\right], & 0 \le x \le l/2, \\ f_{Q_1}\left(\dfrac{m}{-\frac{1}{2}l^2 + lx - \frac{1}{2}x^2}\right)\dfrac{1}{\left|-\frac{1}{2}l^2 + lx - \frac{1}{2}x^2\right|}, & l/2 < x < l. \end{cases} \tag{5.20}$$

The PDF of the shear force, Eq. (5.19), is obtained in a similar way:

$$f_{V(x)}(v) = \begin{cases} \mathbb{E}_{Q_0}\left[f_{Q_1}\left(\dfrac{v - \left(\frac{1}{2}l - x\right)Q_0}{\frac{1}{2}l}\right)\dfrac{2}{l}\right], & 0 \le x \le l/2, \\ f_{Q_1}\left(\dfrac{v}{l-x}\right)\dfrac{1}{l-x}, & l/2 < x < l. \end{cases} \tag{5.21}$$

Finally, we point out that the results derived throughout this section can be extended, using the same reasoning, to a finite number of loads, including the case that the loads occupy different lengths on the beam.

5.3 Case II: Concentrated random loads P_j spanned on the beam

In this section, we obtain the 1-PDF of the solution stochastic process of model (5.1)–(5.2) in the important case that loads are applied at n different spatial points, $x_j, j = 1, \ldots, n$, along the span of the beam. This case can be modelled by taking

$$Q(x) = \sum_{j=1}^{n} P_j \delta\left(x - x_j\right), \tag{5.22}$$

where $\delta(\cdot)$ denotes the Dirac delta distribution.

Let us assume that E and P_j, $j = 1, \ldots, n$, are mutually independent random variables, being $f_E(e)$ and $f_{P_j}(p_j)$, $j = 1, \ldots, n$, their respective PDFs. In Fig. 5.2,

we show a graphical scheme of the model. In a similar way that in the previous section, using the Laplace transform and its properties when computing the Laplace transform of the Dirac delta distribution, we can obtain the stochastic solution of model (5.1)–(5.2), via the following piecewise function

$$Y(x) = \begin{cases} Y^{\mathrm{II}}(x; E, P_1, \ldots, P_n), & 0 < x \leq x_1, \\ Y^{\mathrm{II}}(x; E, P_1, \ldots, P_n) + \dfrac{1}{6Ei} \displaystyle\sum_{k=1}^{j} P_k \left(x - x_k\right)^3, & x_j < x \leq x_{j+1}, \\ & j = 1, \ldots, n-1, \\ Y^{\mathrm{II}}(x; E, P_1, \ldots, P_n) + \dfrac{1}{6Ei} \displaystyle\sum_{k=1}^{n} P_k \left(x - x_k\right)^3, & x_n < x \leq l, \end{cases} \tag{5.23}$$

where

$$Y^{\mathrm{II}}(x; E, P_1, \ldots, P_n) = \frac{1}{2Ei} x^2 \sum_{j=1}^{n} x_j P_j - \frac{1}{6Ei} x^3 \sum_{j=1}^{n} P_j. \tag{5.24}$$

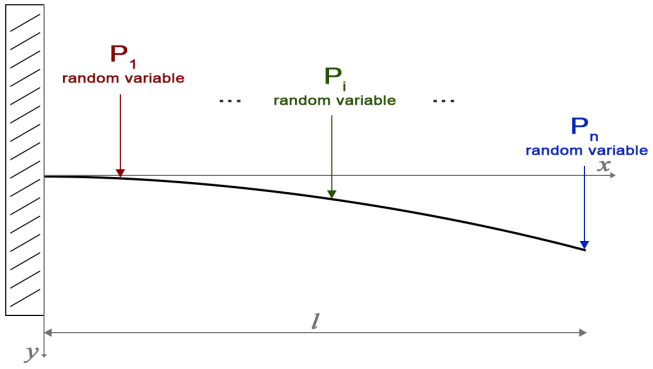

Figure 5.2: Case II: Cantilever beam with concentrated random variables loads at different spatial points.

Once we have obtained the stochastic solution, we will obtain the 1-PDF of (5.23)–(5.24) taking advantage of the RVT method. As the solution is given by means of a piecewise function, the 1-PDF will be determined by applying this method to each piece.

To this end, we first fix $0 < x \leq x_1$. Let us to define a mapping $\mathbf{r} : \mathbb{R}^{n+1} \to \mathbb{R}^{n+1}$ that transforms the random vector $\mathbf{U} = (E, P_1, \ldots, P_n)$ into $\mathbf{V} = (V_1, \ldots, V_{n+1})$ being

$$\begin{array}{rcccl} v_1 & = & r_1(e, p_1, \ldots, p_n) & = & Y^{\mathrm{II}}(x; e, p_1, \ldots, p_n), \\ v_2 & = & r_2(e, p_1, \ldots, p_n) & = & p_1, \\ \vdots & \vdots & \vdots & \vdots & \vdots \\ v_{n+1} & = & r_{n+1}(e, p_1, \ldots, p_n) & = & p_n. \end{array}$$

The inverse mapping of $\mathbf{r}$ is given by the mapping $\mathbf{s} : \mathbb{R}^{n+1} \to \mathbb{R}^{n+1}$ whose components are

$$\begin{array}{rcccl} e & = & s_1(v_1, v_2, \ldots, v_{n+1}) & = & Z^{\mathrm{II}}(x; v_1, v_2, \ldots, v_{n+1}), \\ p_1 & = & s_2(v_1, v_2, \ldots, v_{n+1}) & = & v_2, \\ \vdots & \vdots & \vdots & \vdots & \vdots \\ p_n & = & s_{n+1}(v_1, v_2, \ldots, v_{n+1}) & = & v_{n+1}, \end{array}$$

where

$$Z^{\mathrm{II}}(x; v_1, v_2, \ldots, v_{n+1}) = -\frac{1}{6v_1 i}\left(-3x^2 \sum_{j=1}^{n} x_j v_{j+1} + x^3 \sum_{j=1}^{n} v_{j+1}\right).$$

Note that the absolute value of the Jacobian of $\mathbf{s}$ is

$$|\mathcal{J}| = \left|\frac{\partial s_1(v_1, v_2, \ldots, v_{n+1})}{\partial v_1}\right| = \left|\frac{1}{v_1} Z^{\mathrm{II}}(x; v_1, v_2, \ldots, v_{n+1})\right| \neq 0, \text{ w.p. } 1.$$

Then, according to Th. 2.1, the PDF of $\mathbf{V}$ is given by

$$\begin{array}{rcl} f_{V_1,\ldots,V_{n+1}}(v_1, \ldots, v_{n+1}) & = & f_E\left(Z^{\mathrm{II}}(x; v_1, v_2, \ldots, v_{n+1})\right) f_{P_1}(v_2) \cdots f_{P_n}(v_{n+1}) \\ & & \cdot \left|\frac{1}{v_1} Z^{\mathrm{II}}(x; v_1, v_2, \ldots, v_{n+1})\right|. \end{array}$$

Finally, the 1-PDF of the stochastic solution (5.23)–(5.24), which is given by V_1, is obtained by marginalizing w.r.t. $V_2 = P_1, \ldots, V_{n+1} = P_n$,

$$\begin{aligned} f_{Y(x)}(y) &= \int_{\mathbb{R}^n} f_E\left(-\frac{1}{6yi}\left(-3x^2\sum_{j=1}^{n} x_j p_j + x^3\sum_{j=1}^{n} p_j\right)\right) f_{P_1}(p_1)\cdots f_{P_n}(p_n) \\ &\quad \cdot\frac{1}{6y^2 i}\left|-3x^2\sum_{j=1}^{n} x_j p_j + x^3\sum_{j=1}^{n} p_j\right| \mathrm{d}p_1\cdots\mathrm{d}p_n, \quad 0 < x \le x_1. \end{aligned} \tag{5.25}$$

The above expression involves a multidimensional integral that may be computationally unaffordable in practice. To overcome this drawback, it is interesting to notice that this expression can be rewritten using the operator expectation

$$\begin{aligned} f_{Y(x)}(y) &= \mathbb{E}_{P_1,\ldots,P_n}\left[f_E\left(-\frac{1}{6yi}\left(-3x^2\sum_{j=1}^{n} x_j P_j + x^3\sum_{j=1}^{n} P_j\right)\right)\right. \\ &\quad \left.\cdot\ \frac{1}{6y^2 i}\left|-3x^2\sum_{j=1}^{n} x_j P_j + x^3\sum_{j=1}^{n} P_j\right|\right], \quad 0 < x \le x_1. \end{aligned} \tag{5.26}$$

This expression is particularly useful when applying Monte Carlo simulations to calculate the 1-PDF.

The computation of the 1-PDF on the other subdomains of the stochastic solution (see (5.23)) can be calculated similarly. For simplicity in the presentation, we skip the technical details here. Calculations lead to

$$\begin{aligned} f_{Y(x)}(y) = \mathbb{E}_{P_1,\ldots,P_n}&\left[f_E\left(\frac{1}{6yi}\left(3x^2\sum_{k=1}^{n} x_k P_k - x^3\sum_{k=1}^{n} P_k + \sum_{k=1}^{j}(x-x_k)^3 p_k\right)\right)\right. \\ &\left.\cdot\ \frac{1}{6y^2 i}\left|3x^2\sum_{k=1}^{n} x_k P_k - x^3\sum_{k=1}^{n} P_k + \sum_{k=1}^{j}(x-x_k)^3 p_k\right|\right], \quad x_j < x \le x_{j+1},\ j = 1,\ldots,n-1, \end{aligned} \tag{5.27}$$

and

$$f_{Y(x)}(y) = \mathbb{E}_{P_1,\ldots,P_n}\left[f_E\left(\frac{1}{6yi}\left(3x^2\sum_{k=1}^{n}x_kP_k - x^3\sum_{k=1}^{n}P_k + \sum_{k=1}^{n}(x-x_k)^3P_j\right)\right)\right.$$
$$\left.\cdot\ \frac{1}{6y^2i}\left|3x^2\sum_{k=1}^{n}x_kP_k - x^3\sum_{k=1}^{n}P_k + \sum_{k=1}^{n}(x-x_k)^3P_k\right|\right], \quad x_n < x \le l. \tag{5.28}$$

Now, we will compute the PDF of the slope, $S = Y'(l)$, and the maximum deflection, $D = Y(l)$, at the free end as we did in the previous section. From (5.23)–(5.24), it is easy to see that

$$S = \frac{1}{2Ei}\sum_{j=1}^{n}x_j^2P_j, \quad D = \frac{1}{6Ei}\left(3l\sum_{j=1}^{n}x_j^2P_j - \sum_{j=1}^{n}x_j^3P_j\right), \tag{5.29}$$

and applying the RVT technique with appropriate mappings, we can obtain the PDFs of S and D in terms of the expectation operator

$$f_S(s) = \mathbb{E}_{P_1,\ldots,P_n}\left[f_E\left(\frac{1}{2si}\left(\sum_{j=1}^{n}x_j^2P_j\right)\right)\frac{1}{2s^2i}\left|-\sum_{j=1}^{n}x_j^2P_j\right|\right], \tag{5.30}$$

and

$$f_D(d) = \mathbb{E}_{P_1,\ldots,P_n}\left[f_E\left(\frac{1}{6di}\left(3l\sum_{j=1}^{n}x_j^2P_j - \sum_{j=1}^{n}x_j^3P_j\right)\right)\frac{1}{6d^2i}\left|3l\sum_{j=1}^{n}x_j^2P_j - \sum_{j=1}^{n}x_j^3P_j\right|\right]. \tag{5.31}$$

For the sake of completeness, we finish this section by calculating the PDF of the bending moment and the shear force of the cantilever beam. Applying equations (5.16) and (5.17) to (5.23)–(5.24), we obtain the expressions of the bending moment

$$M(x) = \begin{cases} \sum_{k=1}^{n}P_k(x-x_k), & 0 \le x \le x_1, \\ \sum_{k=j+1}^{n}P_k(x-x_k), & x_j < x \le x_{j+1}, \\ & j = 1,\ldots,n-1, \\ 0, & x_n < x \le l. \end{cases} \tag{5.32}$$

and the shear force

$$V(x) = \begin{cases} \sum_{k=1}^{n} P_k, & 0 \le x \le x_1, \\ \sum_{k=j+1}^{n} P_k, & x_j < x \le x_{j+1}, \\ & j = 1, \dots, n-1, \\ 0, & x_n < x \le l. \end{cases} \tag{5.33}$$

Then, applying RVT technique to expressions (5.32) and (5.33) in a similar way to the previous section, we can obtain the PDF of the bending moment

$$f_{M(x)}(m) = \begin{cases} \mathbb{E}_{P_1,\dots,P_{n-1}}\left[f_{P_n}\left(\frac{m - \sum_{k=1}^{n-1} P_k(x - x_k)}{x - x_n} \right) \frac{1}{|x - x_n|} \right], & 0 \le x \le x_1, \\ \mathbb{E}_{P_{j+1},\dots,P_{n-1}}\left[f_{P_n}\left(\frac{m - \sum_{k=j+1}^{n-1} P_k(x - x_k)}{x - x_n} \right) \frac{1}{|x - x_n|} \right], & x_j \le x \le x_{j+1}, \\ & j = 1, \dots, n-2, \\ f_{P_n}\left(\frac{m}{x - x_n} \right) \frac{1}{|x - x_n|}, & x_{n-1} < x \le x_n, \\ 0, & x_n < x \le l, \end{cases} \tag{5.34}$$

and the PDF of the shear force

$$f_{V(x)}(v) = \begin{cases} \mathbb{E}_{P_2,\dots,P_n}[f_{P_1}\left(v - \sum_{k=2}^{n} P_k\right)], & 0 \le x \le x_1, \\ \mathbb{E}_{P_{j+1},\dots,P_{n-1}}\left[f_{P_n}\left(v - \sum_{k=j+1}^{n-1} P_k \right) \right], & x_j < x \le x_{j+1}, \\ & j = 1, \dots, n-2, \\ f_{P_n}(v), & x_{n-1} < x \le x_n, \\ 0, & x_n < x \le l. \end{cases} \tag{5.35}$$

5.4 Case III: A load modelled via Brownian motion

In this section, we assume that the density downward force, $Q(x)$, is given by the sum of a deterministic value, q_0 (nominal value), and a certain random quantity that depends on the spatial point x on the beam. This latter quantity models the uncertainties due to the heterogeneity of the beam. As for cantilever beams, the key point is clearly located at the free end (in our case, on the right end); then to mathematically analyze the problem, we have chosen a stochastic process whose variance increases with its independent parameter (in our case, the space x) and whose distribution is Gaussian. Specifically, we have selected a standard Wiener process (also termed Brownian motion), $B(x)$, to perform our mathematical analysis, although our subsequent approach also permits considering other stochastic processes to play the role of $B(x)$. Therefore, we shall assume that

$$Q(x) = q_0 + B(x), \quad 0 < x \leq l, \tag{5.36}$$

being $B(x) = B(x, \omega)$ the standard Wiener process. Recall that, $\mu_B(x) = \mathbb{E}[B(x)] = 0$ and $\mathbb{V}[B(x)] = x$, $\forall x > 0$, [54]. Fig. 5.3 shows a graphical representation of the problem.

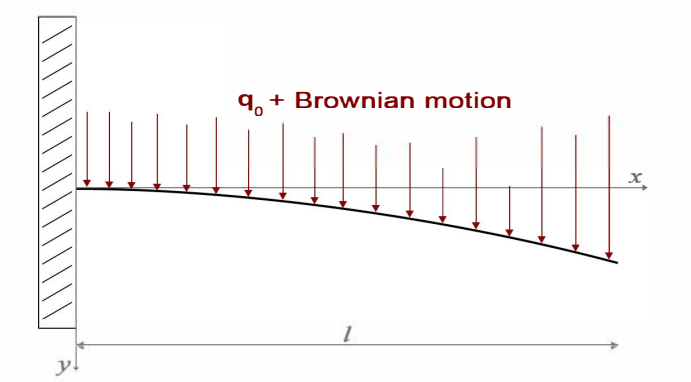

Figure 5.3: Case III: Cantilever beam with $q_0 + B(x)$ as varying load, being $B(x)$ the Brownian motion.

In order to obtain an approximation of the 1-PDF of the solution stochastic process of model (5.1)–(5.2) with $Q(x)$ given by (5.36), we will consider the approximation of $B(x)$ obtained by truncating its Karhunen–Loève expansion, see Section 2.2, at a finite order, say N. Then, the model is approximated via the differential equation

$$\frac{\mathrm{d}^4 Y(x)}{\mathrm{d}x^4} = \frac{1}{Ei}\left(q_0 + \sum_{j=1}^{N} \sqrt{\nu_j}\phi_j(x)\xi_j(\omega)\right), \quad 0 < x < l, \tag{5.37}$$

where

$$\nu_j = \frac{4l^2}{\pi^2(2j-1)^2}, \quad \phi_j(x) = \sqrt{\frac{2}{l}}\sin\left(\frac{(2j-1)\pi}{2l}x\right), \quad j = 1, 2, \ldots, N,$$

and $\xi_j(\omega) \sim \mathrm{N}(0,1)$, $j = 1, 2, \ldots, N$.

The solution stochastic process of model (5.37) together with the boundary conditions (5.2), can be obtained using the Laplace transform. After somewhat technical computations, we obtain

$$\begin{aligned} Y(x) =& \frac{1}{Ei}\left(\frac{x^2}{2}\left(\frac{q_0}{2}l^2 + l\sqrt{\frac{2}{l}}\sum_{j=1}^{N}\xi_j\frac{1-\cos(b_j l)}{b_j^2} - \sqrt{\frac{2}{l}}\sum_{j=1}^{N}\xi_j\frac{b_j l - \sin(b_j l)}{b_j^3}\right)\right. \\ &+\frac{x^3}{6}\left(-q_0 l - \sqrt{\frac{2}{l}}\sum_{j=1}^{N}\xi_j\frac{1-\cos(b_j l)}{b_j^2}\right) + \frac{q_0}{24}x^4 \\ &\left.+\sqrt{\frac{2}{l}}\sum_{j=1}^{N}\xi_j\frac{-6b_j x + b_j^3 x^3 + 6\sin(b_j x)}{6b_j^5}\right), \quad 0 < x \le l, \end{aligned} \tag{5.38}$$

where $b_j = \dfrac{(2j-1)\pi}{2l}$.

We fix $0 < x < l$ and we assume that E and ξ_j, $j = 1, \ldots, N$ are independent continuous random variables with PDFs given by $f_E(e)$ and $f_{\xi_j}(\xi_j)$, $j = 1, \ldots, N$, respectively. Now, we will apply the RVT method taking in Th. 2.1 as $\mathbf{U} = (E, \xi_1, \ldots, \xi_N)$ to obtain the PDF of the random vector $\mathbf{V} = (V_1, V_2, \ldots, V_{N+1})$, defined by the transformation $\mathbf{r}\colon \mathbb{R}^{N+1} \to \mathbb{R}^{N+1}$, whose components are defined

by

$$
\begin{aligned}
v_1 = r_1(e, \xi_1, \ldots, \xi_N) = \frac{1}{ei} \Bigg(\frac{x^2}{2} \Bigg(\frac{q_0}{2} l^2 + l\sqrt{\frac{2}{l}} \sum_{j=1}^{N} \xi_j \frac{1 - \cos(b_j l)}{b_j^2} \\
- \sqrt{\frac{2}{l}} \sum_{j=1}^{N} \xi_j \frac{b_j l - \sin(b_j l)}{b_j^3} \Bigg) + \frac{x^3}{6} \Bigg(-q_0 l - \sqrt{\frac{2}{l}} \sum_{j=1}^{N} \xi_j \frac{1 - \cos(b_j l)}{b_j^2} \Bigg) \\
+ \frac{q_0}{24} x^4 + \sqrt{\frac{2}{l}} \sum_{j=1}^{N} \xi_j \frac{-6 b_j x + b_j^3 x^3 + 6 \sin(b_j x)}{6 b_j^5} \Bigg), \\
v_2 = r_2(e, \xi_1, \ldots, \xi_N) = \xi_1, \\
\vdots \\
v_{N+1} = r_{N+1}(e, \xi_1, \ldots, \xi_N) = \xi_{N+1}.
\end{aligned}
$$

The inverse transformation of $\mathbf{r}$, $\mathbf{s}\colon \mathbb{R}^{N+1} \to \mathbb{R}^{N+1}$, is given by

$$
\begin{aligned}
e = s_1(v_1, v_2, \ldots, v_{N+1}) = \frac{1}{v_1 i} \Bigg(\frac{x^2}{2} \Bigg(\frac{q_0}{2} l^2 + l\sqrt{\frac{2}{l}} \sum_{j=1}^{N} v_{j+1} \frac{1 - \cos(b_j l)}{b_j^2} \\
- \sqrt{\frac{2}{l}} \sum_{j=1}^{N} v_{j+1} \frac{b_j l - \sin(b_j l)}{b_j^3} \Bigg) + \frac{x^3}{6} \Bigg(-q_0 l - \sqrt{\frac{2}{l}} \sum_{j=1}^{N} v_{j+1} \frac{1 - \cos(b_j l)}{b_j^2} \Bigg) \\
+ \frac{q_0}{24} x^4 + \sqrt{\frac{2}{l}} \sum_{j=1}^{N} v_{j+1} \frac{-6 b_j x + b_j^3 x^3 + 6 \sin(b_j x)}{6 b_j^5} \Bigg), \\
\xi_1 = s_2(v_1, v_2, \ldots, v_{N+1}) = v_2, \\
\vdots \\
\xi_N = s_{N+1}(v_1, v_2, \ldots, v_{N+1}) = v_{N+1}.
\end{aligned}
$$

The absolute value of the Jacobian of the inverse mapping $\mathbf{s}$ writes

$$
\begin{aligned}
|\mathcal{J}| = \left| \frac{\partial s_1(v_1, v_2, \ldots, v_{N+1})}{\partial v_1} \right| = \Bigg| -\frac{1}{v_1^2 i} \Bigg(\frac{x^2}{2} \Bigg(\frac{q_0}{2} l^2 + l\sqrt{\frac{2}{l}} \sum_{j=1}^{N} v_{j+1} \frac{1 - \cos(b_j l)}{b_j^2} \\
- \sqrt{\frac{2}{l}} \sum_{j=1}^{N} v_{j+1} \frac{b_j l - \sin(b_j l)}{b_j^3} \Bigg) + \frac{x^3}{6} \Bigg(-q_0 l - \sqrt{\frac{2}{l}} \sum_{j=1}^{N} v_{j+1} \frac{1 - \cos(b_j l)}{b_j^2} \Bigg) \\
+ \frac{q_0}{24} x^4 + \sqrt{\frac{2}{l}} \sum_{j=1}^{N} v_{j+1} \frac{-6 b_j x + b_j^3 x^3 + 6 \sin(b_j x)}{6 b_j^5} \Bigg) \Bigg| \neq 0, \text{ w.p. 1.}
\end{aligned}
$$

Similarly as developed in Cases I and II, the following expression for the 1-PDF of the solution stochastic process is obtained

$$
\begin{aligned}
f_{Y(x)}(y) =& \mathbb{E}_{\xi_1,\ldots,\xi_N}\left[f_E\left(\frac{1}{Ei}\left(\frac{x^2}{2}\left(\frac{q_0}{2}l^2 + l\sqrt{\frac{2}{l}}\sum_{j=1}^{N}\xi_j\frac{1-\cos(b_j l)}{b_j^2}\right.\right.\right.\right. \\
&\left.\left.\left.\left. -\sqrt{\frac{2}{l}}\sum_{j=1}^{N}\xi_j\frac{b_j l-\sin(b_j l)}{b_j^3}\right) + \frac{x^3}{6}\left(-q_0 l - \sqrt{\frac{2}{l}}\sum_{j=1}^{N}\xi_j\frac{1-\cos(b_j l)}{b_j^2}\right)\right.\right.\right. \\
&\left.\left.\left. + \frac{q_0}{24}x^4 + \sqrt{\frac{2}{l}}\sum_{j=1}^{N}\xi_j\frac{-6b_j x + b_j^3 x^3 + 6\sin(b_j x)}{6b_j^5}\right)\right)\right. \\
&\left. \cdot\left| -\frac{1}{E^2 i}\left(\frac{x^2}{2}\left(\frac{q_0}{2}l^2 + l\sqrt{\frac{2}{l}}\sum_{j=1}^{N}\xi_j\frac{1-\cos(b_j l)}{b_j^2} - \sqrt{\frac{2}{l}}\sum_{j=1}^{N}\xi_j\frac{b_j l-\sin(b_j l)}{b_j^3}\right)\right.\right.\right. \\
&\left.\left.\left. + \frac{x^3}{6}\left(-q_0 l - \sqrt{\frac{2}{l}}\sum_{j=1}^{N}\xi_j\frac{1-\cos(b_j l)}{b_j^2}\right) + \frac{q_0}{24}x^4\right.\right.\right. \\
&\left.\left.\left. + \sqrt{\frac{2}{l}}\sum_{j=1}^{N}\xi_j\frac{-6b_j x + b_j^3 x^3 + 6\sin(b_j x)}{6b_j^5}\right)\right|\right], \quad 0 < x \le l.
\end{aligned}
\tag{5.39}
$$

To complete Case III with the same information as the one presented in Cases I and II, we now compute the PDFs of the maximum slope and deflection at the free end of the beam and the PDFs of the bending moment and the shear force. For the sake of simplicity, we directly present the results we obtained. For the maximum slope

$$
\begin{aligned}
S = Y'(l) =& \frac{1}{Ei}\left(\frac{q_0}{8}l^3 + \frac{1}{2}l^2\sqrt{\frac{2}{l}}\sum_{j=1}^{N}\xi_j\frac{1-\cos(b_j l)}{b_j^2} - l\sqrt{\frac{2}{l}}\sum_{j=1}^{N}\xi_j\frac{b_j l-\sin(b_j l)}{b_j^3}\right. \\
&\left. + \sqrt{\frac{2}{l}}\sum_{j=1}^{N}\xi_j\frac{-2 + b_j^2 l^2 + 2\cos(b_j l)}{2b_j^4}\right),
\end{aligned}
\tag{5.40}
$$

its PDF is given by

$$\begin{aligned} f_S(s) =& \mathbb{E}_{\xi_1,\ldots,\xi_N}\left[f_E\left(\frac{1}{si}\left(\frac{q_0}{8}l^3 + \frac{1}{2}l^2\sqrt{\frac{2}{l}}\sum_{j=1}^{N}\xi_j\frac{1-\cos(b_jl)}{b_j^2} - l\sqrt{\frac{2}{l}}\sum_{j=1}^{N}\xi_j\frac{b_jl-\sin(b_jl)}{b_j^3} \right.\right.\right. \\ &\left.\left.\left. + \sqrt{\frac{2}{l}}\sum_{j=1}^{N}\xi_j\frac{-2+b_j^2l^2+2\cos(b_jl)}{2b_j^4}\right)\right) \left| -\frac{1}{\theta^2 i}\left(\frac{q_0}{8}l^3 + \frac{1}{2}l^2\sqrt{\frac{2}{l}}\sum_{j=1}^{N}\xi_j\frac{1-\cos(b_jl)}{b_j^2} \right.\right. \right. \\ &\left.\left.\left. - l\sqrt{\frac{2}{l}}\sum_{j=1}^{N}\xi_j\frac{b_jl-\sin(b_jl)}{b_j^3} + \sqrt{\frac{2}{l}}\sum_{j=1}^{N}\xi_j\frac{-2+b_j^2l^2+2\cos(b_jl)}{2b_j^4}\right)\right|\right], \end{aligned} \tag{5.41}$$

and, for the maximum deflection

$$\begin{aligned} D = Y(l) =& \frac{1}{Ei}\left(\frac{q_0}{8}l^4 + \frac{1}{3}l^3\sqrt{\frac{2}{l}}\sum_{j=1}^{N}\xi_j\frac{1-\cos(b_jl)}{b_j^2} - \frac{1}{2}l^2\sqrt{\frac{2}{l}}\sum_{j=1}^{N}\xi_j\frac{b_jl-\sin(b_jl)}{b_j^3} \right. \\ &\left. + \sqrt{\frac{2}{l}}\sum_{j=1}^{N}\xi_j\frac{-6b_jl+b_j^3l^3+6\sin(b_jl)}{6b_j^5}\right), \end{aligned} \tag{5.42}$$

its PDF is given by

$$\begin{aligned} f_D(d) =& \mathbb{E}_{\xi_1,\ldots,\xi_N}\left[f_E\left(\frac{1}{di}\left(\frac{q_0}{8}l^4 + \frac{1}{3}l^3\sqrt{\frac{2}{l}}\sum_{j=1}^{N}\xi_j\frac{1-\cos(b_jl)}{b_j^2} - \frac{1}{2}l^2\sqrt{\frac{2}{l}}\sum_{j=1}^{N}\xi_j\frac{b_jl-\sin(b_jl)}{b_j^3} \right.\right.\right. \\ &\left.\left.\left. + \sqrt{\frac{2}{l}}\sum_{j=1}^{N}\xi_j\frac{-6b_jl+b_j^3l^3+6\sin(b_jl)}{6b_j^5}\right)\right) \left| -\frac{1}{\delta^2 i}\left(\frac{q_0}{8}l^4 + \frac{1}{3}l^3\sqrt{\frac{2}{l}}\sum_{j=1}^{N}\xi_j\frac{1-\cos(b_jl)}{b_j^2} \right.\right. \right. \\ &\left.\left.\left. - \frac{1}{2}l^2\sqrt{\frac{2}{l}}\sum_{j=1}^{N}\xi_j\frac{b_jl-\sin(b_jl)}{b_j^3} + \sqrt{\frac{2}{l}}\sum_{j=1}^{N}\xi_j\frac{-6b_jl+b_j^3l^3+6\sin(b_jl)}{6b_j^5}\right)\right|\right]. \end{aligned} \tag{5.43}$$

Applying equations (5.16) and (5.17) to (5.38), the following expressions are, respectively, obtained for the bending moment

$$\begin{aligned} M(x) =& -\frac{q_0}{2}\left(l^2+x^2-2xl\right) - \sqrt{\frac{2}{l}}\sum_{j=1}^{N}\xi_j\frac{1-\cos(b_jl)}{b_j^2}(l-x) \\ &- \sqrt{\frac{2}{l}}\sum_{j=1}^{N}\xi_j\frac{b_j(x-l)+\sin(b_jl)-\sin(b_jx)}{b_j^3}, \end{aligned} \tag{5.44}$$

and the shear force

$$V(x) = -q_0(x-l) - \sqrt{\frac{2}{l}} \sum_{j=1}^{N} \xi_j \frac{\cos(b_j l) - \cos(b_j x)}{b_j^2}. \tag{5.45}$$

Its PDFs are given by

$$\begin{aligned} f_{M(x)}(m) = \mathbb{E}_{\xi_2,\ldots,\xi_N} \Big[f_{\xi_1} \Big(\Big(m + \frac{q_0}{2} \left(l^2 + x^2 - 2xl\right) \\ + \sqrt{\frac{2}{l}} \sum_{j=2}^{N} \xi_j \left(\frac{1-\cos(b_j l)}{b_j^2}(l-x) + \frac{b_j(x-l) + \sin(b_j l) - \sin(b_j x)}{b_j^3} \right) \Big) \\ \cdot \left(-\sqrt{\frac{2}{l}} \left(\frac{1-\cos(b_1 l)}{b_1^2}(l-x) + \frac{b_1(x-l) + \sin(b_1 l) - \sin(b_1 x)}{b_1^3} \right) \right)^{-1} \Big) \\ \cdot \left| -\sqrt{\frac{2}{l}} \left(\frac{1-\cos(b_1 l)}{b_1^2}(l-x) + \frac{b_1(x-l) + \sin(b_1 l) - \sin(b_1 x)}{b_1^3} \right) \right|^{-1} \Big], \end{aligned} \tag{5.46}$$

and

$$\begin{aligned} f_{V(x)}(v) = \mathbb{E}_{\xi_2,\ldots,\xi_N} \Bigg[f_{\xi_1} \Bigg(\Bigg(v + q_0(x-l) + \sqrt{\frac{2}{l}} \sum_{j=2}^{N} \xi_j \frac{\cos(b_j l) - \cos(b_j x)}{b_j^2} \Bigg) \\ \cdot \left(-\sqrt{\frac{2}{l}} \left(\frac{\cos(b_1 l) - \cos(b_1 x)}{b_1^2} \right) \right)^{-1} \Bigg) \left| -\sqrt{\frac{2}{l}} \left(\frac{\cos(b_1 l) - \cos(b_1 x)}{b_1^2} \right) \right|^{-1} \Bigg], \end{aligned} \tag{5.47}$$

respectively.

Remark 5.2 *In the previous analysis, we calculated the PDF of several quantities of interest (deflection, shear force, and bending moment) of the beam thanks to the application of the RVT method. It is worthwhile to point out that this technique could also be applied to determine the second probability density function (2-PDF) of the above-mentioned quantities [89]. This would allow us to quantify further statistical properties, such as the correlation of the deflection at two different spatial points. Here, we omit this analysis since it is very similar but involves cumbersome mathematical expressions.*

5.5 Numerical examples

This section is devoted to illustrating the above theoretical findings. We show three different examples corresponding to the theoretical results obtained in Cases I–III developed in each one of the previous Sections 5.2–5.4, respectively. We take the following data for the deterministic parameters of the model (5.1): $l = 10$ m and $i = 722$ cm^4, while for the random parameters, we will assume that the Young's modulus of elasticity, E, has a truncated Gaussian distribution with mean $\mu_E = 210 \cdot 10^9$ Pa (Pascals) and variance $\sigma_E^2 = 420 \cdot 10^7$ Pa^2, i.e. $E \sim \mathrm{N}_{\mathcal{T}}(\mu_E; \sigma_E^2)$ where $\mathcal{T} = [\mu_E - k\sigma_E, \mu_E + k\sigma_E] = [209.9993 \cdot 10^9, 210.0006 \cdot 10^9]$, taking $k = 10$. The particular form of the stochastic process $Q(x)$ will be specified below in each example.

Example 5.1 *(Case I) This example corresponds to Section 5.2, where the cantilever beam supports two different loads. We assume that the loads are defined by random variables whose distributions are Gaussian,* $Q_0 \sim \mathrm{N}\left(\mu_{Q_0} = 40; \sigma_{Q_0}^2 = 0.4\right)$ *and* $Q_1 \sim \mathrm{N}\left(\mu_{Q_1} = 20; \sigma_{Q_1}^2 = 0.2\right)$.

Fig. 5.4 shows the graphical representation of the 1-PDF given by expressions (5.10) *and* (5.11) *at different spatial points* $x \in \{1, \ldots, 10\}$. *As it is expected, we can observe that the variance increases as* x *does.*

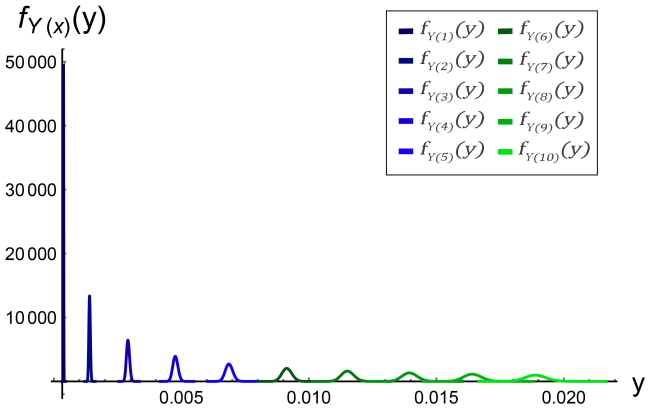

Figure 5.4: 1-PDF, $f_{Y(x)}(y)$, of the solution stochastic process (5.6), computed by (5.10) and (5.11), at different spatial points $x \in \{1, \ldots, 10\}$. Example 5.1.

In Fig. 5.5, we show the plots of the PDFs of the maximum slope, $f_S(s)$, and the maximum deflection, $f_D(d)$, at the free end of the cantilever beam. Computations have been carried out by expressions (5.14) *and* (5.15)*, respectively. In Table 5.1, we include the numerical results for the mean and the standard deviation of random variables S and D.*

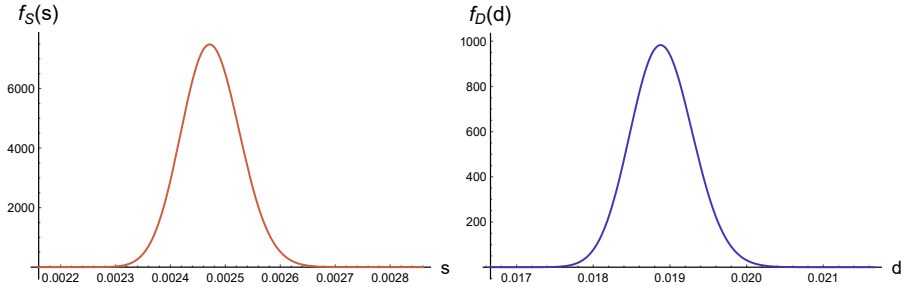

Figure 5.5: Left: PDF of the maximum slope, $f_S(s)$, at free end using expression (5.14). Right: PDF of the maximum deflection, $f_D(d)$, at the free end using (5.15). Example 5.1.

	Mean	**Standard deviation**
Slope at free end	0.0024742	0.00005343
Max. deflection	0.0189006	0.00040673

Table 5.1: Mean and standard deviation of the maximum slope and the maximum deflection of $Y(x)$ at the free end of the beam. Example 5.1.

In Fig. 5.6 and Fig. 5.7, we show a graphical representation of the PDFs of the bending moment, $f_{M(x)}(m)$ and the shear force, $f_{V(x)}(v)$, respectively, at different spatial points $x \in \{0, \ldots, 9\}$. Recall that at the end of the beam ($l = 10$), $M(l) = 0$ and $V(l) = 0$. We can observe in both figures that the variance decreases as the position increases.

Finally, in Fig. 5.8, we show a graphical representation of the mean and standard deviation functions of the solution stochastic process, $Y(x)$. They have been calculated by expressions (2.2) *and* (2.3)*, where $f_{Y(x)}(y)$ is given by* (5.10)–(5.11)*.*

Example 5.2 *(Case II) Here we illustrate the theoretical results for a cantilever beam subject to concentrated loads at specific spatial points. More specifically,*

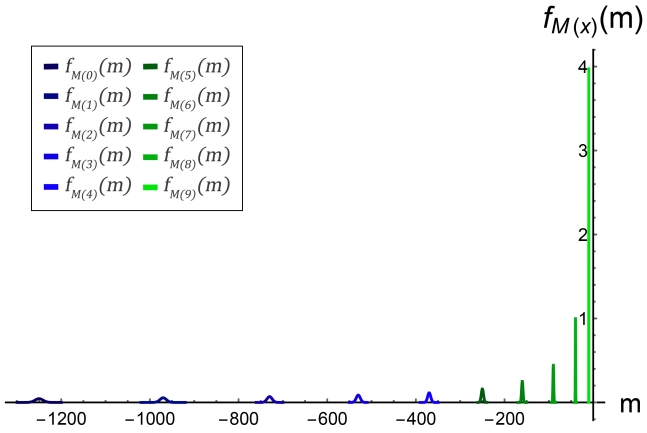

Figure 5.6: PDF of the bending moment, $f_{M(x)}(m)$, using expression (5.20) at different spatial points $x \in \{0, \ldots, 9\}$. Example 5.1.

we assume that four random loads are located at $x_j = 2, 5, 7, 9$, $j = 1, 2, 3, 4$, *respectively. We will assume that all the loads are characterized by a common Gaussian distribution,* $P_j \sim \mathrm{N}(\mu_{P_j} = 20; \sigma^2_{P_j} = 0.02)$, $j = 1, \ldots, 4$.

In Fig. 5.9, we have graphically represented the 1-PDF, $f_{Y(x)}(y)$, *computed by* (5.26)–(5.28), *at the spatial positions* $x = j$, $j = 1, \ldots, 10$.

In Fig. 5.10, we have plotted the PDF of the maximum slope, $f_S(s)$, *and of the maximum deflection,* $f_D(d)$, *at the end of the cantilever beam. These two densities are given by* (5.30) *and* (5.31), *respectively. In Table 5.2, we present the numerical results of the mean and standard deviation of these two random variables.*

	Mean	**Standard deviation**
Slope at free end	0.00104897	0.000022371
Max. deflection	0.00783446	0.000163552

Table 5.2: Mean and standard deviation of the maximum slope and the maximum deflection of $Y(x)$. They have been obtained via the PDFs (5.30) and (5.31), respectively. Example 5.2.

In Fig. 5.11, we show a graphical representation of the PDF of the bending moment, $f_{M(x)}(m)$ *at different spatial points* $x \in \{0, \ldots, 8\}$. *Due to expression* (5.32) *at instants* $x \in \{9, 10\}$, *the value of the PDF computed by* (5.34) *is zero. Fig. 5.12*

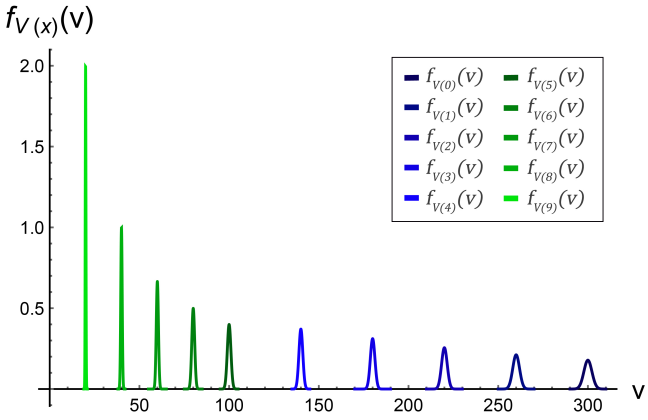

Figure 5.7: PDF of the shear force, $f_{V(x)}(v)$, using expression (5.21) at different spatial points $x \in \{0, \ldots, 9\}$. Example 5.1.

shows the plot of the PDFs of the shear force, $f_{V(x)}(v)$. Notice in this graphical representation that several PDFs match, namely, $f_{V(0)}(v) = f_{V(1)}(v) = f_{V(2)}(v)$, $f_{V(3)}(v) = f_{V(4)}(v) = f_{V(5)}(v)$, $f_{V(6)}(v) = f_{V(7)}(v)$ and $f_{V(8)}(v) = f_{V(9)}(v)$. This is a consequence of the definition of the shear force (see Eq. (5.33)) and the spatial points, $x_j = 2, 5, 7, 9$ (meters), $j = 1, 2, 3, 4$, where the loads have been placed. We can observe in Fig. 5.11 and Fig. 5.12 that the variance decreases as the position increases.

Finally, in Fig. 5.13, we show the mean plus/minus 2 standard deviations of the solution stochastic process, $Y(x)$.

Example 5.3 *(Case III) To illustrate the findings obtained in Section 5.4, we will consider that the density of downward force acting perpendicularly on the beam of length $l = 10\,\mathrm{m}$ is given by $Q(x) = q_0 + B(x)$, $0 < x < l$, $q_0 = 20$, and we will consider a Karhunen-Loève expansion truncated at order N to approximate the Brownian motion, $B(x)$.*

In Fig. 5.14, we show a graphical representation of the 1-PDF, $f_{Y(x)}(x)$, given by (5.39) for different spatial points $x \in \{1, \ldots, 10\}$ considering as truncating order $N = 1$ (later we justify this approximation is enough to achieve reliable results).

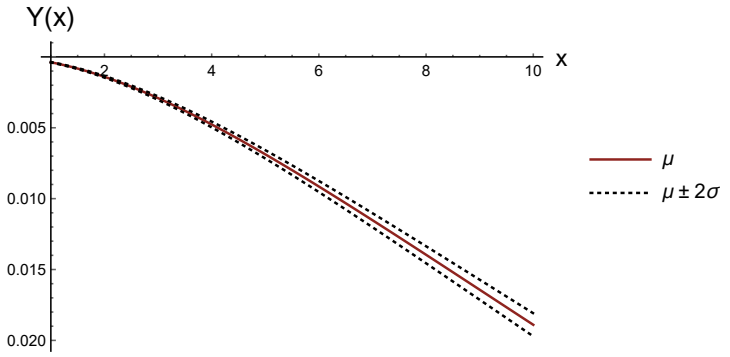

Figure 5.8: Mean (μ) plus/minus 2 standard deviations (σ) of the solution stochastic process, $Y(x)$. Example 5.1.

We can notice that the higher the position, the higher the variability, as expected, since the variability of the Brownian motion, $B(x)$, increases with x.

In Fig. 5.15, we show the PDF of the maximum slope and maximum deflection at the end of the cantilever beam. From both PDFs, we have calculated, in Table 5.3, approximations of the mean and standard deviation of these two random variables.

	Mean	**Standard deviation**
Slope at free end	0.0016496	0.00027951
Max. deflection	0.0164908	0.0020746

Table 5.3: Mean and standard deviation of the maximum slope and deflection at the free end of the cantilever beam, obtained via the PDF (5.41) and (5.43), respectively. Example 5.3.

In Fig. 5.16 and Fig. 5.17, we show, respectively, a graphical representation of the PDFs of the bending moment, $f_{M(x)}(m)$, and the PDFs of the shear force, $f_{V(x)}(v)$, at different spatial points $x \in \{0, \ldots, 9\}$. Recall that $x = 0$ reaches their maximum value (positive or negative) and at $x = l = 10$, $M(l) = 0$ and $V(l) = 0$. To compute these PDFs we have considered again the truncating order $N = 1$. This causes expressions (5.46) *and* (5.47) *to change their structure slightly. So,*

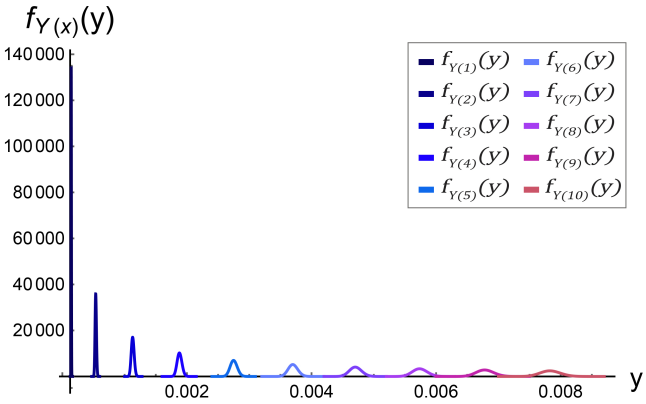

Figure 5.9: 1-PDF, $f_{Y(x)}(y)$, of the solution stochastic process (5.23), computed by (5.26)–(5.28), at the different spatial points $x = j$, $j = 1, 2, \ldots, 10$. Example 5.2.

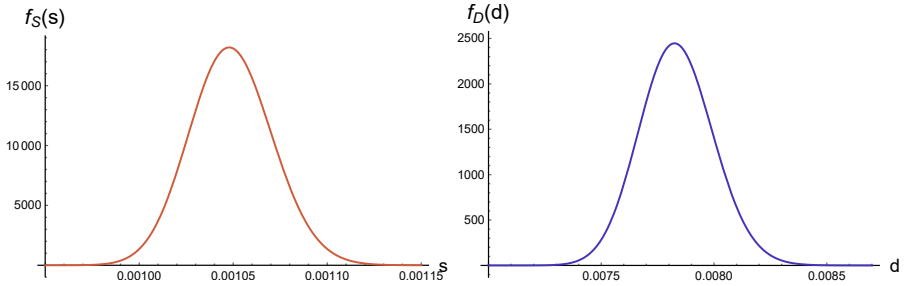

Figure 5.10: Left: PDF, $f_S(s)$, of the maximum slope at free end. Right: PDF, $f_D(d)$, of the maximum deflection at the free end. Example 5.2.

the PDF of the bending moment for $N = 1$ is given by

$$f_{M(x)}(m) = f_{\xi_1}\left(\left(m + \frac{q_0}{2}\left(l^2 + x^2 - 2xl\right)\right)\left(-\sqrt{\frac{2}{l}}\left(\frac{1-\cos(b_1 l)}{b_1^2}(l-x) + \frac{b_1(x-l) + \sin(b_1 l) - \sin(b_1 x)}{b_1^3}\right)\right)^{-1}\right) \cdot \left|-\sqrt{\frac{2}{l}}\left(\frac{1-\cos(b_1 l)}{b_1^2}(l-x) + \frac{b_1(x-l) + \sin(b_1 l) - \sin(b_1 x)}{b_1^3}\right)\right|^{-1}, \tag{5.48}$$

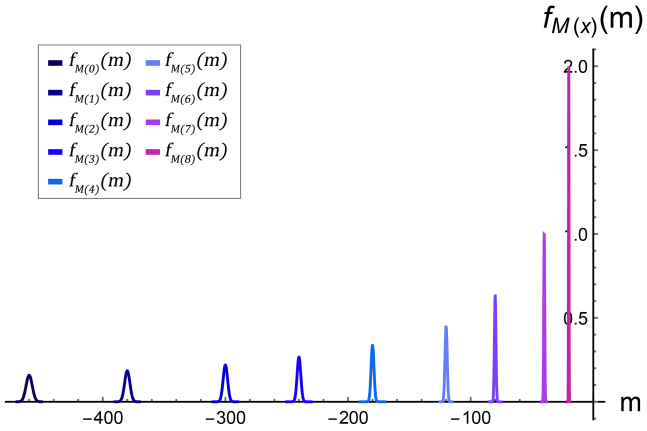

Figure 5.11: PDF of the bending moment, $f_{M(x)}(m)$, using expression (5.34) at different spatial points $x \in \{0, \ldots, 8\}$. Example 5.2.

and the PDF of the shear force is given by

$$f_{V(x)}(v) = f_{\xi_1}\left((v + q_0(x-l))\left(-\sqrt{\frac{2}{l}}\left(\frac{\cos(b_1 l) - \cos(b_1 x)}{b_1^2}\right)\right)^{-1}\right) \cdot \left|-\sqrt{\frac{2}{l}}\left(\frac{\cos(b_1 l) - \cos(b_1 x)}{b_1^2}\right)\right|^{-1}. \tag{5.49}$$

Again, we can observe in both figures that the variance decreases as the position increases.

In Fig. 5.18, we show the mean (μ) plus/minus 2 standard deviations of the solution stochastic process, $Y(x)$, on the whole spatial domain.

Finally, in Table 5.4, we show a comparison of the values of the mean and standard deviation of the maximum deflection of the cantilever beam, D, considering different orders of truncation, $N \in \{1, 2, 3, 10, 50\}$, of $B(x)$ via a Karhunen-Loève expansion. We can observe that approximations are very similar with $N = 1$. This justifies that our previous calculations have been carried out computations with this order. Similar conclusions are derived from the PDFs, as we can observe from Fig. 5.19.

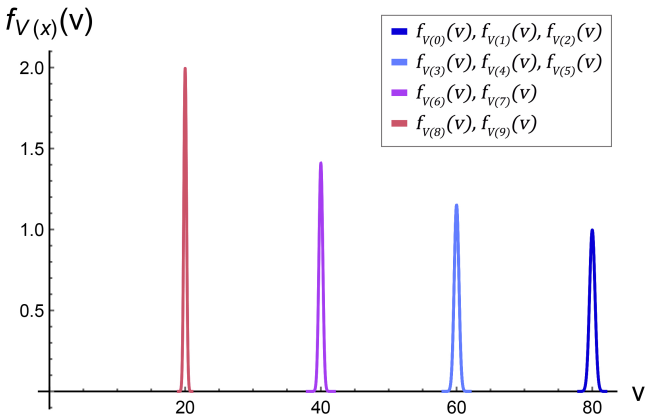

Figure 5.12: PDF of the shear force, $f_{V(x)}(v)$, using expression (5.35) at different spatial points $x \in \{0, \ldots, 9\}$. Example 5.2.

	N = 1	**N = 2**	**N = 3**	**N = 10**	**N = 50**
Mean	0.0164908	0.0164886	0.0164946	0.0164893	0.016493
Standard deviation	0.0020746	0.0020860	0.0020821	0.0020854	0.0020879

Table 5.4: Mean and standard deviation of the maximum deflection, D, at free end, obtained via the PDF (5.43) for different values of the truncation order, N, to approximate the Brownian motion by its Karhunen-Loève expansion, $N \in \{1, 2, 3, 10, 50\}$. Example 5.3.

5.6 Conclusions

Throughout the chapter, we have studied, from a probabilistic standpoint, a foundational model to describe the deflection of a static cantilever beam subject to different loads, which is relevant in the civil engineering literature. Our analysis has several advantages. First, it permits computing not only the mean and the standard deviation of deflection but also its probability density function that provides a fuller description. Secondly, our theoretical findings have been obtained under very general hypotheses since we have considered a complete randomization of model parameters (the density of downward force acting perpendicularly on the beam and the Young's modulus, denoted by $Q(x)$ and E, respectively). Even more, the results obtained in every one of the three cases analysed in the chapter have been established, assuming arbitrary probability density functions for the

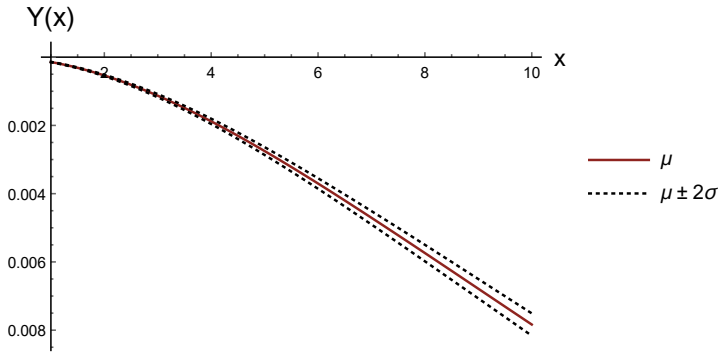

Figure 5.13: Mean (μ) plus/minus 2 standard deviations (σ) of the solution stochastic process, $Y(x)$. Example 5.2.

random parameters involved in the model. This gives a great generality to our results. Besides, we have probabilistically characterized, via the corresponding densities, essential quantities of interest such as the slope, maximum deflection, bending moment, and shear force of the cantilever beam under mild hypotheses. Furthermore, we have shown that the Random Variable Transformation technique provides a comprehensive, systematic, and unifying tool to obtain mathematical results in a variety of scenarios, allowing us to obtain general formulas that are very useful for carrying out computations, as shown in the examples.

Publications associated with this chapter

The results of this chapter have been presented at the International Conference on Mathematical Analysis and Applications in Science and Engineering (ICMAS2SC'22) in Porto (Portugal) from June 27-29, 2022. The talk, titled *Probabilistic analysis of a cantilever beam with random parameters via probability density functions*, was published in the conference proceedings with ISBN 978-989-53496-3-0. Additionally, a complete version of the chapter's findings has been published in the paper [24].

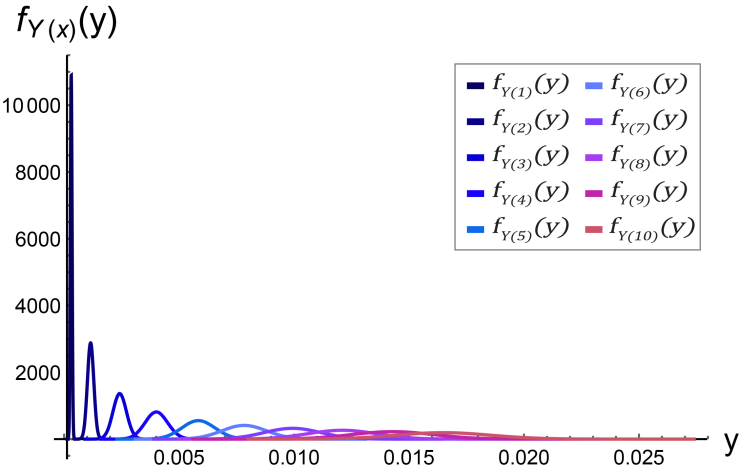

Figure 5.14: 1-PDF, $f_{Y(x)}(y)$, of the solution stochastic process (5.38), computed by (5.39), at different spatial position $x \in \{1, \ldots, 10\}$ of the cantilever beam considering an approximation of the Brownian motion, $B(x)$, via a Karhunen-Loève expansion truncated at order $N = 1$. Example 5.3.

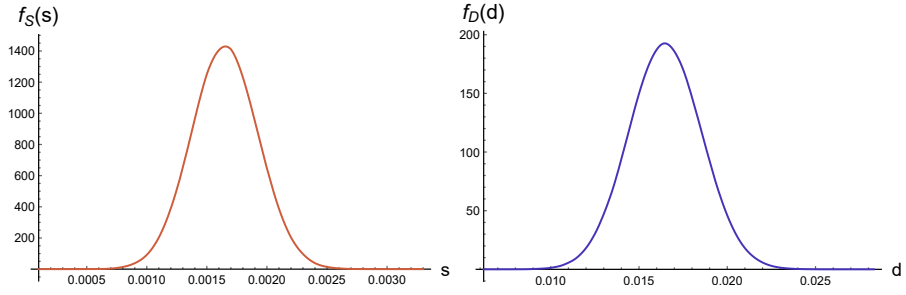

Figure 5.15: Left: PDF, $f_S(s)$, of the maximum slope at free end. Right: PDF, $f_D(d)$, of the maximum deflection at the free end. Example 5.3.

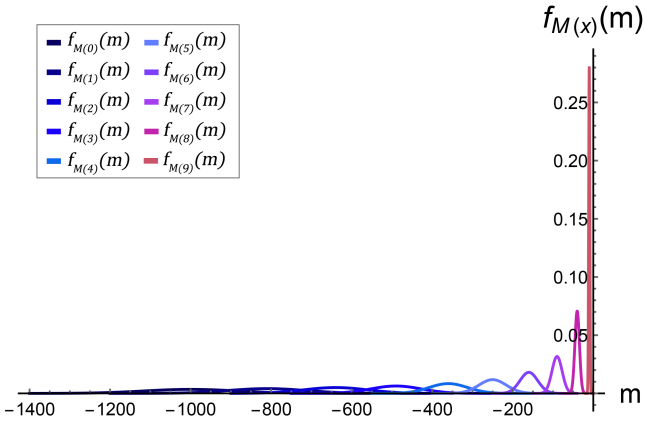

Figure 5.16: PDF of the bending moment, $f_{M(x)}(m)$, using expression (5.46) at different spatial points $x \in \{0, \ldots, 8\}$. Example 5.3.

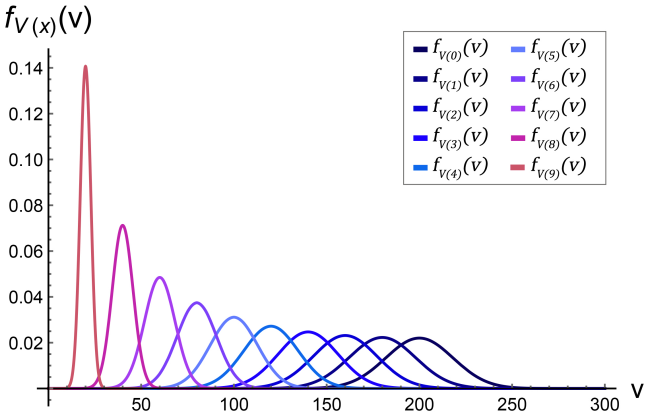

Figure 5.17: PDF of the shear force, $f_{V(x)}(v)$, using expression (5.47) at different spatial points $x \in \{0, \ldots, 9\}$. Example 5.3.

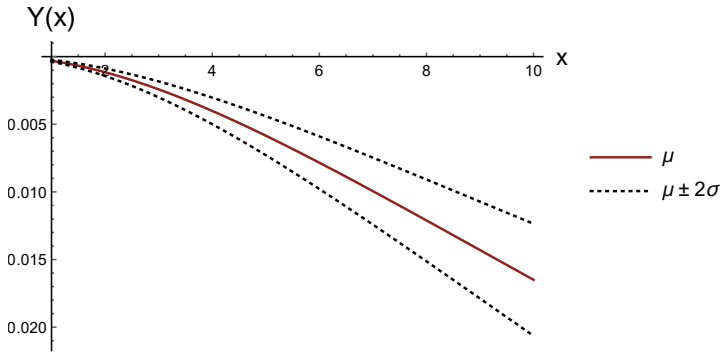

Figure 5.18: Mean (μ) plus/minus 2 standard deviations of the solution stochastic process, $Y(x)$. Example 5.3.

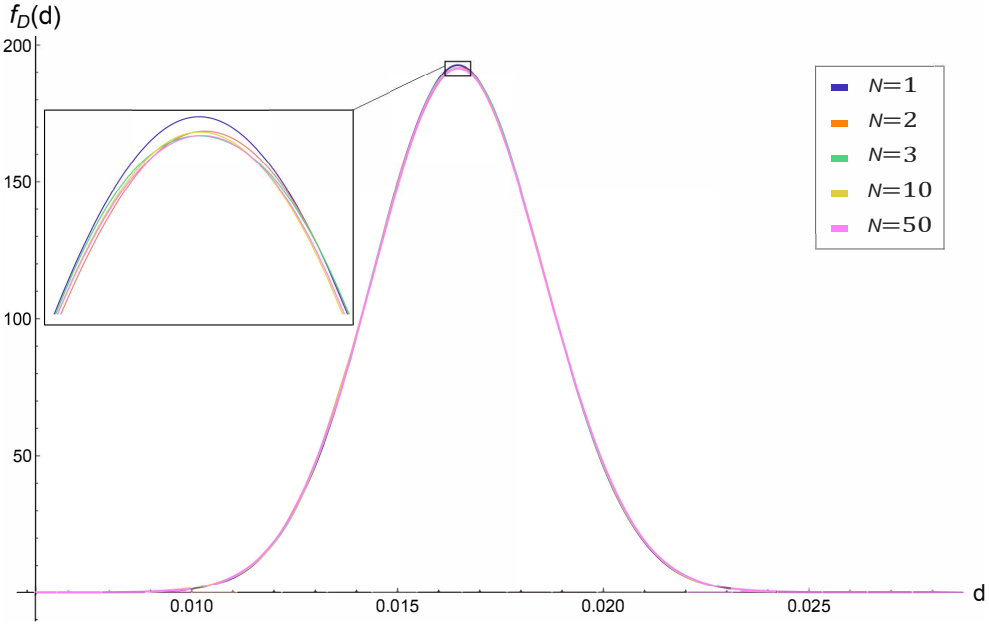

Figure 5.19: PDF of the maximum deflection at free end, $f_D(d)$, for different values of the truncation order, N, to approximate the Brownian motion by its Karhunen-Loève expansion $N \in \{1, 2, 3, 10, 50\}$. Example 5.3.

Chapter 6

Extending the probabilistic analysis of the Euler-Bernoulli model for a stochastic static cantilever beam

In this chapter, we present a comprehensive probabilistic analysis of the deflection of a static cantilever beam based on Euler-Bernoulli's theory. For the sake of generality in our stochastic study, we will assume that all model parameters (Young's modulus and the beam moment of inertia) are random variables with arbitrary probability densities, while the loads applied on the beam are described via a Poisson delta-correlated process. The probabilistic study is based on the calculation of the first probability density function of the solution and the probability density of other key quantities of interest, such as the shear force and the bending moment, which are treated as random variables too. To conduct our study, we will first calculate the first moments of the solution, which is a stochastic process, and we then will take advantage of the Principle of Maximum Entropy. Furthermore, we will present an algorithm, based on Monte Carlo simulations, that allows us to simulate our analytical development computationally. The theoretical findings will be illustrated with numerical examples where different realistic probability distributions are assumed for each model random parameter.

6.1 Introduction

In this chapter, we perform a full probabilistic study of the deflection of a static cantilever beam using the Euler-Bernoulli's model, see Eq. (1.2), with the main novelty, w.r.t. the study performed in Chapter 5, that all its parameters (Young's modulus and the beam moment of inertia) are treated as random variables and that the load applied on the beam is assumed to be described by a Poisson delta-correlated process. Notice that in the previous chapter, we assumed the moment of inertia as a deterministic parameter. We will calculate the solution's 1-PDF via the PME. To achieve this goal, we first calculate the first statistical moments of the solution. To complete the study, we also determine the PDF of the shear force, and the bending moment, which are treated as random variables. We also introduce an algorithm, based on the Monte Carlo method, to carry out simulations from our theoretical findings. It is important to point out that the calculation of the first moments of the solution is based on the so-called generalized functions. This technique is introduced in [35], where authors elegantly analyze other types of beams, different from a cantilever, assuming partial randomization of the models under study. Particularly, they assume the flexural rigidity parameter is deterministic. In the present chapter, apart from studying another type of beam, namely the cantilever, dealing with the full randomization of the corresponding Euler-Bernoulli's model, we also obtain the 1-PDF of the solution, which, as it was pointed out in Chapter 2, is the most important information associated with a stochastic process. Indeed, from the 1-PDF one can determine any one-dimensional statistical moment as well as the probability that the deflection varies on a specific interval of interest. This is key information to, for example, analyze and quantify the main risks that may affect civil structures. As it has been said, the calculation of the 1-PDF will be done utilizing the PME. It is instructive to point out that the PME method has been widely applied in civil engineering. In [107], the authors obtain the PDF of the shear capacity of the reinforced concrete beam using PME and compare it with brute force Monte Carlo simulation, obtaining good approximations. In [21], the PME is modified to estimate the PDF of the material's fiber-reinforced concrete properties using their different order moments. In [42], authors combine polynomial chaos expansions with a variation of the classical PME to approximate the PDF of the response to several structural engineering problems.

In [62], one proposes a new method for constructing the so-called probability box (p-box) model based on the PME. The results are applied to perform a reliability analysis for uncertain engineering structures.

The chapter is organized as follows. Section 6.2 introduces some deterministic and stochastic preliminaries required to conduct the aforementioned probabilistic study of the deflection of a cantilever beam subject to loads and assuming that the model parameters, namely, the material Young's modulus of elasticity and the beam moment of inertia are random variables. In Section 6.3, we carry out the analysis of the stochastic model by first computing, under very general conditions of the model parameters, the mean and variance of the deflection. These two statistical moments will be required later to approximate its 1-PDF taking advantage of the PME method. Apart from the deflection, we will also calculate approximations of the mean, the variance, and the PDF of other relevant physical quantities associated with the beam, such as the bending moment and the shear force. In Section 6.4, we present an algorithm, based on Monte Carlo simulations, that allows us to simulate all the abovementioned physical quantities effectively. The theoretical results obtained in Section 6.3 are compared with the ones obtained via simulations using the algorithm presented in Section 6.4. Finally, conclusions are drawn in Section 6.6.

6.2 Problem setting and preliminaries

As we have seen in the previous chapter, when EI is constant, the Eq. (1.2) can be expressed as follows:

$$\frac{\mathrm{d}^4 Y(x)}{\mathrm{d}x^4} = \frac{1}{EI} Q(x), \quad 0 < x < l. \tag{6.1}$$

This equation, together with the boundary conditions $Y(0) = 0$, $Y'(0) = 0$, $Y''(l) = 0$, and $Y'''(l) = 0$ represent the deflection of a static cantilever beam, see expressions (1.3). The meaning of each quantity in the previous model can be seen in the previous chapter, see model (5.1).

Based on the reasons explained in Section 6.1, we will consider that the distribution of the load supported on the beam, $Q(x)$, is described by a stochastic process.

Specifically, we will assume that $Q(x)$ is determined by concentrated loads, P_i, acting vertically on the beam and randomly spanned according to the following expression,

$$Q(x) = \sum_{i=1}^{N(l)} P_i R_{-1}(x - x_i), \tag{6.2}$$

where P_i are assumed to be i.i.d. random variables, representing concentrated loads acting at the abscissas $x_i \in (0, l)$. $N(l)$ denotes a Poisson counting process with rate $\lambda > 0$. This parameter can be interpreted as the expected number of random loads, P_i, that randomly apply per unit of space on the beam. Following the notation used in [34], we use the term $R_{-1}(x - x_i) := \delta(x - x_i)$ to indicate that P_i, $1 \leq i \leq n$, represent concentrated loads at the spatial points x_i. Here, $\delta(\cdot)$ denotes the Dirac delta function. Furthermore, hereinafter we will assume that E and I are independent random variables, so notice that they do not depend on x. Fig. 6.1 shows a graphical representation of the model.

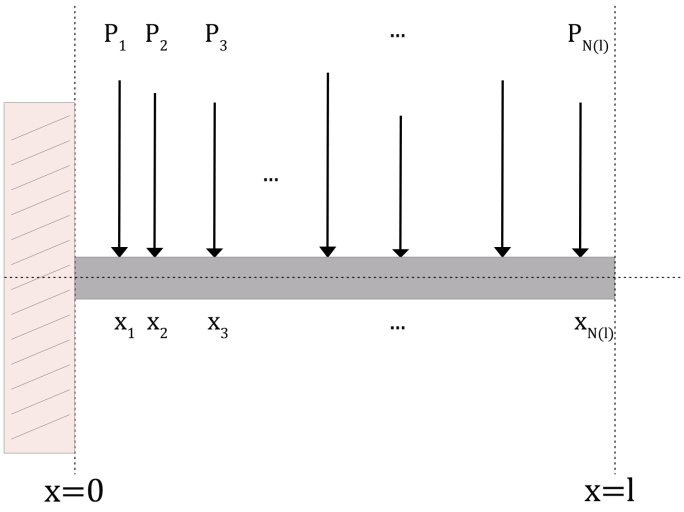

Figure 6.1: Graphical representation of model (6.1), where the distribution of the random concentrated loads, P_i, on the spatial points x_i of the beam is described by the stochastic process given in (6.2).

Remark 6.1 *Throughout this chapter, we will use the most well-known generalized function in $Q(x)$, i.e., the Dirac delta function. We will use this function to represent a concentrated load at an arbitrary spatial point, say x_0. Defining*

$$R_{-1}(x - x_0) := \delta(x - x_0), \tag{6.3}$$

by integration, we obtain $R_0(x - x_0)$, which is the unit step or Heaviside function. If we continue integrating up to order $n \in \mathbb{N}$, we arrive at the following piecewise polynomial function

$$R_n(x - x_0) = \begin{cases} 0, & \text{if } x < x_0, \\ \frac{1}{n!}(x - x_0)^n, & \text{if } x \geq x_0, \end{cases} \tag{6.4}$$

that, for $n = 1, 2, 3$, corresponds to the linear, quadratic, and cubic ramp functions, respectively. Notice that, (6.4) also works for $n = 0$. As it shall be seen later, these functions $R_0(\cdot)$, $R_1(\cdot)$, $R_2(\cdot)$ and $R_3(\cdot)$ will be extensively used in our subsequent calculations.

The stochastic process given by (6.2) is known as the delta-correlated process [95] (also termed Poisson white noise process [41, p.186]). The process $Q(x)$ can be regarded as the formal derivative of its corresponding associated compound Poisson process, $C(x) = \sum_{i=1}^{N(l)} P_i$, $0 < x < l$, i.e. $\frac{\mathrm{d}C(x)}{\mathrm{d}x} = Q(x)$. As we have seen before, this process consists of a Poisson counting process, $N(l)$, and random intensities, P_i, acting at the spatial points on the beam, x_i, $i = 1, \ldots, N(l)$ (this action is mathematically represented by $P_i R_{-1}(x - x_i)$). The loads P_i are distributed along the beam according to a Poisson distribution. This process is widely used to model concentrated loads simulating, for example, cars traveling on a bridge, which has motivated its consideration in our analysis.

We now introduce several statistical properties that will play a key role later for a class of random processes that include, as a particular case, the foregoing random processes $Q(x)$ and

$$G_j(x) := \sum_{i=1}^{N(l)} P_i R_j(x - x_i), \quad j = 0, \ldots, 3, \tag{6.5}$$

are filtered Poisson processes [58], which depend on the loads, P_i, which are randomly spanned on the beam according to a Poisson counting process $N(l)$. Let

$$Z(x) = \sum_{i=1}^{N(l)} U_i v(x, x_i) \tag{6.6}$$

be a stochastic process constructed by superposition of pulses at the spatial points x_i whose shape is defined by a deterministic function $v = v(x, x_i)$ and having pulse intensities given by a family of i.i.d. random variables U_i. As shown in [58], the probabilistic structure of $Z = Z(x)$ can be revealed via the characteristic functional. Indeed, it can be shown that the cumulant function of order m of Z is given by

$$C_Z^{(m)}(x_1, \ldots, x_m) = \lambda \mathbb{E}\left[U^m\right] \int_0^{\min(x_1,\ldots,x_m)} v(\rho, x_1) \cdots v(\rho, x_m) \mathrm{d}\rho. \tag{6.7}$$

Note that we here have used $x_1, \ldots, x_m$ to denote the variables of function C_Z for the sake of consistency with the independent variable x of Z, although any other letter could be used too. As a consequence of the properties of cumulants [58], the mean and the covariance can be obtained as particular cases of $C_{Z(x)}^{(m)}(x_1, \ldots, x_m)$:

$$\mu_Z(x) = \mathbb{E}\left[Z(x)\right] = \lambda \mathbb{E}\left[U\right] \int_0^x v(\rho, x) \mathrm{d}\rho = C_{Z(x)}^{(1)}(x), \tag{6.8}$$

and

$$\begin{aligned} \mathbb{C}\mathrm{ov}_Z(x_1, x_2) &= \mathbb{E}\left[Z(x_1)Z(x_2)\right] - \mathbb{E}\left[Z(x_1)\right]\mathbb{E}\left[Z(x_2)\right] \\ &= \lambda \mathbb{E}\left[U^2\right] \int_0^{\min(x_1,x_2)} v(\rho, x_1) v(\rho, x_2) \mathrm{d}\rho \\ &= C_Z^{(2)}(x_1, x_2). \end{aligned} \tag{6.9}$$

Hence, the variance is given by

$$\sigma_Z^2(x) = C_Z^{(2)}(x, x). \tag{6.10}$$

Later we will also need to handle the cross-covariance of two stochastic processes, say Z_v=$Z_v(x)$ and Z_w=$Z_w(x)$, of the form of (6.6) with different shapes, v and w,

$$Z_v(x) = \sum_{i=1}^{N(l)} U_i v(x, x_i), \quad Z_w(x) = \sum_{i=1}^{N(l)} U_i w(x, x_i). \tag{6.11}$$

In this case, the cross-cumulant function of order $m = 2$, which is just the cross-covariance of Z_v and Z_w, writes

$$C^{(2)}_{Z_v,Z_w}(x_1, x_2) = \lambda \mathbb{E}\left[U^2\right] \int_0^{\min(x_1,x_2)} v(\rho, x_1) w(\rho, x_2) \mathrm{d}\rho. \tag{6.12}$$

As it shall be seen in the next section, these properties will be essential to obtain, in the first step, the mean and the variance of $Y(x)$, i.e., the deflection of the cantilever beam. Afterward, from these two statistics, we will approximate the 1-PDF of the solution taking advantage of the PME. Furthermore, we will determine other engineering probabilistic quantities of interest associated with the beam, such as the bending moment and the shear force.

6.3 Concentrated random loads P_i spanned randomly on the beam

In this section, we will carry out a probabilistic study of model (6.1). For the sake of clarity, we substitute expression (6.2) into Eq. (6.1) and we then obtain

$$\begin{cases} \dfrac{\mathrm{d}^4 Y(x)}{\mathrm{d}x^4} = \dfrac{1}{EI} \displaystyle\sum_{i=1}^{N(l)} P_i R_{-1}(x - x_i), \quad 0 < x < l, \\ Y(0) = 0, \;\; Y'(0) = 0, \;\; Y''(l) = 0, \;\; Y'''(l) = 0. \end{cases} \tag{6.13}$$

To conduct the probabilistic study of model (6.13), we first need to obtain its solution. For this purpose, we take advantage of the one obtained in [35]. The difference between the two of them lies in the type of beam and, therefore, in the boundary conditions of the model. Based on the solution

$$Y(x) = \frac{1}{EI} \sum_{i=1}^{N(l)} P_i R_3(x - x_i) + \frac{1}{6} C_1 x^3 + \frac{1}{2} C_2 x^2 + C_3 x + C_4, \tag{6.14}$$

we use the boundary conditions of model (6.13) in order to compute the integration constants C_1, C_2, C_3, and C_4.

First, we calculate C_4

$$Y(0) = 0 \rightarrow C_4 = 0, \tag{6.15}$$

and C_3

$$Y'(0) = 0 \rightarrow C_3 = 0. \tag{6.16}$$

Second, we calculate C_1 using the third derivative

$$Y'''(l) = 0 \rightarrow \frac{1}{EI} \sum_{i=1}^{N(l)} P_i R_0(l - x_i) + C_1 = 0 \rightarrow C_1 = -\frac{1}{EI} \sum_{i=1}^{N(l)} P_i R_0(l - x_i), \tag{6.17}$$

and finally, we calculate C_2

$$Y''(l) = 0 \rightarrow \frac{1}{EI} \sum_{i=1}^{N(l)} P_i R_1(l - x_i) - \frac{1}{EI} \sum_{i=1}^{N(l)} P_i R_0(l - x_i) l + C_2 = 0, \tag{6.18}$$

$$C_2 = -\frac{1}{EI} \left(\sum_{i=1}^{N(l)} P_i R_1(l - x_i) - \sum_{i=1}^{N(l)} P_i R_0(l - x_i) l \right). \tag{6.19}$$

Now, replacing the obtained integration constants into (6.14) and reorganizing the solution, one obtains

$$Y(x) = \frac{1}{EI} \left(G_3(x) - \frac{1}{6} G_0(l) x^3 - \frac{1}{2} \left(G_1(l) - l G_0(l) \right) x^2 \right), \tag{6.20}$$

where $G_j(x)$ has been defined in (6.5).

The function $G_j(x)$ represents the load function, which is independent of the beam characteristics. However, for the sake of convenience in our subsequent computations, we introduce the following relabeling of the previous stochastic process $G_j(x)$,

$$\widehat{G}_j(x) = \sum_{i=1}^{N(l)} F_i R_j(x - x_i), \quad j = 0, 1, 2, 3, \qquad F_i = \frac{P_i}{EI}, \tag{6.21}$$

where $\widehat{G}_j(x)$ is now also dependent on the beam characteristics. This allows us to rewrite $Y(x)$ given in (6.20) in terms of the stochastic processes $\widehat{G}_j(x)$:

$$Y(x) = \widehat{G}_3(x) - \frac{1}{6}\widehat{G}_0(l)x^3 - \frac{1}{2}\left(\widehat{G}_1(l) - l\widehat{G}_0(l)\right)x^2. \tag{6.22}$$

As has been indicated in Section 6.2, we are interested in approximating the 1-PDF of the deflection of the beam, and for this goal, we shall apply the PME method. So we will first calculate the mean of the deflection, taking the expectation operator in expression (6.20)

$$\mathbb{E}[Y(x)] = \mathbb{E}[\widehat{G}_3(x)] - \frac{1}{6}\mathbb{E}[\widehat{G}_0(l)]x^3 - \frac{1}{2}\left(\mathbb{E}[\widehat{G}_1(l)] - l\mathbb{E}[\widehat{G}_0(l)]\right)x^2. \tag{6.23}$$

In order to provide an explicit representation of $\mathbb{E}[Y(x)]$, we shall compute $\mathbb{E}[\widehat{G}_j(x)]$, $j = 0, \ldots, 3$. Notice that $\mathbb{E}[\widehat{G}_2(x)]$ is not specifically required for computing $\mathbb{E}[Y(x)]$, but it will also be calculated because it will be needed later. To this end, we will take advantage of expectation $\mathbb{E}[Z(x)]$, given in (6.8), of the stochastic process $Z(x)$ defined in (6.6) with the following identification in terms of $\widehat{G}_j(x)$ defined in (6.21): the impulse shapes and pulse intensities are given by $v(x, x_i) := R_j(x - x_i)$, $j = 0, \ldots, 3$, and $U_i := F_i$, respectively. Then, taking into account the definition of functions $R_j(x - x_j)$, given in (6.4), one obtains:

$$\begin{aligned}\mathbb{E}[\widehat{G}_0(x)] = C^{(1)}_{\widehat{G}_0}(x) &= \lambda\mathbb{E}\left[F_i\right]\int_0^x R_0(x-\rho)\mathrm{d}\rho \\ &= \lambda\mathbb{E}\left[F_i\right]\int_0^x \mathrm{d}\rho = \lambda\mathbb{E}\left[F_i\right]x,\end{aligned} \tag{6.24}$$

$$\begin{aligned}\mathbb{E}\left[\widehat{G}_1(x)\right] = C^{(1)}_{\widehat{G}_1}(x) &= \lambda\mathbb{E}\left[F_i\right]\int_0^x R_1(x-\rho)\mathrm{d}\rho \\ &= \lambda\mathbb{E}\left[F_i\right]\int_0^x (x-\rho)\mathrm{d}\rho = \frac{\lambda}{2}\mathbb{E}\left[F_i\right]x^2,\end{aligned} \tag{6.25}$$

$$\begin{aligned}\mathbb{E}[\widehat{G}_2(x)] = C^{(1)}_{\widehat{G}_2}(x) &= \lambda \mathbb{E}\left[F_i\right] \int_0^x R_2(x-\rho)\mathrm{d}\rho \\ &= \lambda \mathbb{E}\left[F_i\right] \int_0^x \frac{1}{2}(x-\rho)^2 \mathrm{d}\rho = \frac{\lambda}{6}\mathbb{E}\left[F_i\right] x^3,\end{aligned} \tag{6.26}$$

and

$$\begin{aligned}\mathbb{E}[\widehat{G}_3(x)] = C^{(1)}_{\widehat{G}_3}(x) &= \lambda \mathbb{E}\left[F_i\right] \int_0^x R_3(x-\rho)\mathrm{d}\rho \\ &= \lambda \mathbb{E}\left[F_i\right] \int_0^x \frac{1}{6}(x-\rho)^3 \mathrm{d}\rho = \frac{\lambda}{24}\mathbb{E}\left[F_i\right] x^4.\end{aligned} \tag{6.27}$$

Then, substituting the above expressions in (6.23), one gets the following expression for the expectation of $Y(x)$:

$$\mathbb{E}[Y(x)] = \frac{\lambda}{2}\mathbb{E}\left[F_i\right]\left(\frac{1}{12}x^4 - \frac{1}{3}lx^3 + \frac{1}{2}l^2x^2\right). \tag{6.28}$$

Now, we compute the covariance of $Y(x)$ using the representation (6.20) and its properties as a positive semidefinite function:

$$\begin{aligned}\mathbb{C}\mathrm{ov}_Y(x_1,x_2) &= \mathbb{E}\left[Y(x_1)Y(x_2)\right] - \mathbb{E}\left[Y(x_1)\right]\mathbb{E}\left[Y(x_2)\right] \\ &= C^{(2)}_{\widehat{G}_3}(x_1,x_2) - \frac{1}{2}C^{(2)}_{\widehat{G}_3\widehat{G}_1}(x_1,l)x_2^2 - \frac{1}{2}C^{(2)}_{\widehat{G}_3\widehat{G}_1}(x_2,l)x_1^2 \\ &\quad + \frac{1}{4}C^{(2)}_{\widehat{G}_1}(l,l)x_1^2x_2^2 + \frac{1}{2}C^{(2)}_{\widehat{G}_3\widehat{G}_0}(x_1,l)\left(lx_2^2 - \frac{1}{3}x_2^3\right) \\ &\quad + \frac{1}{2}C^{(2)}_{\widehat{G}_3\widehat{G}_0}(x_2,l)\left(lx_1^2 - \frac{1}{3}x_1^3\right) \\ &\quad + \frac{1}{4}C^{(2)}_{\widehat{G}_0}(l,l)\left(\frac{1}{9}x_1^3x_2^3 - \frac{l}{3}x_1^3x_2^2 - \frac{l}{3}x_1^2x_2^3 + l^2x_1^2x_2^2\right) \\ &\quad + \frac{1}{2}C^{(2)}_{\widehat{G}_0\widehat{G}_1}(l,l)\left(\frac{1}{6}x_1^3x_2^2 + \frac{1}{6}x_1^2x_2^3 - lx_1^2x_2^2\right).\end{aligned} \tag{6.29}$$

Taking $x_1 = x_2 = x$ in the above expression, using that $C^{(2)}_{\widehat{G}_j}(x,x) = \sigma^2_{\widehat{G}_j}(x)$, and after some algebraic manipulations, one can obtain the variance of $Y(x)$,

$$\begin{aligned}\sigma^2_Y(x) = C^{(2)}_Y(x,x) &= \mathbb{E}\left[Y(x)^2\right] - \mathbb{E}\left[Y(x)\right]^2 \\ &= \sigma^2_{\widehat{G}_3}(x) - C^{(2)}_{\widehat{G}_3\widehat{G}_1}(x,l)x^2 + \frac{1}{4}\sigma^2_{\widehat{G}_1}(l)x^4 + C^{(2)}_{\widehat{G}_3\widehat{G}_0}(x,l)\left(lx^2 - \frac{1}{3}x^3\right) \\ &\quad + \frac{1}{4}\sigma^2_{\widehat{G}_0}(l)\left(\frac{1}{9}x^6 - \frac{2}{3}lx^5 + l^2x^4\right) + \frac{1}{2}C^{(2)}_{\widehat{G}_0\widehat{G}_1}(l,l)\left(\frac{1}{3}x^5 - lx^4\right).\end{aligned} \tag{6.30}$$

In this expression, we now compute the terms of the form $\sigma^2_{\widehat{G}_j}$ and $C^{(2)}_{\widehat{G}_i\widehat{G}_j}$, using (6.10) and (6.12), respectively,

$$\sigma^2_{\widehat{G}_3}(x) = \lambda\mathbb{E}[F_i^2]\int_0^x R_3(x-\rho)R_3(x-\rho)\mathrm{d}\rho = \frac{\lambda}{252}\mathbb{E}\left[F_i^2\right]x^7, \tag{6.31}$$

$$C^{(2)}_{\widehat{G}_3\widehat{G}_1}(x,l) = \lambda\mathbb{E}[F_i^2]\int_0^x R_3(x-\rho)R_1(l-\rho)\mathrm{d}\rho = \frac{\lambda}{24}\mathbb{E}\left[F_i^2\right]x^4\left(l - \frac{1}{5}x\right), \tag{6.32}$$

$$\sigma^2_{\widehat{G}_1}(l) = \lambda\mathbb{E}[F_i^2]\int_0^l R_1(l-\rho)R_1(l-\rho)\mathrm{d}\rho = \frac{\lambda}{3}\mathbb{E}\left[F_i^2\right]l^3, \tag{6.33}$$

$$C^{(2)}_{\widehat{G}_3\widehat{G}_0}(x,l) = \lambda\mathbb{E}[F_i^2]\int_0^x R_3(x-\rho)R_0(l-\rho)\mathrm{d}\rho = \frac{\lambda}{24}\mathbb{E}\left[F_i^2\right]x^4, \tag{6.34}$$

$$\sigma^2_{\widehat{G}_0}(l) = \lambda\mathbb{E}[F_i^2]\int_0^l R_0(l-\rho)R_0(l-\rho)\mathrm{d}\rho = \lambda\mathbb{E}\left[F_i^2\right]l, \tag{6.35}$$

$$C^{(2)}_{\widehat{G}_0\widehat{G}_1}(l,l) = \lambda\mathbb{E}[F_i^2]\int_0^l R_0(l-\rho)R_1(l-\rho)\mathrm{d}\rho = \frac{\lambda}{2}\mathbb{E}\left[F_i^2\right]l^2. \tag{6.36}$$

Substituting these expressions into (6.30) and after simplifying, one gets the following expression of the variance

$$\sigma^2_Y(x) = \frac{\lambda}{12}\mathbb{E}[F_i^2]\left(-\frac{2}{105}x^7 + \frac{1}{3}lx^6 - l^2x^5 + l^3x^4\right). \tag{6.37}$$

Consequently, the second-order moment of the deflection is

$$\mathbb{E}\left[Y^2(x)\right] = \sigma_Y^2(x) + \mathbb{E}[Y(x)]^2 = \frac{\lambda}{12}\mathbb{E}[F_i^2]\left(-\frac{2}{105}x^7 + \frac{1}{3}lx^6 - l^2x^5 + l^3x^4\right) + \frac{\lambda^2}{12}\mathbb{E}[F_i]^2\left(\frac{1}{48}x^8 - \frac{1}{6}lx^7 + \frac{7}{12}l^2x^6 - l^3x^5 + \frac{3}{4}l^4x^4\right). \tag{6.38}$$

This expression will be used later when applying the PME to approximate the 1-PDF of the deflection $Y(x)$.

As we have seen in the previous chapter, two characteristics that are very important when studying beams in engineering are the bending moment, $M(x)$, and the shear force, $T(x)$, defined as

$$M(x) := -EIY''(x), \text{ and } T(x) := -EIY'''(x),$$

respectively [97]. These physical quantities can be calculated differentiating (6.20) and (6.5), and taking into account that, by (6.4), $R_3''(x) = R_1(x)$ and $R_3'''(x) = R_0(x)$, so $G_3''(x) = G_1(x)$ and $G_3'''(x) = G_0(x)$. Consequently,

$$M(x) = -G_1(x) + G_1(l) - G_0(l)(l - x), \tag{6.39}$$

and

$$T(x) = -G_0(x) + G_0(l). \tag{6.40}$$

Applying the expectation operator in (6.39) and (6.40), and using the expressions obtained in (6.24) and (6.25), one calculates the value of the mean of the bending moment

$$\mathbb{E}\left[M(x)\right] = -\frac{1}{2}\lambda\mathbb{E}\left[P_i\right]\left(x^2 + l^2 - 2lx\right), \tag{6.41}$$

and the shear force

$$\mathbb{E}\left[T(x)\right] = -\lambda\mathbb{E}\left[P_i\right](x - l). \tag{6.42}$$

Now, we compute the variance of the bending moment of the beam

$$\begin{aligned}\sigma_M^2(x) &= C_M^{(2)}(x,x) = \mathbb{E}\left[M(x)^2\right] - \mathbb{E}\left[M(x)\right]^2 \\ &= \sigma_{G_1}^2(x) - 2C_{G_1}^{(2)}(x,l) + 2C_{G_1G_0}^{(2)}(x,l)(l-x) + \sigma_{G_1}^2(l) \\ &\quad - 2C_{G_1G_0}^{(2)}(x,l)(l-x) + \sigma_{G_0}^2(l)(l-x)^2.\end{aligned} \tag{6.43}$$

In the above expression, note that $\sigma_{G_1}^2(x)$ can be calculated by (6.33) changing l by x and F_i by P_i, the term $\sigma_{G_0}^2(l)$ can be determined similarly to (6.35) changing F_i by P_i, and the rest of the terms can be expressed in an analogous manner using, respectively, (6.9) and (6.12),

$$C_{G_1}^{(2)}(x,l) = \lambda\mathbb{E}[P_i^2]\int_0^x R_1(x-\rho)R_1(l-\rho)\mathrm{d}\rho = \lambda\mathbb{E}\left[P_i^2\right]\left(\frac{x^2 l}{2} - \frac{x^3}{6}\right), \tag{6.44}$$

$$C_{G_1G_0}^{(2)}(x,l) = \lambda\mathbb{E}[P_i^2]\int_0^x R_1(x-\rho)R_0(l-\rho)\mathrm{d}\rho = \frac{\lambda}{2}\mathbb{E}\left[P_i^2\right]x^2. \tag{6.45}$$

Substituting these expressions in (6.43) and simplifying, one gets

$$\sigma_M^2(x) = \lambda\mathbb{E}\left[P_i^2\right]\left(x^2 l - l^2 x + \frac{1}{3}l^3 - \frac{1}{3}x^3\right). \tag{6.46}$$

Consequently, the second-order statistic of the bending moment, which will be required later to approximate its PDF via the PME, is given by

$$\mathbb{E}\left[M^2(x)\right] = \lambda\mathbb{E}\left[P_i^2\right]\left(x^2 l - l^2 x + \frac{1}{3}l^3 - \frac{1}{3}x^3\right) + \frac{1}{4}\lambda^2\mathbb{E}\left[P_i\right]^2\left(x^2 + l^2 - 2lx\right)^2. \tag{6.47}$$

Now, we complete similar calculations for the shear force. Its variance is given by

$$\sigma_T^2(x) = C_T^{(2)}(x,x) = \mathbb{E}\left[T(x)^2\right] - \mathbb{E}\left[T(x)\right]^2 = \sigma_{G_0}^2(x) - 2C_{G_0}^{(2)}(x,l) + \sigma_{G_0}^2(l). \tag{6.48}$$

Carrying out computations in a similar fashion as before, one obtains

$$\sigma_T^2(x) = -\lambda\mathbb{E}\left[P_i^2\right](x-l). \tag{6.49}$$

The second-order moment is given by

$$\mathbb{E}\left[T^2(x)\right] = \lambda(x-l)\left(-\mathbb{E}\left[P_i^2\right] + \lambda\mathbb{E}\left[P_i\right]^2(x-l)\right). \tag{6.50}$$

6.4 Computational implementation

This section presents an algorithm that allows us to simulate the analytical development shown in the previous section computationally. The proposed algorithm is based on Monte Carlo technique, see Section 2.7. The method consists of a random and repeated sampling of the stochastic process of the load function, $Q(x)$, and of the random variables of the moment of inertia, I, and Young's modulus, E. The objective is to obtain a number of simulations that together provide statistical information on the PDF of the deflection, slope, bending moment, and shear parameters of the beam.

The procedure has been divided into the following steps: (1) first, the beam is discretized (2) then the stochastic process of the load function is simulated for each of the discretized points of the beam, (3) in a third step, the random variables of the moment of inertia and Young's modulus are sampled and (4) with the values obtained, the functions describing the behavior of the beam are evaluated, and (5) finally, the process is repeated until it is obtained a set of simulations which adequately represents the uncertainty of the behavior of the beam.

After the general description, we now give a detailed step-by-step description of the procedure.

Step 1: Beam discretization Given the discrete nature of computer science, it is necessary to deal with the stochastic model in a discrete manner. The Poisson counting process has λx as expected value, where x represents the position in the axis of the beam. Although it is a discrete-continuous process, its simulation is discrete as long as, computationally, you can only evaluate it in a finite set of x. The discretization of the beam is important because the simulation involves assuming that there can only be charge points at the discretized positions and hence an adequate discretization plays a key role to obtain accurate results.

The approximate solution of the model (in our case, the deflection of the beam) between spatial points can be linearly interpolated by knowing the approximations at the adjacent points. Since the solution is not necessarily linear, the distance between points must be small enough so that the error of the approximation is acceptable for the application of the numerical results. Ideally, the beam should be discretized at as many points as possible. However, the computational cost increases proportionally to the number of points used in the discretization. An appropriate strategy to optimize the trade-off between accuracy and computational cost is to generate more points where the greatest uncertainty in the solution is sensed, which generally coincides with the points of greatest structural weakness. If this intuition is not predisposed, the ideal is to consider evenly distributed points.

Step 2: Simulation of the stochastic process

1. $\forall\, i \in \{0, 1, \ldots, D_b\}$ determining a spatial position x_i on beam b (where D_b is the total number of discretized points):

   1.1. $\forall\, m \in \{0, 1, \ldots, C_b\}$, determining the number of load functions c_m to be applied in beam b (where C_b is the total number of loads functions) with intensity Q_c and frequency f_c,

      1.1.1. The number of charge points s_i^m, generated by the charge function c_m at point x_i is obtained sampling from a Poisson distribution with parameter $\lambda := f_c/D_b > 0$, representing the expected value of s_i^m.

      1.1.2. $\forall k \in \{0, 1, \ldots, s_i^m\}$, the value of the point charge P_i is:

$$P_i^k = P_i^{k-1} + Q_c, \tag{6.51}$$

      where $P_i^{k-1} = 0$ if $k = 0$ and where in the case that is a random variable, it is necessary to sample a value of its PDF. The distribution of Q_c can be any positive/negative and continuous/discrete random variable. It can even be a nonparametric distribution constructed from field data.

At the end of the different loops, a value of $P_i^{s_i^m}$ (hereafter P_i) will have been obtained for each x_i.

2. The next step is to obtain the value of the net charge function $G_j(x),\ j = 0, 1, 2, 3$.

   2.1. $\forall\ i\ \in \{0, 1, \ldots, D_b\}$:

      2.1.1. $\forall\ z\ \in \{0, 1, \ldots, D_b\}$:
      If $x_i < x_z$:

$$G_0(x_i) = G_0(x_i) + 0, \tag{6.52}$$

$$G_1(x_i) = G_1(x_i) + 0, \tag{6.53}$$

$$G_2(x_i) = G_2(x_i) + 0, \tag{6.54}$$

$$G_3(x_i) = G_3(x_i) + 0. \tag{6.55}$$

      If $x_i > x_z$:

$$G_0(x_i) = G_0(x_i) + P_i, \tag{6.56}$$

$$G_1(x_i) = G_1(x_i) + P_i(x_i - x_z), \tag{6.57}$$

$$G_2(x_i) = G_2(x_i) + \frac{1}{2}P_i(x_i - x_z)^2, \tag{6.58}$$

$$G_3(x_i) = G_3(x_i) + \frac{1}{3!}P_i(x_i - x_z)^3. \tag{6.59}$$

Step 3: Simulation of the random variables The values of the inertial moment, I_b, and Young's modulus, E_b, are obtained by sampling from their corresponding PDFs. The distribution of these random variables can be any positive parametric one. It can even be a nonparametric distribution constructed from field data.

Step 4: Evaluation of beam performance functions. Once the deterministic values of all the variables have been obtained by simulation, we take advantage of the analytical development introduced in the previous section to determine the behavior of the beam w.r.t. its deflection (Eq. (6.20)) and, therefore, its moment of inertia (Eq. (6.39)) and shear force (Eq. (6.40)).

1. $\forall\, i\ \in \{0, 1, \ldots, D_b\}$:

$$Y_b(x_i) = \frac{1}{E_b I_b}\left[G_3(x_i) - \frac{1}{6}G_0(l)x_i^3 - \frac{1}{2}\left(G_1(l) - lG_0(l)\right)x_i^2\right], \tag{6.60}$$

$$M_b(x_i) = -G_1(x_i) + G_1(l) - G_0(l)(l - x_i), \tag{6.61}$$

$$T_b(x_i) = -G_0(x_i) + G_0(l). \tag{6.62}$$

Step 5: Repeat Steps 1-4 until it is obtained a set of simulations Once all the Steps 1-4 have been simulated, the result of one simulation is obtained. To determine the distribution of deflection, bending moment, and shear force of the beam, it is necessary to perform multiple simulations by repeating Steps 1-4. The greater the number of simulations, N, the better results will be obtained from the statistical analysis.

Once a large set of simulations has been generated, it is possible to construct the 95%PI (probabilistic intervals):

$\forall\, i\ \in \{0, 1, \ldots, D_b\}$:

$$95\%\text{PI of } Y_b(x_i) = \left(\mathbf{P}_{2.5}([Y_b^0, Y_b^1, \ldots, Y_b^n]),\ \mathbf{P}_{97.5}([Y_b^0, Y_b^1, \ldots, Y_b^n])\right), \tag{6.63}$$

$$95\%\text{PI of } M_b(x_i) = \left(\mathbf{P}_{2.5}([M_b^0, M_b^1, \ldots, M_b^n]),\ \mathbf{P}_{97.5}([M_b^0, M_b^1, \ldots, M_b^n])\right), \tag{6.64}$$

$$95\%\text{PI of } T_b(x_i) = \left(\mathbf{P}_{2.5}([T_b^0, T_b^1, \ldots, T_b^n]),\ \mathbf{P}_{97.5}([T_b^0, T_b^1, \ldots, T_b^n])\right), \tag{6.65}$$

where $n \in \{0, 1, \ldots, N\}$ and $\mathbf{P}$ represents the percentile function.

6.5 Numerical example

This section is addressed to apply the theoretical findings established in the previous sections by means of a full illustrative example.

Let us consider a 10m long overhanging beam (cantilever) in form of a balcony or lookout made up of an IPE 450 steel profile whose moment of inertia, I, is 33740cm^4 $\pm 2\%$, and whose Young's modulus, E, is 210Mpa [4]. Due to the heterogeneous properties of the steel, we will assume Young's modulus of the profile has some variability according to a Gaussian distribution with a mean of 210Mpa and a standard deviation of 5%. Just for illustrative purposes, let us assume the maximum capacity allowed in the lookout is 20 people. We will assume that each person weighs, on average, 700N (71.36kg) with a standard deviation of 5%. The above description corresponds with the following deterministic data of our modeling problem: $l = 10$, and $\lambda = 20$. While for the random parameters, and according to the foregoing description, we will assume that the Young's modulus of elasticity, E, has a truncated Gaussian distribution, $E \sim \mathrm{N}_{\mathcal{T}}(210 \cdot 10^9; 0.05 \cdot 210 \cdot 10^9)\mathrm{N/m}^2$, where $\mathcal{T} = [209.9993 \cdot 10^9, 210.0006 \cdot 10^9]$. The moment of inertia, I, has a Gaussian distribution, $I \sim \mathrm{N}(33740 \cdot 10^{-8}; 0.02 \cdot 33740 \cdot 10^{-8})\mathrm{m}^4$. And, finally, let us assume that the intensity of the concentrated loads P_i follows a Gaussian distribution, $P_i \sim \mathrm{N}(700; 35)\mathrm{N}$. We consider that E, I and P_i are independent random variables.

In Table 6.1, we show a comparison of the mean and the variance of the static deflection, $Y(x)$, given by expression (6.28) and (6.37), respectively, and the mean

and variance obtained by Monte Carlo simulation following the procedure described in Section 6.4. We can observe that the values are in full agreement.

x	$\mathbb{E}[Y(x)]$ (Eq. (6.28))	$\mathbb{E}[Y(x)]$ (simulation)	$\sigma^2_Y(x)$ (Eq. (6.37))	$\sigma^2_Y(x)$ (simulation)
0	0	0	0	0
1	0.000463	0.000463	$1.486249 \cdot 10^{-8}$	$1.563205 \cdot 10^{-8}$
2	0.001730	0.001731	$2.140720 \cdot 10^{-7}$	$2.248590 \cdot 10^{-7}$
3	0.003633	0.003634	$9.721975 \cdot 10^{-7}$	$1.019968 \cdot 10^{-6}$
4	0.006023	0.006025	$2.746732 \cdot 10^{-6}$	$2.878598 \cdot 10^{-6}$
5	0.008772	0.008773	$5.974110 \cdot 10^{-6}$	$6.254897 \cdot 10^{-6}$
6	0.011770	0.011770	$1.100046 \cdot 10^{-5}$	$1.150769 \cdot 10^{-5}$
7	0.014928	0.014928	$1.804558 \cdot 10^{-5}$	$1.886364 \cdot 10^{-5}$
8	0.018177	0.018175	$2.719839 \cdot 10^{-5}$	$2.841349 \cdot 10^{-5}$
9	0.021467	0.021464	$3.844254 \cdot 10^{-5}$	$4.013907 \cdot 10^{-5}$
10	0.024769	0.024730	$5.171033 \cdot 10^{-5}$	$5.382120 \cdot 10^{-5}$

Table 6.1: Comparison of the mean, $\mathbb{E}[Y(x)]$, and the variance, $\sigma^2_Y(x)$, of the static deflection of the cantilever beam at different spatial points $x \in \{0, 1, 2, \ldots, 10\}$ using the theoretical approach (Eq. (6.28) and Eq. (6.37) for computing $\mathbb{E}[Y(x)]$ and $\sigma^2_Y(x)$, respectively), and 100000 simulations via Monte Carlo.

Once we have obtained the mean, $\mathbb{E}[Y(x)]$, and the variance, $\sigma^2_Y(x)$, we use the PME to compute the 1-PDF of the static deflection, $f_{Y(x)}(y)$. As we have seen in Section 2.6, for each x, we first solve the system (2.13) for $\lambda_i = \lambda_i(x)$, $i = 0, 1, 2$. Notice that, in our present framework, the x variable in Section 2.6 (the variable of the PDF defined by the PME method), here is denoted by y. For example, for the free-end, $x = 10$, where the mean and variance of the deflection are maxima, the 1-PDF is given by

$$f_{Y(10)}(y) = \mathbb{1}_{\mathcal{D}(Y(10))} e^{-1+0.893356-477.134605y+9633.765685y^2}, \tag{6.66}$$

where we have taken as domain the interval $\mathcal{D}(Y(10)) = [0, 0.096694]$ is constructed using the Chebyshev-Bienaymé's inequality [19] with 10 standard deviations around the mean (and truncating the left-end of the interval to 0 value in order to keep consistent with the physical meaning of the deflection) so that $\int_{\mathcal{D}(Y(10))} f_{Y(10)}(y)\mathrm{d}y \approx 1$. To better compare the results obtained using the PME

against the ones calculated by Monte Carlo, in Fig. 6.2, we show the corresponding using Monte Carlo with simulations 1000, 10000, and 100000 simulations at the spatial point, $x = 10$. Although we can observe a good agreement between them, it is worth to point out that this little discrepancy can be explained because when applying the PME we retain the information provided by the two first moments, then being Gaussian the approximation while the response could be non-Gaussian.

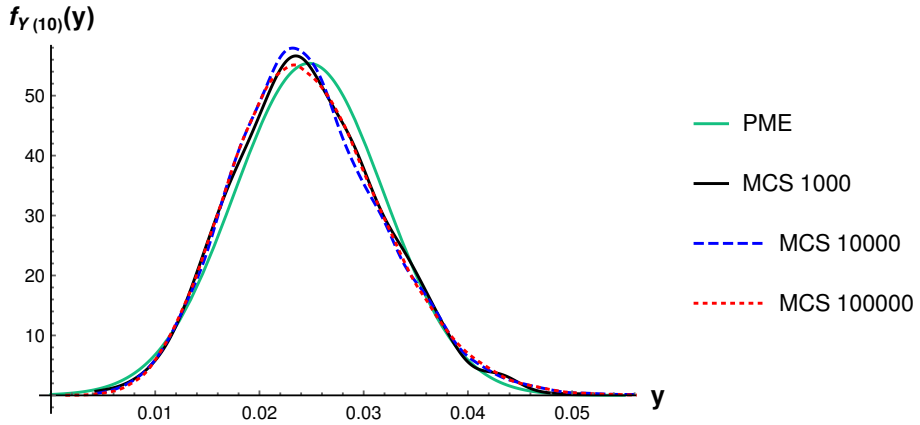

Figure 6.2: 1-PDF of the static deflection of the cantilever beam, $f_{Y(x)}(y)$, at the spatial point $x = 10$ obtained via PME and Monte Carlo using 1000, 10000 and 100000 simulations.

Now, we study the bending moment, $M(x)$. In Table 6.2, we compare the mean and the variance of $M(x)$, given by expression (6.41) and (6.46), respectively, and the ones computed by Monte Carlo using 100000 simulations. We can observe, again, that the values show good agreement.

The 1-PDF of the bending moment, $f_{M(x)}(m)$, can also be computed by the PME. Its approximation at the spatial point $x = 0$, where its mean (in absolute value) and variance are maxima, is given by

$$f_{M(0)}(m) = \mathbb{1}_{\mathcal{D}(M(0))} e^{-1-17.197008-0.000213m-1.524656m^2}, \tag{6.67}$$

where, similarly as it was done for the deflection, the domain of the bending moment at $x = 0$ is given by $\mathcal{D}(M(0)) = [-250931.572337, 0]$. It has been calculated using the Chebyshev-Bienaymé's inequality with 10 standard deviations and taking into account that the bending moment is non-positive.

x	$\mathbb{E}[M(x)]$ (Exp. (6.41))	$\mathbb{E}[M(x)]$ (simulation)	$\sigma^2_M(x)$ (Eq. (6.46))	$\sigma^2_M(x)$ (simulation)
0	-69993.699374	-69878.898675	$3.274244 \cdot 10^8$	$3.291509 \cdot 10^8$
1	-56694.896493	-56586.404173	$2.386924 \cdot 10^8$	$2.399465 \cdot 10^8$
2	-44795.967599	-44696.961390	$1.676413 \cdot 10^8$	$1.685314 \cdot 10^8$
3	-34296.912693	-34206.526813	$1.123065 \cdot 10^8$	$1.128808 \cdot 10^8$
4	-25197.731774	-25118.063711	$7.072368 \cdot 10^7$	$7.103806 \cdot 10^7$
5	-17498.424843	-17432.235020	$4.092805 \cdot 10^7$	$4.104798 \cdot 10^7$
6	-11198.991899	-11145.801799	$2.095516 \cdot 10^7$	$2.096393 \cdot 10^7$
7	-6299.432943	-6258.001079	$8.840460 \cdot 10^6$	$8.808880 \cdot 10^6$
8	-2799.747974	-2768.248438	$2.619395 \cdot 10^6$	$2.586399 \cdot 10^6$
9	-699.936993	-681.106878	$3.274244 \cdot 10^5$	$3.145759 \cdot 10^5$
10	0	0	0	0

Table 6.2: Comparison of the mean, $\mathbb{E}[M(x)]$, and the variance, $\sigma^2_M(x)$, of the bending moment of the cantilever beam at different spatial points $x \in \{0, 1, 2, \ldots, 10\}$ using the theoretical approach (Eq. (6.41) and Eq. (6.46) for computing $\mathbb{E}[M(x)]$ and $\sigma^2_M(x)$, respectively), and 100000 simulations via Monte Carlo.

In Fig. 6.3, we show a graphical representation of the 1-PDF given by (6.67) and the ones obtained by Monte Carlo using 1000, 10000, and 100000 simulations. We can observe the results are fully consistent.

In Table 6.3, we compare the values obtained of the mean, $\mathbb{E}[T(x)]$, and the variance, $\sigma^2_T(x)$, of the shear force, $T(x)$, given by expression (6.42) and (6.49), respectively, and the ones computed by Monte Carlo using 100000 simulations. Note that the results show good agreement.

As before, to complete the probabilistic analysis, we approximate the 1-PDF of the shear force, $f_{T(x)}(t)$, using the PME. It results

$$f_{T(0)}(t) = \mathbb{1}_{\mathcal{D}(T(0))} e^{-1-17.943337+0.001424t-5.088214\cdot 10^{-8}t^2}, \tag{6.68}$$

where $\mathcal{D}(T(0)) = [0, 45347.054670]$.

Finally, in Figure 6.4 we compare the three approximations of 1-PDF obtained by Monte Carlo with 1000, 10000 and 100000 simulations against the one obtained

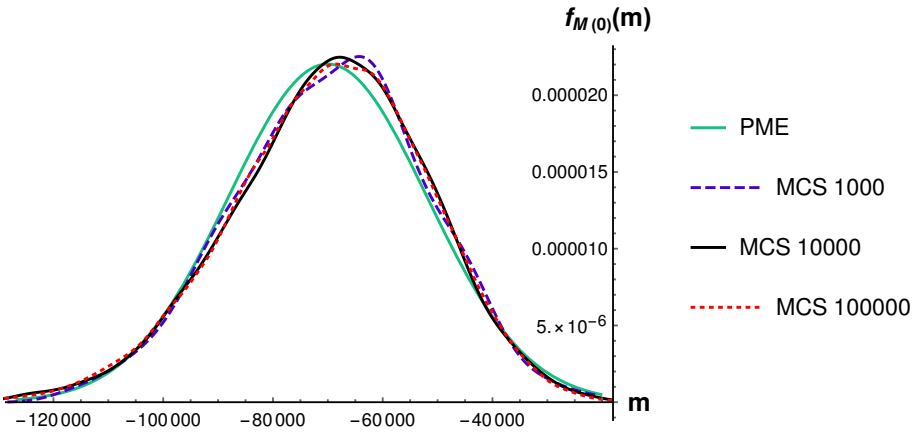

Figure 6.3: 1-PDF of the bending moment of the cantilever beam, $f_{M(x)}(y)$, obtained via PME and Monte Carlo using 1000, 10000, and 100000 simulations at the spatial point $x = 0$.

by Eq. (6.68) at the spatial point $x = 0$. The results show a full agreement as the number of simulation increase.

Now, we are going to compare the theoretical and Monte Carlo approximations of the expectation of all the physical quantities studied for the cantilever, namely, the deflection, the bending moment and the shear force, using as goodness-of-fit the symmetric mean absolute percentage error (SMAPE). Let us recall that for a set of n theoretical values of the previous quantities, say Z_i and their corresponding approximations obtained by Monte Carlo, $\hat{z}_i$, the SMAPE is given by

$$\text{SMAPE} = \frac{100\%}{n} \sum_{i=1}^{n} \frac{|Z_i - \hat{z}_i|}{(|Z_i| + |\hat{z}_i|)/2}. \tag{6.69}$$

In Table 6.4, we show the SMAPE corresponding to the expectation of the deflection, $Y(x)$, the bending moment, $M(x)$, and the shear force, $T(x)$, at the spatial points $x = 0, 1, \ldots, 10$, considering the approximations obtained via Monte Carlo simulations (MCS) with a different number of samples (1000, 10000 and 100000). It must be noticed that we apply the SMAPE with $n = 10$ since we must exclude the term $x = 10$, in the case of the deflection, and $x = 0$, in the case of the bending moment and the shear force, since their values are zero. We can

x	$\mathbb{E}[T(x)]$ (Eq. (6.40))	$\mathbb{E}[T(x)]$ (simulation)	$\sigma_T^2(x)$ (Eq. (6.49))	$\sigma_T^2(x)$ (simulation)
0	13998.739874	13989.984660	$9.822734 \cdot 10^6$	$9.868522 \cdot 10^6$
1	12598.865887	12584.463060	$8.840460 \cdot 10^6$	$8.871837 \cdot 10^6$
2	11198.991899	11184.844909	$7.858187 \cdot 10^6$	$7.891253 \cdot 10^6$
3	9799.117912	9787.433546	$6.875913 \cdot 10^6$	$6.893854 \cdot 10^6$
4	8399.243924	8387.069932	$5.893640 \cdot 10^6$	$5.922317 \cdot 10^6$
5	6999.369937	6985.927374	$4.911367 \cdot 10^6$	$4.941940 \cdot 10^6$
6	5599.495949	5588.894615	$3.929093 \cdot 10^6$	$3.946902 \cdot 10^6$
7	4199.621962	4191.937526	$2.946820 \cdot 10^6$	$2.953221 \cdot 10^6$
8	2799.747974	2792.303398	$1.964546 \cdot 10^6$	$1.971305 \cdot 10^6$
9	1399.873987	1391.025322	$9.822734 \cdot 10^5$	$9.818576 \cdot 10^5$
10	0	0	0	0

Table 6.3: Comparison of the mean, $\mathbb{E}[T(x)]$, and the variance, $\sigma_T^2(x)$, of the shear force of the cantilever beam, at different spatial points $x \in \{0, 1, 2, \ldots, 10\}$ using the theoretical approach (Eq. (6.40) for $\mathbb{E}[T(x)]$ and Eq. (6.49) for $\sigma_T^2(x)$, respectively,), 100000 simulations via Monte Carlo.

observe that the SMAPE is significantly reduced when using 100000 simulations, as expected.

SMAPE (%)	1000 MCS	10000 MCS	MCS 100000
$Y(x)$	0.288816	0.245558	0.032886
$M(x)$	0.824381	1.004208	0.653084
$T(x)$	0.726415	0.442595	0.203296

Table 6.4: Computation of the SMAPE calculated by (6.69) of the theoretical expectation and the mean calculated via Monte Carlo simulations (MCS) with different samples (1000, 10000 and 100000) the deflection, bending moment, and shear force of the cantilever.

We finish this section by comparing the mean and probabilistic intervals of the deflection, bending moment, and shear force, which we have obtained theoretically and by simulations. First, we take advantage of the 1-PDF computed through PME to construct 95% PI. To do this for the deflection $Y(x)$ (similarly is done for the bending moment, $M(x)$, and the shear force, $T(x)$), we need to obtain $k(x)$

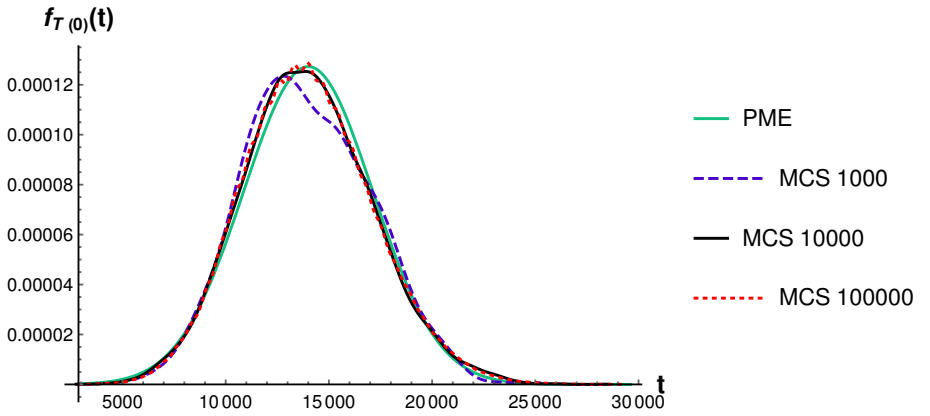

Figure 6.4: 1-PDF of the shear force of the cantilever beam, $f_{T(x)}(t)$, at the spatial point $x = 0$ obtained via PME and Monte Carlo using 1000, 10000 and 100000 simulations.

satisfying

$$\int_{\mathbb{E}[Y(x)]-k(x)\sigma_{Y(x)}}^{\mathbb{E}[Y(x)]+k(x)\sigma_{Y(x)}} f_{Y(x)}(y) = 0.95, \tag{6.70}$$

where $f_{Y(x)}(y)$ is the 1-PDF of the deflection. Second, from the Monte Carlo simulations, we obtain the probabilistic intervals using the algorithm based on the percentile function explained in Step 5 in Section 6.4.

In Fig. 6.5, we show the mean and probabilistic intervals of the deflection, $Y(x)$. We can observe that the results provided using both approaches are very close, showing better agreement in the case of the approximation of the mean $\mathbb{E}[Y(x)]$, as expected. Although the value of $k(x) := k_Y(x)$ obtained from (6.70) may change with the spatial position x, in this case, we have obtained $k_Y(x) \approx 1.96$ for all $x = 1, \ldots, 10$.

Analogously, in Fig. 6.6 and 6.7, we show the corresponding plots for the bending moment, $M(x)$, and the shear force, $T(x)$. Here, it is worth pointing out that the value of k changes as x does. In the case of the bending moment, $k(x) := k_M(x) \approx 1.96$ for $x \in \{0, \ldots, 6\}$, $k_M(7) \approx 1.9$, $k_M(8) \approx 1.75$, and $k_M(9) \approx 1.32$. While for the share force , $k_T(x) \approx 1.96$ for $x \in \{0, \ldots, 6\}$, $k_T(7) \approx 1.95$, $k_T(8) \approx 1.87$, and $k_T(9) \approx 1.51$.

To better understand the behavior indicated for $k = k(x)$ in each of the three cases, let us observe that we have approximated the corresponding 1-PDFs by applying the PME imposing three constraints (first, the one corresponding to the normalization condition and the others two corresponding to the two first statistical moments). In this manner, we determine a (truncated) Gaussian-like approximation. As can be seen in Fig. 6.8, the approximations for $f_{Y(x)}(y)$ are roughly symmetric for every spatial position x (in Fig. 6.8a we show the results including all values of x, and in Fig. 6.8b we zoom-up a few values so that the symmetry can be better graphically assessed). So, the classical Gaussian 2σ rule-of-thumb [19], corresponding to $k \approx 1.96$, is fulfilled. For the case of $f_{M(x)}(m)$, it can be seen that symmetry is roughly preserved for $x \in \{0, \ldots, 6\}$ and deteriorates thereafter (see Fig. 6.8c-6.8d). Consequently, the approximation of $f_{M(x)}(m)$ is no longer Gaussian, and the value of k departs from 1.96. An analogous explanation can be given for the case of $f_{T(x)}(t)$ (see Fig. 6.8e-6.8f). In this latter case, it is worth pointing out that we can also observe that in the case of the calculation of the percentiles of $f_{T(x)}(t)$, there are steps in the functions. This is because the shear force is defined by a linear function of $G_0(x)$, see Eq. (6.62), which corresponds to the step function. The differences in the smoothness of the steps are due to the influence of the random intense load, P_i, in extreme cases. Simulating this parameter as a deterministic one, it has been observed that both functions reduce the smoothness of their steps. This verification has also been done with the parameters corresponding to the structural characteristics, E and I, observing that their variability has no impact on the smoothness of the steps.

6.6 Conclusions

In this chapter, we have performed a full probabilistic analysis of a cantilever beam using the Euler-Bernoulli's theory. For the sake of generality, in our study, we have assumed that all the model parameters (the moment of inertia, I, and Young's modulus, E) are independent random variables with arbitrary density functions, and the load acting on the beam is described by means of the delta-correlated process. The adopted approach has made it possible to compute the mean and the variance of the static deflection, the bending moment, and the shear force, with the purpose of later obtaining the first probability density function, taking

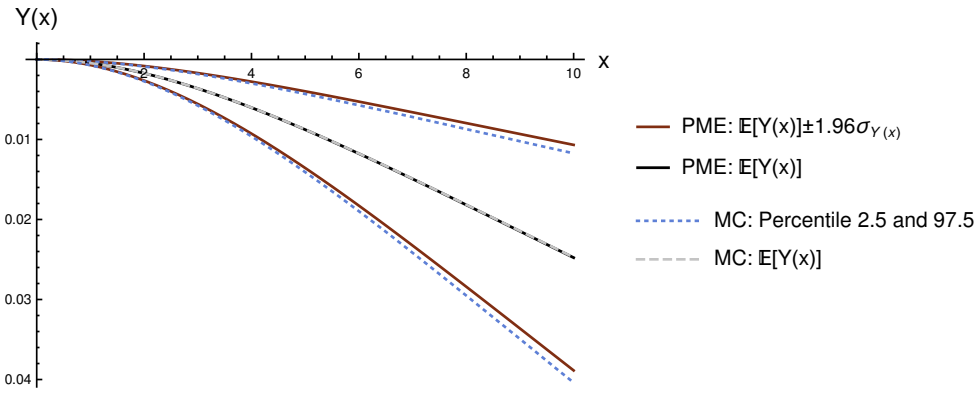

Figure 6.5: Comparison of the mean and probabilistic intervals of the static deflection, $Y(x)$, using the PME and Monte Carlo simulations (MC).

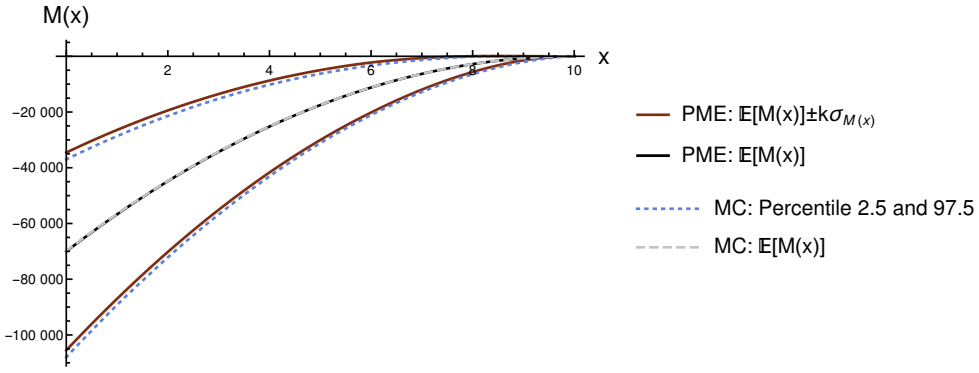

Figure 6.6: Comparison of the mean and probabilistic intervals of the bending moment, $M(x)$, using the PME and Monte Carlo simulations (MC).

advantage of the Principle of Maximum Entropy. In the numerical example, we have compared these results with simulations obtained using a Monte Carlo-based algorithm, with good results.

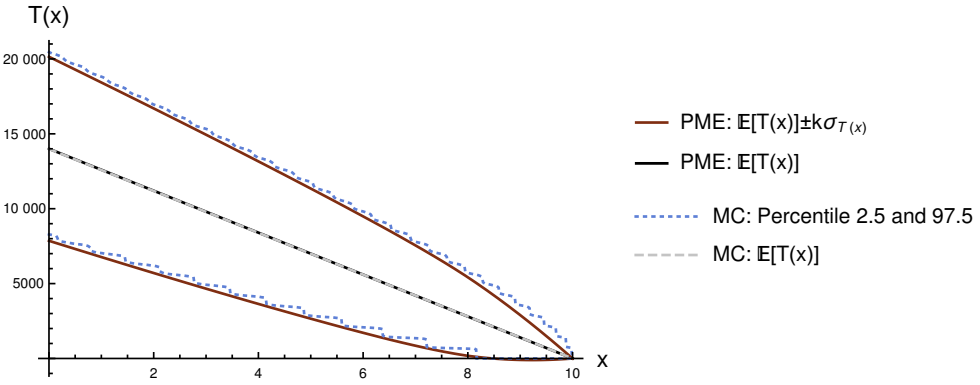

Figure 6.7: Comparison of the mean and probabilistic intervals of the shear force, $T(x)$, using the PME and Monte Carlo simulations (MC).

Publications associated with this chapter

The results of this chapter have been presented at the 6th International Symposium on Uncertainty Quantification and Stochastic Modeling (Uncertainties 2023) in Fortaleza (Brazil) from July 30 to August 4, 2023 with the talk titled *Uncertainty-Based Analysis of a Cantilever Beam with Random Parameters Subject to Correlated Noise*. Additionally, a complete version of the chapter's findings has been published in the paper [22].

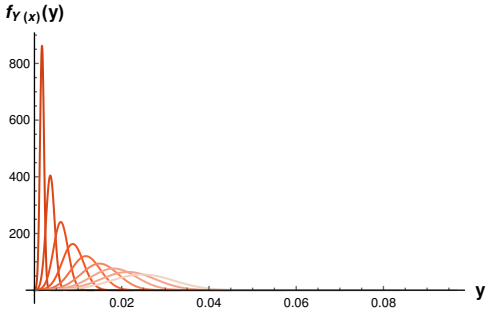

(a) 1-PDF of the deflection at the spatial points $x \in \{1, 2, 3, 4, 5, 6, 7, 8, 9\}$.

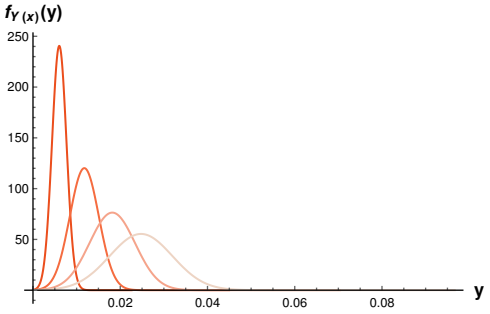

(b) 1-PDF of the deflection at the spatial points $x \in \{2, 4, 6, 8\}$.

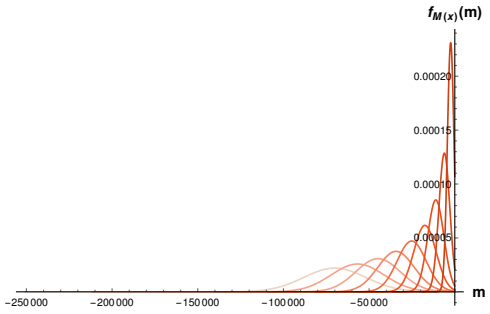

(c) 1-PDF of the bending moment at the spatial points $x \in \{0, 1, 2, 3, 4, 5, 6, 7, 8\}$.

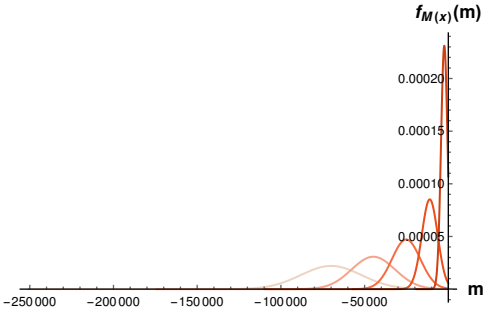

(d) 1-PDF of the bending moment at the spatial points $x \in \{0, 2, 4, 6, 8\}$.

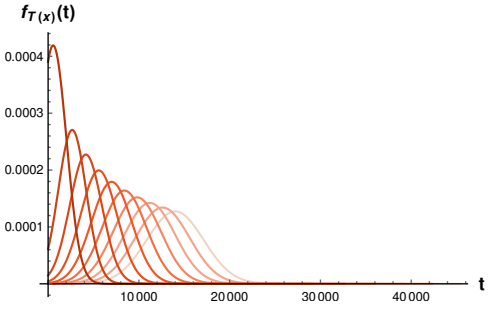

(e) 1-PDF of the shear force at the spatial points $x \in \{0, 1, 2, 3, 4, 5, 6, 7, 8, 9\}$.

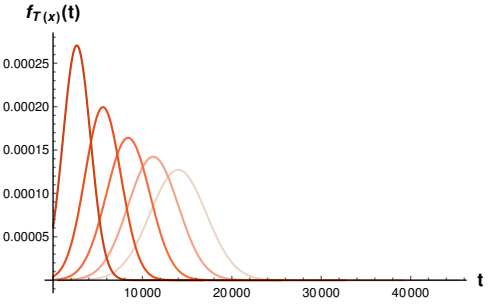

(f) 1-PDF of the shear force at the spatial points $x \in \{0, 2, 4, 6, 8\}$.

Figure 6.8: 1-PDF of the different studied characteristics of the cantilever beam.

Chapter 7

Probabilistic analysis of a foundational class of generalized second-order linear differential equations in Classic Mechanics

A number of relevant models in Classical Mechanics are formulated by means of the differential equation $y''(t) + At^{\beta}y(t) = 0$. In this chapter, we improve the results recently established for a randomized reformulation of this model that includes a generalized derivative. The stochastic analysis permits solving that generalized model by computing reliable approximations of the probability density function of the solution, which is a stochastic process. The approximations are built by the Random Variable Transformation method. We prove that these approximations converge to the exact density under mild conditions on the data. Finally, several numerical examples illustrate our theoretical findings.

7.1 Introduction

The homogeneous linear second-order differential equation

$$y''(t) + f(t)y(t) = 0, \tag{7.1}$$

plays a key role in a number of problems mainly appearing in Physics and Engineering. It describes simple harmonic motion or free undamped motion of a spring of mass m and constant $k > 0$. In this case, one obtains the simplest formulation of (7.1), where $f(t)$ is the *spring constant*, $f(t) = \varpi^2 := \frac{k}{m}$ (ϖ is called the circular frequency of the spring) [81]. On the other hand, there are real-world situations where it is more realistic to assume that the spring constant changes over time. For example, if the spring/mass system is in motion for a long period, the spring will weaken due to wear and tear; if the temperature of the environment is rapidly decreasing, this will affect the spring material. In these two scenarios, that fall within the so called aging spring theory, possible choices for $f(t)$ are $\frac{k}{m}\mathrm{e}^{-at}$, $\alpha > 0$ and $\frac{k}{m}t$, respectively [110, p. 197]. This latter choice, in a more general form, $f(t) = At$, leads to the so-called Airy's differential equation,

$$y''(t) + Aty(t) = 0, \tag{7.2}$$

that is encountered in the study of radiowave propagation (diffraction of radio waves around the surface of the Earth) and in physical optics (the diffraction of the light) [1, p. 89]. The differential equation (7.1) also appears in the theory of elasticity to model the problem of determining when a uniform vertical column will buckle under its own weight. In this context, the independent variable t is better denoted by x representing the deflection w.r.t. the stable (vertical) position and $f(x) = \frac{g\rho}{EI}x$, where g denotes the gravitational acceleration, E is the Young's modulus of the material of the column, I is its cross-sectional moment of inertia and ρ is the linear density of the column [6]. Many other applications of model (7.2) can be found in [102].

On the one hand, over the last decades classical ordinary differential equations, as (7.1), have been reformulated in terms of generalized or fractional derivatives aimed at better modelling complex phenomena such as acoustic attenuations in Acoustics

[49], anomalous diffusion processes in complex media in Fluids [33] or memory effects in materials (viscoelasticity, aging, etc.) in Structural Mechanics [80]. On the other hand, when ordinary or fractional differential equations are applied to real-world problems, one requires setting their parameters (initial/boundary conditions, forcing term and/or coefficients) using the available information, which is usually collected from measurements and metadata that often contain epistemic and/or aleatoric uncertainties coming from measurement errors and/or lack of knowledge, respectively. One can delineate two main different forms of this type of equation depending on the way that uncertainty is considered in the equation, namely, Stochastic Fractional Differential Equations (SFDEs) and Random Fractional Differential Equations (RFDEs). In the former case, uncertainties are driven by one (or more) prefixed types of stochastic processes such as the fractional Brownian motion [67, Ch. 6] and/or the fractional Lèvy process [82]. In the framework of RFDEs, uncertainties are directly assigned to every parameter of the equation via specific probability distributions that must be previously chosen so that they properly represent the physical meaning of the corresponding model parameter and the solution captures the uncertainties in the model response [87].

In this chapter, we are concerned with studying a generalization of (7.2), that takes into account the previous considerations, namely, a fractional derivative and a full randomization of model parameters. Additionally, a power-law generalized coefficient is also included. Specifically, in this contribution, we deal with the following Random Fractional Initial Value Problem (RFIVP)

$$\begin{cases} ({}^{C}D_0^{\alpha}Y)(t) - B\,t^{\beta}Y(t) = 0, & t > 0, \quad n = -\lfloor -\alpha \rfloor, \quad n-1 \leq \alpha \leq n, \\ Y^{(j)}(0) = A_j, & j = 0, \ldots, n-1, \end{cases} \tag{7.3}$$

where $\lfloor \cdot \rfloor$ stands for the floor function, $({}^{C}D_0^{\alpha}Y)(t)$ denotes the Caputo derivative of order $\alpha > 0$, interpreted in the random mean square sense [14], of the stochastic process $Y(t)$. The initial conditions $A_0, A_1, \ldots, A_{n-1}$ and the coefficient B are assumed random variables belonging to the space $\mathrm{L}_2(\Omega)$ (see Section 2.1).

To study the RFIVP (7.3), from a probabilistic standpoint, entails computing its solution, $Y(t)$, which is a stochastic process, but also determining its main statistical

information. It includes the computation of the first moments of $Y(t)$, such as the mean and the variance functions, and its *fidis*, particularly the 1-PDF [89].

Under the following hypotheses:

H1: $A_0, A_1, \ldots, A_{n-1}$ and B are (mutually) independent random variables,

H2: There exist positive constants η, $\mathcal{H}$ and p, such that

$$||B^m||_2 \leq \eta \mathcal{H}^{m-1}((m-1)!)^p, \qquad \forall m \geq m_0 \geq 1, \text{ integers},$$

in [12], the authors have recently studied the RFIVP (7.3). Specifically, in that article, one constructs the solution stochastic process by means of the following finite sum of n random generalized power series

$$Y(t) = \sum_{j=0}^{n-1} Y_j(t), \tag{7.4}$$

where

$$\begin{aligned} Y_j(t) &= \sum_{m=0}^{\infty} X_{m,j} t^{\gamma m + j}, \qquad X_{m,j} = B^m A_j g_{m,j}, \\ g_{m,j} &= \prod_{k=1}^{m} \frac{\Gamma(k\gamma + j + 1 - \alpha)}{\Gamma(k\gamma + j + 1)}, \qquad \gamma = \alpha + \beta. \end{aligned} \tag{7.5}$$

Besides constructing the foregoing solution and studying its convergence, in the mean square sense, in [12], one also constructs approximations for the mean and for the variance functions of the solution by truncating $Y_j(t)$ at certain order, say M. Then, taking advantage of this punctual statistical information, the PME [69] was applied to construct reliable approximations of the 1-PDF of the solution. The accuracy in the approximations of the 1-PDF, via this approach, heavily depends on controlling two main sources of errors, first, the ones associated with the approximations of the mean and the variance, and secondly, the associated with the application of the PME with *only* these two (approximate) statistical moments. The aforementioned errors involved in the calculation of the mean and

the variance could, theoretically, be reduced at the expense of increasing the order of truncation, M, of the random generalized power series solution (7.4)–(7.5) and/or by constructing approximations for higher statistical moments. However, both strategies might be unaffordable in many cases. Motivated by these drawbacks, in this chapter, we propose a direct method to approximate the 1-PDF of the solution stochastic process of the RFIVP (7.3), that avoids approximating the first statistical moments of the solution and the application of the PME.

Our subsequent study will be based on the representation of the solution given in (7.4)–(7.5), hence the foregoing hypotheses **H1** and **H2** must be fulfilled. Specifically, hereinafter, we will assume the following assumptions:

A1: $A_0, A_1, \ldots, A_{n-1}$ and B are (mutually) independent random variables whose respective domains will be denoted by $\mathcal{D}(A_j)$, $j = 0, 1, \ldots, n-1$ and $\mathcal{D}(B)$.

A2: B is a bounded random variable that takes values away from the origin, i.e., there exist positive lower and upper bounds, b_l and b_u, such that

$$0 < b_l \leq |B(\omega)| \leq b_u < \infty, \quad \forall \omega \in \Omega.$$

Now, we give two key remarks. The first one justifies that assumption **A2** guarantees that hypothesis **H2** fulfills, while in the second one shows that the random variables A_j, $j = 0, 1, \ldots, n-1$, defining the initial conditions, have finite expectation. This latter fact will be used later.

Remark 7.1 *In [16, Subsect. 3.3], one proves that the boundedness of random variable B is equivalent to the following condition about the exponential growth of its absolute moments*

$$\exists\, \rho, \mathcal{H} > 0: \quad ||B^m||_2 \leq \rho \mathcal{H}^m, \qquad \forall m \geq m_0 \geq 1, \quad \textit{integers},$$

*Notice that, this condition can be obtained from the inequality stated in assumption **A2** just taking $p = 0$ and relabeling the constant η as $\rho = \eta\mathcal{H}$. Furthermore, as it is proved in [12], the random generalized power series solution* (7.4)–(7.5) *is mean square convergent on the whole real line. Almost surely convergence on*

*the whole real line is also guaranteed since, by assumption **A2**, B is a bounded random variable.*

Remark 7.2 *As $A_0, A_1, \ldots, A_{n-1} \in \mathrm{L}_2(\Omega)$, then $\mathbb{E}[A_j^2] < \infty$, and by the Schwarz's inequality, $\mathbb{E}[|A_j|]) < (\mathbb{E}[A_j^2])^{1/2} < \infty$. This fact will used later.*

The key tool to conduct our subsequent analysis is the RVT method. As we have seen in Section 2.5, this result permits determining the PDF, say $f_{\mathbf{Y}}(\mathbf{y})$, of a random vector, $\mathbf{Y}$, that results from mapping another random vector, $\mathbf{Z}$, whose PDF, $f_{\mathbf{Z}}(\mathbf{z})$, is known. Notice that, for convenience, we have changed the notation in this chapter with respect to the theorem.

7.2 Computing the 1-PDF of the solution stochastic process by applying the RVT method

To compute the 1-PDF of the solution of the RFIVP (7.4), by means of the application of Theorem 2.1, we will first consider the truncation of (7.4),

$$Y^M(t) = \sum_{j=0}^{n-1} Y_j^M(t), \tag{7.6}$$

where

$$Y_j^M(t) = \sum_{m=0}^{M} X_{m,j} t^{\gamma m + j} = A_j \sum_{m=0}^{M} B^m g_{m,j} t^{\gamma m + j}. \tag{7.7}$$

For fixed t, expression (7.6)–(7.7) can be interpreted as a continuous mapping of the random variables, $A_0, A_1, \ldots A_{n-1}$ and B, whose joint PDF can be expressed as $f_{A_0,A_1,\ldots,A_{n-1},B} = f_{A_0} f_{A_1} \cdots f_{A_{n-1}} f_B$, by assumption **A1**. Then, in order to apply Theorem 2.1 with $k = n+1$, we identify $\mathbf{Z} = (Z_1, Z_2, \ldots, Z_n, Z_{n+1}) = (A_0, A_1, \ldots, A_{n-1}, B)$, and define $\mathbf{Y}$ via the following transformation $\mathbf{r} : \mathbb{R}^{n+1} \longrightarrow$

$\mathbb{R}^{n+1}$ of $\mathbf{Z}$ whose components are

$$\begin{array}{rcccl}
y_1 & = & r_1(z_1, z_2, \ldots, z_n, z_{n+1}) & = & z_1 \displaystyle\sum_{m=0}^{M} z_{n+1}^m g_{m,0} t^{\gamma m} \\
 & & & & + \displaystyle\sum_{j=1}^{n-1} \sum_{m=0}^{M} z_{j+1} z_{n+1}^m g_{m,j} t^{\gamma m + j}, \\
y_2 & = & r_2(z_1, z_2, \ldots, z_n, z_{n+1}) & = & z_2, \\
\vdots & \vdots & \vdots & \vdots & \vdots \\
y_n & = & r_n(z_1, z_2, \ldots, z_n, z_{n+1}) & = & z_n, \\
y_{n+1} & = & r_{n+1}(z_1, z_2, \ldots, z_n, z_{n+1}) & = & z_{n+1}.
\end{array} \tag{7.8}$$

The inverse mapping of $\mathbf{r}$, $\mathbf{s} = \mathbf{r}^{-1}$, is given by

$$\begin{array}{rcccl}
z_1 & = & s_1(y_1, y_2, y_3, \ldots, y_n, y_{n+1}) & = & \dfrac{y_1 - \displaystyle\sum_{j=1}^{n-1} \sum_{m=0}^{M} y_{j+1} y_{n+1}^m g_{m,j} t^{\gamma m + j}}{\displaystyle\sum_{m=0}^{M} y_{n+1}^m g_{m,0} t^{\gamma m}}, \\
z_2 & = & s_2(y_1, y_2, y_3, \ldots, y_n, y_{n+1}) & = & y_2, \\
\vdots & \vdots & \vdots & \vdots & \vdots \\
z_n & = & s_n(y_1, y_2, y_3, \ldots, y_n, y_{n+1}) & = & y_n, \\
z_{n+1} & = & s_{n+1}(y_1, y_2, y_3, \ldots, y_n, y_{n+1}) & = & y_{n+1},
\end{array} \tag{7.9}$$

being its Jacobian

$$J = \left| \frac{\partial s_1}{\partial y_1}(y_1, y_2, y_3, \ldots y_n, y_{n+1}) \right| = \frac{1}{\left| \sum_{m=0}^{M} y_{n+1}^m g_{m,0} t^{\gamma m} \right|} \neq 0.$$

The expression in the denominator of the Jacobian depends on the random variable B, which is absolutely continuous, so the denominator is distinct from zero w.p. 1. Hence, it is well-defined.

Applying Theorem 2.1, one gets

$$\begin{aligned} &f_{Y_1,Y_2,\ldots,Y_n,Y_{n+1}}(y_1,y_2,\ldots,y_n,y_{n+1}) \\ &= f_{Z_1}\left(\frac{y_1-\sum_{j=1}^{n-1}\sum_{m=0}^{M} y_{j+1}y_{n+1}^m g_{m,j}t^{\gamma m+j}}{\sum_{m=0}^{M} y_{n+1}^m g_{m,0}t^{\gamma m}}\right) f_{Z_2}(y_2)\cdots f_{Z_n}(y_n) f_{Z_{n+1}}(y_{n+1}) \\ &\quad \cdot \frac{1}{\left|\sum_{m=0}^{M} y_{n+1}^m g_{m,0}t^{\gamma m}\right|}. \end{aligned} \tag{7.10}$$

For fixed t, $Y_1 = Y^M(t)$, and marginalizing w.r.t. $Y_2 = A_1, \ldots, Y_n = A_{n-1}, Y_{n+1} = B$, the 1-PDF of the truncated solution (7.6)–(7.7) is given by

$$\begin{aligned} f_{Y^M(t)}(y) = &\int_{\mathcal{D}(A_1)} \cdots \int_{\mathcal{D}(A_{n-1})} \int_{\mathcal{D}(B)} f_{A_0}\left(\frac{y-\sum_{j=1}^{n-1}\sum_{m=0}^{M} a_j b^m g_{m,j}t^{\gamma m+j}}{\sum_{m=0}^{M} b^m g_{m,0}t^{\gamma m}}\right) \\ &\cdot f_{A_1}(a_1)\cdots f_{A_{n-1}}(a_{n-1}) f_B(b) \frac{1}{\left|\sum_{m=0}^{M} b^m g_{m,0}t^{\gamma m}\right|}\,\mathrm{d}a_1\cdots\mathrm{d}a_{n-1}\mathrm{d}b. \end{aligned} \tag{7.11}$$

So far, the 1-PDF, $f_{Y^M(t)}(y)$, of the truncated solution, $Y^M(t)$, has been obtained via a semi-explicit expression (in terms of a multidimensional integral). Now, we will impose mild conditions on the data so that $f_{Y^M(t)}(y)$ converges to $f_{Y(t)}(y)$, where

$$\begin{aligned} f_{Y(t)}(y) = &\int_{\mathcal{D}(A_1)} \cdots \int_{\mathcal{D}(A_{n-1})} \int_{\mathcal{D}(B)} f_{A_0}\left(\frac{y-\sum_{j=1}^{n-1}\sum_{m=0}^{\infty} a_j b^m g_{m,j}t^{\gamma m+j}}{\sum_{m=0}^{\infty} b^m g_{m,0}t^{\gamma m}}\right) \\ &\cdot f_{A_1}(a_1)\cdots f_{A_{n-1}}(a_{n-1}) f_B(b) \frac{1}{\left|\sum_{m=0}^{\infty} b^m g_{m,0}t^{\gamma m}\right|}\,\mathrm{d}a_1\cdots\mathrm{d}a_{n-1}\mathrm{d}b. \end{aligned} \tag{7.12}$$

For the sake of clarity in the presentation of the forthcoming development, we introduce the following notation

$$s_j^M(t) = \sum_{m=0}^{M} b^m g_{m,j}t^{\gamma m+j}, \quad s_j(t) = \sum_{m=0}^{\infty} b^m g_{m,j}t^{\gamma m+j}, \qquad j = 0,1,\ldots n-1. \tag{7.13}$$

Then, expressions (7.11) and (7.12), can be written, respectively, as

$$\begin{aligned} f_{Y^M(t)}(y) = \int_{\mathcal{D}(A_1)} \cdots \int_{\mathcal{D}(A_{n-1})} \int_{\mathcal{D}(B)} f_{A_0}\left(\frac{y - \sum_{j=1}^{n-1} a_j s_j^M(t)}{s_0^M(t)}\right) \\ \cdot f_{A_1}(a_1) \cdots f_{A_{n-1}}(a_{n-1}) f_B(b) \frac{1}{\left|s_0^M(t)\right|} \, \mathrm{d}a_1 \cdots \mathrm{d}a_{n-1} \mathrm{d}b, \end{aligned} \tag{7.14}$$

and

$$\begin{aligned} f_{Y(t)}(y) = \int_{\mathcal{D}(A_1)} \cdots \int_{\mathcal{D}(A_{n-1})} \int_{\mathcal{D}(B)} f_{A_0}\left(\frac{y - \sum_{j=1}^{n-1} a_j s_j(t)}{s_0(t)}\right) \\ \cdot f_{A_1}(a_1) \cdots f_{A_{n-1}}(a_{n-1}) f_B(b) \frac{1}{|s_0(t)|} \, \mathrm{d}a_1 \cdots \mathrm{d}a_{n-1} \mathrm{d}b. \end{aligned} \tag{7.15}$$

Now, let us derive a lower bound for $S_0(t)$ and $S_0^M(t)$, and an upper bound for $S_j(t)$ and $S_j^M(t)$, $j = 1, \ldots n-1$, in a certain neighborhood, that will be required later when studying the convergence $f_{Y^M(t)}(y) \longrightarrow f_{Y(t)}(y)$ as $M \to \infty$. Let us first observe that, from the initial condition and the form of the solution, one gets

$$\begin{aligned} A_0 = Y(0) = Y_0(0) = \sum_{m=0}^{\infty} X_{m,0} t^{\gamma m}\Big|_{t=0} = \sum_{m=0}^{\infty} B^m A_0 g_{m,0} t^{\gamma m}\Big|_{t=0} \\ = A_0 \sum_{m=0}^{\infty} B^m g_{m,0} t^{\gamma m}\Big|_{t=0} = A_0 S_0(0). \end{aligned} \tag{7.16}$$

Observe that in the above expression, we have used capital letters to denote the series $S_0(t)$ evaluated at $t = 0$ because, in this setting, it represents a random power series. Later, when this series as well as $S_j(t)$, $j = 1, \ldots, n-1$ are considered via its samples or trajectories, for consistency with the notation, hereinafter they will be denoted using lower-case letters, i.e. $s_j(t)$, $j = 0, 1, \ldots, n-1$. Since the random variable A_0 is different from zero w.p. 1 (because it is absolutely continuous), then by the last expression, one deduces $S_0(0) = 1$ w.p. 1. From this fact and taking into account that $S_0(t)$ is a random power series evaluated at $t := t^\gamma$, so

continuous w.p. 1, it is guaranteed that

$$\exists\, \delta_0 > 0 :\ 0 < m_{s,0} \leq \min\{|s_0^M(t)|, |s_0(t)|\}, \qquad \forall t :\ |t| \leq \delta_0, \quad \forall M \geq 0 \text{ integer}. \tag{7.17}$$

On the other hand, by Remark 7.1 and the definition of $S_j^M(t)$, $j = 1, \ldots, n-1$, which are random power series evaluated at $t := t^{\gamma m + j}$ and convergent on the whole real line, it is known that each $S_j^M(t)$ is almost surely uniformly convergent in every compact set of $\mathbb{R}$. This guarantees that

$$\exists\, M_{s,j} > 0 :\ \max\{|s_j^M(t)|, |s_j(t)|\} \leq M_{s,j}, \qquad \forall t :\ |t| \leq T, T > 0,\ \forall M > 0, \text{ integer } j = 1, \ldots, n-1. \tag{7.18}$$

Finally, as $S_j^M(t)$ converges uniformly to $S_j(t)$, for each $j = 0, 1, \ldots, n-1$ and given $\epsilon_j > 0$, then

$$\exists\, M_0 > 0 \text{ integer} :\ |s_j^M(t) - s_j(t)| < \epsilon_j, \quad \forall M \geq M_0 \text{ integer and } \forall t :\ |t| \leq T,\ T > 0. \tag{7.19}$$

Hereinafter, and according to (7.17), we will work in a neighborhood of $t = 0$ (possibly small), where the RFIVP (7.3) is formulated, and where the bounds (7.17)–(7.19) are guaranteed. We will prove the convergence $f_{Y^M(t)}(y) \longrightarrow f_{Y(t)}(y)$ as $M \to \infty$ for each t in that neighborhood. To this end, besides assumptions **A1** and **A2**, we will suppose that

A3: The PDF of the first random initial condition A_0, f_{A_0}, is Lipschitz in $\mathbb{R}$, i.e. exists $L_0 > 0$ such that

$$|f_{A_0}(a_2) - f_{A_0}(a_1)| \leq L_0 |a_2 - a_1|, \qquad \forall a_2, a_1 \in \mathbb{R}.$$

Let us observe that

$$|\ f_{Y(t)}(y) - f_{Y^M(t)}(y)| \leq \int_{\mathcal{D}(A_1)} \cdots \int_{\mathcal{D}(A_{n-1})} \int_{\mathcal{D}(B)} \left| f_{A_0}\left(\frac{y - \sum_{j=1}^{n-1} a_j s_j(t)}{s_0(t)} \right) \frac{1}{|s_0(t)|} \right.$$

$$- f_{A_0}\left(\frac{y-\sum_{j=1}^{n-1} a_j s_j^M(t)}{s_0^M(t)}\right)\frac{1}{\left|s_0^M(t)\right|}\Bigg| f_{A_1}(a_1)\cdots f_{A_{n-1}}(a_{n-1}) f_B(b)\,\mathrm{d}a_1\cdots\mathrm{d}a_{n-1}\mathrm{d}b. \tag{7.20}$$

Now, we first add and subtract $f_{A_0}\left(\frac{y-\sum_{j=1}^{n-1} a_j S_j^M(t)}{S_0^M(t)}\right)\frac{1}{|S_0(t)|}$ inside the absolute value. We then arrange the terms and we apply the triangular inequality. Finally, we take into account that any PDF is a non-negative function to remove the unnecessary absolute values. The last expression then writes

$$\begin{aligned}
\left|\, f_{Y(t)}(y) - f_{Y^M(t)}(y)\right| \leq \int_{\mathcal{D}(A_1)}\cdots\int_{\mathcal{D}(A_{n-1})}\int_{\mathcal{D}(B)} \Bigg\{ & \underbrace{f_{A_0}\left(\frac{y-\sum_{j=1}^{n-1} a_j s_j^M(t)}{s_0^M(t)}\right)}_{\text{(I)}} \\
& \cdot \underbrace{\left|\frac{1}{|s_0(t)|}-\frac{1}{\left|s_0^M(t)\right|}\right|}_{\text{(II)}} + \underbrace{\left|f_{A_0}\left(\frac{y-\sum_{j=1}^{n-1} a_j s_j(t)}{s_0(t)}\right) - f_{A_0}\left(\frac{y-\sum_{j=1}^{n-1} a_j s_j^M(t)}{s_0^M(t)}\right)\right|}_{\text{(III)}} \\
& \cdot \underbrace{\frac{1}{|s_0(t)|}}_{\text{(IV)}} \Bigg\} f_{A_1}(a_1))\cdots f_{A_{n-1}}(a_{n-1}) f_B(b)\,\mathrm{d}a_1\cdots\mathrm{d}a_{n-1}\mathrm{d}b.
\end{aligned} \tag{7.21}$$

We are going to bound the terms (I)–(IV). For the term (I), let us denote by $F_0 = f_{A_0}(0)$ (remember that by assumption **A3** this value exists), then first applying **A3**, secondly the triangular inequality together with bounds (7.17) and (7.18), one gets

$$\begin{aligned}
f_{A_0}\left(\frac{y-\sum_{j=1}^{n-1} a_j s_j^M(t)}{s_0^M(t)}\right) &\leq \left|f_{A_0}\left(\frac{y-\sum_{j=1}^{n-1} a_j s_j^M(t)}{s_0^M(t)}\right) - f_{A_0}(0)\right| + F_0 \\
&\leq L_0\left|\frac{y-\sum_{j=1}^{n-1} a_j s_j^M(t)}{s_0^M(t)}\right| + F_0 \\
&\leq \frac{L_0}{m_{s,0}}\left(|y| + \sum_{j=1}^{n-1}|a_j| M_{s,j}\right) + F_0.
\end{aligned}$$

Let us now bound the term (II) by applying (7.17) and (7.19) for $j = 0$,

$$\left|\frac{1}{|s_0(t)|} - \frac{1}{|s_0^M(t)|}\right| = \frac{\left||s_0^M(t)| - |s_0(t)|\right|}{|s_0(t)||s_0^M(t)|} \leq \frac{|s_0^M(t) - s_0(t)|}{|s_0(t)||s_0^M(t)|} \leq \frac{\epsilon_0}{m_{s,0}^2}.$$

The term (IV) can be similarly bounded applying (7.17)

$$\frac{1}{|s_0(t)|} \leq \frac{1}{m_{s,0}}.$$

Finally, let us bound the term (III). To this end, we first apply assumption **A3**, and secondly, the triangular inequality together with bounds (7.17)–(7.19),

$$\begin{aligned}
&| f_{A_0}\left(\frac{y - \sum_{j=1}^{n-1} a_j s_j(t)}{s_0(t)}\right) - f_{A_0}\left(\frac{y - \sum_{j=1}^{n-1} a_j s_j^M(t)}{s_0^M(t)}\right)\Bigg| \\
&\leq L_0 \left|\frac{y - \sum_{j=1}^{n-1} a_j s_j(t)}{s_0(t)} - \frac{y - \sum_{j=1}^{n-1} a_j s_j^M(t)}{s_0^M(t)}\right| \\
&= L_0 \left|\frac{y s_0^M(t) - s_0^M(t)\sum_{j=1}^{n-1} a_j s_j(t) - y s_0(t) + s_0(t)\sum_{j=1}^{n-1} a_j s_j^M(t)}{s_0(t)s_0^M(t)}\right| \\
&= L_0 \left|\frac{y\left(s_0^M(t) - s_0(t)\right) + \sum_{j=1}^{n-1} a_j\left(s_0(t)s_j^M(t) - s_0^M(t)s_j(t)\right)}{s_0(t)s_0^M(t)}\right| \\
&\leq L_0 \frac{|y||s_0^M(t) - s_0^M(t)| + \sum_{j=1}^{n-1}|a_j|\left|s_0(t)s_j^M(t) - s_0^M(t)s_j(t)\right|}{|s_0(t)||s_0^M(t)|} \\
&= L_0 \frac{|y||s_0^M(t) - s_0^M(t)| + \sum_{j=1}^{n-1}|a_j|\left|s_0(t)s_j^M(t) - s_j(t)s_0(t) + s_j(t)s_0(t) - s_0^M(t)s_j(t)\right|}{|s_0(t)||s_0^M(t)|} \\
&\leq L_0 \frac{|y||s_0^M(t) - s_0^M(t)| + \sum_{j=1}^{n-1}|a_j|\left(|s_0(t)||s_j^M(t) - s_j(t)| + |s_j(t)||s_0(t) - s_0^M(t)|\right)}{|s_0(t)||s_0^M(t)|} \\
&\leq L_0 \frac{|y|\epsilon_0 + \sum_{j=1}^{n-1}|a_j|\left(M_{s,0}\epsilon_j + M_{s,j}\epsilon_0\right)}{m_{s,0}^2}.
\end{aligned}$$

Substituting the previous bounds in (7.21), one gets

$$\left|f_{Y(t)}(y) - f_{Y^M(t)}(y)\right|$$

$$
\begin{aligned}
&\leq \int_{\mathcal{D}(A_1)} \cdots \int_{\mathcal{D}(A_{n-1})} \int_{\mathcal{D}(B)} \left\{ \left(\frac{L_0}{m_{s,0}} \left(|y| + \sum_{j=1}^{n-1} |a_j| M_{s,j} \right) + F_0 \right) \frac{\epsilon_0}{m_{s,0}^2} \right. \\
&\left. + \left(L_0 \frac{|y|\varepsilon_0 + \sum_{j=1}^{n-1} |a_j| \left(M_{s,0}\epsilon_j + M_{s,j}\epsilon_0 \right)}{m_{s,0}^2} \right) \frac{1}{m_{s,0}} \right\} \\
&\cdot f_{A_1}(a_1) \cdots f_{A_{n-1}}(a_{n-1}) f_B(b)\, \mathrm{d}a_1 \cdots \mathrm{d}a_{n-1} \mathrm{d}b.
\end{aligned}
$$

If we denote $\epsilon := \max \epsilon_j$, and $\mathcal{M} := \max M_{s,j}$, $j = 0, 1, \ldots, n-1$, one gets

$$
\begin{aligned}
&\left| f_{Y(t)}(y) - f_{Y^M(t)}(y) \right| \\
&\leq \int_{\mathcal{D}(A_1)} \cdots \int_{\mathcal{D}(A_{n-1})} \int_{\mathcal{D}(B)} \left\{ \left(\frac{L_0}{m_{s,0}} \left(|y| + \mathcal{M} \sum_{j=1}^{n-1} |a_j| \right) + F_0 \right) \frac{\epsilon}{m_{s,0}^2} \right. \\
&\quad \left. + L_0 \frac{|y|\epsilon + 2\mathcal{M}\epsilon \sum_{j=1}^{n-1} |a_j|}{m_{s,0}^3} \right\} f_{A_1}(a_1) \cdots f_{A_{n-1}}(a_{n-1}) f_B(b)\, \mathrm{d}a_1 \cdots \mathrm{d}a_{n-1} \mathrm{d}b \\
&= \int_{\mathcal{D}(A_1)} \cdots \int_{\mathcal{D}(A_{n-1})} \int_{\mathcal{D}(B)} \left(\frac{L_0 |y| \epsilon}{m_{s,0}^3} + \frac{L_0 \mathcal{M} \epsilon}{m_{s,0}^3} \sum_{j=1}^{n-1} |a_j| + \frac{F_0 \epsilon}{m_{s,0}^2} \right. \\
&\quad \left. + \frac{L_0 |y| \epsilon}{m_{s,0}^3} + \frac{2 L_0 \mathcal{M} \epsilon}{m_{s,0}^3} \sum_{j=1}^{n-1} |a_j| \right) f_{A_1}(a_1) \cdots f_{A_{n-1}}(a_{n-1}) f_B(b)\, \mathrm{d}a_1 \cdots \mathrm{d}a_{n-1} \mathrm{d}b \\
&= \epsilon \left(\frac{2L_0|y|}{m_{s,0}^3} + \frac{F_0}{m_{s,0}^2} \right) \int_{\mathcal{D}(A_1)} \cdots \int_{\mathcal{D}(A_{n-1})} \int_{\mathcal{D}(B)} f_{A_1}(a_1) \cdots f_{A_{n-1}}(a_{n-1}) f_B(b)\, \mathrm{d}a_1 \cdots \mathrm{d}a_{n-1} \mathrm{d}b \\
&\quad + \frac{3 L_0 \mathcal{M} \epsilon}{m_{s,0}^3} \sum_{j=1}^{n-1} \int_{\mathcal{D}(A_1)} \cdots \int_{\mathcal{D}(A_{n-1})} \int_{\mathcal{D}(B)} |a_j| f_{A_1}(a_1) \cdots f_{A_{n-1}}(a_{n-1}) f_B(b)\, \mathrm{d}a_1 \cdots \mathrm{d}a_{n-1} \mathrm{d}b \\
&= \epsilon \left(\frac{2L_0|y|}{m_{s,0}^3} + \frac{F_0}{m_{s,0}^2} \right) \underbrace{\left(\int_{\mathcal{D}(A_1)} f_{A_1}(a_1)\, \mathrm{d}a_1 \right)}_{=1} \cdots \underbrace{\left(\int_{\mathcal{D}(A_{n-1})} f_{A_{n-1}}(a_{n-1})\, \mathrm{d}a_{n-1} \right)}_{=1} \\
&\quad \cdot \underbrace{\left(\int_{\mathcal{D}(B)} f_B(b)\, \mathrm{d}b \right)}_{=1} + \frac{3 L_0 \mathcal{M} \epsilon}{m_{s,0}^3} \sum_{j=1}^{n-1} \underbrace{\left(\int_{\mathcal{D}(A_1)} f_{A_1}(a_1)\, \mathrm{d}a_1 \right)}_{=1} \cdots \underbrace{\left(\int_{\mathcal{D}(A_{j-1})} f_{A_{j-1}}(a_{j-1})\, \mathrm{d}a_{j-1} \right)}_{=1} \\
&\quad \cdots \underbrace{\left(\int_{\mathcal{D}(A_j)} |a_j| f_{A_j}(a_j)\, \mathrm{d}a_j \right)}_{=\mathbb{E}[|A_j|]} \cdots \underbrace{\left(\int_{\mathcal{D}(A_{n-1})} f_{A_{n-1}}(a_{n-1})\, \mathrm{d}a_{n-1} \right)}_{=1} \underbrace{\left(\int_{\mathcal{D}(B)} f_B(b)\, \mathrm{d}b \right)}_{=1} \\
&\quad \cdot f_{A_1}(a_1) \cdots f_{A_{n-1}}(a_{n-1}) f_B(b)\, \mathrm{d}a_1 \cdots \mathrm{d}a_{n-1} \mathrm{d}b
\end{aligned}
$$

$$= \epsilon \left(\frac{2L_0|y|}{m_{s,0}^3} + \frac{F_0}{m_{s,0}^2} \right) + \epsilon \frac{3L_0\mathcal{M}}{m_{s,0}^3} \sum_{j=1}^{n-1} \mathrm{E}[|A_j|]$$

$$= \epsilon \left(\frac{2L_0|y|}{m_{s,0}^3} + \frac{F_0}{m_{s,0}^2} + \frac{3L_0\mathcal{M}}{m_{s,0}^3} \sum_{j=1}^{n-1} \mathrm{E}[|A_j|] \right).$$

Taking into account Remark 7.2, the above sum of the expectations is finite. So, the following result has been established:

Theorem 7.1 *Consider the random fractional initial value problem* (7.3)*, where its data satisfies the assumptions* ***A1****–****A3****. Then, the probability density function,* $f_{Y^M(t)}(y)$*, defined by* (7.11)*, corresponding to the approximate solution of order* M *given in* (7.6)*–*(7.7)*, converges to the probability density function,* $f_{Y(t)}(y)$*, given by* (7.12) *of the exact solution* (7.4)*–*(7.5) *as* $M \to \infty$ *for each* (t, y)*.*

7.3 Numerical examples

This section is devoted to illustrating the previous theoretical findings with two numerical examples, where we graphically show the convergence of the sequence of PDFs, $f_{Y^M(t)}(y)$, to $f_{Y(t)}(y)$, as M increases. Additionally, as assumptions **A1** and **A2** guarantee hypotheses **H1** and **H2** fulfill, then $Y^M(t)$, given by (7.6)–(7.7), is mean square convergent to $Y(t)$, given by (7.4)–(7.5). As a consequence, the mean and the variance of the solution exist, and then they can be approximated by

$$\mathbb{E}[Y^M(t)] = \int_{-\infty}^{\infty} y f_{Y^M(t)}(y)\,\mathrm{d}y \tag{7.27}$$

and

$$\begin{aligned} \mathbb{V}[Y^M(t)] &= \mathbb{E}[(Y^M(t))^2] - (\mathbb{E}[Y^M(t)])^2 \\ &= \int_{-\infty}^{\infty} y^2 f_{Y^M(t)}(y)\,\mathrm{d}y - \left(\int_{-\infty}^{\infty} y f_{Y^M(t)}(y)\,\mathrm{d}y \right)^2, \end{aligned} \tag{7.28}$$

respectively, (see [89, Th. 4.2.1] and [89, Th. 4.3.1], respectively).

Example 7.1 *The first example aims to show that the results obtained with the approach presented in this chapter are in full agreement with the ones obtained*

in [12]. To check that the results given in [12, Example 1] agree with the ones in the present example, let us assume that the values of A_0 *and* A_1 *and* B *are close to that example, so ensuring assumptions* ***A1****–****A3*** *fulfill. Firstly, let us consider* $\beta = 1$ *and* $\alpha = 1.9$*. In [12] the random variable* B *is considered as a negative beta distribution of parameters 2 and 3. According to Assumption* ***A2*** *the random variable* B *must be bounded and away from 0. To guarantee this assumption is satisfied while the spirit of [12, Example 1] holds true, we here take* B *as a negative Beta distribution of parameters* 2 *and* 3 *truncated at the interval* $[0.05, 1]$*, i.e.* $B \sim -\mathrm{Be}_{[0.05,1]}(2,3)$*. The initial conditions* A_0 *and* A_1 *are taken as in [12, Example 1]. So* A_0 *is a Normal distribution with mean* 1 *and standard deviation* 1*, i.e.* $A_0 \sim \mathrm{N}(1;1)$*, hence* $\mathbb{E}[A_0] = 1$ $\mathbb{E}[A_0^2] = 2$*. It is important to remark that the PDF of a Gaussian distribution has bounded derivative on the whole real line, so applying the Mean Value theorem, it is straightforward to check that it is globally Lipschitz continuous [3]. As a consequence, assumption* ***A3*** *fulfills. The random variable* A_1 *is assumed to have a uniform distribution of mean* 2 *and standard deviation* 1*, i.e.* $A_1 \sim U(2-\sqrt{3}, 2+\sqrt{3})$*. Additionally, we will assume that* A_0*,* A_1 *and* B *are independent, so assumption* ***A1*** *holds.*

In Figure 7.1, we graphically show the approximations, $f_{Y^M(t)}$*, of the 1-PDF* (7.11) *at the time instants* $t \in \{0.5, 1, 1.5, 2\}$ *for different orders of truncation,* $M \in \{1, 5, 10\}$*. In each panel, we have performed a zoom to better illustrate the convergence as* M *increases.*

In Table 7.1, we collect the approximations of the mean and the variance of the solution using (7.27) *and* (7.28)*, respectively. We point out these figures agree with the ones obtained in [12, Example 1]. To numerically verify the convergence of the 1-PDFs as* M *increases, Table 7.2 collects the* L_1*-norm of the difference between consecutive approximations of the 1-PDF w.r.t. the order of truncation, i.e.*

$$e_M(t) := \|f_{Y_{M+1}(t)}(y) - f_{Y_M(t)}(y)\|_1 = \int_{\mathcal{D}_t} |f_{Y_{M+1}(t)}(y) - f_{Y_M(t)}(y)| \, \mathrm{d}y. \quad (7.29)$$

Here, we have taken the same domain of integration, $\mathcal{D}_t$*, as the one used for plotting the PDF for* t *fixed. As we can observe, the error decreases with* M*, so correctly illustrating convergence as expected.*

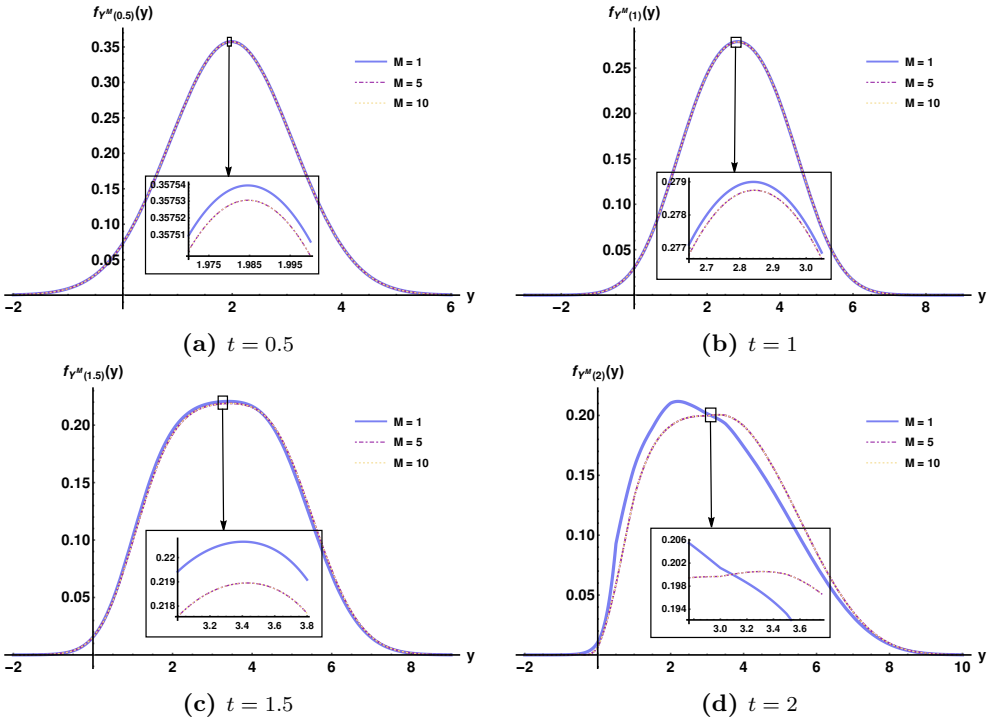

(a) $t = 0.5$ **(b)** $t = 1$

(c) $t = 1.5$ **(d)** $t = 2$

Figure 7.1: Approximations of $f_{Y^M(t)}$, given in (7.11), of 1-PDF of the solution stochastic process at the time instants $t \in \{0.5, 1, 1.5, 2\}$ for different orders of truncation $M \in \{1, 5, 10\}$. Example 7.1 with $\alpha = 1.9$.

We complete this example showing the corresponding approximations when $\alpha = 1.2$ at the same foregoing time instants and using the same orders of truncation. The approximations of the 1-PDF of the solution are shown in Figure 7.2, while Table 7.3 collects the figures for the mean and the variance. In Table 7.4, we collect the L_1-norm for the difference for consecutive approximations. We can graphically and numerically observe convergence as the order of truncation increases, respectively.

Example 7.2 *In this second example, we deal with the case that $\alpha = 2.5$, so $n = -\lfloor -2.5 \rfloor = 3$, and three initial conditions, A_0, A_1 and A_2 are then required. We take $A_0 \sim \mathrm{N}(2; 3^2)$, hence* **A3** *is fulfilled. The random variables A_1 and A_2 are assumed $A_1 \sim \mathrm{Be}(1, 1)$ and $A_2 \sim \mathrm{U}(2, 4)$. In order to guarantee assumption* **A2** *holds true, we will assume that B has a Gamma distribution of parameters $(2, 2)$*

$\mathbb{E}[Y^M(t)] \mid \mathbb{V}[Y^M(t)]$	$\mathbf{t = 0.5}$	$\mathbf{t = 1}$	$\mathbf{t = 1.5}$	$\mathbf{t = 2}$
$\mathbf{M = 1}$	1.9841 | 1.22372	2.84533 | 1.7836	3.37137 | 2.39698	3.26288 | 3.04415
$\mathbf{M = 5}$	1.9842 | 1.22378	2.84807 | 1.7872	3.40555 | 2.42417	3.46492 | 2.99021
$\mathbf{M = 10}$	1.9842 | 1.22378	2.84807 | 1.7872	3.40555 | 2.42417	3.46492 | 2.99021

Table 7.1: Approximations of the mean and variance at time instants $t \in \{0.5, 1, 1.5, 2\}$ using different orders of truncation $M \in \{1, 5, 10\}$. These values have been calculated using (7.27) and (7.28), respectively. Example 7.1 with $\alpha = 1.9$.

$e_M(t)$; $\alpha = 1.9$	$\mathbf{t = 0.5}$	$\mathbf{t = 1}$	$\mathbf{t = 1.5}$	$\mathbf{t = 2}$
$\mathbf{M = 1}$	0.00003521008	0.00184215438	0.01988455842	0.11839990407
$\mathbf{M = 5}$	$2.5804011 \cdot 10^{-17}$	$1.4576956 \cdot 10^{-12}$	$1.6507047 \cdot 10^{-9}$	$4.0953768 \cdot 10^{-7}$
$\mathbf{M = 10}$	0.	0.	0.	$3.4694469 \cdot 10^{-17}$

Table 7.2: Values of the L_1-norm defined in (7.29) for different orders of truncation, $M \in \{1, 5, 10\}$, at the time instants $t \in \{0.5, 1, 1.5, 2\}$. The order of the fractional derivative is $\alpha = 1.9$. Example 7.1.

truncated at the interval $[0.05, 15]$*, i.e.* $A_2 \sim \mathrm{Ga}_{[0.05,15]}(2, 2)$*. In Figure 7.3, we show the approximations* $f_{Y^M(t)}$ *for the PDF of the solution at the time instants* $t \in \{0.5, 1, 1.5, 2\}$ *for different orders of truncation. In each panel of Figure 7.3 is graphically observed convergence as* M *increases. From the plots, and particularly looking at the magnified plots, we can observe that, for* t *fixed, the approximations improve when* M *increases, while for* M *fixed, the approximations deteriorate as* t *increases, as expected.*

7.4 Conclusions

In this chapter, we have provided an alternative approach to approximate the first probability density function of the solution stochastic process of a generalized model formulated via a differential equation that appears in a number of relevant problems of Classical Mechanics. The proposed approach avoids double approximations, and hence their associated errors, based on first approximating the moments of the solution and secondly applying the Principle of Maximum Entropy. The mild conditions assumed to conduct our study permit applying our theoretical results to a wide variety of real-world scenarios where probability distributions must be inferred from all the model data.

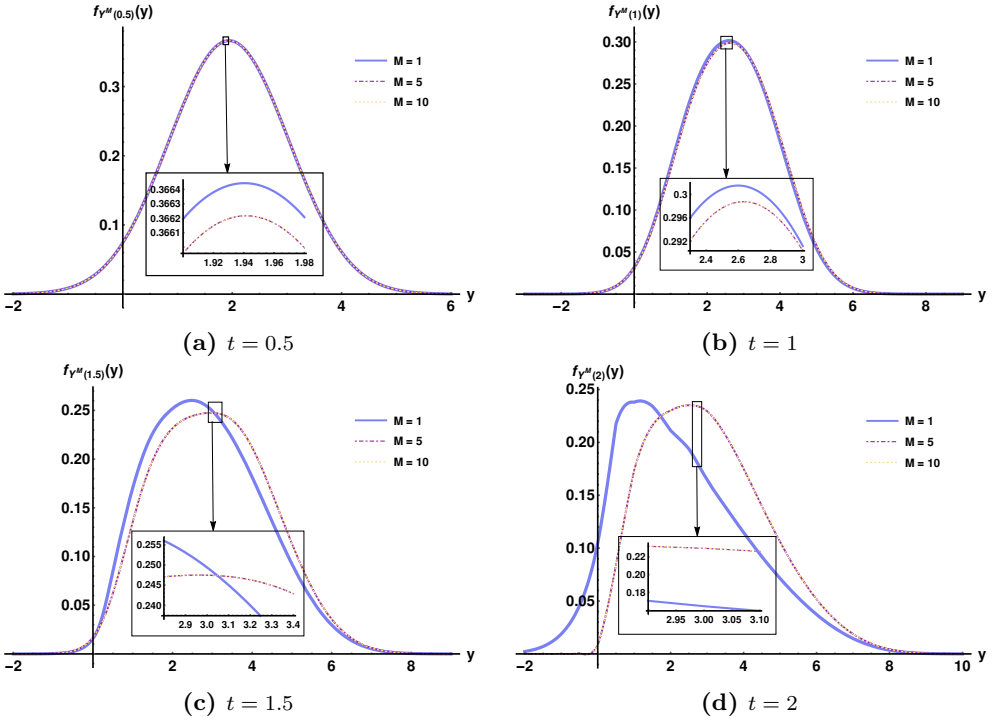

(a) $t = 0.5$ **(b)** $t = 1$

(c) $t = 1.5$ **(d)** $t = 2$

Figure 7.2: Approximations of $f_{Y^M(t)}$, given in (7.11), of 1-PDF of the solution stochastic process at the time instants $t \in \{0.5, 1, 1.5, 2\}$ for different orders of truncation $M \in \{1, 5, 10\}$. Example 7.1 with $\alpha = 1.2$.

Publications associated with this chapter

A complete version of the chapter's findings has been published in the paper [13].

$\mathbb{E}[Y^M(t)] \mid \mathbb{V}[Y^M(t)]$	$\mathbf{t = 0.5}$	$\mathbf{t = 1}$	$\mathbf{t = 1.5}$	$\mathbf{t = 2}$
$\mathbf{M = 1}$	1.94084 | 1.16605	2.62433 | 1.53783	2.82825 | 1.99607	2.3131 | 3.18559
$\mathbf{M = 5}$	1.94185 | 1.16743	2.65148 | 1.56298	3.01537 | 2.03536	3.03015 | 2.53089
$\mathbf{M = 10}$	1.94185 | 1.16743	2.65148 | 1.56298	3.01539 | 2.03536	3.03099 | 2.52984

Table 7.3: Approximations of the mean and variance at time instants $t \in \{0.5, 1, 1.5, 2\}$ using different orders of truncation $M \in \{1, 5, 10\}$. These values have been calculated using (7.27) and (7.28), respectively. Example 7.1 with $\alpha = 1.2$.

$e_M(t)$; $\alpha = \mathbf{1.2}$	$\mathbf{t = 0.5}$	$\mathbf{t = 1}$	$\mathbf{t = 1.5}$	$\mathbf{t = 2}$
$\mathbf{M = 1}$	0.00093398498	0.02108848639	0.13985203151	0.48984846327
$\mathbf{M = 5}$	$6.5739242 \cdot 10^{-12}$	$6.1373116 \cdot 10^{-8}$	0.00001457034	0.00091111341
$\mathbf{M = 10}$	0.	$3.1576341 \cdot 10^{-16}$	$5.6654917 \cdot 10^{-12}$	$8.4097494 \cdot 10^{-9}$

Table 7.4: Values of the L_1-norm defined in (7.29) for different orders of truncation, $M \in \{1, 5, 10\}$, at the time instants $t \in \{0.5, 1, 1.5, 2\}$. The order of the fractional derivative is $\alpha = 1.2$. Example 7.1.

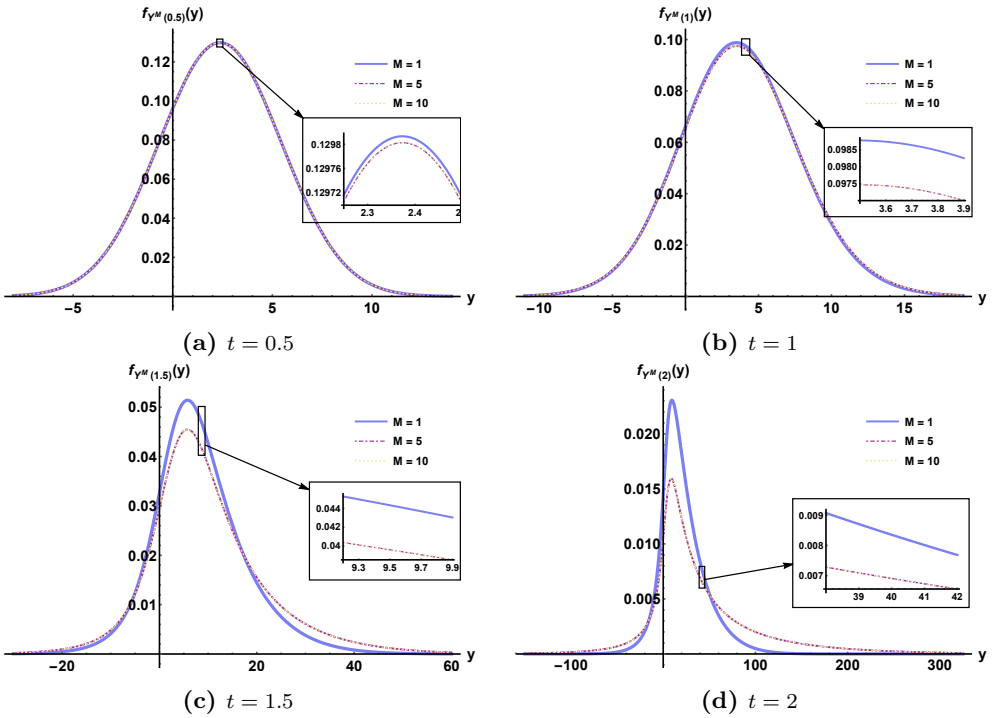

(a) $t = 0.5$ **(b)** $t = 1$

(c) $t = 1.5$ **(d)** $t = 2$

Figure 7.3: Approximations of $f_{Y^M(t)}$, given in (7.11), of 1-PDF of the solution stochastic process at the time instants $t \in \{0.5, 1, 1.5, 2\}$ for different orders of truncation $M \in \{1, 5, 10\}$. Example 7.2 with $\alpha = 2.5$.

Chapter 8

General Conclusions

In the development of this thesis, the importance of the calculation of the so-called first probability density function of the response of some mechanical engineering models has been highlighted, since obtaining it has been our main objective in all the chapters. Indeed, the computation of the first probability density function is very advantageous since from it one can calculate any one-dimensional moment of the response, such as the mean (or expectation) and the variance functions but also higher-order moments, such as kurtosis and skewness, provided they exist. In this manner, the probabilistic system's response can be completely characterised (as it happens in the Gaussian case) or better approximated in many scenarios. Furthermore, the first probability density function permits computing key information about the mechanical system such as the probability that the response (e.g., the position and/or velocity of an oscillator; the deflection of a beam; etc.) lies within an interval of specific interest.

In Chapters 3 and 4, it has been shown that the combination of the classical stochastic perturbation method and the Principle of Maximum Entropy allows to obtain approximations of the stationary probability density function of nonlinear oscillators in scenarios where the restoring term depends on both position and

velocity. Although the study is limited to the case where the external force is a stationary Gaussian process (with zero-mean), which permits taking advantage of the so-called random mean square calculus, it can be also useful to approximate the response of nonlinear oscillators when the external input can locally be approximated via a stationary Gaussian process using the central limit theorem. Nevertheless, we want to point out that our approach has several limitations that need to be further explored in forthcoming studies. First, and as it also happens when utilizing the deterministic perturbation technique, in the stochastic setting we have been restricted to obtain reliable approximations to the stationary probability density function of the system's response only for small values of the perturbative parameter. This fact stems from the need to truncate the expansion of the solution, represented via the perturbation method, to first order. In this manner, we have been able to take advantage of the rich properties that linear Gaussian processes have. Furthermore, when the Principle of Maximum Entropy has been applied, we have worked with a few statistical moments due to the aforementioned application of the stochastic perturbation technique. In future works, it may be interesting to explore two possible ways of improvement the above-mentioned limitations. On the one hand, and maintaining the order of perturbation to the linear term, one can explore the possibility of approximating more statistical moments. Nevertheless, we guess that, due to its complexity, this must be only carried out by means of purely computational development. On the other hand, it could be interesting to extend the study exhibited in Chapters 3 and 4 by working with truncations of second order when applying the stochastic perturbation method. However, the nonlinear nature of such an approximation can be very challenging in combination with the properties of Gaussian stochastic processes. The study could be extended, in the case of Chapter 3, to a restoring term in the form of an arbitrary polynomial whose variable is the oscillator position and, in the case of Chapter 4, to a polynomial of two variables, position and velocity. This would allow us to approximate, in both cases, the more general scenario in which the restoring term is defined by an analytical function (in one or two variables) by its Taylor truncation to an appropriate order.

In Chapters 5 and 6, a static deflection model has been studied using the Euler-Bernoulli beam theory. In both chapters, an explicit solution of the model has

been obtained, but we have had to adopt different approaches to determine its probability density function. On the one hand, in Chapter 5, it has been feasible to calculate it using the Random Variable Transformation method. This approach has allowed for a detailed and accurate probabilistic analysis of the structural system under study. On the other hand, in Chapter 6, it has not been possible to apply the Random Variable Transformation method because of the load spanned in the beam is described by a correlated delta process involving a random number of pulses. In this case, first we have obtained the first statistical moments of the response and then we have applied the Principle of Maximum Entropy to address the approximation of the probability density function of the solution. An interesting point that has not been widely documented in the literature is the possibility of extending the Random Variable Transformation method when we are dealing with a process defining via a random number of addends, such as those found in Chapter 6. In future works, we aim to explore this generalization of the Random Variable Transformation method, with the objective of effectively applying this approach in situations where complex stochastic processes are involved, such as the one presented in this case.

In Chapter 7, we have shown that the Random Variable Transformation method is a powerful tool to obtain the first probability density function of oscillators described by differential equations with Caputo fractional derivatives and with data (initial position and velocity, and the oscillator's constant) that depend on random variables with arbitrary distributions. The study we have carried out is a first step on a simple type of oscillators, but from the analysis, we can conclude that it can be extended to oscillators with greater complexity both in its formulation through other differential equations with generalised derivatives and involving uncertainty via not only random variables but also stochastic processes. In this sense, we believe that the ideas developed in this chapter have great potential in the emerging field of fractional differential equations and their applications in Probabilistic Mechanics Engineering.

Bibliography

[1] R.P. Agarwal, S. Hodis, and D. O'Regan. *500 Examples and Problems of Applied Differential Equations*. Springer Nature, 2019. ISBN: 978-3-030-26384-3 (cit. on p. 144).

[2] A.A. Andronov, A.A. Vitt, and S.E. Khaikin. *Theory of Oscillators*. Electrical Engineering. New York: Dover Books, 2011. ISBN: 978-0486655086 (cit. on p. 3).

[3] T.M. Apostol. *Mathematical Analysis*. Addison-Wesley series in mathematics. Addison-Wesley, 1974. ISBN: 9780201002881 (cit. on p. 157).

[4] ASM Handbook Committee. *Properties and Selection: Irons, Steels, and High-Performance Alloys*. ASM International, 1990. ISBN: 978-1-62708-161-0 (cit. on p. 132).

[5] T.M. Atanacković, S. Pilipović, B. Stanković, and D. Zorica. *Fractional Calculus With Applications in Mechanics: Wave Propagation, Impact and Variational Principles*. Wiley, 2014. ISBN: 9781118909065 (cit. on p. 6).

[6] B. Balachandran and E. Magrab. *Vibrations*. Cencage Learning, 2009. ISBN: 978-0-534-55206-0 (cit. on p. 144).

[7] H.T. Banks, H. Shuhua, and W. Clayton. *Modelling and Inverse Problems in the Presence of Uncertainty*. Monographs and Research Notes in Mathematics. CRC Press, 2014. ISBN: 978-1482206425 (cit. on p. 43).

[8] R. Bellman. *Perturbation Techniques in Mathematics, Engineering and Physics*. Dover Books on Physics. New York: Dover Publications, 2003. ISBN: 978-0486432588 (cit. on p. 26).

[9] B. Biondi and S. Caddemi. "Euler–Bernoulli beams with multiple singularities in the flexural stiffness". In: *European Journal of Mechanics - A/Solids*

26.5 (2007), pp. 789–809. ISSN: 0997-7538. DOI: 10.1016/j.euromechsol.2006.12.005 (cit. on p. 4).

[10] P. Blondeel, P. Robbe, C. Van Hoorickx, G. Lombaert, and S. Vandewalle. "Multilevel Monte Carlo applied to a structural engineering model with random material parameters". In: *Proceedings of ISMA2018 and USD2018*. Ed. by W. Desmet, B. Pluymers, D. Moens, and W. Rottiers. Leuven: Wiley-VCH Verlag, 2018, pp. 5027–5042. ISBN: 9789073802995 (cit. on p. 80).

[11] J.L. Bogdanoff, J.E. Goldberg, and M.C. Bernard. "Response of a simple structure to a random earthquake-type disturbance". In: *Bulletin of the Seismological Society of America* 51 (2 1961), pp. 293–310. DOI: 10.1785/BSSA0510020293 (cit. on p. 3).

[12] C. Burgos, J.-C. Cortés, A. Debbouche, L. Villafuerte, and R.-J. Villanueva. "Random fractional generalized Airy differential equations: A probabilistic analysis using mean square calculus". In: *Applied Mathematics and Computation* 352 (2019), pp. 15–29. DOI: 10.1016/j.amc.2019.01.039 (cit. on pp. 6, 146 sq., 157).

[13] C. Burgos, J.-C. Cortés, E. López-Navarro, C.M.A. Pinto, and R.-J. Villanueva. "Probabilistic analysis of a foundational class of generalized second-order linear differential equations in classic mechanics". In: *The European Physical Journal Plus* 137.5 (2022). DOI: 10.1140/epjp/s13360-022-02691-x (cit. on p. 160).

[14] C. Burgos, J.-C. Cortés, L. Villafuerte, and R.-J. Villanueva. "Extending the deterministic Riemann–Liouville and Caputo operators to the random framework: A mean square approach with applications to solve random fractional differential equations". In: *Chaos, Solitons & Fractals* 102 (2017). Future Directions in Fractional Calculus Research and Applications, pp. 305–318. DOI: 10.1016/j.chaos.2017.02.008 (cit. on p. 145).

[15] J. Calatayud, J.-C. Cortés, and M. Jornet. "The damped pendulum random differential equation: A comprehensive stochastic analysis via the computation of the probability density function". In: *Physica A: Statistical Mechanics and its Applications* 512 (2018), pp. 261–279. DOI: 10.1016/j.physa.2018.08.024 (cit. on p. 26).

[16] J. Calatayud, J.-C Cortés, M. Jornet, and L. Villafuerte. "Random non-autonomous second order linear differential equations: mean square analytic solutions and their statistical properties". In: *Advances in Difference Equations* 392 (2018). DOI: 10.1186/s13662-018-1848-8 (cit. on p. 147).

[17] J. Calatayud, J.-C. Cortés, M. Jornet, and R.-J. Villanueva. *An introduction to random variables, random vectors and stochastic processes*. Editorial Universitat Politècnica de València, 2019. ISBN: 978-84-9048-824-9 (cit. on pp. 7, 15).

[18] J.A.M. Carrer, R.F. Scuciato, and L.F.T. Garcia. "The Boundary Element Method Applied to the Analysis of Euler–Bernoulli and Timoshenko Continuous Beams". In: *Iran J Sci Technol Trans Civ Eng* 44 (2020), 875–888. DOI: 10.1007/s40996-020-00359-z (cit. on p. 4).

[19] G. Casella and R.L. Berger. *Statistical Inference*. India: Cengage Learning, 2007. ISBN: 978-8131503942 (cit. on pp. 47, 133, 139).

[20] L. Chen, J. Qian, H. Zhu, and J.Q. Sun. "The closed-form stationary probability distribution of the stochastically excited vibro-impact oscillators". In: *Journal of Sound and Vibration* 439 (2019), pp. 260–270. DOI: 10.1016/j.jsv.2018.09.061 (cit. on p. 27).

[21] Q. Chen, H. Zhu, and J.W. et al. Ju. "A stochastic micromechanical model for fiber-reinforced concrete using maximum entropy principle". In: *Acta Mechanica* 229 (2018), pp. 2719–2735. DOI: 10.1007/s00707-018-2135-1 (cit. on p. 116).

[22] J.-C. Cortés, E. López-Navarro, P. Martínez-Rodríguez, J.-V. Romero, and M.-D. Roselló. "Extending the analysis of the Euler–Bernoulli model for a stochastic static cantilever beam: Theory and simulations". In: *Probabilistic Engineering Mechanics* 74 (2023), p. 103493. DOI: 10.1016/j.probengmech.2023.103493 (cit. on p. 141).

[23] J.-C. Cortés, E. López-Navarro, J.-V. Romero, and M.-D. Roselló. "Approximating the Density of Random Differential Equations with Weak Nonlinearities via Perturbation Techniques". In: *Mathematics* 9.3 (2021), p. 204. DOI: 10.3390/math9030204 (cit. on pp. 58, 76).

[24] J.-C. Cortés, E. López-Navarro, J.-V. Romero, and M.-D. Roselló. "Probabilistic analysis of a cantilever beam subjected to random loads via probability density functions". In: *Computational and Applied Mathematics* 42.1 (2023). DOI: 10.1007/s40314-023-02194-0 (cit. on p. 110).

[25] J.-C. Cortés, E. López-Navarro, J.-V. Romero, and M.-D. Roselló. "Probabilistic analysis of random nonlinear oscillators subject to small perturbations via probability density functions: theory and computing". In: *The European Physical Journal Plus* 136.723 (2021). DOI: 10.1140/epjp/s13360-021-01672-w (cit. on p. 55).

[26] S. H. Crandall. "Perturbation Techniques for Random Vibration of Nonlinear Systems". In: *The Journal of the Acoustical Society of America* 35.11 (1963), pp. 1700–1705. DOI: 10.1121/1.1918792 (cit. on pp. 26, 58, 72).

[27] S.H. Crandall. *Random Vibration*. New York: John Wiley & Sons, 1958 (cit. on p. 26).

[28] L. Cveticanin. *Strongly Nonlinear Oscillators: Analytical Solutions*. New York: Springer, 2014. ISBN: 978-3-319-05272-4 (cit. on p. 3).

[29] A. Di Matteo. "Response of nonlinear oscillators with fractional derivative elements under evolutionary stochastic excitations: A Path Integral approach based on Laplace's method of integration". In: *Probabilistic Engineering Me-*

chanics 71 (2023), p. 103402. DOI: 10.1016/j.probengmech.2022.103402 (cit. on p. 6).

[30] M.A. El-Beltagy and A.S. Al-Johany. "Numerical approximation of higher-order solutions of the quadratic nonlinear stochastic oscillatory equation using WHEP technique". In: *Journal of Applied Mathematics* ID-685137 (2013), pp. 1–21. DOI: 10.1155/2013/685137 (cit. on p. 27).

[31] M.A. El-Beltagy and A.S. Al-Johany. "Toward a solution of a class of non-linear stochastic perturbed PDEs using automated WHEP algorithm". In: *Applied Mathematical Modelling* 37 (12–13 2013), pp. 7174–7192. DOI: 10.1016/j.apm.2013.01.038 (cit. on p. 27).

[32] M.A. El-Tawil and A.S. Al-Johany. "Approximate solution of a mixed non-linear stochastic oscillator". In: *Computers & Mathematics with Applications* 58 (11–12 2009), pp. 2236–2259. DOI: 10.1016/j.camwa.2009.03.057 (cit. on p. 26).

[33] L.R. Evangelista and E.K. Lenzi. *Fractional Diffusion Equations and Anomalous Diffusion*. Cambridge University Press, 2018. ISBN: 9781316534649 (cit. on p. 145).

[34] G. Falsone. "The Use of Generalised Functions in the Discontinuous Beam Bending Differential Equations". In: *International Journal of Engineering Education* 18.3 (2002), pp. 337–343 (cit. on p. 118).

[35] G. Falsone and D. Settineri. "Exact stochastic solution of beams subjected to delta-correlated loads". In: *Structural Engineering and Mechanics* 47.3 (2013), pp. 307–329. DOI: 10.12989/sem.2013.47.3.307 (cit. on pp. 116, 121).

[36] A. Farsi, A.D. Pullen, J.P. Latham, J. Bowen, M. Carlsson, E.H. Stitt, and M. Marigo. "Full deflection profile calculation and Young's modulus optimization for engineered high-performance materials". In: *Scientific Reports* 7.1 (Apr. 2017). DOI: 10.1038/srep46190 (cit. on p. 78).

[37] C. Fua, Y. Xu, Y. Yang, K. Lu, F. Gu, and A. Ball. "Response analysis of an accelerating unbalanced rotating system with both random and interval variables". In: *Journal of Sound and Vibration* 466 (2020), p. 115047. DOI: 10.1016/j.jsv.2019.115047 (cit. on p. 27).

[38] V.K. Garg and Y.-C. Wang. "1 - Signal Types, Properties, and Processes". In: *The Electrical Engineering Handbook*. Ed. by WAI-KAI CHEN. Burlington: Academic Press, 2005, pp. 951–956. ISBN: 978-0-12-170960-0. DOI: 10.1016/B978-012170960-0/50069-4 (cit. on p. 46).

[39] M. Gitterman. "Stochastic oscillator with random mass: New type of Brownian motion". In: *Physica A: Statistical Mechanics and its Applications* 395 (2014), pp. 11–21. DOI: 10.1016/j.physa.2013.10.020 (cit. on p. 27).

[40] M. Gitterman. *The Noisy Oscillator: Random Mass, Frequency, Damping*. World Scientific, 2013. ISBN: 978-981-4440-48-6 (cit. on p. 26).

[41] M. Grigoriu. *Stochastic Calculus: Applications in Science and Engineering*. Boston: Birkhauser, 2002. ISBN: 978-0-8176-4242-6 (cit. on p. 119).

[42] J. Guo, J. Zhao, and S. Zeng. "Structural reliability analysis based on analytical maximum entropy method using polynomial chaos expansion". In: *Structural and Multidisciplinary Optimization* 58 (3 2018), pp. 1187–1203. DOI: 10.1007/s00158-018-1961-z (cit. on p. 116).

[43] T.D. Hien and P.-C. Nguyen. "Evaluation of Response Variability of Euler-Bernoulli Beam Resting on Foundation Due to Randomness in Elastic Modulus". In: *ICSCEA 2019*. Ed. by J. N. Reddy, C.M. Wang, V.H. Luong, and A.T. Le. Singapore: Springer Singapore, 2020, pp. 1087–1092. ISBN: 978-981-15-5144-4 (cit. on p. 4).

[44] T.D. Hien, B.T. Thanh, N.N. Long, N. Van Thuan, and D.T. Hang. "Investigation Into The Response Variability of A Higher-Order Beam Resting on A Foundation Using A Stochastic Finite Element Method". In: *CIGOS 2019, Innovation for Sustainable Infrastructure*. Ed. by C. Ha-Minh, D. Dao,

F. Benboudjema, S. Derrible, D. Huynh, and A. Tang. Singapore: Springer Singapore, 2020, pp. 117–122. ISBN: 978-981-15-0802-8 (cit. on p. 78).

[45] E.J. Hinch. *Perturbation Methods*. Cambridge University Press, 1991. ISBN: 9781139172189 (cit. on pp. 20, 26).

[46] R.A. Ibrahim. *Parametric Random Vibration*. Dover Books on Engineering. New York: Dover Publications, 2008. ISBN: 978-0486462622 (cit. on p. 26).

[47] T. Iwiński. *Theory of Beams: The Application of the Laplace Transformation Method to Engineering Problems*. Commonwealth and international library. Pergamon Press, 1967 (cit. on p. 83).

[48] S. Janson. *Gaussian Hilbert Spaces*. Cambridge University Press, 1997. ISBN: 9780511526169 (cit. on p. 18).

[49] H. Joumaa and M. Ostoja-Starzewski. "Acoustic-elastoodynamic interaction in isotropic fractal media". In: *The European Physical Journal Special Topics* 222 (2013), pp. 1951–1960. DOI: 10.1140/epjst/e2013-01976-x (cit. on p. 145).

[50] M. Kaminski. *The Stochastic Perturbation Method for Computational Mechanics*. New York: Wiley, 2013. ISBN: 9780470770825 (cit. on p. 21).

[51] H. Khakurel, M.F.N. Taufique, A. Roy, G. Balasubramanian, G. Ouyang, J. Cui, D.D. Johnson, and R. Devanathan. "Machine learning assisted prediction of the Young's modulus of compositionally complex alloys". In: *Scientific Reports* 11.1 (Aug. 2021). DOI: 10.1038/s41598-021-96507-0 (cit. on p. 78).

[52] Y. Khan and A. Mirzabeigy. "Improved accuracy of He's energy balance method for analysis of conservative nonlinear oscillator". In: *Neural Computing and Applications* 25 (3–4 2014), pp. 889–895. DOI: 10.1007/s00521-014-1576-2 (cit. on p. 3).

[53] Y. Khan, H. Vázquez-Leal, and L. Hernández-Martínez. "Removal of noise oscillation term Appearing in the nonlinear equation solution". In: *Journal of Applied Mathematics* ID 387365 (2012), pp. 1–9. DOI: 10.1155/2012/387365 (cit. on p. 3).

[54] P.E. Kloeden and E. Platen. *Numerical Solution of Stochastic Differential Equations*. Vol. 23. Stochastic Modelling and Applied Probability. Berlin Heidelberg: Springer-Verlag, 1992. ISBN: 978-3-540-54062-5 (cit. on pp. 1, 45, 48, 75, 96).

[55] T.F. Korzeniowski and K. Weinberg. "A comparison of stochastic and data-driven FEM approaches to problems with insufficient material data". In: *Computer Methods in Applied Mechanics and Engineering* 350 (2019), pp. 554–570. DOI: 10.1016/j.cma.2019.03.009 (cit. on p. 80).

[56] V.C. Le and T.T.M. Ta. "Constrained shape optimization problem in elastic mechanics". In: *Computational and Applied Mathematics* 40 (7 2021), p. 240. DOI: 10.1007/s40314-021-01632-1 (cit. on p. 79).

[57] M. Li. *Theory of Fractional Engineering Vibrations*. De Gruyter, 2021. ISBN: 9783110726152 (cit. on p. 6).

[58] Y.K. Lin. *Probabilistic Theory of Structural Dynamics*. McGraw-Hill, 1967 (cit. on pp. 17, 120).

[59] Y.K. Lin and G.Q. Cai. *Probabilistic Structural Dynamics: Advanced Theory and Applications*. McGraw-Hill, 1995. ISBN: 978-0070380387 (cit. on p. 28).

[60] G. Lindgren. *Stationary Stochastic Processes. Theory and Applications*. New York: Chapman and Hall/CRC, 2012. ISBN: 9780429097980 (cit. on p. 28).

[61] G. Lindgren, H. Rootzen, and M. Sandsten. *Stationary Stochastic Processes for Scientists and Engineers*. New York: Chapman and Hall/CRC, 2013. ISBN: 9780429190292 (cit. on p. 28).

[62] X. Liu, X. Wang, J. Xie, and B. Li. "Construction of probability box model based on maximum entropy principle and corresponding hybrid reliability analysis approach". In: *Structural and Multidisciplinary Optimization* 61 (2 2020), pp. 599–617. DOI: 10.1007/s00158-019-02382-9 (cit. on p. 117).

[63] M. Loève. *Probability Theory*. Graduate texts in mathematics v. 1. Springer, 1977. ISBN: 9783540902102 (cit. on p. 7).

[64] G.J. Lord, C.E. Powell, and T. Shardlow. *An Introduction to Computational Stochastic PDEs*. Cambridge University Press, 2014. ISBN: 9781139017329 (cit. on pp. 16, 80).

[65] N. Malkiel, O. Rabinovitch, and I. Elishakoff. "Exact solutions for stochastic Bernoulli–Euler beams under deterministic loading". In: *Acta Mechanica* 232.6 (Mar. 2021), pp. 2201–2224. DOI: 10.1007/s00707-020-02895-1 (cit. on p. 4).

[66] M. Mazhdrakov, D. Benov, and N. Valkanov. *The Monte Carlo Method. Engineering Applications*. Sofia: ACMO Academic Press, 2018. ISBN: 9786199068434 (cit. on p. 23).

[67] J.L. McCauley. *Stochastic Calculus and Differential Equations for Physics and Finance*. Cambridge University Press, 2013. ISBN: 9780521763400 (cit. on p. 145).

[68] N.W. McLachlan. *Laplace Transforms and Their Applications to Differential Equations*. Vol. 103. New York: Dover Publ. INc., 2014. ISBN: 978-0486788111 (cit. on pp. 33, 60).

[69] J. V. Michalowicz, J. M. Nichols, and F. Bucholtz. *Handbook of Differential Entropy*. CRC Press, Taylor & Francis Group, 2018. ISBN: 978-1138374799 (cit. on pp. 22 sq., 146).

[70] J.V. Michalowicz, J.M. Nichols, F. Bucholtz, and C.C. Olson. "An Isserlis' Theorem for Mixed Gaussian Variables: Application to the Auto-Bispectral

Density". In: *Journal of Statistical Physics* 136.1 (2009), 89–102. DOI: 10.1007/s10955-009-9768-3 (cit. on p. 18).

[71] C. Mittelstedt. *Structural Mechanics in Lightweight Engineering*. Springer International Publishing, 2021. ISBN: 9783030751937 (cit. on p. 86).

[72] Ali H. Nayfeh. *Perturbation Methods*. Wiley Classics Library. Wiley VCH, 2000. ISBN: 9780471399179 (cit. on pp. 20, 26).

[73] D.E. Newland. *An Introduction to Random Vibrations, Spectral and Wavelet Analysis*. New York: Longman Group UK Ltd, 1994. ISBN: 9780582215849 (cit. on p. 26).

[74] W.L. Oberkampf, S.M. De Land, B.M. Rutherford, K.V. Diegert, and K.F. Alvin. "Error and uncertainty in modeling and simulation". In: *Reliability Engineering & System Safety* 75 (3 2002), pp. 333–357. DOI: 10.1016/S0951-8320(01)00120-X (cit. on p. 1).

[75] A. Öchsner. *Classical Beam Theories of Structural Mechanics*. Springer International Publishing, 2021. ISBN: 978-3-030-76035-9 (cit. on pp. 4, 78, 86).

[76] S. Pryse and S. Adhikari. "Neumann enriched polynomial chaos approach for stochastic finite element problems". In: *Probabilistic Engineering Mechanics* 66 (2021), p. 103157. DOI: 10.1016/j.probengmech.2021.103157 (cit. on pp. 5, 80).

[77] Z. Ren, W. Xu, and S. Zhang. "Reliability analysis of nonlinear vibro-impact systems with both randomly fluctuating restoring and damping terms". In: *Communications in Nonlinear Science and Numerical Simulation* 82 (2020), p. 105087. DOI: 10.1016/j.cnsns.2019.105087 (cit. on p. 28).

[78] T. Reppel1, T.F. Korzeniowski, and K. Weinberg. "Effect of uncertain parameters on the deflection of beams". In: *Proceedings in Applied Mathematics & Mechanics*. Ed. by M. Schöberl J. Eberhardsteiner. Vienna:

Wiley-VCH Verlag, 2019, e201900318. DOI: 10.1002/pamm.201900318 (cit. on p. 80).

[79] P.F. Rizos, N. Aspragathos, and A.D. Dimarogonas. "Identification of crack location and magnitude in a cantilever beam from the vibration modes". In: *Journal of Sound and Vibrations* 138.3 (May 1990), pp. 381–388. DOI: 10.1016/0022-460X(90)90593-O (cit. on p. 79).

[80] Yury Rossikhin and Marina Shitikova. "Fractional calculus in structural mechanics". In: *Volume 7 Applications in Engineering, Life and Social Sciences, Part A*. Ed. by Dumitru Băleanu and António Mendes Lopes. Berlin, Boston: De Gruyter, 2019, pp. 159–192. ISBN: 9783110571905. DOI: doi:10.1515/9783110571905-009 (cit. on pp. 6, 145).

[81] M. Samiullah. *A First Course in Vibrations and Waves*. Oxford, 2015. ISBN: 978-0198729792 (cit. on p. 144).

[82] K.-I. Sato. *Lèvy Processes and Infinitely Divisible Distributions*. Cambridge University Press, 1999. ISBN: 9780521553025 (cit. on p. 145).

[83] J.L. Schiff. *The Laplace Transform: Theory and Applications*. New York: Springer, 1999. ISBN: 9781449255008 (cit. on p. 83).

[84] R.A. Shetty, S.A. Deepak, K. Sudheer Kini, and G.L. Dushyanthkumar. "Bending Deflection Solutions of Thick Beams Using a Third-Order Simple Single Variable Beam Theory". In: *Recent Advances in Structural Engineering and Construction Management*. Ed. by K.K Hau, A.K. Gupta, S. Chaudhary, and T. Gupta. Singapore: Springer Nature Singapore, 2023, pp. 233–246. ISBN: 978-981-19-4040-8 (cit. on p. 4).

[85] J.G. Simmonds and J.E. Mann. *A First Look at Perturbation Theory*. Dover Books on Physics. New York: Dover Publications, 2013. ISBN: 9780486315584 (cit. on p. 26).

[86] H. Singh, H.M. Srivastava, and J.J. Nieto. *Handbook of Fractional Calculus for Engineering and Science*. Chapman and Hall/CRC, 2022. ISBN: 9781003263517 (cit. on p. 6).

[87] R.C. Smith. *Uncertainty Quantification: Theory, Implementation, and Applications*. Computational Science & Engineering. SIAM, 2013. ISBN: 978-1-61197-322-8 (cit. on p. 145).

[88] K. Sobczyk. *Stochastic Differential Equations with Applications to Physics and Engineering*. Springer Dordrecht, 1991. ISBN: 978-0-7923-0339-8 (cit. on p. 16).

[89] T.T. Soong. *Random Differential Equations in Science and Engineering*. Vol. 103. New York: Academic Press, 1973. ISBN: 9780080956121 (cit. on pp. 1 sq., 7, 17 sqq., 28, 33, 43, 50, 58, 61, 72, 79, 101, 146, 156).

[90] C. Soyarslan, M. Pradas, and S. Bargmann. "Effective elastic properties of 3D stochastic bicontinuous composites". In: *Mechanics of Materials* 137 (2019), p. 103098. DOI: 10.1016/j.mechmat.2019.103098 (cit. on p. 78).

[91] R.F. Steidel. *An Introduction to Mechanical Vibrations*. New York: Wiley, 1989. ISBN: 978-0-471-84545-4 (cit. on pp. 33, 61).

[92] J.J. Stoker. *Nonlinear Vibrations*. New York: Wiley (Interscience), 1950 (cit. on p. 21).

[93] H.V. Storch and F.W. Zwiers. *Statistical Analysis in Climate Research*. Cambridge University Press, 1999. ISBN: 9780511612336 (cit. on pp. 42 sq.).

[94] J.L. Strand. "Random ordinary differential equations". In: *Journal of Differential Equations* 7 (3 1970), pp. 538–553. DOI: 10.1016/0022-0396(70)90100-2 (cit. on p. 72).

[95] R.L. Stratonovich. *Topics in the theory of random noise*. New York: Gordon and Breach, 1963 (cit. on p. 119).

[96] E.N. Strømmen. *Structural Dynamics*. Springer Series in Solid and Structural Mechanics. Springer International Publishing, 2013. ISBN: 9783319018027 (cit. on p. 86).

[97] E.N. Strømmen. *Structural Mechanics*. Springer International Publishing, 2020. ISBN: 9783030443207. DOI: 10.1007/978-3-030-44318-4 (cit. on pp. 88, 126).

[98] L. Su and G. Ahmadi. "Earthquake response of linear continuous structures by the method of evolutionary spectra". In: *Engineering Structures* 10 (1 1988), pp. 47–56. DOI: 10.1016/0141-0296(88)90016-8 (cit. on p. 3).

[99] E. Talvila. "Necessary and sufficient conditions for differentiating under the integral sign". In: *The American Mathematical Monthly* 108 (6 2001), pp. 544–548. DOI: 10.1080/00029890.2001.11919782 (cit. on p. 69).

[100] C.W.S. To. *Nonlinear Random Vibration: Analytical Techniques and Applications*. CRC Press, 2000. ISBN: 9789026516375 (cit. on p. 28).

[101] F. Uribe, I. Papaioannou, W. Betz, E. Ullmann, and D. Straub. "Random Fields in Bayesian Inference: Effects of the Random Field Discretization". In: *Safety, Reliability, Risk, Resilience and Sustainability of Structures and Infrastructure*. Ed. by C. Bucher, B.R. Ellingwood, and D.M. Frangopol. TU-Verlag, 2017, pp. 799–808. ISBN: 978-3-903024-28-1 (cit. on p. 80).

[102] O. Vallee and M. Soares. *Airy Functions and Applications to Physics*. Imperial College Press, 2010. ISBN: 978-1-911299-48-6 (cit. on p. 144).

[103] N.G. Van Kampen. *Stochastic Processes in Physics and Chemistry*. Elsevier, 2007. ISBN: 9780444529657 (cit. on p. 17).

[104] S. Wu, Y. Sun, Y. Li, and Q. Fei. "Stochastic Dynamic Load Identification on an Uncertain Structure With Correlated System Parameters". In: *ASME. Journal of Vibrations and Acoustics* 141 (4 2019), pp. 041013–1. DOI: 10.1115/1.4043412 (cit. on p. 80).

[105] D. Xiu. *Numerical Methods for Stochastic Computations: A Spectral Method Approach*. Princeton University Press, 2010. ISBN: 978-1-4008-3534-8 (cit. on p. 23).

[106] A. Yildirim, H. Askari, Z. Saadatnia, M. KalamiYazdic, and Y. Khan. "Analysis of nonlinear oscillations of a punctual charge in the electric field of a charged ring via a Hamiltonian approach and the energy balance method". In: *Computers & Mathematics with Applications* 62 (1 2011), pp. 486–490. DOI: 10.1016/j.camwa.2011.05.029 (cit. on p. 3).

[107] N.J. Yogalakshmi and K. Balaji Rao. "Shear capacity distribution of reinforced concrete beams: An information theoretic entropy approach". In: *Advances in Structural Engineering* 24.15 (2021), pp. 3452–3471. DOI: 10.1177/13694332211029734 (cit. on p. 116).

[108] D. Zhang, P. Li, Y. Zhu, and Y. Yang. "Aeroelastic instability of an inverted cantilevered plate with cracks in axial subsonic airflow". In: *Applied Mathematical Modelling* 107 (2022), pp. 782–801. DOI: 10.1016/j.apm.2022.03.019 (cit. on p. 79).

[109] H.T. Zhu, G.K. Er, V.P. Iu, and K.P. Kou. "Probabilistic solution of nonlinear oscillators excited by combined Gaussian and Poisson white noises". In: *Journal of Sound and Vibration* 330 (2011), pp. 2900–2909. DOI: 10.1016/j.jsv.2011.01.005 (cit. on p. 27).

[110] D.G. Zill. *A First Course in Differential Equations with Modeling Applications*. Boston: Brooks/Cole Cencage Learning, 2013. ISBN: 978-1-111-82705-2 (cit. on p. 144).

Differential equations in Engineering are fundamental tools for modelling and analysing dynamical systems. Differential equations allow engineers to describe how physical quantities change over time and/or space, such as vibratory systems, mechanical structures, etc. However, many real-world systems are influenced by uncertainties. For instance, measurement errors, incomplete understanding of complex physical phenomena, random fluctuations like noise in electronic circuits, and unpredictable variations in material properties are aleatoric factors. Understanding both deterministic and random/stochastic differential equations is, therefore, vital for developing robust and reliable engineering solutions in a random world. This thesis presents a comprehensive probabilistic analysis of three classes of mechanical engineering problems, such as vibratory systems (oscillators), mechanical structures (deflection of beams), and a foundational mechanical problem modelled by a random fractional differential equation. Throughout our work, we have applied different mathematical techniques to achieve a deeper understanding of these system's behavior under random excitations.